TR- 81
1976

Simulation of Pollutant Movement in Groundwater Aquifers

R. Khaleel
D.L. Reddell

Texas Water Resources Institute

Texas A&M University

RESEARCH PROJECT COMPLETION REPORT

Project Number A-030-TEX

(July 1, 1974 - September 30, 1976)

Agreement Numbers

14-31-0001-5044
14-31-0001-6045

SIMULATION OF POLLUTANT MOVEMENT IN GROUNDWATER AQUIFERS

Principal Investigators

Raziuddin Khaleel
Donald L. Reddell

The work upon which this publication is based was supported in part by funds provided by the United States Department of the Interior, Office of Water Research & Technology, as authorized under the Water Resources Research Act of 1964, P. L. 88-379.

Technical Report No. 81
Texas Water Resources Institute
Texas A&M University

May 1977

ABSTRACT

Simulation of Pollutant Movement

in Groundwater Aquifers

by

Raziuddin Khaleel

and

Donald L. Reddell

A three-dimensional model describing the two-phase (air-water) fluid flow equations in an integrated saturated-unsaturated porous medium was developed. Also, a three-dimensional convective-dispersion equation describing the movement of a conservative, noninteracting tracer in a nonhomogeneous, anisotropic porous medium was developed. Finite difference forms of these two equations were derived. The two models were linked by the pore water-velocity term.

The computer simulator was developed to handle a variety of boundary conditions, such as, constant pressure, constant head, a no-flow boundary, a constant flux, and a time-dependent flux based on rainfall rate. The two-phase fluid flow equations were solved using an implicit scheme to solve for water or air pressures and an explicit scheme to solve for water and air saturations. The tensorial nature of the dispersion coefficient in a cartesian coordinate system was recognized and the method of characteristics with a numerical tensor transformation was used to solve the convective-dispersion equations.

The numerical simulator was tested on problems for which analytical solutions, numerical solutions, and experimental data are available. The

two-phase infiltration model yielded excellent results upon comparison with analytical solutions, numerical simulations, and experimental data. The inclusion of air as a second phase in infiltration problems led to interesting results. The infiltration rate decreased rapidly to a value well below the saturated hydraulic conductivity. As the compressed air was released, the infiltration rate increased for a short period of time, then decreased slightly and remained below the saturated hydraulic conductivity until the end of simulation. This is in contrast to one-phase flow problems in which the saturated hydraulic conductivity is considered to be the lower bound of infiltration rate.

The longitudinal and lateral concentration distributions obtained with and without tensor transformation in a homogeneous, isotropic medium and a uniform flow field were compared with known analytical solutions. Excellent agreement was obtained between the numerical solution with tensor transformation and the analytical solution. The solution without the tensor transformation resulted in a steeper concentration distribution than the analytical solution.

A typical two-dimensional drainage problem in agriculture was solved in a nonhomogeneous, integrated saturated-unsaturated medium using the total simulator of fluid flow and convective-dispersion equations. A variety of outputs, such as an equipotential map or a moving points' concentration map showing isochlors were obtained at selected time steps. The limitations of the assumptions of a homogeneous and isotropic medium are illustrated by the accumulation of moving points at a transition from a higher to lower permeability. A field-size problem describing the migration of septic-tank wastes around the perimeter of a lake was also considered and solved using the total simulator.

This study was an initial thrust at developing a total numerical simulator for miscible displacement in the entire flow domain of saturated and unsaturated regions. The simulator can be applied to environmental problems concerning groundwater contamination from waste disposal sites, provided the values of the input parameters, such as the field dispersivities, are known under field conditions. The uniqueness of the model developed in this study are (1) infiltration was treated as a two-phase (air-water) process, (2) the complete subsurface regime was considered as a unified whole because the flow in the saturated region was integrated with that in the unsaturated region, (3) the model allows consideration of nonhomogeneous porous media and a combination of a variety of realistic boundary conditions, and (4) the tensorial nature of the dispersion coefficients was recognized.

ACKNOWLEDGEMENTS

The authors wish to express appreciation to Dr. Edward A. Hiler for his constant encouragement and constructive comments during this study. Thanks are also extended to Dr. Robert E. Stewart and Dr. Jack R. Runkles for their review of the manuscript and helpful comments and corrections.

The authors are also grateful to the Department of Agricultural Engineering (Dr. E. A. Hiler, Head) and the Texas Water Resources Institute (Dr. J. R. Runkles, Director) for providing the financial assistance for this study. The money for the computer analysis necessary for this work was received from the Department of Agricultural Engineering and is gratefully acknowledged.

TABLE OF CONTENTS

Chapter Page

APPENDICES (cont.)

LIST OF FIGURES

Figure Page

Figure | Page

Figure Page

LIST OF SYMBOLS

Symbol	Definition	Units
A_n	Coefficients of ordinary differential equations and defined in equation (3)	---
[A]	Square coefficient matrices for air or water and defined by the equation (40) or (42)	---
a	Subscript used to denote air	---
a_I	Longitudinal dispersivity	L
a_{II}	Lateral dispersivity	L
a_{ijmn}	Coefficient of dispersivity, a fourth rank tensor	L
b	Width of injected tracer along input boundary	L
c	Subscript used to denote capillary pressure	---
C	Mass concentration of tracer	ML^{-3}
C_ℓ	Concentration of the ℓth moving point	ML^{-3}
C_o	Reference concentration	ML^{-3}
C_p	Mass concentration of tracer in produced fluid	ML^{-3}
$\hat{C}$	Concentration of tracer in fluid element	ML^{-3}
$\overset{o}{C}$	Deviation of concentration at a point from cross-sectional average	ML^{-3}
D	Diffusivity	L^2T^{-1}
D	Dispersion coefficient	L^2T^{-1}
D^*_{ij}	Total dispersion coefficient, a second rank tensor	L^2T^{-1}
D_d	Molecular diffusion coefficient	L^2T^{-1}
D_{ij}	Dispersion coefficient, a second rank tensor	L^2T^{-1}

Symbol	Definition	Units
D_L	Longitudinal dispersion coefficient	L^2T^{-1}
D_T	Lateral (or transverse) dispersion coefficient	L^2T^{-1}
d	Particle size of the porous media or median grain diameter	L
d_{50}	Mean grain size diameter	L
$E^{\pm}_{x_i x_i}$	Coefficients for finite difference scheme and defined by equations (D-19)	---
$F^{\pm}_{x_i x_j}$	Coefficients for finite difference scheme and defined by equations (D-19)	---
F_1	Even function of Peclet number	---
F_2	Even function of Reynolds number	---
$G^{\pm}_{x_i x}$	Coefficients of finite difference scheme and defined by equations (D-19)	---
g	Gravitational acceleration	LT^{-2}
$\bar{g}$	Average value of a variable over a cross-sectional area of the representative elementary volume (REV)	---
$\overset{o}{g}$	Deviation of a variable at a point from the cross-sectional average	---
$\hat{g}$	The value of a variable at a point in the porous medium as defined by equation (C-13)	---
H_A	Elevation head at half the drain spacing	L
H_B	Elevation head at the drain or at the lake	L
$H^{\pm}_{x_i x_j}$	Coefficients for finite difference scheme and defined by equations (D-19)	---
h	Elevation above datum	L
i	Infiltration rate at the soil surface	LT^{-1}
i_f	"Feasible" infiltration rate	LT^{-1}
ij	Subscript used to denote tensor where i and j = 1, 2, 3	---

Symbol	Definition	Units
i,k	Subscript used to denote row and columns of a two-dimensional finite difference grid	---
i,j,k	Subscript used to denote row and columns of a three-dimensional finite difference grid	---
ijkℓ	Subscript used to denote tensor where i,j,k and ℓ = 1, 2, 3	---
J	Diffusive mass flux of the tracer	$ML^{-2}T^{-1}$
J_i^*	Tracer mass flux components (i = 1, 2, 3) averaged over cross-sectional area of volume element (relative to pore area)	$ML^{-2}T^{-1}$
J_i	Diffusive mass flux components (i = 1, 2, 3) in fluid element	$ML^{-2}T^{-1}$
K	Hydraulic conductivity	LT^{-1}
K_o	Hydraulic conductivity associated with the initial water content	LT^{-1}
k_r	Relative permeability to fluid	---
k_{x_i}	Absolute permeability in x_i-direction	L^2
k_s	Saturated permeability	L^2
L	Displacement vector	L
L_{ij}	Displacement, a second rank tensor	L
ℓhs	Left hand side of an equation	---
ℓ_1,ℓ_2,ℓ_3	Length in x_1-, x_2-, and x_3-directions	L
ℓ_1',ℓ_2',ℓ_3'	Length in rotated cartesian coordinates	L
M	Total mass flow rate	MT^{-1}
M_t	Mass flow rate of tracer	MT^{-1}
M_p	Mass flow rate of source or sink	MT^{-1}
M_{tp}	Tracer mass flow rate of source or sink	MT^{-1}
M_{VE}	Mass of volume element	M

Symbol	Definition	Units
M_{tREV}	Tracer mass of REV	M
m	Number of rows in matrix	---
NC	Number of grids in x_1-direction	---
NR	Number of grids in x_3-direction	---
$N^{\pm}_{x_i}$	Coefficients calculated for the finite difference scheme and defined in equations (B-11)	---
$N^{\pm\pm}_{x_i}$	Coefficients calculated for the finite difference scheme and defined in equations (B-11)	---
n	Number of columns in matrix	---
P	Concentration distribution defined as the normal probability distribution and given by equation (7)	---
P	Fluid pressure	$ML^{-1}T^{-2}$
P_A	Atmospheric pressure	$ML^{-1}T^{-2}$
P_e	Peclet number	---
Q	Rate of fluid production	L^3T^{-1}
q	Volume flux of fluid	LT^{-1}
R	Gas constant = 2.71 X 10^6 dyne-cmgm^{-1}(°K)$^{-1}$	---
R	Reynolds number	---
[rhs]	Column vector for air or water and defined by the equation (40) or (42)	---
rhs	Right hand side of an equation	---
S	Coefficient in equation (3)	---
S	Saturation of fluid	---
S_e	Effective water saturation	---
S_{ar}	Residual air saturation	---
S_{wr}	Residual water saturation	---

Symbol	Definition	Units
S_{cw}	Critical water saturation	---
S_w^*	Water saturation defined in equation (69)	---
S_{error}	Saturation error = 1 - (S_w + S_a)	---
s	Subscript used to denote saturated condition	---
T	Temperature	°K
T_{ij}	Tortuosity factor, a second rank tensor	---
$\hat{T}_{ij}$	Tortuosity on microscopic scale, a second rank tensor	---
$\mathring{T}_{ij}$	Deviation of tortuosity at a point from cross-sectional average	---
t	Time	T
t+1	New time level	T
t-1	Previous time level	T
t+Δ	Time level between t and t+1	T
V_1, V_2, V_3	Seepage velocity components (flow rate per unit pore area)	LT^{-1}
V_1', V_2', V_3'	Seepage velocity components in rotated cartesian coordinates	LT^{-1}
V	Magnitude of velocity vector	LT^{-1}
V	Velocity vector	LT^{-1}
V_m, V_n	Components of velocity vector in the m and n directions respectively	LT^{-1}
$\hat{V}$	Volume-averaged velocity of fluid element	LT^{-1}
$\hat{V}_t$	Velocity of tracer in fluid element	LT^{-1}
$\mathring{V}_i$	Deviation of velocity at a point from cross-sectional average (i = 1, 2, 3)	LT^{-1}
$V_{1_\ell}, V_{2_\ell}, V_{3_\ell}$	Velocity components of ℓth moving point	LT^{-1}

Symbol	Definition	Units
$V'_{1_\ell}, V''_{1_\ell}, V'_{3_\ell}, V''_{3_\ell}$	Velocity at grid interfaces defined by equations (59), (60), (62), and (63) respectively	LT^{-1}
w	Subscript used to denote water	---
x_1, x_2, x_3	Cartesian coordinates	L
x'_1, x'_2, x'_3	Rotated cartesian coordinates	L
$x_{1_\ell}, x_{2_\ell}, x_{3_\ell}$	Coordinates of the ℓth moving point	L
x,y,z	Cartesian coordinates	L
$\bar{x}, \bar{y}, \bar{z}$	Cartesian coordinates defined in equation (7)	L
z	Spatial dimension in the vertical direction	L
α_1, β_1	Coefficients defined by equation (22)	---
α_2, β_2	Coefficients defined by equation (23)	---
β	Angle in degrees between the displacement vector and x_1-direction (Figure 1)	---
$\Delta x_1, \Delta x_2, \Delta x_3$	Dimensions of volume element or REV	L
$\Delta x'_1, \Delta x'_2, \Delta x'_3$	Grid dimensions in rotated coordinates	L
$\Delta A_1, \Delta A_2, \Delta A_3$	Cross-sectional area of volume element perpendicular to x_1, x_2, and x_3 directions (i.e., $\Delta A_1 = \Delta x_2\ \Delta x_3$)	L^2
$\Delta x^{\pm}_1, \Delta x^{\pm}_2, \Delta x^{\pm}_3$	Dimensions defined by equations (B-7)	L
$\Delta h^{\pm}_{x_1}, \Delta h^{\pm}_{x_2}, \Delta h^{\pm}_{x_3}$	Dimensions defined by equations (B-12)	L
ΔC	Change in concentration due to dispersion	ML^{-3}
ΔS^+	Change in fluid saturation	---
$\Delta \bar{V}$	Volume of volume element ($\Delta \bar{V} = \Delta x_1 \Delta x_2 \Delta x_3$)	L^3
Δt	Time increment	T
Δt_o	Time increment in previous time step	T
σ	Length along axis of channel	L

Symbol	Definition	Units
ξ	Length along streamline	L
ρ	Fluid density	ML^{-3}
ρ_p	Density of produced fluid	ML^{-3}
ϕ	Porosity	---
μ	Dynamic viscosity	$ML^{-1}T^{-1}$
ν	Kinematic viscosity	L^2T^{-1}
δ_{ij}	Kronecker delta	---
λ	Pore-size distribution index	---
η	$2 + 3\lambda$	---
θ	Volumetric water content	L^3L^{-3}
ϕ	Potential function	---
ψ	Stream function	---
ψ	Fluid pressure head expressed as a water height	L
ψ_{at}	Threshold air pressure expressed as a water height	L
ψ_{atm}	Atmospheric pressure expressed as a water height = 1033.3 cm of water	L
ψ_b	Bubbling or air entry pressure expressed as a water height	L
erf	Error function	---
erfc	Complimentary error function	---

CHAPTER I

INTRODUCTION

An optimum soil and water management program should provide for a minimum of pollution into underground water systems. Major sources of pollution in underground water may result from the runoff of fertilizers and other chemicals when applied to cropland, from the wastes produced by livestock feedlots, and from the disposal of domestic or industrial wastes on land. Most of these pollutants are miscible with the native groundwater. A portion of the pollutants will remain in the unsaturated porous medium or root zone of the soil but, due to deep percolation, a portion may also percolate deeper and enter the saturated groundwater aquifer. The movement of these water-soluble pollutants underground changes the concentration of the native groundwater, and a concentration of dissolved salts in excess of a permissible maximum creates a water quality hazard. It is important, therefore, to investigate the processes controlling the movement of pollutants through integrated saturated-unsaturated porous media systems. Understanding the mechanics of miscible fluid displacement makes it possible to monitor the concentration of dissolved contaminants over space and time, and to design optimum management schemes for preventing or minimizing soil and water pollution.

The mixing of miscible fluids in a porous medium was named dispersion by Scheidegger (1954) and is the macroscopic outcome of the

---

Literature citations follow the style of the Transactions of the ASAE (American Society of Agricultural Engineers).

actual movements of individual tracer particles through the many pores of a porous medium. According to Bear (1972), convection and molecular diffusion are the two processes involved in dispersion. Convection depends upon the magnitude and direction of flow velocities within the porous medium and upon the geometry of the porous structure. Molecular and ionic diffusion primarily depends on time and is more significant at low flow velocities.

The dispersion process is described by a second order, nonlinear, convective-diffusion partial differential equation in which a coefficient of dispersion replaces the standard coefficient of diffusion. Even though the porous medium can be homogeneous and isotropic, the dispersion coefficient is an anisotropic quantity and must be treated as a second-rank tensor (de Josselin de Jong, 1958). It is formed from the contraction of a fourth order tensor which depends on the porous medium and a second order tensor which is a function of flow (Bear, 1961a; Scheidegger, 1961).

The complexity of the partial differential equation describing the dispersion process invariably limits any analytical solution to systems with simple initial and boundary conditions, simple geometries and a highly idealized porous media. However, practical problems involve complex flow geometries in nonhomogeneous and anisotropic media. With recent advances in computer technology, an interest in using computer or numerical simulation to describe the dispersion process has developed. Numerical techniques used to solve the convective-dispersion equation are the method of finite differences and the finite element scheme. The application of the finite element technique to dispersion

problems is rather recent but is quickly gaining momentum.

Objectives

The objective of this research was to develop a computer simulator describing the miscible displacement of pollutants in an integrated saturated-unsaturated porous medium. Instead of the traditional one-phase (water only) approach, a two-phase (air-water) flow model, as developed in the petroleum industry (Breitenbach et al., 1968a, 1968b), was employed to solve the fluid flow equations. Specifically, the objectives were:

1. Develop a numerical model describing the miscible displacement of pollutants or salts in a three-dimensional, nonhomogeneous, saturated-unsaturated porous media with a transient, nonuniform flow field. A two-dimensional problem in a nonhomogeneous, isotropic medium with a homogeneous (no density and viscosity variations due to concentration changes) and conservative fluid was analyzed using the numerical model.

2. Develop a two-phase (air-water) computer simulation model for solving the fluid flow equations.

3. Develop a numerical tensor transformation which considers the tensorial nature of the dispersion coefficient in a cartesian coordinate system.

Methods of Investigation

The techniques of this investigation were directed toward using the computer as a model simulator. The differential equations

describing two-phase (air-water) fluid flow and convection-dispersion in a saturated-unsaturated porous medium were developed and written in finite difference form (Appendices A through D). A mixed implicit-explicit technique, in which the water or air pressures are solved implicitly and the water and air saturations explicitly, was used to solve the two-phase fluid flow equations simultaneously. The fluid flow velocities were obtained and the method of characteristics (Garder et al., 1964) with a tensor transformation was then used to solve the convective-dispersion equation. The solution of the miscible displacement problem was accomplished by solving the two-phase flow equations for the water velocities at all points within the flow domain. The resulting water velocity distribution was then used in the dispersion equation to solve for the concentration distribution within the flow domain. The above procedure is described in detail in Chapter IV.

The validity of the computer simulation was tested on simple problems for which exact or analytical solutions are available. Also, a two-dimensional infiltration problem with simultaneous movement of water and salt in a saturated-unsaturated porous medium was considered.

CHAPTER II

LITERATURE REVIEW

The literature concerning fluid flow and dispersion in porous media is quite extensive. This review was divided into two distinct categories for discussion purposes: one dealing with fluid flow in porous media and the other with dispersion in porous media. Further subdivisions in each category are made for clarity. Within this framework, significant experimental works are cited.

Fluid Flow in Porous Media

The Traditional Unsaturated Approach

Richards (1931) extended Darcy's law to unsaturated flow. The resulting equation (now known as Richards' equation) has remained the basis for the majority of the work concerning flow in unsaturated porous media. Richards combined Darcy's law and the continuity equation for the liquid and obtained a one dimensional equation with the following form:

$$\frac{\partial \theta}{\partial t} = \frac{\partial}{\partial z}\left[K(\psi)\,\frac{\partial h}{\partial z}\right] , \qquad (1)$$

where θ = volumetric water content (L^3L^{-3}),

t = time (T),

z = spatial dimension (L),

ψ = pressure potential (L),

h = total hydraulic head = $\psi+z$, (L), and

K = hydraulic conductivity (LT^{-1}).

Equation (1) is called the pressure head form of Richards' equation. The other form of Richards' equation is called the diffusivity or water content form where θ is the dependent variable as shown in equation (2):

$$\frac{\partial \theta}{\partial t} = \frac{\partial}{\partial z}\left[D(\theta)\,\frac{\partial \theta}{\partial z}\right] + \frac{\partial K(\theta)}{\partial z} \quad , \tag{2}$$

where D = diffusivity = $\dfrac{K(\theta)}{(\partial\theta/\partial\psi)}$.

The conversion to either the water content or pressure head form is accomplished by the use of functional relationships among K, θ and ψ. The pressure head form is somewhat more general than the diffusivity form because it can be applied to both the saturated and unsaturated flow domains. In saturated soil, the specific water capacity $(d\theta/d\psi)$ is zero and therefore the diffusivity becomes indeterminate.

A series of papers by Philip (1969) presented the classical analysis of flow in unsaturated porous media. Philip (1969) obtained an approximate solution to equation (2) subject to boundary conditions of constant water content at the upper surface and also for a ponded water boundary condition. The initial condition treated by Philip was that of a uniform water content. The equation for the infiltration rate, $i(t)$, derived from this analysis was

$$i(t) = \frac{S}{2}\,t^{-1/2} + (A_2 + k_0) + \frac{3}{2}A_3 t^{1/2} + 2A_4 t + \ \ldots \quad . \tag{3}$$

A series of ordinary differential equations requiring numerical solution was presented from which each of the coefficients S, A_2, A_3, A_4, ... A_n can be calculated. The constant K_0 is the hydraulic

conductivity associated with the initial water content.

Theoretically, Philip's series expansion as given by equation (3) is valid for short times and diverges as $t \to \infty$. For times larger than 10^6 seconds, Philip used an asymptotic solution (the profile at infinity).

Parlange (1971a, 1971b, 1975) proposed another approximate solution to Richards' equation. He used an iterative approach to solve for the coefficients S and A_n (n = 1, 2, ...) instead of using the numerical solution for the ordinary differential equations proposed by Philip. An advantage of Parlange's method is that his solution is valid for large times and the so-called water content profile at infinity evolves naturally from his approximations. This occurs because his approximation makes use of the steady-state water content profile which becomes the proper profile at infinity as the infiltration rate approaches the saturated hydraulic conductivity.

Analytical work such as that done by Philip and Parlange has contributed immensely to understanding the physics of infiltration. It is unfortunate that such analytical work is invariably limited to systems with simple initial and boundary conditions, simple geometries and highly idealized media.

With the advent of high-speed digital computers, the method of finite differences was applied to equation (1) and several researchers (Hanks and Bowers, 1962; Whisler and Klute, 1965; Whisler and Klute, 1967; Hanks et al., 1969; Bresler et al., 1969; Smith and Woolhiser, 1971) have developed methods to solve problems that better approximate the real situations. For example, Whisler and Klute (1965, 1967)

studied infiltration into stratified soils under conditions of a non-uniform saturation distribution and included the effect of hysteresis in their calculations. Smith and Woolhiser (1971) numerically solved Richards' equation for stratified soil conditions and included the effect of a time-varying boundary condition.

The Saturated-Unsaturated Approach

Soil physicists working in the unsaturated domain have given very little attention to the saturated flow processes that occur below the root zone of the soil. In the same manner, groundwater hydrologists have avoided studies which included consideration of the unsaturated zone. In recent years, however, several studies have been reported that included an integrated saturated-unsaturated flow domain (Rubin, 1968, Freeze, 1969; Freeze, 1971; Skaggs and Tang, 1976). An excellent reference dealing with research in both the saturated and unsaturated zones was provided by Remson et al. (1971).

The pressure head form of Richards' equation as given by equation (1) is equally applicable to both the saturated and unsaturated flow domains. In the unsaturated zone, the flow parameters are:

$$\psi < 0 \ ,$$

$$K = K(\theta),$$

$$\theta = \theta(\psi), \text{ and}$$

$$\frac{\partial \theta}{\partial \psi} \neq 0 \ .$$

In the saturated zone,

$$\psi \geq 0 \ ,$$

$$K = K_s,$$

$$\theta = \theta_s, \text{ and}$$

$$\frac{\partial \theta}{\partial \psi} = 0$$

where the subscript s refers to the saturated condition.

Rubin (1968) studied a two-dimensional, ditch drainage problem using an alternating-direction implicit (ADI) finite-difference scheme. His results showed that transient water flow within the unsaturated zone and the outflow from the seepage zone may significantly affect the progress of water-table decline and the total outflow rates.

Using a numerical technique similar to that of Rubin (1968), Vauclin et al. (1974) studied a recharge and a drainage problem. The flow domain was two-dimensional and included an integrated saturated-unsaturated region. They compared their numerical results with experiments run in the laboratory on a slab of soil 3 m long, 2 m high and 5 cm thick. A fair agreement was generally obtained.

Luthin et al. (1975) studied a coupled saturated-unsaturated, transient flow toward a well using an implicit finite-difference scheme. They also obtained experimental data from a sector tank for the transient flow toward a well. A good agreement was obtained between the numerical and experimental water content profiles.

With the extensive literature available on numerical solutions to flow problems in porous media, it was surprising to note virtually no mention of mass balance errors in any of them. However, the cumulative mass balance over time represents an independent check of the accuracy with which the finite difference equations are being solved. Thus, during the course of calculations, it is advantageous to keep a running

check on the mass balance of all fluids in the system to detect any machine or programming errors, should they occur. This is simply done by computing the total mass entering the system, the total mass leaving the system, and the change in mass storage within the system.

Two-Phase Approach

All of the work reviewed so far treated fluid flow in porous media from a single-phase point of view. In other words, all analytical, numerical and laboratory work centered around the thesis that the movement of water may be defined without reference to the movement of other fluids (air) contained within the pores. Such assumptions in most cases are far from realistic. When water enters a soil, air must be removed and vice-versa. The fluid flow in porous media, therefore, involves the flow of two largely immiscible fluids: air and water.

Soil physicists define soil water pressure, P_w, relative to atmospheric pressure, P_A, and express it as a water height. This quantity, ψ, which has been given a variety of names (suction, tension, potential, etc.), is defined by the relation

$$\psi = \frac{P_w - P_A}{\rho_w g} \quad , \tag{4}$$

where ρ_w = density of water (ML^{-3}), and

g = acceleration due to gravity (LT^{-2}) .

For an air (non-wetting) - water (wetting) system, capillary pressure, P_c, is defined as (DeWeist, 1969):

$$P_c = P_a - P_w \quad , \tag{5}$$

where P_a is the air pressure in the soil. The quantity ψ broadened a growing communication gap between soil physicists and hydrologists on one side and fluid mechanists and petroleum engineers on the other (Morel-Seytoux, 1973). Yet ψ and P_c are simply related by the formula of equivalence

$$\psi = - \frac{P_c}{\rho_w g} + \frac{P_a - P_A}{\rho_w g} = - h_c + \frac{P_a - P_A}{\rho_w g} \quad . \tag{6}$$

Equation (6) shows that ψ corresponds numerically (and in absolute value) to the capillary pressure (expressed as a water height, h_c) only when the soil air pressure, P_a, is equal to the atmospheric pressure, P_A.

Free and Palmer (1940) conducted extensive experiments to determine a relationship between infiltration rate and air movement. Their results showed that the infiltration rate was significantly reduced when air was trapped and not allowed to escape freely. Experiments by Horton (1940) tended to confirm this. Peck (1965) conducted experiments on vertical columns closed at the bottom. His results indicated that the infiltration rate was reduced by a factor of nine in the bounded column. Dixon and Linden (1972) and Linden and Dixon (1973, 1975) conducted a series of experiments to observe the impedance of infiltration rate by air pressure build-up. Results indicated that displaced air tended to increase air pressure during border irrigation and impede infiltration.

Most of the literature concerning the numerical solution of immiscible fluid flow equations is found in petroleum engineering journals. Breitenbach et al. (1968a, 1968b) developed multiphase

flow equations for each of the oil, water and gas phases and combined them to give equations describing fluid flow in porous media. They also presented several numerical techniques, such as, Gaussian elimination, successive overrelaxation (SOR) and the iterative alternating direction implicit procedure (ADIPIT) for solving the set of finite difference equations. Phuc and Morel-Seytoux (1972) analyzed infiltration as a two-phase (air-water) problem. A mixed implicit and explicit scheme was employed to solve the appropriate partial differential equations simultaneously. Brustkern and Morel-Seytoux (1970) solved the two-phase infiltration problem by introducing the fractional flow function and the total velocity concepts. The total velocity is the algebraic sum of the liquid and air phase fluxes and the fractional flow of water is the ratio of the water velocity to the total velocity. Their analytical approach yields saturation profiles at various time steps. The significant aspect of their work was that an increase in infiltration rate after the release of compressed air was obtained analytically and the solution was valid for large as well as small times. A numerical solution similar to that of Phuc and Morel-Seytoux (1972) was obtained by Green et al. (1970) to determine the saturation profile. The equations were solved using an implicit scheme. Field experiments were conducted and excellent agreement was reported with the numerical results.

Using the fractional flow function concept, an extensive analytical treatment of the two-phase infiltration problem was conducted by McWhorter (1971) for various boundary conditions. His experimental results showed the infiltration rate curve to have a unique shape when

the effects of air on the infiltration rate are pronounced. Sonu (1973) studied water and air movement in bounded layered soils and obtained analytical solutions for various boundary conditions and initial saturation profiles. Brutsaert et al. (1971) used the multiphase flow equations to solve the free-surface gravity well flow problem.

The preceding review of literature on fluid flow in porous media has revealed the following facts:

1. A fair simulation of the physical process of fluid flow in porous media must take into account the simultaneous movement of fluids in the saturated and unsaturated domains.

2. The theory of transient flow in porous media is governed by complex non-linear partial differential equations not readily amenable to analytical solutions. As a result, numerical techniques have been widely used.

3. Flow problems in a porous medium really involve a two-phase flow system of air and water and thus it is essentially a case of the simultaneous flow of two immiscible fluids (air and water). An accurate description of fluid flow in a porous medium must, therefore, consider the two-phase flow problem.

4. Numerical techniques developed for multiphase fluid flow in the petroleum industry seem to offer excellent possibilities for solving air-water flow problems in porous media. Phuc and Morel-Seytoux (1972) used a mixed implicit-explicit approach to solve an infiltration problem in one dimension. This needs to be extended to other dimensions.

Dispersion in Porous Media

The literature review on dispersion is divided into five categories: statistical approach, tensorial nature of the dispersion coefficient, analytical solutions, experimental studies, and numerical solutions.

Statistical Approach

The basic postulate of the statistical approach is that the rules of probability are employed to predict the spatial distribution at any later time of a cloud of many tracer particles that were initially in a close proximity, and that move under the same average conditions (Bear, 1972). Using this approach, Scheidegger (1954) obtained the normal probability distribution:

$$P(x,y,z,t) = (4\pi Dt)^{-3/2} \exp\{-[(x-\bar{x})^2 + (y-\bar{y})^2 + (z-\bar{z})^2]/(4Dt)\} \qquad (7)$$

where D = dispersion coefficient (L^2T^{-1}),

x,y,z = coordinates in a three-dimensional field (L),

t = time (T),

P = concentration distribution of tracer (ML^{-3}),

V_x, V_y, V_z = the components of a uniform velocity field (LT^{-1}), and

$\bar{x} = V_x t$, $\bar{y} = V_y t$, $\bar{z} = V_z t$.

According to Bear (1972), convection and molecular diffusion are the two basic phenomena involved in dispersion. Diffusion is a direct result of thermal motion of the individual fluid molecules and takes

place under the influence of a concentration gradient. Convection is the result of individual fluid particles traveling at variable velocities through irregular shaped pores and along tortuous microscopic pathlines of the porous medium. Scheidegger (1954) neglected molecular diffusion in his probability analysis. He also assumed the medium was isotropic, and that the probability of a particle moving a given distance was the same in all directions. However, De Josselin de Jong (1958) also used statistical analysis to develop a model which indicated that dispersion was an anisotropic quantity and that Scheidegger's assumption of isotropic tracer spreading was erroneous. Although the porous medium may be isotropic, the spreading of the tracer is not isotropic, but greater in the direction of mean flow (longitudinal dispersion) and smaller in the direction perpendicular to mean flow (transverse or lateral dispersion). The concept of longitudinal and transverse dispersion is supported by experimental evidence (de Josselin de Jong, 1958; Bear, 1961b).

Saffman (1959, 1960) studied the relationship between molecular diffusion and convection or mechanical dispersion in his model. His first model (1959) considered dispersion to be large compared to molecular diffusion and his second model (1960) considered diffusion and dispersion to be of the same order of magnitude.

Tensorial Nature of Dispersion Coefficient

Several investigators (Scheidegger, 1961; de Josselin de Jong and Bossen, 1961) have suggested that the dispersion of a tracer in fluid flow through a saturated, homogeneous porous media is described by the equation

$$\frac{\partial C}{\partial t} + \frac{\partial}{\partial x_i}(V_i C) = \frac{\partial}{\partial x_i}\left(D_{ij}\frac{\partial C}{\partial x_j}\right) \quad , \tag{8}$$

where C = tracer concentration (ML^{-3}),

D_{ij} = second order dispersivity tensor (L^2T^{-1}), and

V_i = component of velocity vector (LT^{-1}) in a cartesian coordinate system of x_i ($i = 1, 2, 3$).

The double summation convention of tensor notation is implied in the use of equation (8). The inherent difficulty in using equation (8) is that of determining components of the dispersivity tensor which depends on the geometry of the medium, the motion of the fluid and the properties of the fluid and tracer.

Bear (1972) observed, in determining the tracer distribution resulting from a point injection in a uniform flow field, that the components of V_i of the velocity vector $\vec{V}$, or L_i of the displacement $\vec{L}$ play no role in the analysis. Therefore, although the vector of mean displacement $\vec{L}$ can be separated into its components $L\cos\beta$ and $L\sin\beta$, to obtain the dispersion itself, each component has to be further resolved to yield displacement vectors in the directions of mean flow and perpendicular to it (Figure 1).

The four components $L\cos^2\beta$, $L\sin\beta\cos\beta$, $L\cos\beta\sin\beta$, and $L\sin^2\beta$ thus define the displacement in the x_1, x_3 coordinates by means of displacements in the direction of flow and perpendicular to it. Thus displacement is defined as a second rank tensor which in two dimensions takes the form:

$$\left[L_{ij}\right] = \begin{bmatrix} L\cos^2\beta & L\sin\beta\cos\beta \\ L\sin\beta\cos\beta & L\sin^2\beta \end{bmatrix} . \tag{9}$$

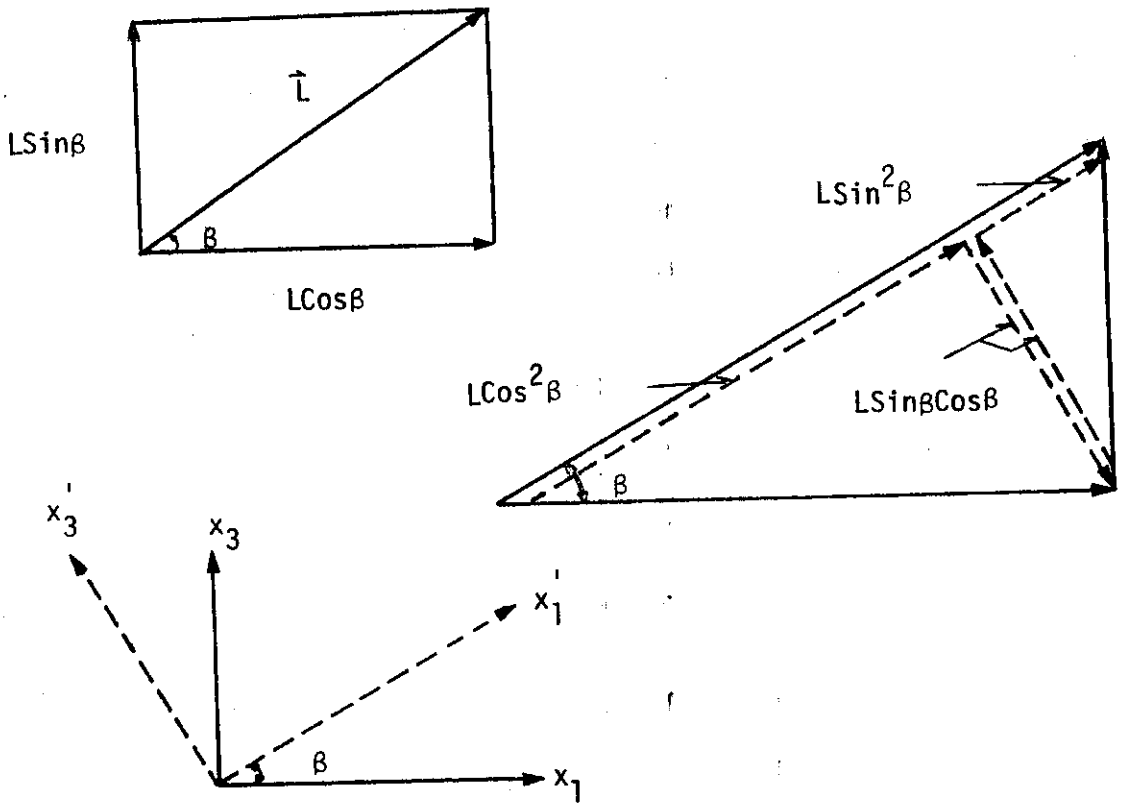

Figure 1. Resolution of the displacement $\vec{L}$.

For a uniform flow field with L = Vt, equation (9) may be written as

$$\left[L_{ij}\right] = \frac{L}{V^2}\begin{bmatrix} (V\cos\beta)^2 & V\sin\beta\cos\beta \\ V\sin\beta\cos\beta & (V\sin\beta)^2 \end{bmatrix} = \left[\frac{V_i V_j}{V}\right] t. \qquad (10)$$

Bear (1972) expressed the dispersion coefficient, D_{ij}, (a second rank tensor) as the contraction of a fourth rank dispersivity tensor, a_{ijkl}, and a second rank velocity tensor, $V_i V_j / V$,

$$D_{ij} = a_{ijkl}\frac{V_i V_j}{V}, \qquad (11)$$

where the tensor summation convention is employed.

Scheidegger (1961) studied the symmetry properties of a_{ijkl} (i, j, k, l = 1, 2, 3) and found that in a general three-dimensional space it had 81 components. However, due to certain symmetry properties, a_{ijkl} only had 36 components in the general case for an anisotropic media. For an isotropic media, the dispersivity tensor reduced to only two components, a_I and a_{II}, with

$$\begin{aligned} a_{1111} &= a_{2222} = a_I \\ a_{1122} &= a_{2211} = a_{II} \\ a_{1212} &= a_{1221} = a_{2121} = a_{2112} = 1/2\ (a_I - a_{II}) \\ &\text{and all other a's} = 0. \end{aligned} \tag{12}$$

The longitudinal and lateral dispersion coefficients are related to the dispersivities by

$$\begin{aligned} D_L &= a_I V \\ D_T &= a_{II} V \quad . \end{aligned} \tag{13}$$

Poreh (1965) showed from physical and dimensional reasoning that

$$\frac{D_{ij}}{D_d} = F_1 \delta_{ij} + F_2\ V_i V_j\ \left(\frac{d}{D_d}\right)^2 \quad , \tag{14}$$

where d = median grain diameter (L),

F_1, F_2 = even functions of Vd/ν and Vd/D_d, the Reynolds' and Peclet numbers, respectively,

ν = kinematic viscosity (L^2T^{-1}),

D_d = molecular diffusion coefficient (L^2T^{-1}), and

δ_{ij} = kronecker delta.

Analytical Solutions

Analytical solutions to dispersion problems in porous media have been obtained by many investigators. Common to these studies is the assumption of a step function for the input concentration, that is, the concentration of the displacing fluid is changed instantaneously from zero to some value and maintained at this concentration thereafter. In addition, it is commonly assumed that only mass transport by means of convection and dispersion takes place; that is, additional mass transfer mechanisms are neglected.

Longitudinal dispersion. A semi-infinite column ($x_3 > 0$) of homogeneous and isotropic porous media with a plane source maintained at $x_3 = 0$ is shown in Figure 2. The flow is maintained at a constant specific discharge, q, in the x_3-direction. For an isotropic media, the axes of the dispersivity tensor are assumed to coincide with the velocity vector. Thus equation (8) reduces to

$$\frac{\partial C}{\partial t} = D_L \frac{\partial^2 C}{\partial x_3^2} - V_3 \frac{\partial C}{\partial x_3} \quad , \tag{15}$$

where D_L is the longitudinal dispersion coefficient.

Initial and boundary conditions are given by

$$\begin{aligned} C(0,t) &= C_0 \; ; \quad t \geq 0 \\ C(x_3,0) &= 0 \; ; \quad x_3 \geq 0 \\ C(\infty,t) &= 0 \; ; \quad t \geq 0 \end{aligned} \tag{16}$$

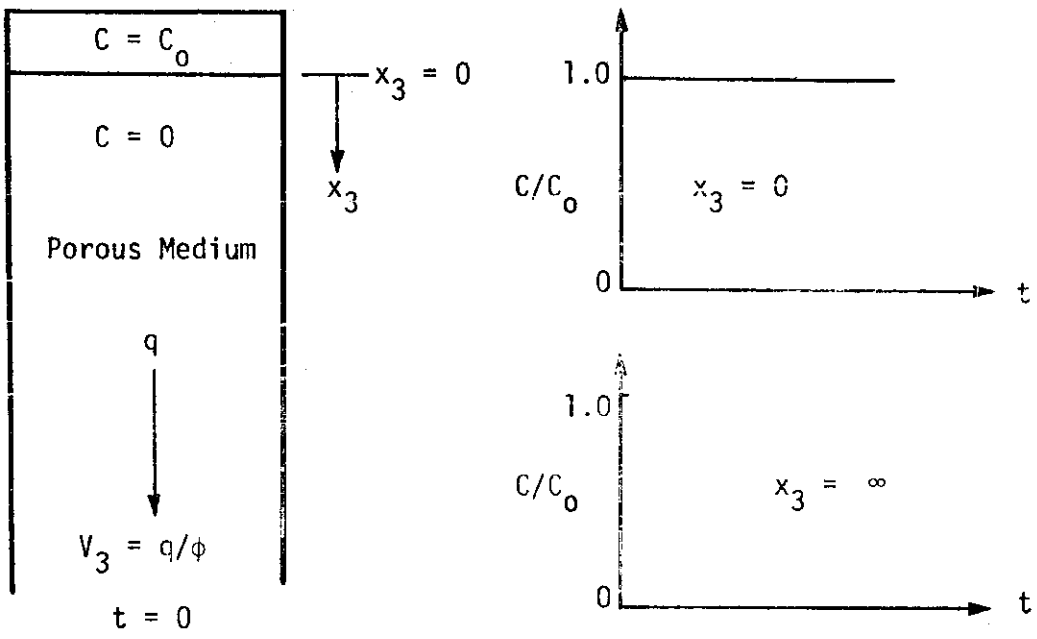

Figure 2. Schematic sketch of longitudinal dispersion column setup.

Ogata and Banks (1961) used Laplace transforms to obtain the solution

$$\frac{C}{C_0} = \frac{1}{2}\left[\operatorname{erfc}\left(\frac{x_3 - V_3 t}{2 D_L t}\right) + \exp\left(\frac{V_3 x_3}{D_L}\right)\operatorname{erfc}\left(\frac{x_3 + V_3 t}{2 D_L t}\right)\right] \qquad (17)$$

where erfc (u) = 1 - erf (u). Ogata and Banks showed that the second term in equation (17) may be neglected in most cases. For instance, if $D_L < 0.002\ V_3 x_3$, a maximum error of less than 3 percent is introduced by neglecting the second term. Therefore, unless the region close to the source is considered, an approximate solution to equations (15) and (16) is

$$\frac{C}{C_0} = \frac{1}{2}\left[\operatorname{erfc}\left(\frac{x_3 - v_3 t}{2 D_L t}\right)\right] \qquad (18)$$

Longitudinal and lateral dispersion. If a rectangular column ($0 \leq x_3 \leq \ell_3$, $0 \leq x_1 \leq \ell_1$) is used and a tracer source is maintained over a portion of the input area ($0 \leq x_1 \leq b$) as shown in Figure 3, then both longitudinal and lateral dispersion will occur.

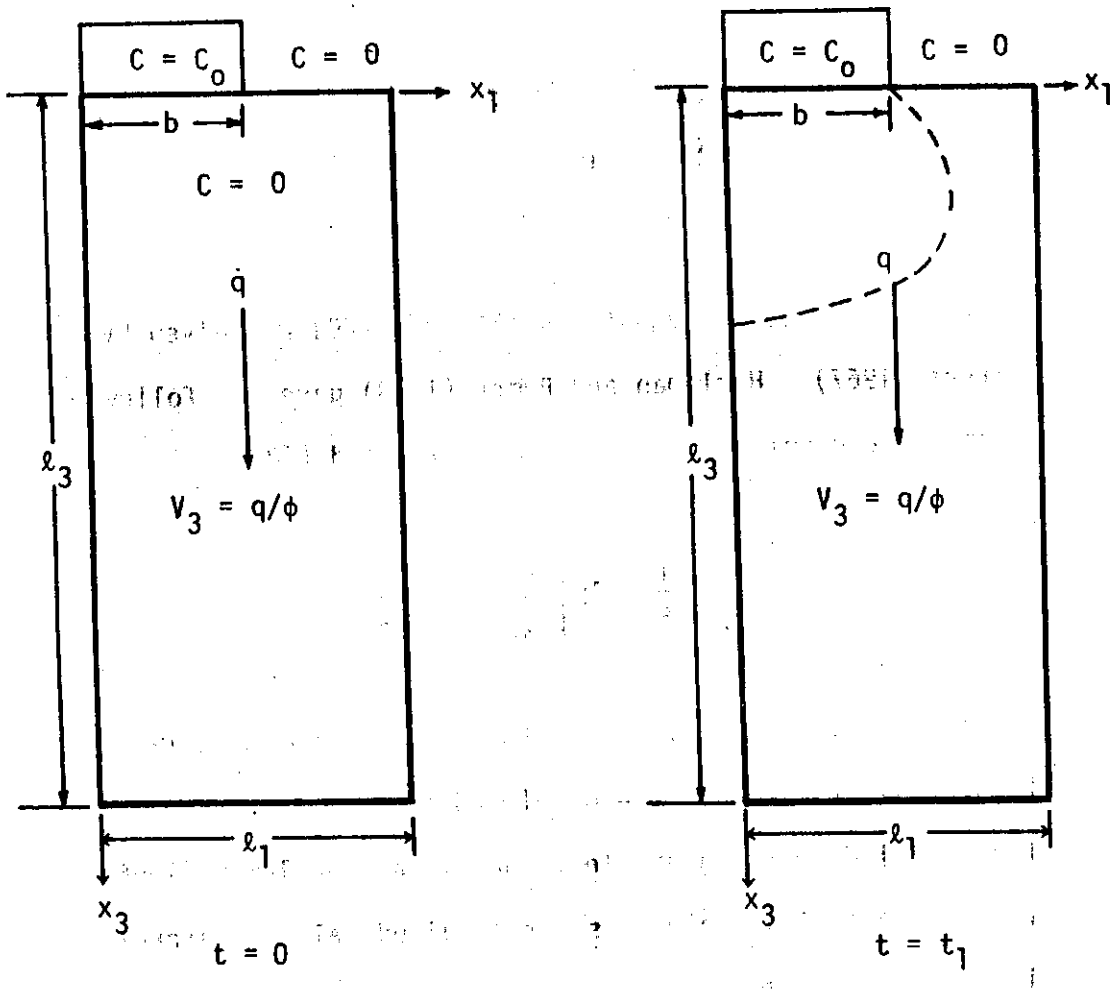

Figure 3. Schematic sketch of longitudinal and lateral dispersion column setup.

Assuming a homogeneous and isotropic medium with undirectional flow in the x_3 direction and $\partial C/\partial x_1 = 0$, equation (8) becomes

$$\frac{\partial C}{\partial t} = D_L \frac{\partial^2 C}{\partial x_3^2} + D_T \frac{\partial^2 C}{\partial x_1^2} - V_3 \frac{\partial C}{\partial x_3} \quad . \tag{19}$$

The initial and boundary conditions are given by

$$C(x_3, 0, t) = C_0; \qquad 0 \leq x_1 \leq b; \quad t \geq 0$$

$$C(x_1, 0, t) = 0; \qquad b < x_1 < \ell_1; \quad t \geq 0$$

$$\frac{\partial C}{\partial x_1}(0, x_3, t) = 0 , \qquad t \geq 0$$

$$\frac{\partial C}{\partial x_1}(\ell_3, x_3, t) = 0 , \qquad t \geq 0$$

$$C(x_1, \infty, t) = \text{Bounded}$$

$$C(x_1, x_3, 0) = 0, \quad 0 \leq x_1 \leq \ell_1 ; \quad x_3 > 0 \quad . \tag{20}$$

A series solution to equations (19) and (20) was given by Bruch and Street (1967). Harleman and Rumer (1963) gave the following approximate steady-state solution to equations (19) and (20),

$$\frac{C}{C_0} = \frac{1}{2} \operatorname{erfc}\left[\frac{x_1 - b}{2\sqrt{D_T x_3 / V_3}}\right] \quad . \tag{21}$$

In their work on wastewater recharge and dispersion, Hoopes and Harleman (1965, 1967) have developed several approximate solutions to the radial dispersion problem. Shamir and Harleman (1966, 1967) developed analytical solutions for longitudinal and lateral dispersion in layered porous media.

Experimental Studies

Literature describing experimental studies is not quite as extensive as other aspects of the dispersion phenomenon. However, to solve the theoretical and analytical equations of dispersion, the longitudinal and lateral dispersion coefficients are needed.

The analytical solutions reported previously are mostly used to experimentally determine the longitudinal dispersion coefficient, D_L. Harleman and Rumer (1963) related D_L to the Reynolds number, $R = Vd/\nu$,

$$\frac{D_L}{\nu} = \alpha_1 \left(\frac{Vd}{\nu}\right)^{\beta_1} \tag{22}$$

where V = fluid velocity (LT^{-1}),

d = particle size of the porous media (L),

ν = kinematic viscosity (L^2T^{-1}), and

α_1, β_1 = coefficients which are dependent on the porous medium and flow regime, respectively.

Values ranging from 0.66 to 1.92 for α_1 and 1.06 to 1.20 for β_1 were reported by different investigators (Harleman and Rumer, 1963; Hoopes and Harleman, 1965; Ebach and White, 1958; Bruch, 1970). Harleman and Rumer also developed a permeability (k) - longitudinal dispersion coefficient (D_L) relationship similar to equation (22) in which d is replaced by $\sqrt{k}$.

An expression similar to equation (22) has also been used to determine lateral dispersion

$$\frac{D_T}{\nu} = \alpha_2 \left(\frac{Vd}{\nu}\right)^{\beta_2} \tag{23}$$

Again, values ranging from 0.036 to 0.11 for α_2 have been reported by various investigators (Harleman and Rumer, 1963; Hoopes and Harleman, 1965; Bruch and Street, 1970). All of these investigators used a value of 0.70 for β_2.

All the experiments reported here were run under saturated flow conditions. The flow rates in those experiments were very large compared to those typically measured under unsaturated conditions. The Reynolds number versus dispersion coefficient relationships are not valid for all values of R. At small velocities, as found in unsaturated flow, molecular diffusion is very important (Biggar and Nielson, 1960). Bear (1972) presented a relationship with a wide range of Peclet numbers, P_e (= Vd/D_d) versus D_L/D_d. A plot of P_e versus D_L/D_d was divided into five regions, and characteristics of each region were discussed by Bear. Fewer experiments are available to characterize the lateral dispersion coefficient. However, the relationship between P_e versus D_T/D_d is expected to be similar to the P_e versus D_L/D_d relationship (Bear, 1972).

Lau et al. (1957) performed some field tests to evaluate various tracers, and found the chloride ion to be the best. Field-oriented laboratory experiments have been conducted by Hoopes and Harleman (1965, 1967) on wastewater recharge and by Rumer and Harleman (1963) on salt-water intrusion along coastal aquifers.

Numerical Solutions

The problem of miscible displacement has been treated extensively in the petroleum industry. Peaceman and Rachford (1962) applied a

'distance-centered' finite difference approximation (CDA) and a 'backward-in-distance' approximation (BDA). For both approximations, a Crank-Nicholson scheme was used for the space derivatives. The truncation error was too high in the BDA, and excessive numerical dispersion occurred. The CDA solutions showed oscillations that were particularly severe near the displacement front.

Garder et al. (1964) developed the method of characteristics (MOC) to overcome these difficulties. This technique does not introduce numerical dispersion. The development and application of this technique to groundwater problems was presented by Pinder and Cooper (1970), Reddell and Sunada (1970), Bredehoeft and Pinder (1973) and Konikow and Bredehoeft (1974). The MOC is described in detail in Chapter IV.

Hoopes and Harleman (1965) used an explicit finite difference scheme to obtain a solution for the problem of radial flow from a well. In addition, they studied dispersion between two wells fully penetrating a confined aquifer, one pumping and the other recharging at the same rate.

Shamir and Harleman (1966) presented a numerical scheme general enough to handle any problem of dispersion in a steady flow field, with any boundary and initial conditions. They used the convective equation in ϕ and ψ (ϕ = equipotential function and ψ = stream function) coordinates and devised a numerical scheme to use Stone and Brian's (1963) results for one-dimensional dispersion. They kept the scheme computationally efficient by using an alternating direction implicit (ADI) solution method. Stone and Brian's weighting scheme for the

convective and time terms was used without modification. This process took care of convection and longitudinal dispersion. The lateral or transverse dispersion was also solved by an ADI scheme, which was more efficient than either an explicit or a fully implicit scheme.

Lantz (1971) quantitatively evaluated the value of numerical dispersion (Peaceman and Rachford, 1962; Bresler and Hanks, 1969). Over a wide range of spatial and time steps, the truncation error is presented and can provide a guideline for choosing the spatial and time increments such that the effect of numerical dispersion can be minimized. Chaudhari (1971) added a negative dispersion term to the continuity equation to account for the numerical dispersion. Using an approach similar to Chaudhari (1971), Bresler (1973) used a higher order finite difference approach that supposedly eliminated the effects of numerical dispersion.

Several investigators (Nalluswami, 1971; Cavendish et al., 1973; Pinder, 1973; Segol et al., 1975; Pickens and Lennox, 1976) proposed a numerical solution to the dispersion problem based on variational methods by using a Galerkin-type finite element technique. Their studies indicated that both gains in speed and accuracy can be achieved with the finite element technique.

The preceding literature review on dispersion has revealed the following facts:

1. Even though the porous medium can be homogeneous and isotropic, the dispersion coefficient is an anisotropic quantity and must be treated as a second-rank tensor;

2. The dispersion coefficient is linearly related to the components of velocity as given by equation (11);

3. An analytical solution to the longitudinal dispersion problem is given by equation (17);

4. An approximate steady state solution to the longitudinal and lateral dispersion problem is given by equation (21);

5. The longitudinal and lateral dispersion coefficients can be obtained by using P_e versus D_L/D_d and P_e versus D_T/D_d relationships (Bear, 1972);

6. The method of characteristics (MOC) appears to be one of the best numerical techniques currently available for simulating dispersion. It has been widely used and tested. Reddell and Sunada (1970), Pinder and Cooper (1970), Bredehoeft and Pinder (1973) and Konikow and Bredehoeft (1974) used the MOC for saturated groundwater flow, while Smajstrla et al. (1975) used it for unsaturated flow; and

7. Finally, to get a complete simulation of the dispersion problem, a combination of the dispersion models used in saturated and unsaturated porous media is necessary.

CHAPTER III

MATHEMATICAL MODEL

The solution of the dispersion problem requires the simultaneous solution of a set of coupled equations: (1) the equations governing two-phase (air-water) fluid flow, and (2) the equation governing the convective-dispersion transport of a dissolved tracer.

Fluid Flow Equations

The equations appropriate for this case are those of two-phase fluid flow in porous media. The two fluid phases are air and water, and soil is the porous medium. Thus, a set of fundamental flow equations for the immiscible movement of air-water through the entire porous medium (saturated-unsaturated) are (1) Darcy's law for each fluid phase, (2) continuity equations for each fluid phase, (3) a total fluid conservation equation, (4) an equation defining the capillary pressure, and (5) an equation of state describing the density of air as a function of air pressure. These equations combine together to yield the Water or Air Pressure Equation, the Water Saturation Equation, and the Air Saturation Equation. A detailed development of these Fluid Flow Equations is given in Appendix A. Using shorthand tensor notation, the Water Pressure Equation is written as

$$\left(\frac{1}{\rho_w \phi \Delta \bar{V}}\right) \frac{\partial}{\partial x_i}\left[\frac{\rho_w^2 \, k_{x_i} \, k_{rw} \Delta A_i}{\mu_w} \frac{\partial \psi_w}{\partial x_i}\right] \Delta x_i \; +$$

$$\left(\frac{1}{\rho_a \phi \Delta \bar{V}}\right) \frac{\partial}{\partial x_i} \left[\frac{\rho_a \rho_w k_{x_i} k_{ra} \Delta A_i}{\mu_a} \frac{\partial \psi_w}{\partial x_i} \right] \Delta x_i =$$

$$-\left(\frac{1}{\rho_a \phi \Delta \bar{V}}\right) \frac{\partial}{\partial x_i} \left[\frac{\rho_a \rho_w k_{x_i} k_{ra} \Delta A_i}{\mu_a} \frac{\partial \psi_c}{\partial x_i} \right] \Delta x_i -$$

$$\left(\frac{1}{\rho_w \phi \Delta \bar{V}}\right) \frac{\partial}{\partial x_i} \left[\frac{\rho_w^2 k_{x_i} k_{rw} \Delta A_i}{\mu_w} \frac{\partial h}{\partial x_i} \right] \Delta x_i -$$

$$\left(\frac{1}{\rho_a \phi \Delta \bar{V}}\right) \frac{\partial}{\partial x_i} \left[\frac{\rho_a^2 k_{x_i} k_{ra} \Delta A_i}{\mu_a} \frac{\partial h}{\partial x_i} \right] \Delta x_i +$$

$$\frac{S_w}{\phi \Delta \bar{V} g} \frac{\partial}{\partial t} (\phi \Delta \bar{V}) + \frac{S_w}{\rho_w g} \frac{\partial \rho_w}{\partial t} + \frac{S_a}{\phi \Delta \bar{V} g} \frac{\partial}{\partial t} (\phi \Delta \bar{V}) +$$

$$\frac{S_a}{\rho_a g} \frac{\partial \rho_a}{\partial t} + \frac{\rho_P Q_w}{\rho_w \phi \Delta \bar{V} g} + \frac{\rho_P Q_a}{\rho_a \phi \Delta \bar{V} g} \quad , \tag{24}$$

where Δx_i ($i = 1, 2, 3$) = dimensions of volume element (L),

ΔA_i ($i = 1, 2, 3$) = cross sectional area of element perpendicular to x_i (that is, $\Delta A_1 = \Delta x_2 \Delta x_3$, etc.) ($L^2$),

t = time T ,

$\Delta \bar{V} = \Delta x_1 \Delta x_2 \Delta x_3$ = volume of element (L^3),

x_i ($i = 1, 2, 3$) = cartesian coordinate system (x_1, x_2, x_3) (L),

ρ_w = density of water (ML^{-3}),

ρ_a = density of air (ML^{-3}),

μ_w = dynamic viscosity of water ($ML^{-1}T^{-1}$),

μ_a = dynamic viscosity of air $(ML^{-1}T^{-1})$,

k_{rw} = relative permeability to water, dimensionless,

k_{ra} = relative permeability to air, dimensionless

k_{x_i} = absolute permeability in x_i - direction (L^2),

ϕ = porosity of the medium, dimensionless,

g = acceleration due to gravity (LT^{-2}),

ψ_w = water pressure in head of water (L),

ψ_a = air pressure in head of water (L),

ψ_c = capillary pressure in head of water (L),

h = gravitational head above datum (L),

S_w = water saturation, dimensionless,

S_a = air saturation, dimensionless,

Q_w = water production rate (L^3T^{-1}),

Q_a = air production rate (L^3T^{-1}), and

ρ_p = density of fluid passed in the source or sink (ML^{-3}).

The Air Pressure Equation is

$$\left(\frac{1}{\rho_w \phi \Delta \overline{V}}\right) \frac{\partial}{\partial x_i}\left[\frac{\rho_w^2 k_{x_i} k_{rw} \Delta A_i}{\mu_w} \frac{\partial \psi_a}{\partial x_i}\right] \Delta x_i +$$

$$\left(\frac{1}{\rho_a \phi \Delta \overline{V}}\right) \frac{\partial}{\partial x_i}\left[\frac{\rho_a \rho_w k_{x_i} k_{rw} \Delta A_i}{\mu_a} \frac{\partial \psi_a}{\partial x_i}\right] \Delta x_i =$$

$$\left(\frac{1}{\rho_w \phi \Delta \overline{V}}\right) \frac{\partial}{\partial x_i}\left[\frac{\rho_w^2 k_{x_i} k_{rw} \Delta A_i}{\mu_w} \frac{\partial \psi_c}{\partial x_i}\right] \Delta x_i -$$

$$\left(\frac{1}{\rho_w \phi \Delta \overline{V}}\right) \frac{\partial}{\partial x_i}\left[\frac{\rho_w^2 k_{x_i} k_{rw} \Delta A_i}{\mu_w} \frac{\partial h}{\partial x_i}\right] \Delta x_i -$$

$$\left(\frac{1}{\rho_a \phi \Delta \bar{V}}\right) \frac{\partial}{\partial x_i} \left[\frac{\rho_a^2 k_{x_i} k_{ra} \Delta A_i}{\mu_a} \frac{\partial h}{\partial x_i} \right] \Delta x_i \quad +$$

$$\frac{S_w}{\phi \Delta \bar{V} g} \frac{\partial}{\partial t} (\phi \Delta \bar{V}) + \frac{S_w}{\rho_w g} \frac{\partial \rho_w}{\partial t} + \frac{S_a}{\phi \Delta \bar{V} g} \frac{\partial}{\partial t} (\phi \Delta \bar{V}) +$$

$$\frac{S_a}{\rho_a g} \frac{\partial \rho_a}{\partial t} + \frac{\rho_p Q_w}{\rho_w \phi \Delta \bar{V} g} + \frac{\rho_p Q_a}{\rho_a \phi \Delta \bar{V} g} \quad . \tag{25}$$

The Water Saturation Equation is

$$\frac{\partial S_w}{\partial t} = \left(\frac{1}{\rho_w \phi \Delta \bar{V}}\right) \frac{\partial}{\partial x_i} \left[\frac{\rho_w^2 g k_{x_i} k_{rw}}{\mu_w} \left(\frac{\partial \psi_w}{\partial x_i} + \frac{\partial h}{\partial x_i} \right) \Delta A_i \right] \Delta x_i$$

$$- \frac{\rho_p Q_w}{\rho_w \phi \Delta \bar{V}} - \frac{S_w}{\phi \Delta \bar{V}} \frac{\partial}{\partial t} (\phi \Delta \bar{V}) - \frac{S_w}{\rho_w} \frac{\partial \rho_w}{\partial t} \quad . \tag{26}$$

The Air Saturation Equation is

$$\frac{\partial S_a}{\partial t} = \left(\frac{1}{\rho_a \phi \Delta \bar{V}}\right) \frac{\partial}{\partial x_i} \left[\left(\frac{\rho_a \rho_w g k_{x_i} k_{ra}}{\mu_a} \frac{\partial \psi_a}{\partial x_i} \right. \right. +$$

$$\left. \left. \frac{\rho_a^2 g k_{x_i} k_{ra}}{\mu_a} \frac{\partial h}{\partial x_i} \right) \Delta A_i \right] \Delta x_i - \frac{\rho_p Q_a}{\rho_a \phi \Delta \bar{V}} -$$

$$\frac{S_a}{\phi \Delta \bar{V}} \frac{\partial}{\partial t} (\phi \Delta \bar{V}) - \frac{S_a}{\rho_a} \frac{\partial \rho_a}{\partial t} \quad . \tag{27}$$

The following assumptions were made in deriving the above equations:

1. Darcy's law is valid for both wetting (water) and nonwetting (air) phases;
2. The two fluids, air and water, are homogeneous and immiscible;
3. The water as a wetting phase fluid is incompressible and the air as a nonwetting phase fluid is compressible;
4. The flow is isothermal; and
5. There is no mutual solubility in two fluid phases.

Convective-Dispersion Equation

A relationship for determining tracer concentration was derived by using a continuity equation for the dissolved tracer. The problem was formulated on a microscopic basis and then averaged over a cross sectional area of the porous medium to give a macroscopic convective-dispersion equation. A detailed derivation of this equation is given in Appendix C. The general convective-dispersion equation is

$$\frac{\partial}{\partial t}(\phi S_w \Delta \bar{V} C) = \frac{\partial}{\partial x_i}\left[D^*_{ij}\frac{\partial C}{\partial x_j}\phi S_w \Delta A_i\right]\Delta x_i - \frac{\partial}{\partial x_i}(CV_i \phi S_w \Delta A_i)\Delta x_i - C_p Q_w \tag{28}$$

where $D^*_{ij} = D_{ij} + D_d T_{ij}$ = coefficient of hydrodynamic dispersion, a second rank tensor (L^2T^{-1}),

D_{ij} = mechanical dispersion coefficient, a second rank tensor (L^2T^{-1}),

D_d = molecular diffusion coefficient (L^2T^{-1}),

T_{ij} = porous medium "tortuosity" factor, a second rank tensor, dimensionless,

C = mass concentration of tracer (ML^{-3}),

V_i = pore velocity (flow rate per unit pore area) of miscible fluid in i-th direction (LT^{-1}),

C_p = concentration of tracer in produced fluid (ML^{-3}), and

all other terms are as defined previously. Assumptions made in deriving equation (28) are as follows:

1. The diffusive mass flux is proportional to the concentration gradient;
2. The convective mixing (called dispersion) is proportional to the concentration gradient;
3. Only the wetting phase is considered in the convective-dispersion section of the problem;
4. Any diffusion due to temperature or velocity gradients is neglected; and
5. The fluid tracer is conservative.

Assuming further a homogeneous fluid in which there is no variation of density and viscosity due to changes in concentration, and rearranging equation (28), the result is

$$\frac{\partial C}{\partial t} = \frac{1}{(\phi S_w \Delta \overline{V})} \frac{\partial}{\partial x_i} \left[D^*_{ij} \frac{\partial C}{\partial x_j} \phi S_w \Delta A_i \right] \Delta x_i - V_i \frac{\partial C}{\partial x_i}$$

$$- \left(C_p - \frac{C \rho_p}{\rho_w} \right) \frac{Q_w}{\Delta \overline{V}} \quad . \tag{29}$$

Pore Water Velocity

The convective-dispersion equation is coupled to the fluid flow equation by the pore velocity. The pore velocity of the miscible fluid is related to the volume flux of water, q_{w_i}, by the relation:

$$q_{w_i} = V_i \phi S_w \tag{30}$$

where $$q_{w_i} = - \frac{k_{x_i} k_{rw} \rho_w g}{\mu_w} \left(\frac{\partial \psi_w}{\partial x_i} + \frac{\partial h}{\partial x_i} \right) \tag{31}$$

Parameters of Dispersion

The coefficient of hydrodynamic dispersion, D^*_{ij}, appearing in equation (29) has been analyzed by many investigators. It depends on the flow pattern and on some basic medium characteristics. In general, D^*_{ij} which includes the effects of both mechanical (or convective) dispersion and molecular diffusion, is a function of the Peclet number, P_e,

$$P_e = \frac{Vd}{D_d} \tag{32}$$

where d = mean grain size diameter or any other characteristic medium length (L).

As discussed earlier in Chapter II, the mechanical dispersion coefficient, D_{ij}, is

$$D_{ij} = a_{ijmn} \frac{V_m V_n}{V} \tag{33}$$

where a_{ijmn} = dispersivity of the medium, a fourth rank tensor (L),

V_m, V_n = components of velocity in the m and n directions, respectively (LT^{-1}), and

V = magnitude of velocity (LT^{-1}).

For an isotropic medium, Bear (1960, 1961a) relates the medium's dispersivity a_{ijmn} to two constants: a_I = longitudinal dispersivity and a_{II} = transverse dispersivity of the medium. For two dimensions:

$$a_{1111} = a_{2222} = a_I ,$$

$$a_{1122} = a_{2211} = a_{II} ,$$

$$a_{1212} = a_{1221} = a_{2112} = a_{2121} = \frac{1}{2}(a_I - a_{II}),$$

and all other a's = 0. (34)

The longitudinal and lateral dispersion coefficients are related to the dispersivities by

$$D_L = a_I V, \quad (35a)$$

and $$D_T = a_{II} V . \quad (35b)$$

For an isotropic medium, the diffusion tensor, $D_d T_{ij}$, is given as

$$D_d T_{11} = D_d T_{22} = D_d T_{33} = D_d T$$

and all other $D_d T_{ij}$'s = 0 (36)

where T = tortuosity factor, dimensionless.

Expanding equation (33) and using equations (34) through (36), the following functional relationship for the nine components of the hydrodynamic dispersion coefficient are obtained for an isotropic

medium:

$$
\begin{aligned}
D^*_{11} &= D_L \frac{V_1 V_1}{V^2} + D_T \frac{V_2 V_2}{V^2} + D_T \frac{V_3 V_3}{V^2} + D_d T, \\
D^*_{22} &= D_T \frac{V_1 V_1}{V^2} + D_L \frac{V_2 V_2}{V^2} + D_T \frac{V_3 V_3}{V^2} + D_d T, \\
D^*_{33} &= D_T \frac{V_1 V_1}{V^2} + D_T \frac{V_2 V_2}{V^2} + D_L \frac{V_3 V_3}{V^3} + D_d T, \\
D^*_{21} &= D^*_{12} = (D_L - D_T) \frac{V_1 V_2}{V^2}, \\
D^*_{31} &= D^*_{13} = (D_L - D_T) \frac{V_1 V_3}{V^2},
\end{aligned}
$$

and

$$
D^*_{32} = D^*_{23} = (D_L - D_T) \frac{V_2 V_3}{V^2}. \qquad (37)
$$

CHAPTER IV

NUMERICAL MODEL

The numerical model consists of finite difference analogs to the differential equations presented in Chapter III. The detailed derivation of the finite difference analogs is given in Appendices B and D. Since only two-dimensional problems are dealt with in this study, the numerical simulator is presented in two-dimensional form. The grid system used in the following finite difference equation is shown in Figure 4.

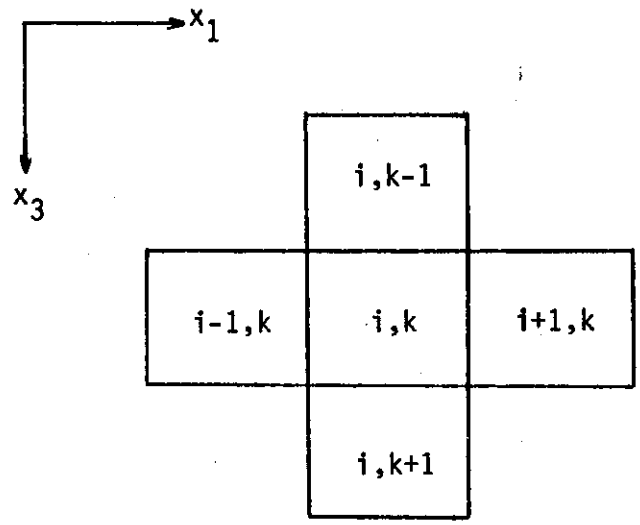

Figure 4. Two-dimensional grid system used in finite difference equations.

Finite Difference Form of Two-Dimensional Fluid Flow Equations

The fluid flow equations are the Water Pressure Equation (24), the Air Pressure Equation (25), the Water Saturation Equation (26), and the Air Saturation Equation (27). Using an implicit, centered-in-space finite difference scheme to approximate the time and space derivatives, the two-dimensional finite difference form of the Water Pressure Equation is

$$
\begin{aligned}
&(N^{+}_{x_1 w} + N^{+}_{x_1 a})\, \psi^{t+1}_{w_{i+1,k}} + (N^{-}_{x_1 w} + N^{-}_{x_1 a})\, \psi^{t+1}_{w_{i-1,k}} + \\
&(N^{+}_{x_3 w} + N^{+}_{x_3 a})\, \psi^{t+1}_{w_{i,k+1}} + (N^{-}_{x_3 w} + N^{-}_{x_3 a})\, \psi^{t+1}_{w_{i,k-1}} - \\
&(N^{+}_{x_1 w} + N^{+}_{x_1 a} + N^{-}_{x_1 w} + N^{-}_{x_1 a} + N^{+}_{x_3 w} + N^{+}_{x_3 a} + N^{-}_{x_3 w} + N^{-}_{x_3 a})\, \psi^{t+1}_{w_{i,k}} = \\
&-\Big[N^{+}_{x_1 a} \psi^{t}_{c_{i+1,k}} + N^{-}_{x_1 a} \psi^{t}_{c_{i-1,k}} + N^{+}_{x_3 a} \psi^{t}_{c_{i,k+1}} + N^{-}_{x_3 a} \psi^{+}_{c_{i,k-1}} - \\
&(N^{+}_{x_1 a} + N^{-}_{x_1 a} + N^{+}_{x_3 a} + N^{-}_{x_3 a})\, \psi^{t}_{c_{i,k}} + (N^{+}_{x_1 w} + N^{++}_{x_1 a})\, \Delta h^{+}_{x_1} + \\
&(N^{-}_{x_1 w} + N^{--}_{x_1 a})\, \Delta h^{-}_{x_1} + (N^{+}_{x_3 w} + N^{++}_{x_3 a})\, \Delta h^{+}_{x_3} + (N^{-}_{x_3 w} + N^{--}_{x_3 a})\, \Delta h^{-}_{x_3} \Big] \\
&+ \frac{1}{g(\phi \Delta \bar{V})^{t}_{i,k}} \frac{\{(\phi \Delta \bar{V})^{t}_{i,k} - (\phi \Delta \bar{V})^{t-1}_{i,k}\}}{\Delta t_0} + \frac{S^{t}_{w_{i,k}}}{g \rho^{t}_{w_{i,k}}} \frac{\{\rho^{t}_{w_{i,k}} - \rho^{t-1}_{w_{i,k}}\}}{\Delta t_0} + \\
&\frac{S^{t}_{a_{i,k}}}{g \rho^{t}_{a_{i,k}}} \frac{\{\rho^{t}_{a_{i,k}} - \rho^{t-1}_{a_{i,k}}\}}{\Delta t_0} + \frac{(\rho_p)_{i,k}}{g(\phi \Delta \bar{V})^{t}_{i,k}} \left[\left(\frac{Q_w}{\rho_w}\right)_{i,k} + \left(\frac{Q_a}{\rho_a}\right)_{i,k}\right] . \qquad (38)
\end{aligned}
$$

The subscripts i and k indicate the grid column and grid row number respectively, and t indicates the time level. The coefficients are as defined in Appendix B. The dimension of the volume element, $\Delta\bar{V}$, is evaluated with $\Delta x_2 = 1$.

The two-dimensional finite-difference form of the Air Pressure Equation is

$$
\begin{aligned}
&(N^{+}_{x_1 w} + N^{+}_{x_1 a})\,\psi^{t+1}_{a_{i+1,k}} + (N^{-}_{x_1 w} + N^{-}_{x_1 a})\,\psi^{t+1}_{a_{i-1,k}} + \\
&(N^{+}_{x_3 w} + N^{+}_{x_3 a})\,\psi^{t+1}_{a_{i,k+1}} + (N^{-}_{x_3 w} + N^{-}_{x_3 a})\,\psi^{t+1}_{a_{i,k-1}} - \\
&\left\{N^{+}_{x_1 w} + N^{+}_{x_1 a} + N^{-}_{x_1 w} + N^{-}_{x_1 a} + N^{+}_{x_3 w} + N^{+}_{x_3 a} + N^{-}_{x_3 w} + N^{-}_{x_3 a} + \right. \\
&\left. \frac{S^{t}_{a_{i,k}}}{(\psi^{t}_{a_{i,k}} + 1033.3)\Delta tg}\right\}\psi^{t+1}_{a_{i,k}} = N^{+}_{x_1 w}\psi^{t}_{c_{i+1,k}} + N^{-}_{x_1 w}\psi^{t}_{c_{i-1,k}} + N^{+}_{x_3 w}\psi^{t}_{c_{i,k+1}} \\
&+ N^{-}_{x_3 w}\psi^{t}_{c_{i,k-1}} - (N^{+}_{x_1 w} + N^{-}_{x_1 w} + N^{+}_{x_3 w} + N^{-}_{x_3 w})\,\psi^{t}_{c_{i,k}} - (N^{+}_{x_1 w} + \\
&N^{++}_{x_1 a})\,\Delta h^{+}_{x_1} - (N^{-}_{x_1 w} + N^{--}_{x_1 a})\,\Delta h^{-}_{x_1} - (N^{+}_{x_3 w} + N^{++}_{x_3 a})\,\Delta h^{+}_{x_3} - \\
&(N^{-}_{x_3 w} + N^{--}_{x_3 a})\,\Delta h^{-}_{x_3} + \frac{1}{g(\phi\Delta V)^{t}_{i,k}}\,\frac{\{(\phi\Delta\bar{V})^{t}_{i,k} - (\phi\Delta\bar{V})^{t-1}_{i,k}\}}{\Delta t_0} + \\
&\frac{S^{t}_{w_{i,k}}}{g\rho^{t}_{w_{i,k}}}\,\frac{(\rho^{t}_{w_{i,k}} - \rho^{t-1}_{w_{i,k}})}{\Delta t_0} + \frac{(\rho_p)_{i,k}}{g(\phi\Delta\bar{V})^{t}_{i,k}}\left[\left(\frac{Q_w}{\rho_w}\right)_{i,k} + \left(\frac{Q_a}{\rho_a}\right)_{i,k}\right] . \qquad (39)
\end{aligned}
$$

where 1033.3 is the atmospheric pressure in cm. of water.

A rectangular grid system of m rows and n columns is superimposed onto the region of interest, and equation (38) or (39) is written for each grid. Since equation (38) or (39) contains unknown pressures from each of the four adjacent grids plus an unknown pressure for the grid in question, the result of writing equation (38) or (39) for mxn grids is a set of mn simultaneous algebraic equations. Equation (38) may be written in matrix form as

$$\left[A_w\right]\left\{\psi_w^{t+1}\right\} = \left\{rhs_w\right\} \tag{40}$$

where $\left[A_w\right]$ = mn x mn matrix containing the coefficients of unknown water pressures,

$\left\{\psi_w\right\}$ = mn column vector containing the unknown water pressures at time t+1, and

$\left\{rhs_w\right\}$ = mn column vector containing the right hand side terms of equation (38).

The implicit solution of equation (40) yields water pressures, ψ_w, at time level t+1. The air pressures, ψ_a, at time t+1 are

$$\psi_{a_{i,k}}^{t+1} = \psi_{c_{i,k}}^{t} + \psi_{w_{i,k}}^{t+1} . \tag{41}$$

If the air pressures are solved implicitly, equation (39) is used instead of equation (38). Equation (39) may be written in matrix form as

$$\left[A_a\right]\left\{\psi_a^{t+1}\right\} = \left\{rhs_a\right\} . \tag{42}$$

where $\left[A_a\right]$ = mn x mn matrix containing the coefficients of unknown air pressures,

$\left\{\psi_a\right\}$ = mn column vector containing the unknown air pressures at time t+1, and

$\left\{rhs_a\right\}$ = mn column vector containing the right hand side terms of equation (39).

The implicit solution of equation (42) yields air pressures, ψ_a, at time level t+1. The water pressures, ψ_w, at time t+1 are

$$\psi_{w_{i,k}}^{t+1} = -\psi_{c_{i,k}}^{t} + \psi_{a_{i,k}}^{t+1} \tag{43}$$

Therefore, either equations (40) and (41) are used to obtain the water and air pressures at time t+1, or equations (42) and (43) are used to obtain the air and water pressures at time t+1. Once the water and air pressures are known at new time t+1 using either one of the two sets of equations, the next step is to solve explicitly for the water saturations, S_w and the air saturations, S_a, at time t+1. The finite difference form of the Water Saturation Equation (26) in two dimensions is

$$\Delta S_{w_{i,k}}^{+} = g\Delta t \left[N_{x_1w}^{+}\psi_{w_{i+1,k}}^{t+1} + N_{x_1w}^{-}\psi_{w_{i-1,k}}^{t+1} + N_{x_3w}^{+}\psi_{w_{i,k+1}}^{t+1}\right.$$

$$\left. N_{x_3w}^{-}\psi_{w_{i,k-1}}^{t+1} - (N_{x_1w}^{+} + N_{x_1w}^{-} + N_{x_3w}^{+} + N_{x_3w}^{-})\,\psi_{w_{i,k}}^{t+1}\right] +$$

$$N^{+}_{x_1 w}\Delta h^{+}_{x_1} + N^{-}_{x_1 w}\Delta h^{-}_{x_1} + N^{+}_{x_3 w}\Delta h^{+}_{x_3} + N^{-}_{x_3 w}\Delta h^{-}_{x_3}\Big] -$$

$$\Delta t\left[\left(\frac{\rho_P Q_w}{\rho_w \phi \Delta \bar{V}}\right)^{t}_{i,k} - S^{t}_{w_{i,k}} \frac{\{(\phi\Delta\bar{V})^{t}_{i,k} - (\phi\Delta\bar{V})^{t-1}_{i,k}\}}{(\phi\Delta\bar{V})^{t}_{i,k}\Delta t_0}\right.$$

$$\left.\left(\frac{S_w}{\rho_w}\right)^{t} \frac{(\rho^{t}_{w_{i,k}} - \rho^{t-1}_{w_{i,k}})}{\Delta t_0}\right], \tag{44}$$

where $\Delta S^{+}_{w_{i,k}} = S^{t+1}_{w_{i,k}} - S^{t}_{w_{i,k}}$.

The new water saturation, S_w, at time t+1 is, therefore:

$$S^{t+1}_{w_{i,k}} = \Delta S^{+}_{w_{i,k}} + S^{t}_{w_{i,k}} . \tag{45}$$

If equations (40) and (41) are used to obtain the water and air pressures at time t+1, the finite difference form of the Air Saturation equation (27) in two dimensions is

$$\Delta S^{+}_{a_{i,k}} = g\Delta t\left[N^{+}_{x_1 a}\psi^{t+1}_{a_{i+1,k}} + N^{-}_{x_1 a}\psi^{t+1}_{a_{i-1,k}} + N^{+}_{x_3 a}\psi^{t+1}_{a_{i,k+1}} +\right.$$

$$N^{-}_{x_3 a}\psi^{t+1}_{a_{i,k-1}} - (N^{+}_{x_1 a} + N^{-}_{x_1 a} + N^{+}_{x_3 a} + N^{-}_{x_3 a})\,\psi^{t+1}_{a_{i,k}} +$$

$$\left.N^{++}_{x_1 a}\Delta h^{+}_{x_1} + N^{--}_{x_1 a}\Delta h^{-}_{x_1} + N^{++}_{x_3 a}\Delta h^{+}_{x_3} + N^{--}_{x_3 a}\Delta h^{-}_{x_3}\right] -$$

$$\Delta t\left[\left(\frac{\rho_P Q_a}{\rho_a \phi \Delta \bar{V}}\right)^{t}_{i,k} - S^{t}_{a_{i,k}} \frac{\{(\phi\Delta\bar{V})^{t}_{i,k} - (\phi\Delta\bar{V})^{t-1}_{i,k}\}}{(\phi\Delta\bar{V})^{t}_{i,k}\Delta t_0}\right.$$

$$\left.\left(\frac{S_a}{\rho_a}\right)^{t}_{i,k} \frac{(\rho^{t}_{a_{i,k}} - \rho^{t-1}_{a_{i,k}})}{\Delta t_0}\right] , \tag{46}$$

where $\Delta S^{+}_{a_{i,k}} = S^{t+1}_{a_{i,k}} - S^{t}_{a_{i,k}}$.

If equations (42) and (43) are used to obtain the air and water pressures at time t+1, the finite difference form of the Air Saturation equation (27) in two dimensions is

$$\Delta S^{+}_{a_{i,k}} = g\Delta t \left[N^{+}_{x_1 a} \psi^{t+1}_{a_{i+1,k}} + N^{-}_{x_1 a} \psi^{t+1}_{a_{i-1,k}} + N^{+}_{x_3 a} \psi^{t+1}_{a_{i,k+1}} + N^{-}_{x_3 a} \psi^{t+1}_{a_{i,k-1}} - (N^{+}_{x_1 a} + N^{-}_{x_1 a} + N^{+}_{x_3 a} + N^{-}_{x_3 a}) \psi^{t+1}_{a_{i,k}} + N^{++}_{x_1 a} \Delta h^{+}_{x_1} + N^{--}_{x_1 a} \Delta h^{-}_{x_1} + N^{++}_{x_3 a} \Delta h^{+}_{x_3} + N^{--}_{x_3 a} \Delta h^{-}_{x_3} \right] -$$

$$\Delta t \left[\left(\frac{\rho_P Q_a}{\rho_a \phi \Delta \bar{V}} \right)^{t}_{i,k} - S^{t}_{a_{i,k}} \frac{\{(\phi \Delta \bar{V})^{t}_{i,k} - (\phi \Delta \bar{V})^{t-1}_{i,k}\}}{(\phi \Delta \bar{V})^{t}_{i,k} \Delta t_0} - \frac{S^{t}_{a_{i,k}} (\psi^{t+1}_{a_{i,k}} - \psi^{t}_{a_{i,k}})}{(1033.3 + \psi^{t}_{a_{i,k}})} \right] . \qquad (47)$$

The new air saturation, S_a, at time t+1 is, therefore,

$$S^{t+1}_{a_{i,k}} = \Delta S^{+}_{a_{i,k}} + S^{t}_{a_{i,k}} \qquad (48)$$

The saturation error at each time step is computed as

$$(S_{error})_{i,k} = 1 - (S^{t+1}_{w_{i,k}} + S^{t+1}_{a_{i,k}}) \quad . \qquad (49)$$

If the right hand side of equation (49) does not converge to unity within the tolerance level, an iteration of the flow equations may be necessary. The original values of the flow coefficients, $N^+_{x_1 w}$, $N^+_{x_1 a}$, etc. need to be updated at each iteration.

Finite Difference Form of Two-Dimensional Dispersion Equation

The numerical technique used in this study to solve the dispersion equation is the Method of Characteristics (MOC) introduced by Garder et al. (1964). As discussed in Chapter II, the MOC does not introduce numerical dispersion and the MOC approach can be extended to two or three dimensions. The succeeding discussion follows the development by Garder et al. (1964).

In the MOC, instead of solving equation (29) directly, characteristic equations are determined and solved. The second order terms of equation (29) are regarded as given functions of x_1, x_2, x_3, and t, and equation (29) treated as a first order equation. Such an equation will then have four characteristic curves which are the solutions to the following ordinary differential equations:

$$\frac{dx_1}{dt} = V_1, \tag{50a}$$

$$\frac{dx_2}{dt} = V_2, \tag{50b}$$

$$\frac{dx_3}{dt} = V_3, \tag{50c}$$

and

$$\frac{dC}{dt} = \frac{1}{(\phi S_w \Delta A_i)} \frac{\partial}{\partial x_i} \left[D^*_{ij} \frac{\partial C}{\partial x_j} \phi S_w \Delta A_i \right] . \tag{50d}$$

A fifth characteristic curve could be written for the production term, $(C_p - C\rho_p/\rho_w)\, Q_w/\Delta\overline{V}$. However, the production term will be treated as a boundary condition of the moving points described below.

In addition to the usual division of the flow region into a grid system, a set of moving points is introduced into the numerical solution. Initially, the moving points are uniformly distributed throughout the grid system with a given concentration. At each time interval, the moving points in a two-dimensional system are relocated using a finite difference form of equations (50a) and (50c):

$$x_{1_\ell}^{t+1} = x_{1_\ell}^{t} + \Delta t\, V_{1_\ell}^{t+1} , \tag{51a}$$

and

$$x_{3_\ell}^{t+1} = x_{3_\ell}^{t} + \Delta t\, V_{3_\ell}^{t+1} \tag{51b}$$

where

$t + 1$ = new time level,

t = old time level,

Δt = time increment,

x_{1_ℓ} and x_{3_ℓ} = coordinates of the ℓ-th moving point in the x_1 - and x_3 - directions, and

V_{1_ℓ} and V_{3_ℓ} = velocities of the ℓ-th moving point in the x_1 - and x_3 - directions.

When all the moving points have been relocated, each grid in the grid system is temporarily assigned a concentration, $C_{i,k}^{t+\Delta}$, which is the average of the concentrations $C_\ell^{t+\Delta}$ of all the moving points lying inside the grid at time $t + 1$. Next, the change in concentration due to dispersion, $\Delta C_{i,k}$, is calculated using an explicit, centered-in-space

finite difference approximation to equation (50d). This equation is developed in detail in Appendix D. The two-dimensional form is

$$\Delta C_{i,k} = E^{+}_{x_1x_1}\left(C^{t+\Delta}_{i+1,k} - C^{t+\Delta}_{i,k}\right) - E^{-}_{x_1x_1}\left(C^{t+\Delta}_{i,k} - C^{t+\Delta}_{i-1,k}\right) +$$

$$E^{+}_{x_3x_3}\left(C^{t+\Delta}_{i,k+1} - C^{t+\Delta}_{i,k}\right) - E^{-}_{x_3x_3}\left(C^{t+\Delta}_{i,k} - C^{t+\Delta}_{i,k-1}\right) +$$

$$G^{+}_{x_1x_3}\left(C^{t+\Delta}_{i,k+1} + C^{t+\Delta}_{i+1,k+1} - C^{t+\Delta}_{i,k-1} - C^{t+\Delta}_{i+1,k-1}\right) - G^{-}_{x_1x_3}\left(C^{t+\Delta}_{i-1,k+1}\right.$$

$$\left. + C^{t+\Delta}_{i,k+1} - C^{t+\Delta}_{i,k-1} - C^{t+\Delta}_{i-1,k-1}\right) + G^{+}_{x_3x_1}\left(C^{t+\Delta}_{i+1,k+1} + C^{t+\Delta}_{i+1,k} -\right.$$

$$\left. C^{t+\Delta}_{i-1,k+1} - C^{t+\Delta}_{i-1,k}\right) - G^{-}_{x_3x_1}\left(C^{t+\Delta}_{i+1,k} + C^{t+\Delta}_{i+1,k-1} - C^{t+\Delta}_{i-1,k} -\right.$$

$$\left. C^{t+\Delta}_{i-1,k-1}\right) \quad . \tag{52}$$

Each moving point is then assigned a concentration according to

$$C^{t+\Delta t}_{\ell} = C^{t+\Delta}_{\ell} + \Delta C_{i,k} \quad . \tag{53}$$

To complete the step from time t to t+1, the concentration of the stationary grid points are calculated according to

$$C^{t+1}_{i,k} = C^{t+\Delta}_{i,k} + \Delta C_{i,k} \tag{54}$$

Finite Difference Form of Velocity Equation

In the method of characteristics described above, a determination of seepage velocity is necessary for relocating the moving points at each time step. The water pressures, ψ_w, obtained from either equation (40) or equation (43) are assigned to the centers of each grid. Using these pressures (ψ_w) and equations (30) and (31), the seepage velocity at the interface of two grids may be calculated. Referring to Figure 4, a finite difference form of the horizontal seepage velocity at (i+1/2,k) can be written as

$$(V_1)^{t+1}_{i+1/2,k} = -\left(\frac{k_{x_1} k_{rw} \rho_w g}{\mu_w \phi S_w}\right)_{i+1/2,k} \left[\frac{\left(\psi_{w_{i+1,k}} - \psi_{w_{i,k}}\right)}{\Delta x_1} + \frac{\left(h_{i+1,k} - h_{i,k}\right)}{\Delta x_1}\right], \tag{55}$$

where all the symbols are as previously defined. The vertical seepage velocity at (i, k+1/2) may be calculated as

$$(V_3)^{t+1}_{i,k+1/2} = -\left(\frac{k_{x_3} k_{rw} \rho_w g}{\mu_w \phi S_w}\right)_{i,k+1/2} \left[\frac{\left(\psi_{w_{i,k+1}} - \psi_{w_{i,k}}\right)}{\Delta x_3} + \frac{\left(h_{i,k+1} - h_{i,k}\right)}{\Delta x_3}\right]. \tag{56}$$

The horizontal seepage velocity at (i-1/2,k) is

$$(V_1)^{t+1}_{i-1/2,k} = -\left(\frac{k_{x_1} k_{rw} \rho_w g}{\mu_w \phi S_w}\right)_{i-1/2,k} \left[\frac{\left(\psi_{w_{i,k}} - \psi_{w_{i-1,k}}\right)}{\Delta x_1} + \frac{\left(h_{i,k} - h_{i-1,k}\right)}{\Delta x_1}\right] \tag{57}$$

The vertical seepage velocity at (i,k-1/2) is

$$(V_3)^{t+1}_{i,k-1/2} = -\left(\frac{k_{x_3} k_{rw} \rho_w g}{\mu_w \phi S_w}\right)_{i,k-1/2} \left[\frac{\left(\psi_{w_{i,k}} - \psi_{w_{i,k-1}}\right)}{\Delta x_3} + \frac{\left(h_{i,k} - h_{i,k-1}\right)}{\Delta x_3}\right] . \quad (58)$$

Using equations (55) through (58), the seepage velocities of moving points are obtained using a three-way linear interpolation scheme as described in the following paragraph.

Let a moving point at any time be positioned on the lower right hand corner of grid (i,k) (Figure 5). The seepage velocity, V'_{1_ℓ}, is obtained by linear interpolation between the interface velocities, $(V_1)_{i-1/2,k}$ and $(V_1)_{i-1/2,k+1}$,

$$V'_{1_\ell} = (V_1)_{i-1/2,k} - \frac{x_{3_\ell} - (x_3)_{i-1/2,k}}{\Delta x_3}\left[(V_1)_{i-1/2,k} - (V_1)_{i-1/2,k+1}\right]. \quad (59)$$

The seepage velocity, V''_{1_ℓ}, is obtained by linear interpolation between the interface velocities, $(V_1)_{i+1/2,k}$ and $(V_1)_{i+1/2,k+1}$,

$$V''_{1_\ell} = (V_1)_{i+1/2,k} - \frac{x_{3_\ell} - (x_3)_{i+1/2,k}}{\Delta x_3}\left[(V_1)_{i+1/2,k} - (V_1)_{i+1/2,k+1}\right] . \quad (60)$$

The seepage velocity, V_{1_ℓ}, of the ℓ-th moving point is then obtained by linear interpolation between V'_{1_ℓ} and V''_{1_ℓ},

$$V_{1_\ell} = V'_{1_\ell} - \frac{x_{1_\ell} - (x_1)_{i-1/2,k}}{\Delta x_1}\left(V'_{1_\ell} - V''_{1_\ell}\right) . \quad (61)$$

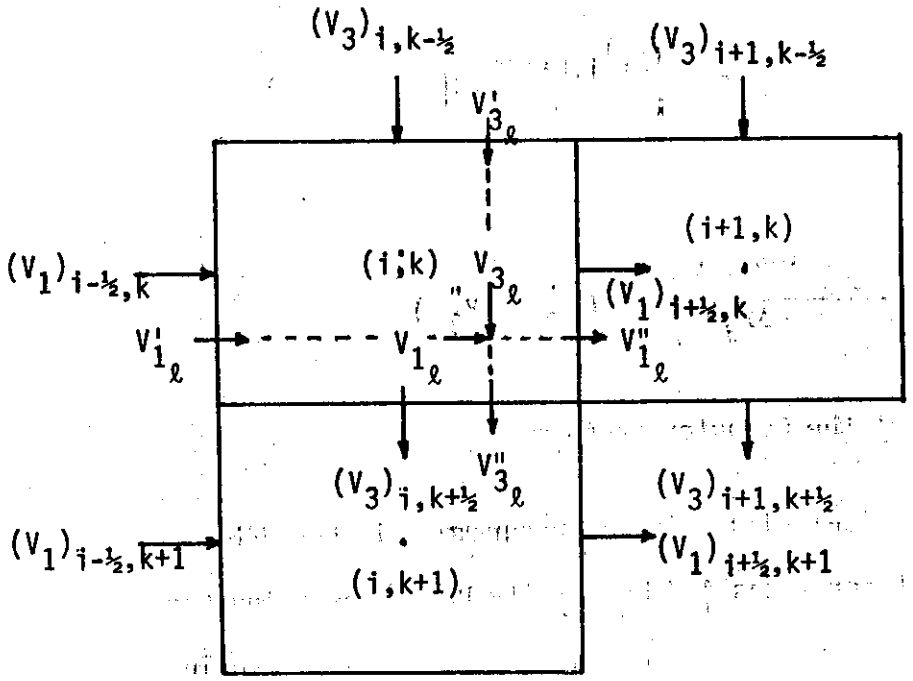

Figure 5. A three-way interpolation scheme to calculate seepage velocities of moving points.

Similarly, the seepage velocity, V_{3_ℓ}, of the ℓ-th moving point is obtained using equations (62) through (64):

$$V'_{3_\ell} = (V_3)_{i,k-1/2} - \frac{x_{1_\ell} - (x_1)_{i,k-1/2}}{\Delta x_1} \left[(V_3)_{i,k-1/2} - (V_3)_{i+1,k-1/2} \right], \tag{62}$$

$$V''_{3_\ell} = (V_3)_{i,k+1/2} - \frac{x_{1_\ell} - (x_1)_{i,k+1/2}}{\Delta x_1} \left[(V_3)_{i,k+1/2} - (V_3)_{i+1,k+1/2} \right], \tag{63}$$

and

$$V_{3_\ell} = V'_3 - \frac{x_{3_\ell} - (x_3)_{i,k-1/2}}{\Delta x_3} \left(V'_{3_\ell} - V''_{3_\ell} \right) . \tag{64}$$

Description of the Computer Program

The numerical simulator was programmed in FORTRAN IV for the AMDAHL 470 at the Texas A&M University Data Processing Center. A flow chart of the program is shown in Appendix E, and a reprint of the program used in solving the two-phase, two-dimensional infiltration and dispersion problem in a saturated-unsaturated porous medium is given in Appendix F.

The MAIN program governs the sequence of operations to be performed. Subroutine READIN reads in the physical data needed to solve the problem. It reads in the saturated permeabilities, porosity, initial densities and viscosities for both air and water, initial water and air pressure distribution, boundary conditions, and the water saturation - relative water permeability - relative air permeability - capillary pressure relationships.

Subroutine INICON sets up the number, coordinates, and concentra-

tion of each of the moving points in the two-dimensional grid system. It also reads in the relative concentration, C/C_0, of the incoming tracer. Finally, it computes the initial average grid concentration.

Subroutine INIPRT prints out all of the initial data read in by subroutines READIN and INICON. All of the two-dimensional matrices are printed out using subroutine MATROP.

Subroutine MATSOL sets up the coefficient matrix, $[A_w]$, and the right hand side column vector, $\{rhs_w\}$, for solving implicitly the water pressure vector, $\{\psi_w\}$, at time $t+\Delta t$ using subroutine BSOLV. Subroutine MATSOL, as is presently written, may take care of one or a combination of the following boundary conditions: (1) a constant water pressure boundary, (2) a constant or a variable flux boundary, (3) a no-flow boundary, and (4) a constant head reservoir boundary. Initially, MATSOL sets up the coefficient matrix, $[A_w]$, for a no-flow boundary condition around the boundary grids of the two-dimensional grid system. MATSOL then checks the boundary conditions and makes appropriate changes in $[A_w]$ and $\{rhs_w\}$. Once the water pressures, $\{\psi_w\}$, are known at time $t+\Delta t$, the air pressures, $\{\psi_a\}$, at time $t+\Delta t$, are calculated using the definition of capillary pressure. If the air pressures, instead of the water pressures, are solved implicitly, a procedure analogous to the one described above is followed. The air pressures are solved implicitly using BSOLV and the water pressures are obtained using capillary pressure definition. With the updated water and air pressures, water and air saturation changes are calculated explicitly. New water and air saturations, S_w and S_a, at time $t+\Delta t$ and the saturation error, $1 - (S_w + S_a)$, are then computed.

If the saturation error is too large, more than one iteration in a time step may be necessary and the entire set of operations described under MATSOL is repeated. Also, during the computation of new saturations, the magnitude of maximum saturation change at any grid point is obtained. If this saturation change is too large, the time step size is appropriately decreased and the necessary calculations are repeated. In practice, the rules for selecting the original time step size are such that this flow path is infrequently taken. In selecting the time step size at the beginning of calculations, a maximum change in water saturation of 0.05 is allowed during any one time step.

Subroutine SLPROP is used to update the water saturation-capillary pressure and water saturation-relative permeabilities relationships.

Subroutine BSOLV uses a Gaussian elimination technique to solve the matrix given by equations (40) or (42). The two-dimensional, two-phase flow equations when written out result in a coefficient matrix which is a banded matrix with five diagonals. Thurnau (1963) developed an algorithm called BANDSOLVE to solve such matrices. Computer storage is not necessary for the matrix elements above and below the band. Thus, having a minimum band width is desirable. The grids are numbered along the shorter dimension of the two-dimensional grid system to reduce the size of the band width.

Subroutine VELOCY calculates the velocities at each grid interface by use of equations (55) through (58). This subroutine also calculates the longitudinal and lateral dispersion coefficients using a Peclet number versus dispersion coefficient relationship. With values for

the dispersion coefficients and velocity components, equation (37) is used to calculate the components of the dispersion tensor.

Subroutine MOVPT uses a three-way linear interpolation scheme as given by equations (59) through (64) to obtain the velocity components of each moving point. Each moving point is then moved to a new location using equations (51a) and (51b). A section of this subroutine determines which of the moving points has moved out of the model. These points are tagged and introduced at an inflow boundary with the appropriate boundary condition. The coordinates of these reintroduced points are assigned randomly within the inflow boundary using subroutine RANDU. RANDU generates random numbers having a uniform distribution and ranging from 0 to 1. An attempt is made to keep a minimum number of moving points in all grids at all times. If, at any time, the number of moving points in a grid drops below a specified minimum number, new points are introduced in that grid to bring it to a minimum number. The coordinates of these new points depend on the grid or grids from which the fluid is emanating, and their concentrations are based on a three-way interpolation scheme similar to that used for velocity. After each point has been moved to a new location, the average grid concentration is calculated by arithmetically averaging the concentrations of the moving points located in that grid.

Subroutine DISP uses equation (52) and the average grid concentrations from subroutine MOVPT to determine the change in concentration due to dispersion. The average grid concentration and the concentration of each moving point are then corrected for this dispersion.

Subroutine MATBAL then calculates a mass balance for both the air and water phase and the tracer. Both cumulative and differential mass balance errors are calculated.

To conclude a time step, the density of water is updated for changes in concentration. A test for printout is made. Subroutine OUTPUT prints out the results using subroutine MATROP. A set of plot routines, PLOT1, PLOT2, PLOT3, and PLOT4 are used to plot a moving points' concentration map. The program, at this point, has gone through one time step. The total simulation time is now incremented and the entire set of operations repeated until a maximum number of time steps or a finish time has been exceeded.

CHAPTER V

RESULTS AND DISCUSSION

The accuracy of the Numerical Model was tested on several problems for which exact or analytical solutions were available. The two-phase fluid flow and dispersion segments of the computer program were tested independently with various boundary conditions. Also, a two-dimensional infiltration problem with simultaneous movement of water and salt in a saturated-unsaturated porous medium was solved using the numerical simulator.

Two-Phase Fluid Flow Models

Constant Pressure Boundary

The accuracy of the Two-Phase Numerical Simulator was checked by solving an infiltration problem using Yolo Light clay. Other simulation results using this particular soil are available. For example, Philip (1969) obtained an analytical solution using Yolo Light clay. The numerical results from this simulator could, therefore be compared with Philip's analytical solution.

A schematic of this particular infiltration problem is shown in Figure 6. Data used for this numerical simulation were: Δx_1 = 10 cm, Δx_3 = 10 cm, depth of model, ℓ_3 = 120 cm, length of model, ℓ_1 = 30 cm, number of rows, NR = 12 and number of columns, NC = 3. The total simulation time was 53.3 hours. The upper boundary condition was that of infiltration into the center column from a saturated surface layer of zero thickness and zero water pressure

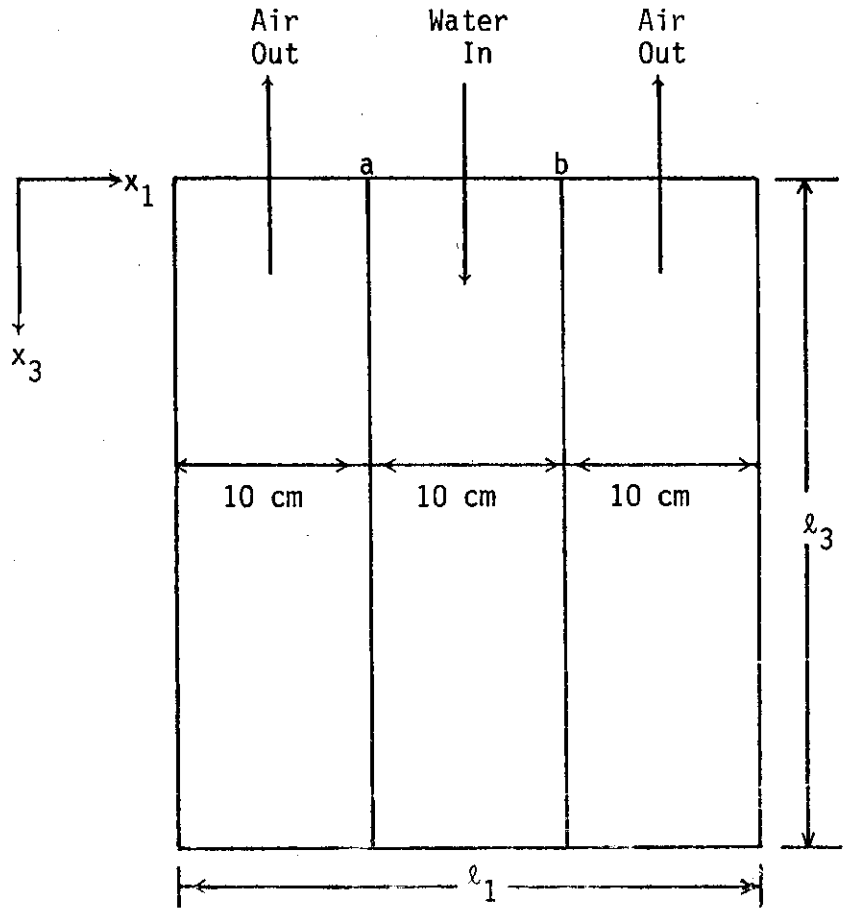

Figure 6. Schematic sketch of constant pressure boundary infiltration problem.

head. Air was allowed to escape through the upper boundary of the two adjacent columns. Mathematically, the boundary conditions were:

$$\frac{\partial \psi_w}{\partial x_3} = 0, \ \psi_a = \psi_{atm} = 0; \qquad x_3 = 0, \ 0 \leq x_1 < a, \ t \geq 0$$

$$x_3 = 0, \ b < x_1 \leq \ell_1, \ t \geq 0$$

$$\psi_w = 0, \ \frac{\partial \psi_a}{\partial x_3} = 0; \qquad x_3 = 0, \ a \leq x_1 \leq b, \ t \geq 0$$

$$\frac{\partial \psi_w}{\partial x_1} = 0, \ \frac{\partial \psi_a}{\partial x_1} = 0; \qquad x_1 = 0, \ 0 \leq x_3 \leq \ell_3, \ t \geq 0$$

$$x_1 = \ell_1, \ 0 \leq x_3 \leq \ell_3, \ t \geq 0$$

$$\frac{\partial \psi_w}{\partial x_3} = 0, \quad \frac{\partial \psi_a}{\partial x_3} = 0; \qquad 0 \leq x_1 \leq \ell_1, \; x_3 = \ell_3, \; t \geq 0. \tag{65}$$

The initial condition was that of a uniform water saturation of 0.48. This corresponds to a uniform water pressure potential of -660 cm of water.

Although this infiltration problem was being solved using two-dimensional and two-phase (air-water) flow equations, the resulting infiltration rates and water saturation profiles were not expected to deviate significantly from those using one-dimensional and one-phase (water) flow equations. Air was allowed to escape at all times. The effect of air on infiltration rates would, therefore, be minimal. Water was infiltrating into the center column and although lateral movement of water was allowed within the system, the resulting saturation profiles in the center column were not expected to be significantly different from those using one-dimensional flow. Therefore, with the assumed boundary conditions and physics of the problem, the two-dimensional, two-phase flow equations collapse into one-dimensional, one-phase flow equations. The advantage of going through this exercise was that the results from this infiltration simulation using the two-dimensional, two-phase flow simulator could be compared with Philip's (1969) analytical solution using one-dimensional, one-phase flow equations. A run with this infiltration problem would, therefore, be an indicator of the accuracy of the two-phase simulator.

Capillary pressure head and hydraulic conductivity as functions of volumetric water content for Yolo Light clay were presented by

Hiler and Bhuiyan (1971). Those relationships were used to determine the capillary pressure head, relative water permeability and relative air permeability of Yolo Light clay as functions of water saturation. The relative permeabilities as functions of water saturation were determined from the following relationships (Brooks and Corey, 1966):

$$k_{rw} = S_e^2 \frac{\int_0^{S_w} dS_w/\psi_c^2}{\int_0^1 dS_w/\psi_c^2}, \tag{66a}$$

and

$$k_{ra} = (1 - S_e)^2 \frac{\int_{S_w}^1 dS_w/\psi_c^2}{\int_0^1 dS_w/\psi_c^2}. \tag{66b}$$

where S_e = effective saturation = $(S_w - S_{wr})/(1 - S_{wr})$,

S_w = water saturation,

ψ_c = capillary pressure head (L),

k_{rw} = relative permeability for the wetting phase or water, and

k_{ra} = relative permeability for the nonwetting phase or air,

S_{wr} = residual water saturation. S_{wr} is the value of S_w approached astmptotically as the capillary pressure is reduced. For $S_w < S_{wr}$, the wetting phase may be assumed to be discontinuous and the

flow to cease.

Evaluation of the relative permeabilities, k_{rw} and k_{ra}, required knowledge of the capillary pressure head-water saturation function $\psi_c(S_w)$ and its asymptote S_{wr}. The value of S_{wr} was obtained by a trial and error procedure. The effective saturation, S_e was plotted against the capillary pressure head, ψ_c, on log-log paper for several trial values of S_{wr}. The plot that resulted in a straight line yielded the correct value of S_{wr}. For Yolo Light clay, the value of S_{wr} was found to be equal to 0.125. The integrals in equations (66a) and (66b) were obtained graphically. A plot was made of S_w - $(1/\psi_c^2)$ relationship. Using the trapezoidal rule, the integrals were then evaluated as the area under the curves.

The resulting functional relationships for Yolo Light clay are shown in Figures 7 and 8. These data were introduced into the numerical model in tabular form. A tabular interpolation scheme was used in the model to find values of P_c, k_{rw}, and k_{ra} corresponding to specific values of saturation. Additional data needed for this problem were: $k_s = 1.085 \times 10^{-10}$ cm^2, and $\phi = 0.50$.

Figure 9 shows a plot of the predicted saturation profiles at various times in the center column. As expected, the saturation values obtained using the two-phase (air-water) flow model were identical with those obtained with a one-phase (water) flow model. Infiltration rates and cumulative infiltration amounts were also identical for the two models. This was expected since air was allowed to escape upwards from the two-phase model at all times. Thus, air pressures were never large enough in the two-phase model to reduce infiltration rates below those of the one-phase flow model.

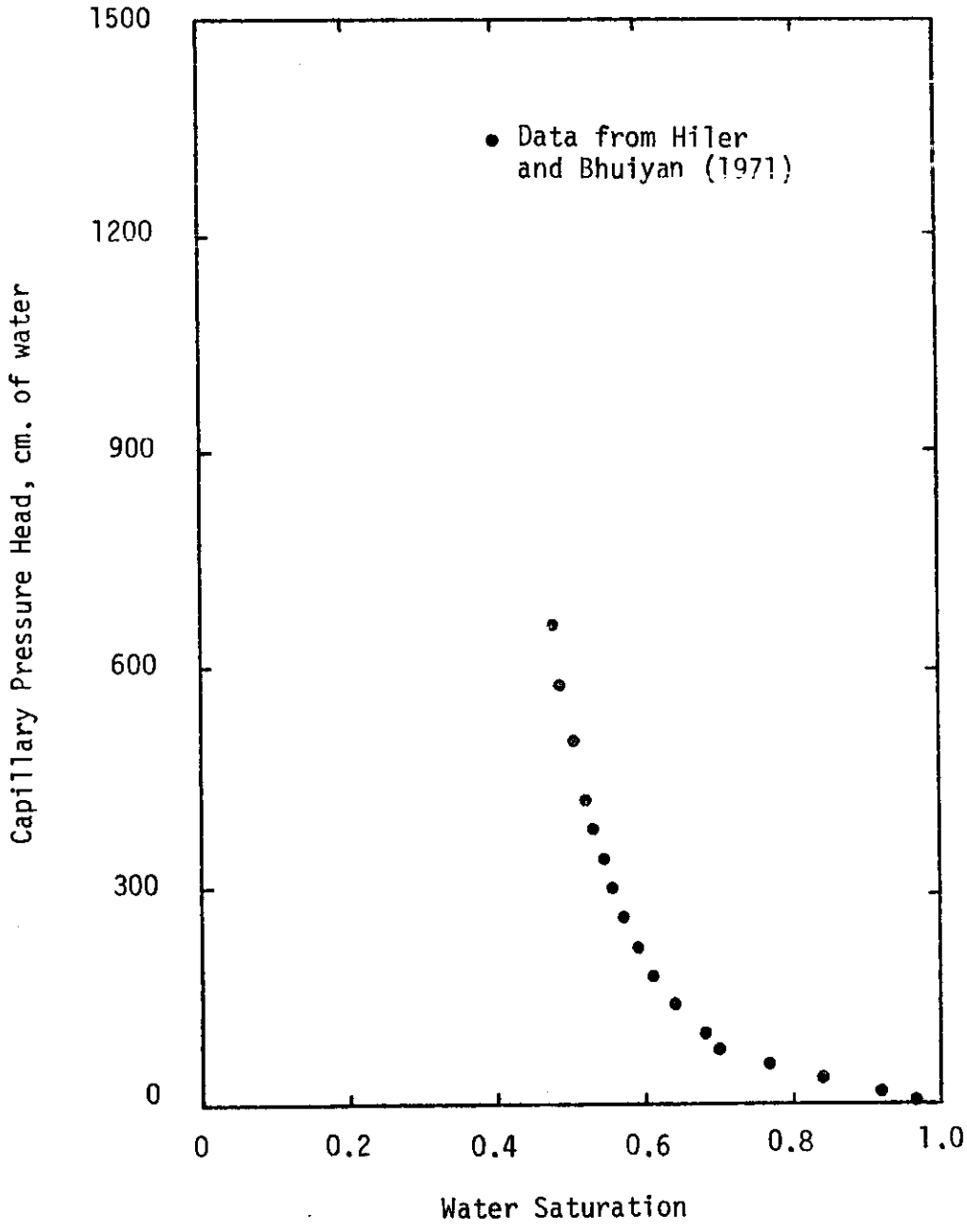

Figure 7. Capillary pressure head as a function of water saturation for Yolo Light clay.

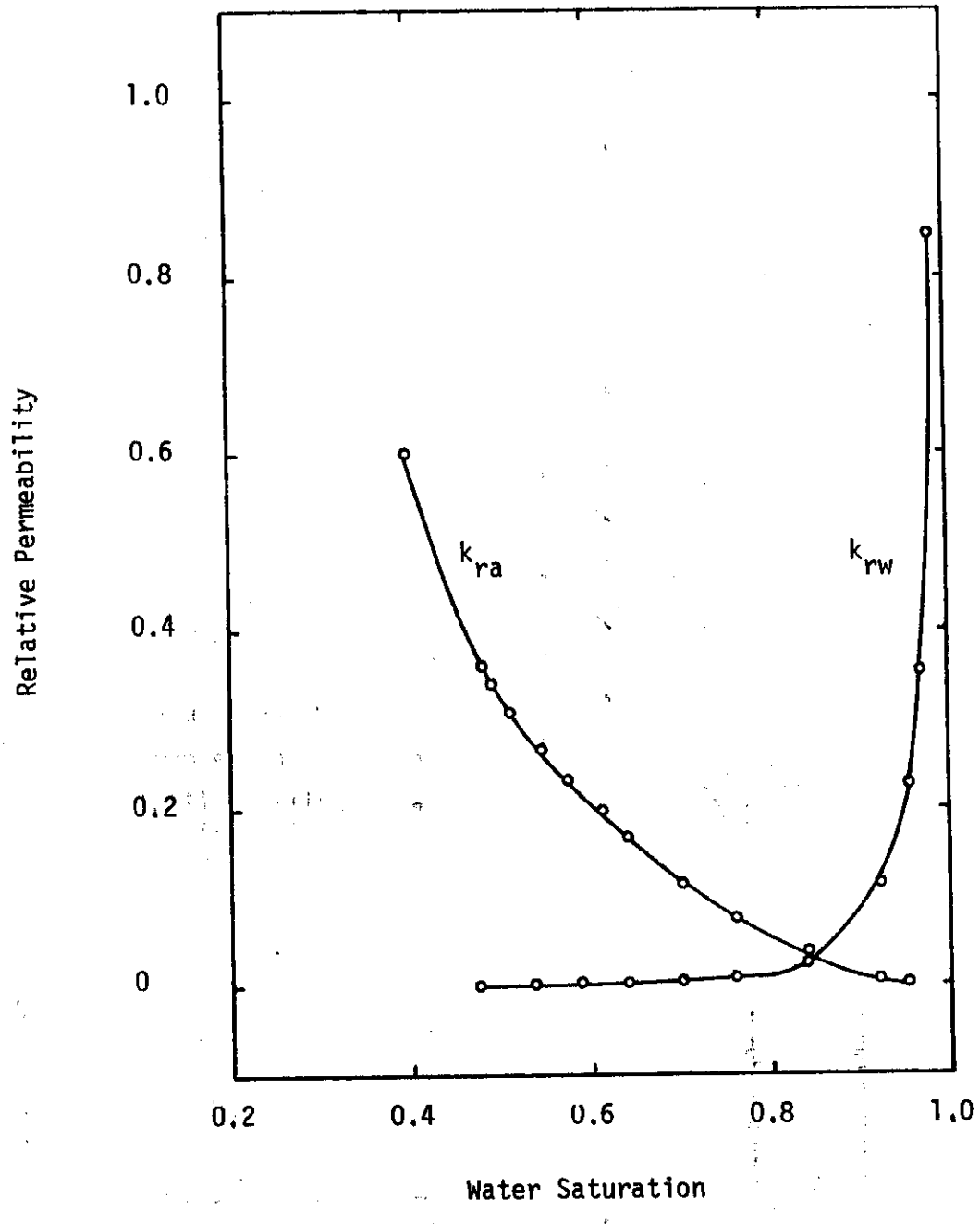

Figure 8. Relative Permeability as a function of water saturation for Yolo Light clay.

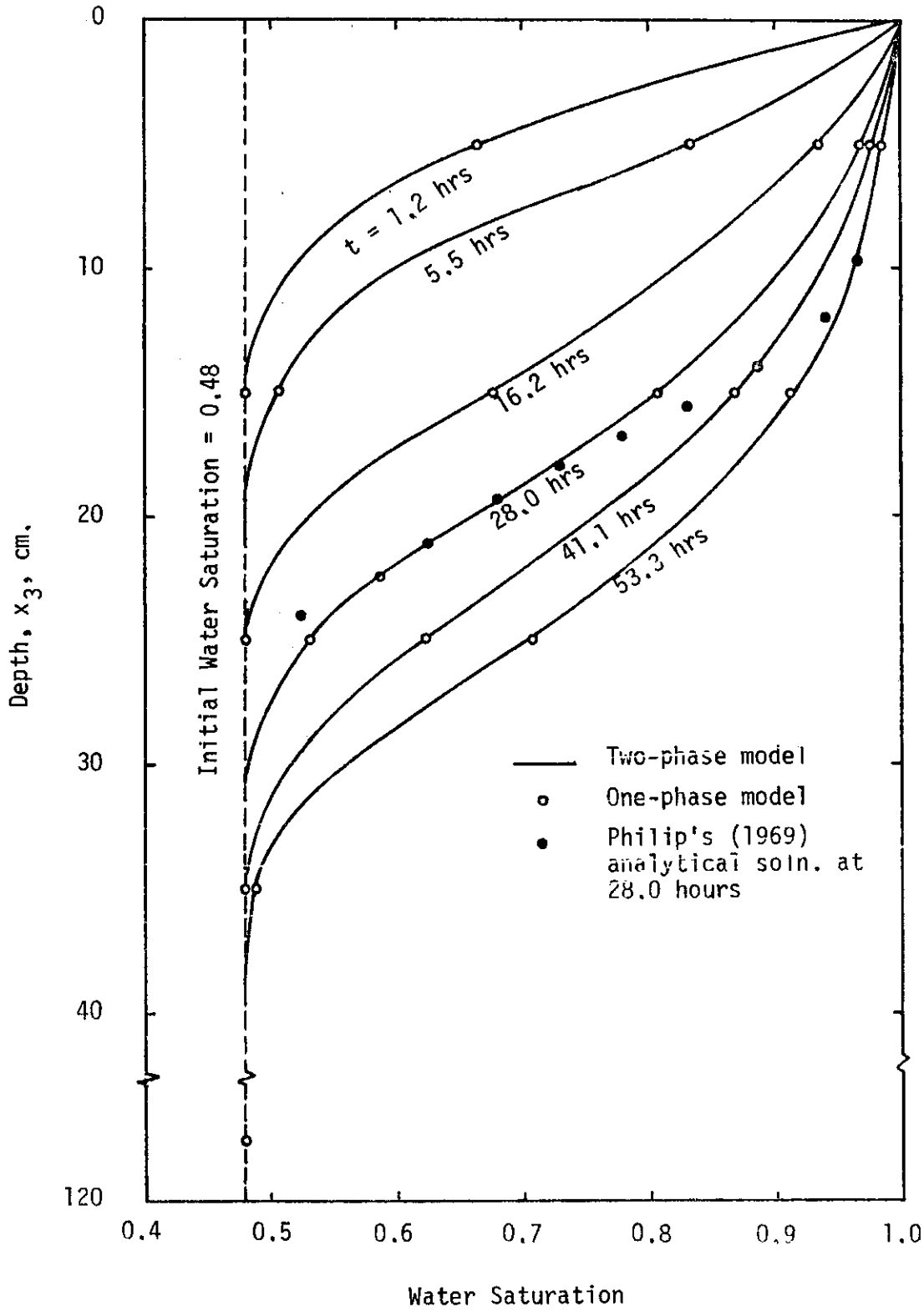

Figure 9. Water saturation profiles for vertical infiltration into Yolo Light clay with Δx_3 = 10 cm.

An analytical solution for one-phase infiltration from a surface layer of infinitesimal thickness was developed by Philip (1969), and a plot of Philip's solution at approximately 28 hours is shown in Figure 9. Close agreement between Philip's solution and the two-phase model was expected since the upper boundary condition used by Philip was identical with that on the center column of the numerical model. Agreement was good at large depths but deviated at shallow depths. The analytical solution of Philip allowed more saturation to occur in grids near the surface than was allowed by the numerical two-phase model.

Since the numerical results obtained using one-phase and two-phase flow models were identical, the error in the saturation profiles at 28 hours was presumed to be the result of using large spatial dimensions in the x_3-direction. To check this hypothesis, a run was made using Δx_3 and Δx_1 equal to 2 cm. The one-phase flow model was employed and the following functional relationships were used for capillary pressure head and relative water permeability as functions of water saturation for Yolo Light clay:

$$S_e = \left(\frac{S_w - S_{wr}}{1 - S_{wr}}\right) = \left(\frac{\psi_b}{\psi_c}\right)^{\lambda}, \quad \psi_c > \psi_b$$

$$= 1, \quad \psi_c \leq \psi_b \tag{67a}$$

and

$$k_{rw} = \left(\frac{\psi_b}{\psi_c}\right)^{\eta}, \quad \psi_c > \psi_b$$

$$= 1, \quad \psi_c \leq \psi_b \tag{67b}$$

where ψ_b = bubbling pressure = 16.5 cm of water for Yolo Light clay,

λ = pore-size distribution index = 0.244,

$\eta = 2 + 3\lambda$, and

all other terms are as defined before.

The bubbling pressure corresponds closely to the smallest capillary pressure at which the air phase is continuous. The pore-size distribution index, λ, is a number representing the medium structure. These parameters were determined in the same manner as the residual water saturation, S_{wr}. The bubbling pressure, ψ_b, was determined by extrapolating, to $S_e = 1$, the linear portion of the $\psi_c - S_e$ curve on logarithmic scale. The pore-size distribution index, λ, was the slope of the $\psi_c - S_e$ plot.

Figure 10 shows a comparison of Philip's analytical solution with the one-phase flow model at 28 hours using equations (67a) and (67b) and $\Delta x_3 = 2$ cm. Agreement between the two is excellent. The use of functional relationships like equations (67a) and (67b) and the use of a smaller value of Δx_3 allowed the numerical procedure to better approximate Philip's solution. No runs were, however, made to separate the effects of using functional relationships and smaller grid dimensions. The effect of using functional relationships was believed to be minimal in yielding accurate saturation profiles. Figures 11 and 12 show plots of infiltration rates and cumulative infiltration amounts against time using one-phase and two-phase models; agreement with Philip's analytical solution was excellent.

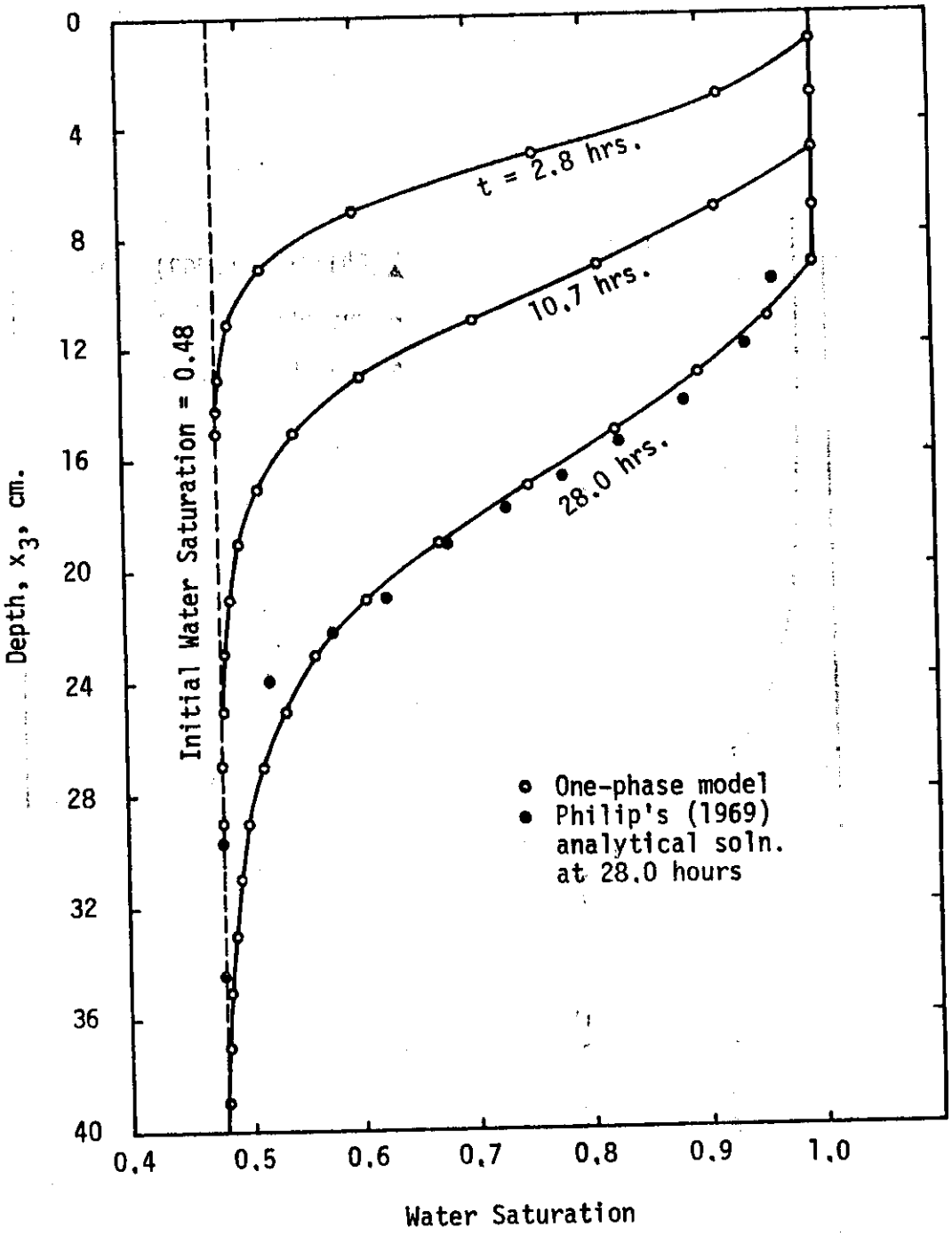

Figure 10. Water saturation profiles for vertical infiltration into Yolo Light clay with Δx_3 = 2 cm.

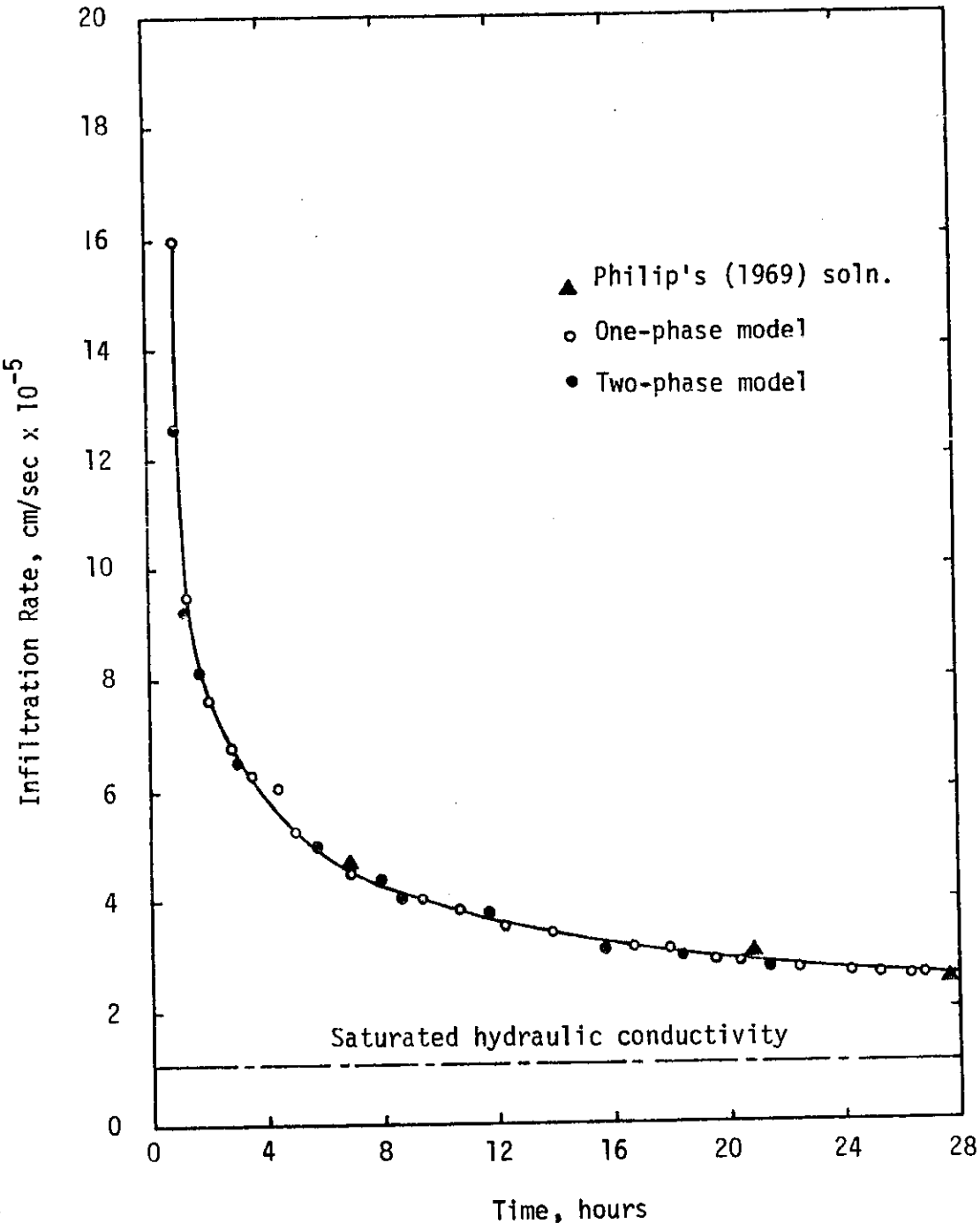

Figure 11. Infiltration rate as a function of time for Yolo Light clay.

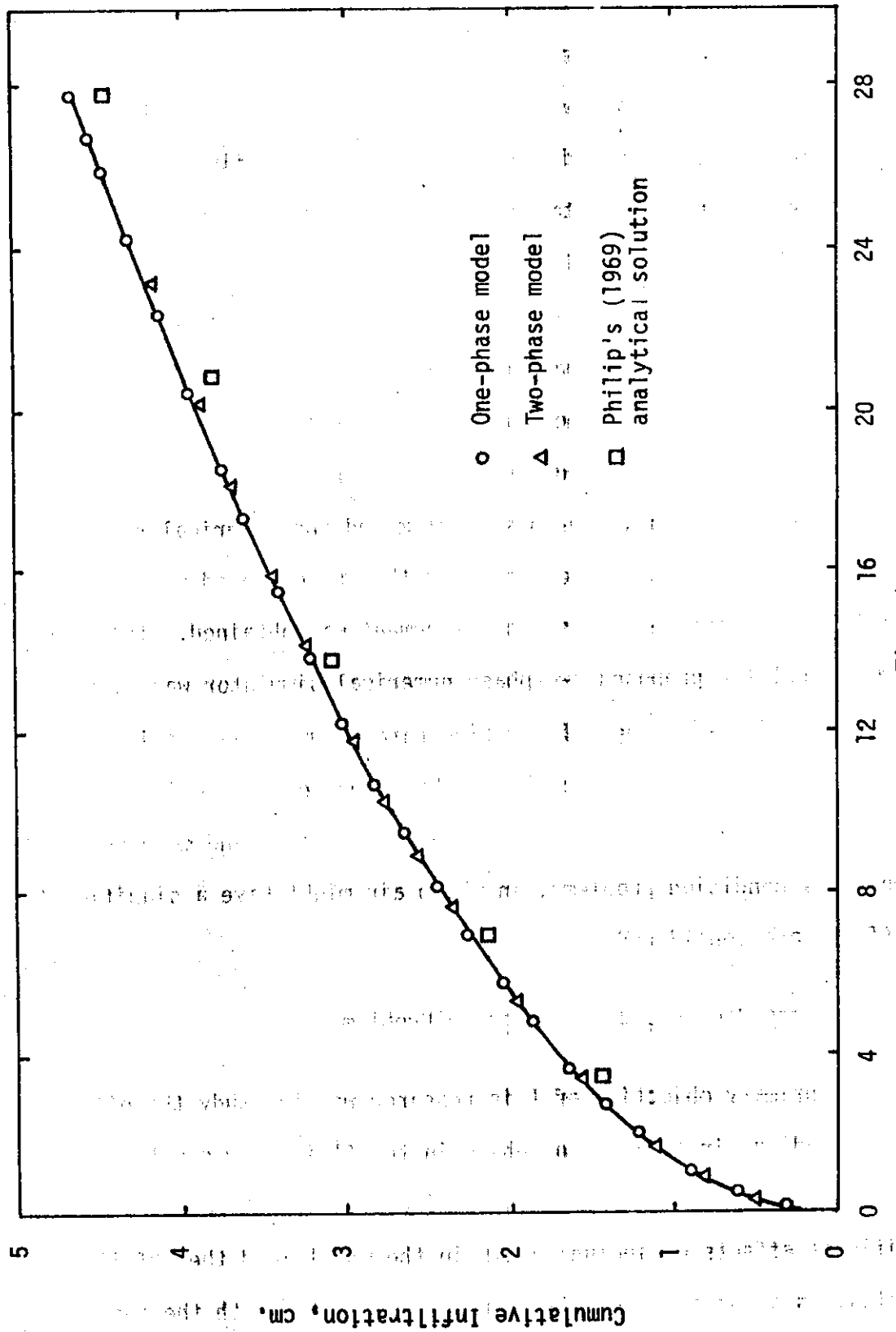

Figure 12. Cumulative infiltration amount with time for Yolo Light clay.

The constant pressure boundary problem was a first test on the accuracy of the two-phase flow numerical simulator. As expected, the results of this study indicated no significant effect of including air as a second phase in the two-phase flow equations. The numerical results obtained using one-phase and two-phase flow models were almost identical. This might lead one to conclude that inclusion of air in infiltration problems is not worth the effort. But the physics of this particular problem and the boundary conditions were such that the effect of air on the numerical results was negligible. The two-dimensional, two-phase equations collapsed into one-dimensional, one-phase system and the numerical results from this infiltration problem could then be compared with Philip's analytical solution. Excellent agreement was obtained. This indicates that the proposed two-phase numerical simulator was doing a good job of predicting infiltration rates, cumulative infiltration amounts and saturation profiles. The effect of air on infiltration is explored further in the following sub-sections and more realistic boundary condition problems, in which air might have a significant effect, are considered.

A Time-Dependent Boundary Condition Problem

A primary objective of this research was to study the effects of including air as a second phase in the fluid flow equations. The problem treated in the previous section did not indicate any significant effects of including air in the model, and the infiltration rates, as shown in Figure 11, were identical for both the one-phase

(water) and two-phase (air-water) fluid flow models. This was due to the nature of the boundary conditions considered in the previous problem where water was allowed to enter through only one of the upper boundary grids while air moved out of all the other surface grids.

To study the effects of air on infiltration, a time-dependent boundary condition using rainfall was selected. Phuc and Morel-Seytoux (1972) used an one-dimensional model to study the effects of air movement and compressibility on infiltration rates. The two-dimensional and two-phase flow model developed for this study was used to solve the rainfall-infiltration problem presented by Phuc and Morel-Seytoux (1972).

A schematic of this particular problem is shown in Figure 13. Data used for this numerical simulation were: Δx_3 = 15 cm,

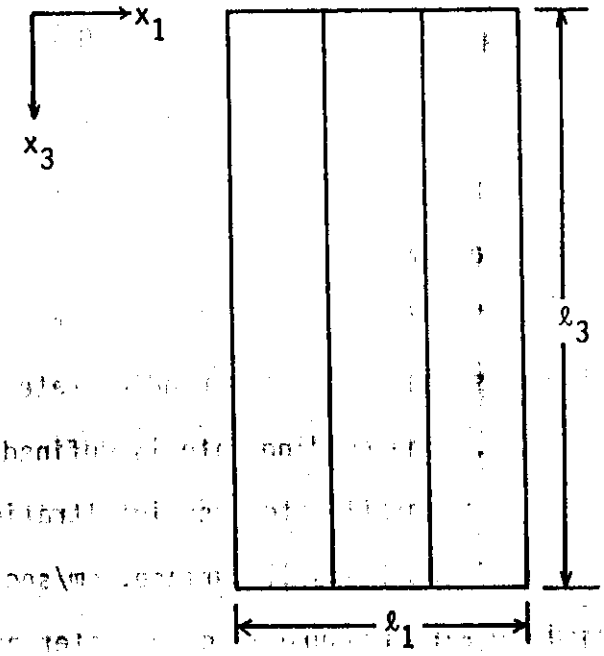

Figure 13. Schematic sketch of rainfall-infiltration problem.

$\Delta x_1 = 15$ cm, $\ell_3 = 495$ cm, $\ell_1 = 45$ cm, NR = 33, and NC = 3. The upper boundary condition, as described later, was applied across the entire upper surface boundary of the two-dimensional model so that the numerical results obtained using the two-dimensional model could be compared with those of Phuc and Morel-Seytoux's one-dimensional model. Mathematically, the boundary conditions were:

$$\left.\begin{aligned} i(t) &= q_w(t), \quad \text{if} \quad i_f(t) \geq q_w(t) \\ &= i_f(t), \quad \text{if} \quad q_w(t) > i_f(t) \end{aligned}\right\} \quad x_3 = 0,\ 0 \leq x_1 < \ell_1,\ t \geq 0,$$

$$\left.\begin{aligned} q_a(t) &= 0 \quad , \quad \text{if} \quad \psi_a(x_3 \simeq 0) < \psi_{at} \\ &> 0 \quad , \quad \text{if} \quad \psi_a(x_3 \simeq 0) \geq \psi_{at} \end{aligned}\right\} \quad x_3 = 0,\ 0 \leq x_1 \leq \ell_1,\ t \geq 0,$$

$$\frac{\partial \psi_a}{\partial x_1} = \frac{\partial \psi_w}{\partial x_1} = 0; \qquad x_1 = 0,\ 0 \leq x_3 \leq \ell_3,\ t \geq 0$$

$$x_1 = \ell_1,\ 0 \leq x_3 \leq \ell_3,\ t \geq 0,$$

$$\frac{\partial \psi_a}{\partial x_3} = \frac{\partial \psi_w}{\partial x_3} = 0; \qquad x_3 = \ell_3,\ 0 \leq x_1 \leq \ell_1,\ t \geq 0\ , \tag{68}$$

where $i(t)$ = infiltration rate at the soil surface, cm/sec,

$q_w(t)$ = water flux at the soil surface, as calculated by Darcy's law, cm/sec,

$i_f(t)$ = "feasible" infiltration rate, cm/sec, and is defined as the sum of the ponding rate and the rainfall rate. The ponding rate is defined as the excess of rainfall rate over infiltration rate.

$q_a(t)$ = flux of air at the soil surface, cm/sec,

ψ_{at} = threshold air pressure in cm of water and is equal to the sum of atmospheric pressure head, ponding

depth and the air entry pressure head. The ponding depth is equal to the ponding rate multiplied by the time over which ponding occurs. The air entry pressure head corresponds to the capillary pressure at which air phase is continuous. It is the same as bubbling pressure, ψ_b, and was assumed to be 20 cm of water for the soil used in this particular problem. ($x_3 \simeq 0$) denotes the grid immediately beneath the soil surface.

The upper boundary condition is described more in detail. A rainfall hyetograph, as shown in Figure 14, was chosen and used in combination with the upper time-dependent boundary condition. The intensities of the rainfall hyetograph were chosen so that the rainfall rate would exceed the infiltration rate and ponding would occur. The saturated hydraulic conductivity of the soil, or gravity flow, was equal to 0.0005 cm/sec. The maximum rainfall intensity was, therefore, more than twice the saturated hydraulic conductivity of the soil. If the "feasible" infiltration rate was higher than the water flux, as calculated by Darcy's law, then the rate of infiltration was equal to the Darcian flux only. If, on the other hand, the calculated value of the flux was higher than the "feasible" infiltration rate, then the infiltration rate was equal to the "feasible" infiltration rate. If water was available at the soil surface due to rainfall or ponding, the soil surface was assumed saturated and the air pressure at the surface was at atmospheric pressure. Air, initially at atmospheric pressure throughout

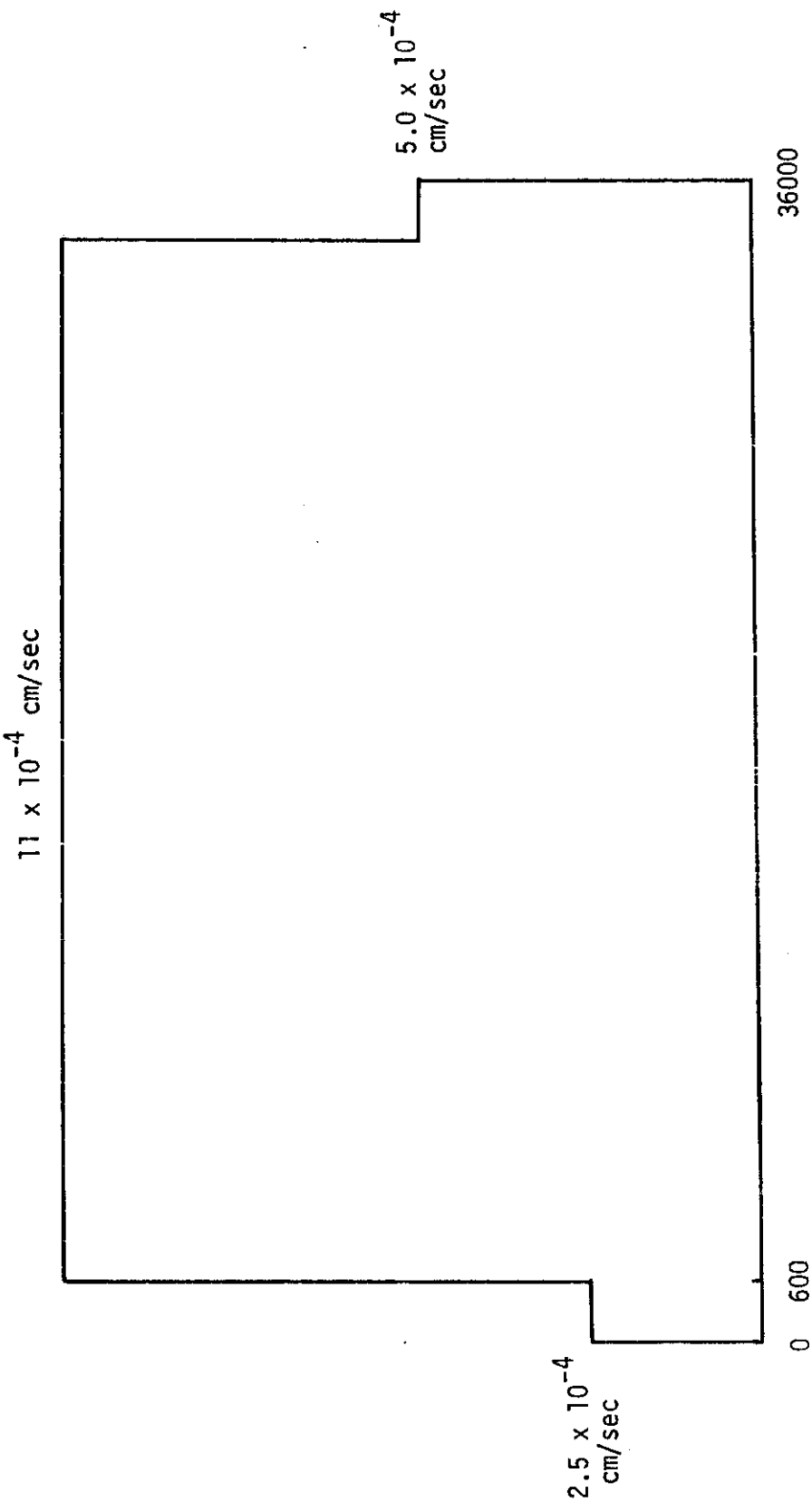

Figure 14. 10-hour rainfall hyetograph (Phuc and Morel-Seytoux, 1972).

the medium, was trapped by the advancing wetting fluid and compressed. If the air pressure in the grid immediately below the soil surface (that is, $x_3 \simeq 0$) exceeded a threshold value, a very small desaturation equal to 0.0001 of the soil surface was assumed and air was allowed to escape through the top of the column.

An initial uniform water saturation profile of $S_w = 0.30$ was assumed to exist in the soil. The numerical model described in Chapter IV was used to solve the fluid flow equations. Air pressures were obtained implicitly using equation (42) and water saturations were obtained explicitly from equation (44). Capillary pressure as a function of saturation was given by Phuc and Morel-Seytoux (1972) as follows:

$$\psi_c = 925.58\left(\frac{1}{S_w^* + 0.4} - \frac{1}{100 + 0.4}\right) + 0.838 \arctan\left(\frac{100 - S_w^*}{0.5}\right) + 11.843 \arctan\left(\frac{100 - S_w^*}{0.5}\right), \tag{69}$$

where $$S_w^* = 100\left(\frac{S_w - S_{wr}}{S_{cw} - S_{wr}}\right)$$

S_{wr} = residual water saturation = 0.02,

S_{cw} = critical water saturation = $1 - S_{ar}$, and

S_{ar} = residual air saturation = 0.088.

The relative permeabilities as functions of saturation were given by the relationships,

$$k_{rw}(S_w) = \left(\frac{S_w - S_{wr}}{S_{cw} - S_{wr}}\right)^{3.6113} \tag{70}$$

and

$$k_{ra}(S_w) = \left(\frac{S_{cw} - S_w}{S_{cw} - S_{wr}}\right). \qquad (71)$$

The time increment, Δt, was not allowed to exceed $\Delta x_3^2/2$, or, 112.5 seconds. The following data were also needed: $\phi = 0.10$, and $k_s = 5.68 \times 10^{-9}$ cm^2.

Results from the rainfall-infiltration simulation are presented in Figures 15, 16, and 17. These figures show the infiltration rate due to the rainfall hyetograph, the air pressure build-up profiles, and the water saturation profiles.

Figure 15 shows the changes in infiltration rate with time resulting from the rainfall hyetograph given in Figure 14. The infiltration rate equals the rainfall rate for the first 900 seconds compared to the 1550 seconds obtained by Phuc and Morel-Seytoux (1972). Beyond 900 seconds, ponding of water occurs at the surface. In calculating infiltration rates from numerical models, most previous investigators have encountered some difficulty because of the scatter of points about the actual infiltration curve (Hanks and Bowers, 1962). Results from Phuc and Morel-Seytoux (1972) are also shown in Figure 15, and they exhibited the widely scattered pattern discussed by Hanks and Bowers (1962). It is significant to note that the two-phase, two-dimensional model developed in this study exhibited none of this instabililty problem. On the contrary, results from the two-phase model of this study gave a very smooth curve of infiltration rate versus time.

As shown in Figure 15, results from the two-phase model differ considerably in the initial stages from those obtained by

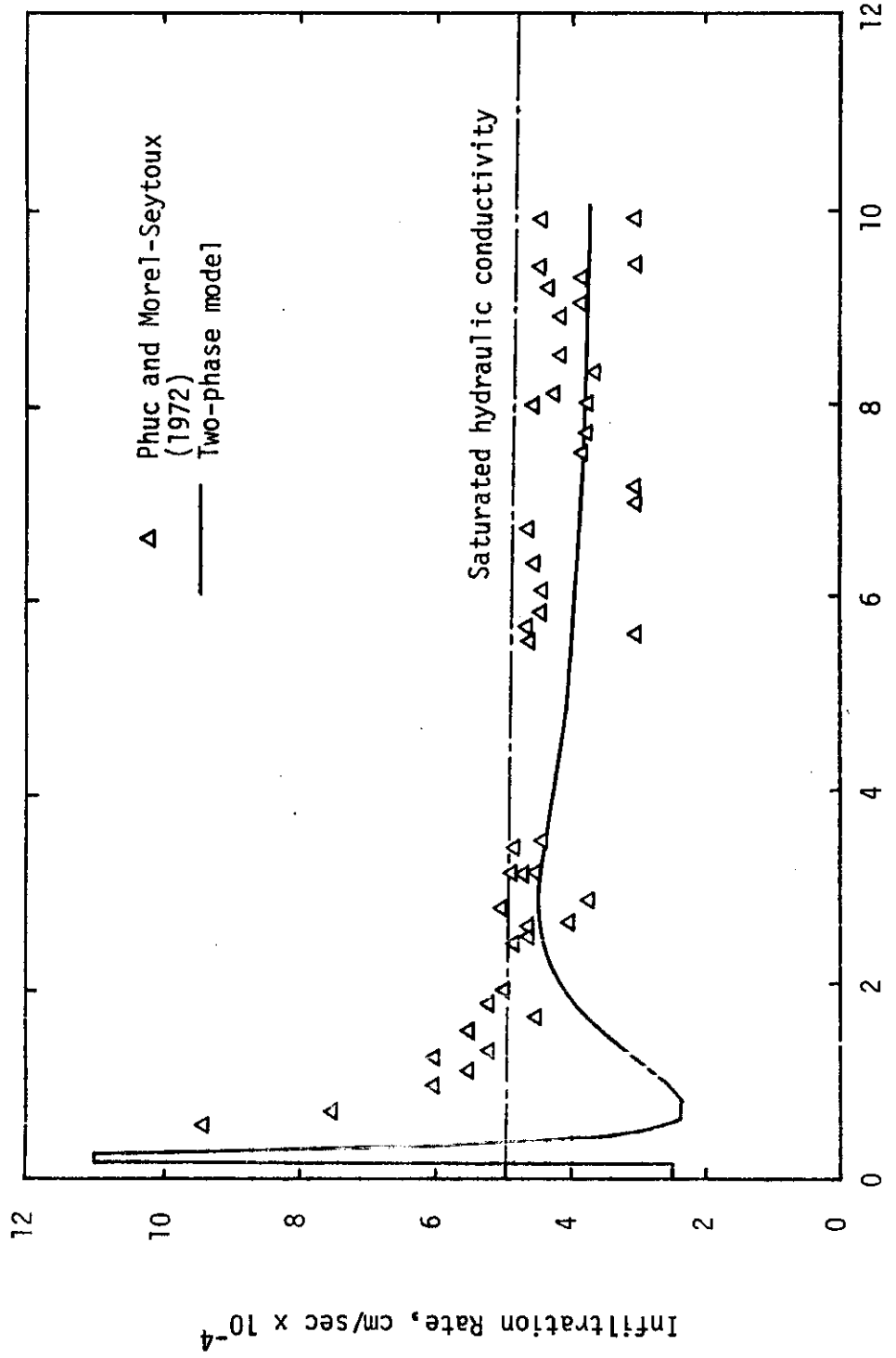

Figure 15. Comparison of infiltration rates predicted by the two-phase model used in this study with those from Phuc and Morel-Seytoux (1972).

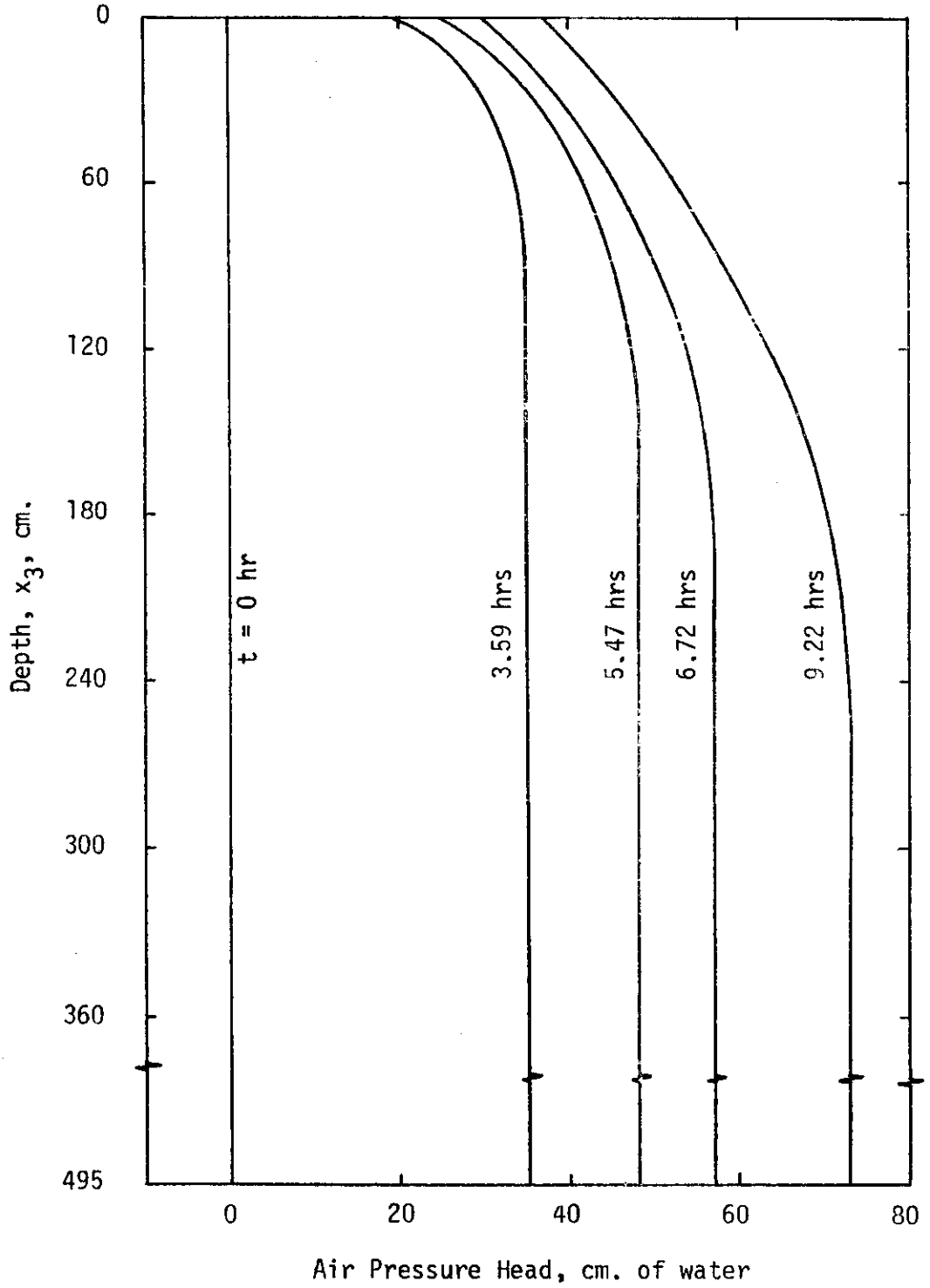

Figure 16. Air pressure profiles during infiltration into a closed bottom soil column.

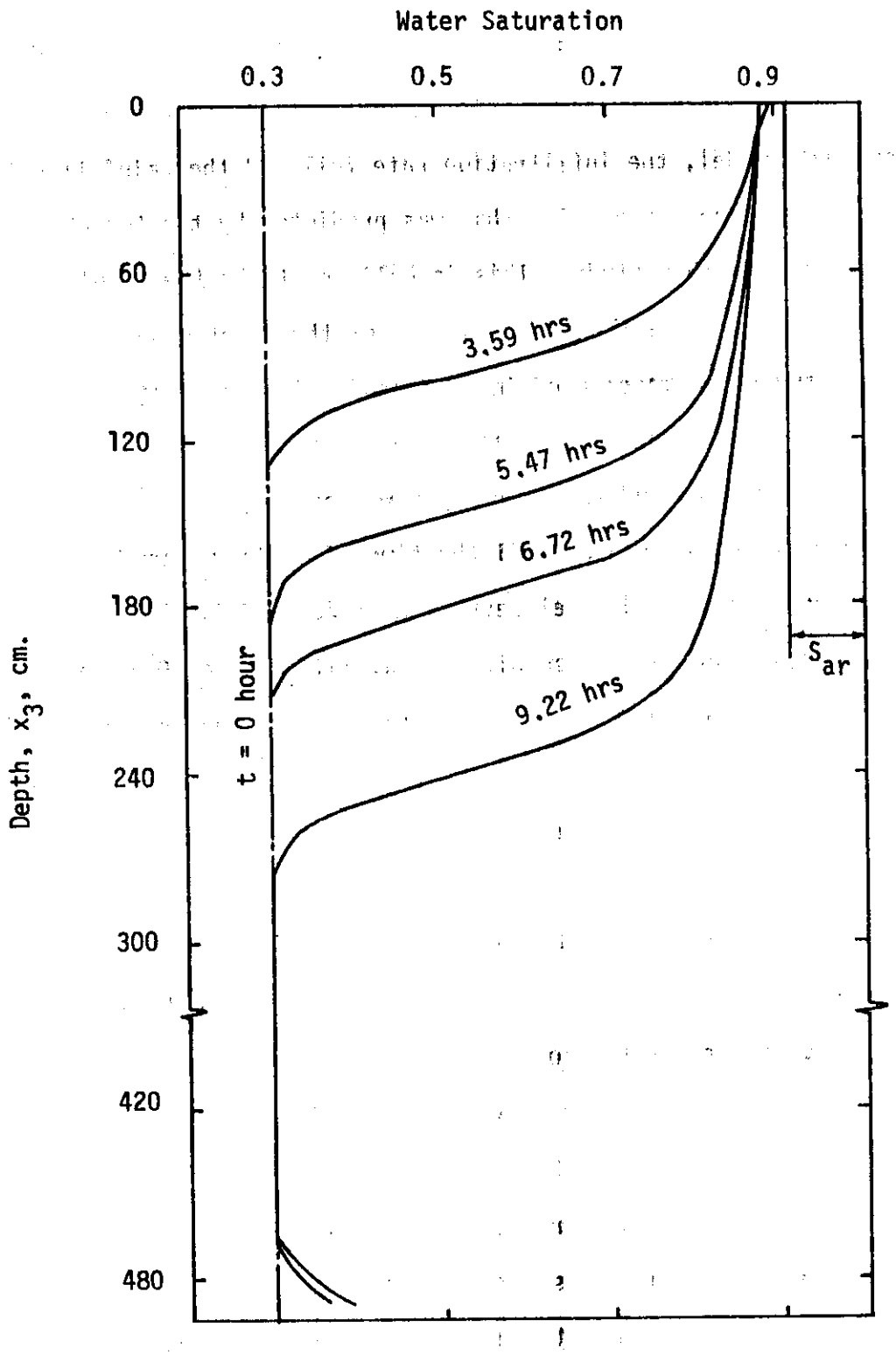

Figure 17. Water saturation profiles during infiltration into a closed bottom soil column.

Phuc and Morel-Seytoux (1972). The ponding times in the two studies also differ significantly. This implies that in Phuc and Morel-Seytoux's model, the infiltration rate followed the rainfall rate for a longer period of time than was predicted by the two-phase model used in this study. This is believed to be the result of slight discrepancies in the treatment of the upper boundary condition. In the two-phase model used in this study, if water was available at the soil surface due to rainfall or ponding, the soil surface was assumed saturated and the saturation was equal to 0.912. The saturation remained at 0.912 until the time of ponding. On the contrary, in Phuc and Morel-Seytoux's (1972) model, the saturation at the soil surface started with an initial value of 0.30 and increased to a maximum of 0.912 at the time of ponding. The value of the air entry pressure was not given in Phuc and Morel-Seytoux's work. An air entry pressure of 20 cm was assumed for the two-phase model used in this study. An air entry pressure less than 20 cm would reduce the threshold pressure and therefore would result in higher infiltration rates than those shown in Figure 15 prior to the start of air counterflow.

The infiltration rate curve in Figure 15 has a unique shape after air counterflow starts. After air counterflow starts, a hump was observed in the infiltration rate. Initially, the air pressure is zero in the column and saturation is equal to 0.912 at the soil surface. When water infiltrates the soil, air is trapped inside and compressed. When the air pressure in the medium exceeds the threshold pressure, air starts to move in the direction opposite to

water movement. This results in a desaturation of the medium and an increase in air permeability. This occurs even though there is ponding of water at the surface. Because of this desaturation, the hydraulic conductivity is decreased. Thus, the infiltration rate must decrease to a value less than the hydraulic conductivity at $(1 - S_{ar})$. The infiltration rate curve shown in Figure 15 depicts this proces very well.

As soon as the trapped air escapes from the medium, the infiltration rate increases and then finally reaches a limiting value slightly below the saturated hydraulic conductivity. The infiltration rate decreases to a value below the saturated hydraulic conductivity because the air pressure build-up represents a retarding force and causes a reduced permeability to liquid by increasing the capillary pressure. All previous studies (Figure 11) using a one-phase flow model have shown the saturated hydraulic conductivity or gravity flow as the lower limit for the infiltration rate. But as shown in Figure 15, the infiltration rates obtained from this work and those obtained by Phuc and Morel-Seytoux (1972) clearly dip below the saturated hydraulic conductivity. Experimental evidence is available to show that the infiltration rate does decrease below the saturated hydraulic conductivity (McWhorter, 1971).

Figure 16 shows the air pressure profiles at various times. Figure 17 shows the water saturation profiles at various times. The water saturation at the soil surface decreases below the saturation at $(1 - S_{ar})$ as trapped air escapes from the medium.

The results from the rainfall-infiltration simulation, unlike

the constant pressure boundary problem considered in the previous section, showed that inclusion of air in the two-phase flow model does have an influence on the infiltration rates. Unlike one-phase flow, the infiltration rates obtained using the two-phase model decreased below the saturated hydraulic conductivity. This is in agreement with the results obtained by Phuc and Morel-Seytoux (1972). However, in contrast to the results obtained by Phuc and Morel-Seytoux (1972), in which the infiltration rates exhibited a widely scattered pattern, a very smooth curve of infiltration rate versus time was obtained from the two-phase model used in this study. An excellent agreement was obtained comparing the infiltration rates from the two-phase model with those of Phuc and Morel-Seytoux (1972) towards the end of simulation. But in the initial stages, both after and prior to initiation of air counterflow, results from the two-phase model deviated considerably from those obtained by Phuc and Morel-Seytoux (1972). Unlike their results, a dip-and-hump was observed in the infiltration rates both after and prior to initiation of air counterflow. This unique shape of the infiltration rate curve is investigated further in the following section.

Comparison with Experimental Data

In the previous two sections, the numerical results obtained using the two-phase model were compared with analytical solutions or other numerical simulations. No experimental data were available to compare with the numerical solutions. McWhorter (1971) studied experimentally the two-phase infiltration process and it is now

possible to compare the results from the two-phase model with his experimental work. He studied an infiltration case in which liquid was provided at the soil surface at a constant ponding depth of 0.8 cm.

The numerical model used in this study to compare with McWhorter's (1971) experimental data was two-dimensional. Data used for this numerical simulation were: Δx_3 = 5.61 cm, Δx_1 = 5.61 cm, ℓ_3 = 185 cm, ℓ_1 = 15 cm, NR = 33, NC = 3, $k_s = 2.52 \times 10^{-8}$ cm^2, ϕ = 0.396, S_{wr} = 0.29, and ψ_b = 22.0 cm. The upper boundary condition of constant ponding depth of 0.8 cm was applied across the entire upper surface boundary of the two-dimensional model. The other three boundaries of the two-dimensional model were impervious and the boundary conditions were zero flux for both air and water. Again, similar to the time-dependent boundary condition problem considered in the previous section, air was trapped inside the medium until the air pressure near the surface reached a threshold value at which air began to escape from the top of the column. An air entry pressure of 22 cm and a desaturation of 0.0001 of water saturation at the soil surface were used in the two-phase model. The porous medium was a Poudre sand whose hydraulic properties are given in Figures 18 and 19. The imbibition cycle of the capillary pressure versus saturation curve (Figure 18) was used. The wetting fluid was a light hydrocarbon oil called Philips core test fluid whose density was 0.756 gm/cm^3. The initial condition was of uniform saturation of 0.29. The time step size was not allowed to exceed a maximum of $\Delta x_3^2/2$.

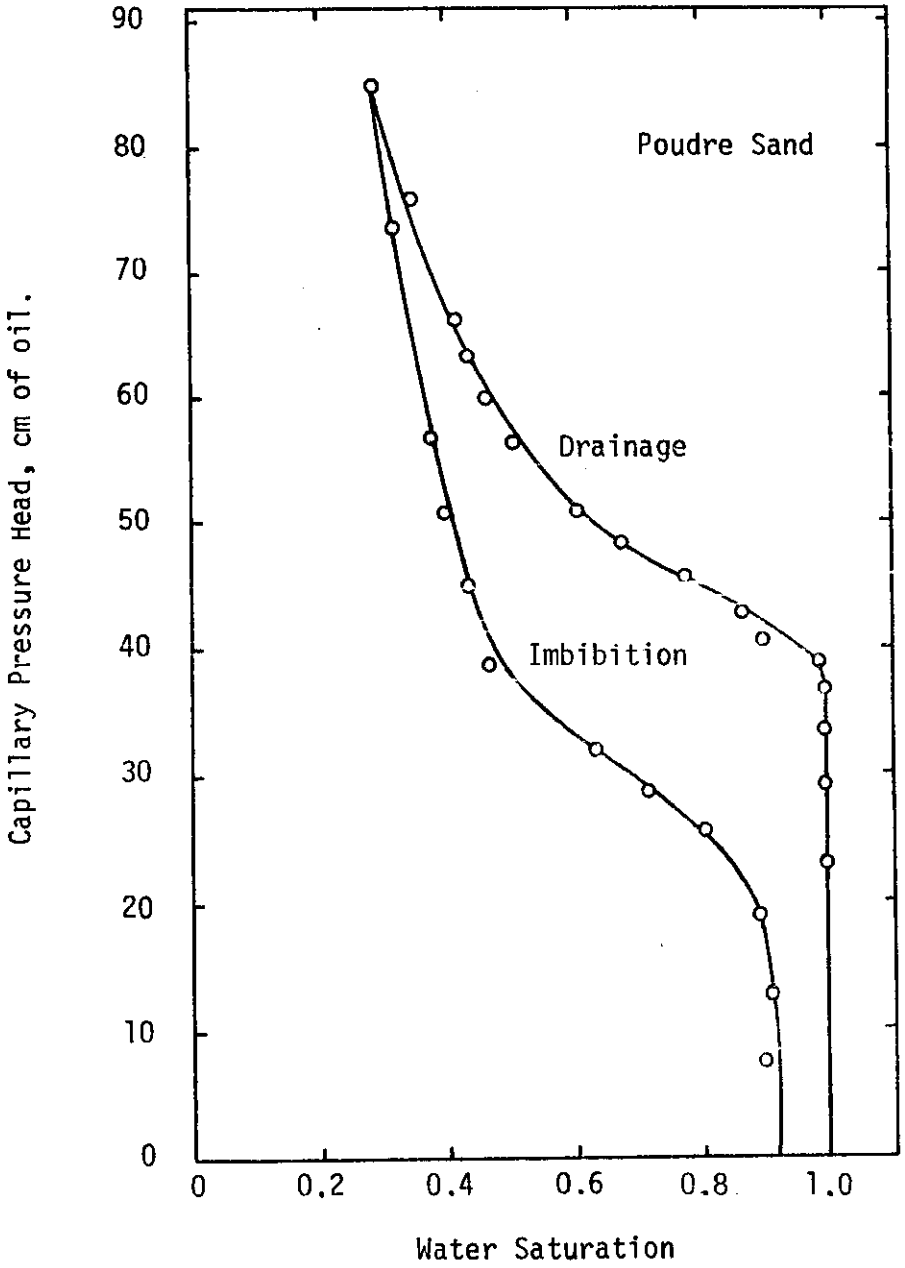

Figure 18. Capillary pressure head as a function of water saturation for Poudre Sand.

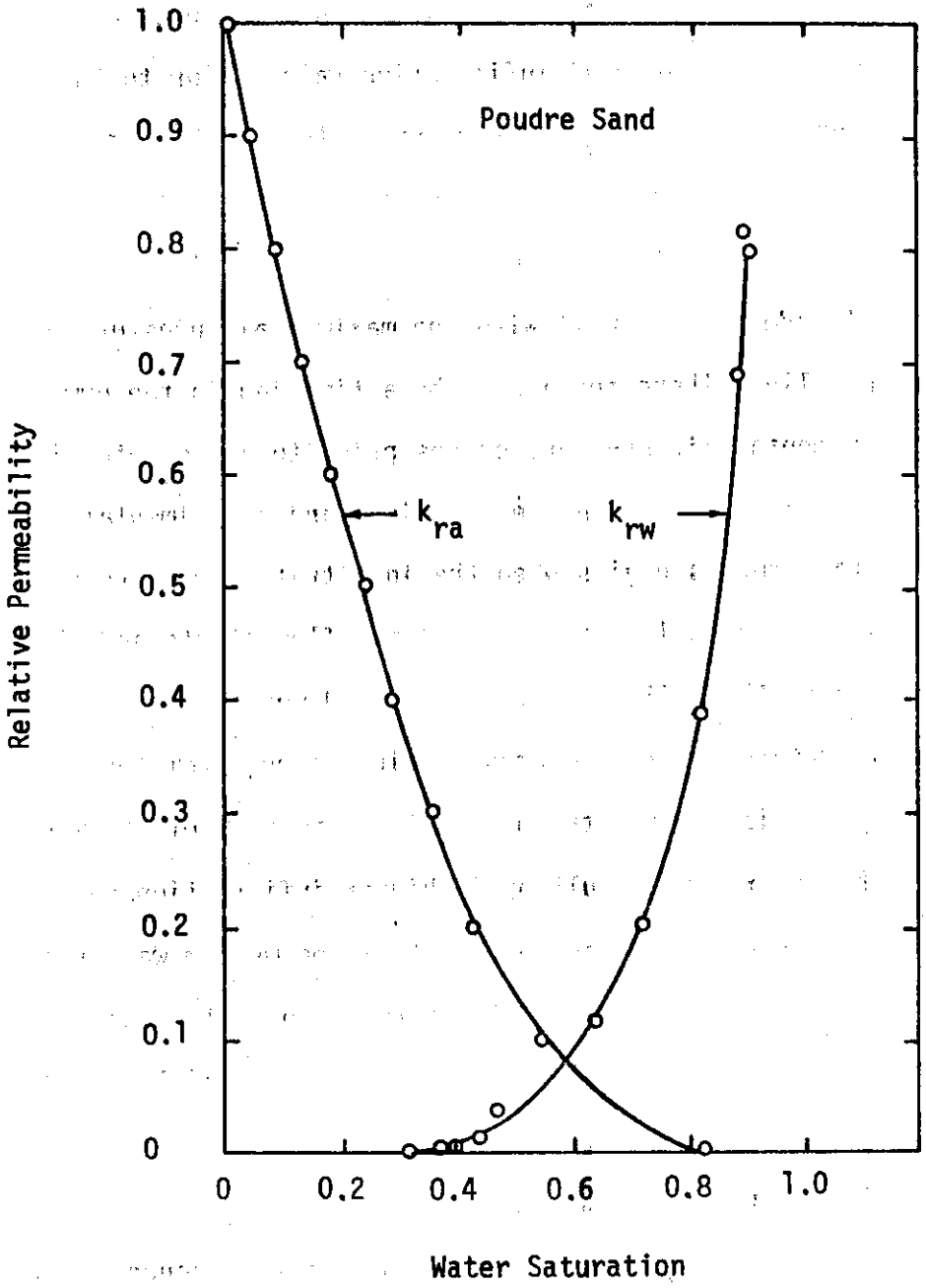

Figure 19. Relative permeability as a function of water saturation for Poudre sand.

Variations of infiltration rate and air pressure with time are shown in Figure 20. Excellent agreement was found between the numerical and experimental infiltration rates prior to the initiation of air counterflow. Air pressures predicted by the numerical model prior to air counterflow were higher than those determined experimentally. However, the maximum air pressure predicted by the numerical model agrees well with the maximum air pressure obtained experimentally. There appears to be a time lag in the numerical and experimental air pressure curves prior to air counterflow.

The deviation between the numerical and experimental infiltration rate curves begins when the infiltration rate reaches its lowest value. At this point, air counterflow starts and the desaturation of the soil begins. The upward moving air front breaks the soil surface and the compressed air escapes from the surface violently. This changes the hydraulic properties of the media during the experiment resulting in higher infiltration rates. Contrary to this, the escape of air from the medium was treated in the numerical model by a gradual desaturation of the soil surface resulting in lower infiltration rates. This particular boundary condition, immediately after initiation of air counterflow, is difficult to simulate in the numerical model. The discrepancies between the numerical and the experimental air pressure and infiltration rate curves, after the initiation of air counterflow, are due to problems in simulating such boundary conditions numerically. However, the fact that the experimental and numerical curves behaved in a similar fashion is the most significant aspect of this

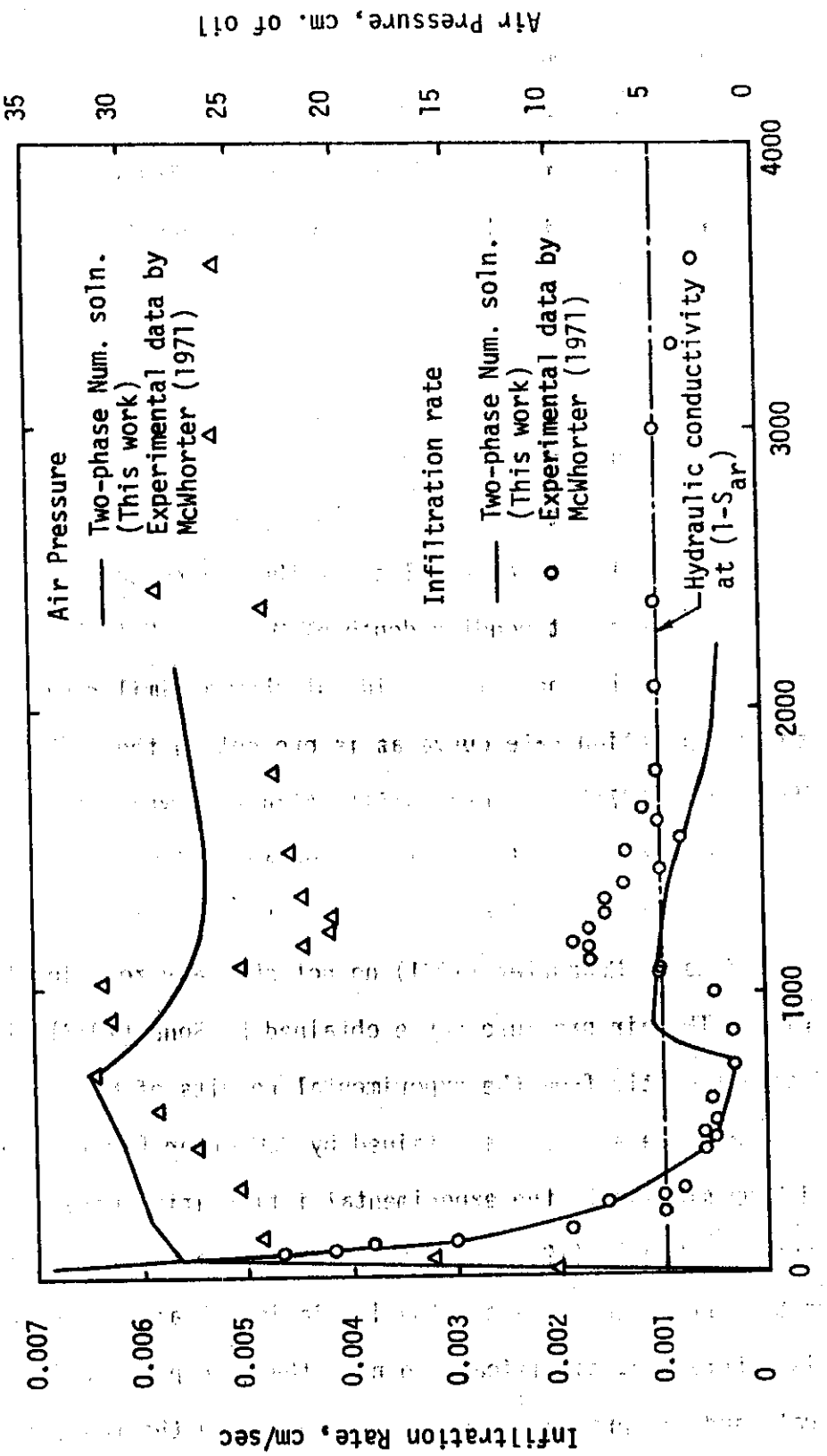

Figure 20. Comparison of experimental and numerical results for infiltration into 185-cm Poudre sand.

comparison.

The rainfall-infiltration problem considered in the previous section resulted in a dip-and-hump in the infiltration rate curve prior to and after initiation of air counterflow. The presence of this unique shape of the infiltration rate curve when the effect of air on infiltration is pronounced is verified by the experimental data of McWhorter (1971). The numerical results obtained from the two-phase model used in this study showed excellent agreement with McWhorter's (1971) experimental data.

Sonu (1973) also attempted to compare McWhorter's (1971) experimental data with his numerical results for the 185-cm column of Poudre sand and a constant ponding depth of 0.8 cm. But the numerical results obtained by Sonu (1973) did not show a similar dip and hump in the infiltration rate curve as is present in the experimental data of McWhorter (1971). A zero infiltration rate was obtained by Sonu (1973) and this zero rate continued for about 3.0 to 3.5 minutes before the infiltration rate started to increase. The experimental data of McWhorter (1971) do not show any zero infiltration rate. The air pressure curve obtained by Sonu (1973) also deviated significantly from the experimental results of McWhorter (1971). The air pressure curve obtained by McWhorter (1971) showed a dip-and-hump similar to the experimental infiltration rate curve. On the contrary, Sonu's (1973) results predicted no changes in air pressures both prior to and after the initiation of air counterflow.

It is, therefore, significant to note that the predicted infiltration rate and air pressure curves obtained using the two-phase

numerical model in this study behave in a similar fashion with those determined experimentally by McWhorter (1971). This study is, therefore, believed to be a first successful attempt at comparing McWhorter's (1971) experimental data with the numerical results using a two-phase model. Quantitatively, there were some differences between the numerical and experimental infiltration rate and air pressure curves. These differences are believed to be due to changes in medium characteristics as the compressed air escapes through the soil surface resulting in a sharp drop in the air pressure and a corresponding sharp increase in infiltration rate. This phenomenon of change in hydraulic properties is present during the experiment. However, it is difficult to accurately simulate such drastic changes in boundary conditions in the numerical model. The fact that the experimental and numerical curves behave in a similar fashion provides strong evidence for the accuracy of the two-phase numerical simulator developed in this study.

In the preceding sections, the accuracy of the two-phase numerical simulator developed in this study was tested with analytical solutions, experimental data, and other numerical simulations from the literature. It is apparent from the comparisons that the two-phase flow model developed in this study is sufficiently accurate. The usefulness of the two-phase model is also apparent when the results from the two-phase model were compared with laboratory experiments of McWhorter (1971). Air indeed has a significant effect on infiltration when a permeable layer is underlain by a relatively impermeable layer and there is no lateral passage to

permit the trapped air to escape. It has been recognized from infiltration experiments in the laboratory that an air vent is needed to allow the air to escape from the medium, minimizing the influence of the air on the advancing wetting front. Even in field experiments, if the soil is covered by a fine and hard crust and the medium is bounded below by either the water table or an impervious bed rock, the effect of air on infiltration is pronounced. It is interesting to quote Philip (1969):

> ..., as this author is well aware from his personal experiences in the Riverina of Australia, limits to air escape may well affect infiltration into large inundated areas. In fact, soil air pressures have been developed which were great enough to lift the pavements of highways passing through the flooded region.

Numerical Solution of Dispersion Equation using Tensor Concept

The accuracy of the convective-dispersion model developed in this study was verified by comparing the simulation results with available analytical or exact solutions. The method of characteristics (MOC) was used to numerically solve the convective-dispersion equation. Much can be learned about the accuracy of numerical solutions for two-dimensional flow fields by examining the one-dimensional flow case. An exact analytical solution of the one-dimensional flow problem is available for any input concentration; in particular for the step concentration input considered in this work. This solution was given earlier by equation (17).

Longitudinal Dispersion

A numerical solution was obtained using the data from Garder et al. (1964): Δt = 100 sec, Δx_3 = 3.81 cm, D_L = 2.94 x 10^{-3} cm^2 sec^{-1}, ϕ = 0.34, V_3 = 0.01411 cm sec^{-1}, ℓ_3 = 182.88 cm, number of grids = 48, and moving points per grid = 4. The results are shown in Figure 21, and good agreement is indicated between the numerical and analytical solutions. Reddell and Sunada (1970) made extensive studies on the number of moving points required per grid for the MOC to give accurate results. Contrary to Garder et al. (1964), they concluded that both the number and relative position of the moving points influenced the average grid concentration.

To check the numerical solution using the tensorial form of the dispersion coefficient (equation 37), a coordinate transformation was made similar to the one suggested by Reddell and Sunada (1970). The coordinate axes were rotated so that an angle of 45° existed between the velocity vector and the transformed coordinate axes. The problem was solved numerically in the rotated coordinate system (x_1', x_3'). This forced the numerical model to use the tensor transformation for the dispersion coefficient. However, the physics of the problem was not changed, and equation (17) still provides an analytical solution to the problem in the (x_1, x_3) coordinate system.

A rectangular region, $0 \leq x_3 \leq \ell_3$ and $0 \leq x_1 \leq \ell_1$, was considered in which the flow is along the x_3-axis with a steady, uniform seepage velocity, V_3 (Figure 22). With the coordinates rotated at an angle of 45° to the velocity vector V_3, the numerical solution was carried out in the rectangular region defined by $0 \leq x_3' \leq \ell_3'$

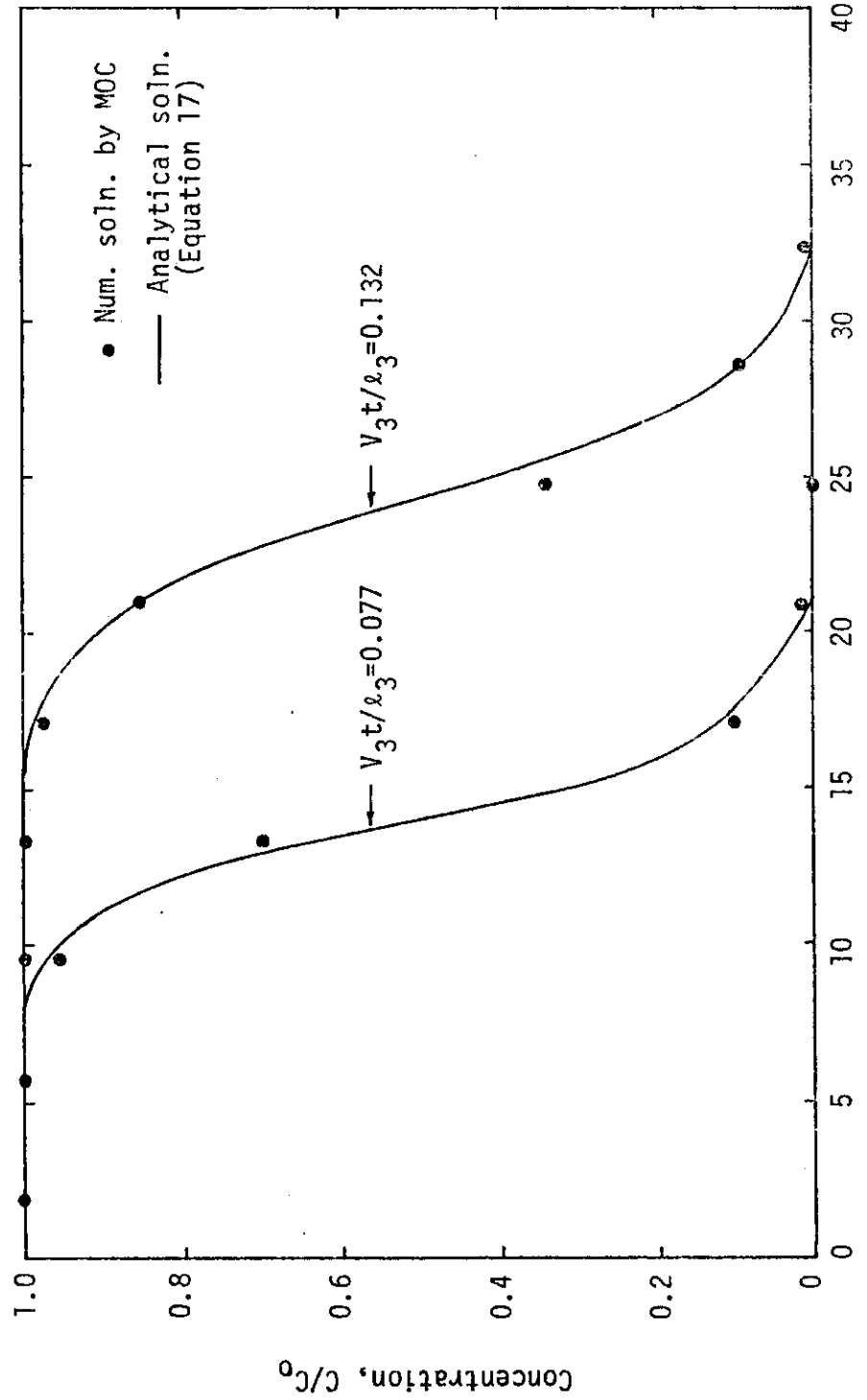

Figure 21. Comparison of analytical and numerical solution to the longitudinal dispersion problem used by Garder et al. (1964).

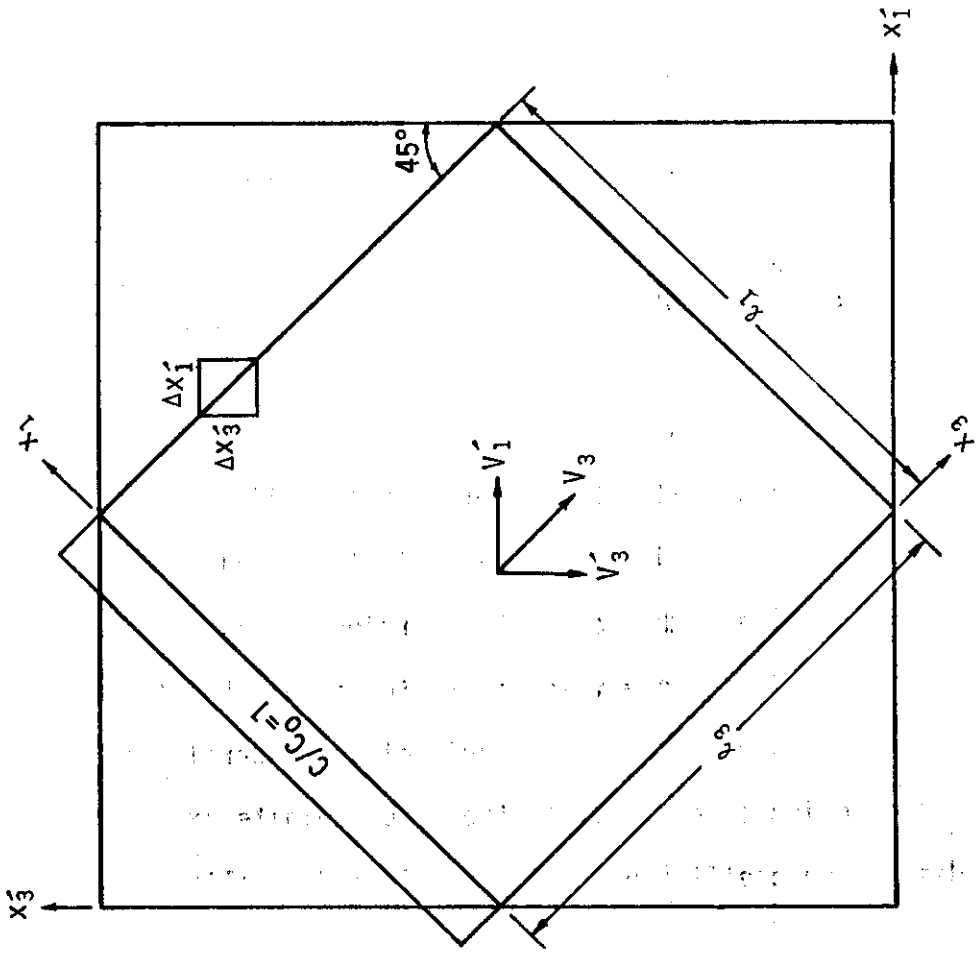

Figure 22. Schematic sketch of coordinate axes rotation used for comparing numerical and analytical solutions of the longitudinal dispersion problem.

and $0 \leq x_1' \leq \ell_1'$. A steady, uniform seepage velocity with components $V_3' = 0.707\ V_3$ and $V_1' = 0.707\ V_3$ existed in the transformed region. A fluid with a relative concentration of $C/C_0 = 1.0$ was injected across the entire interface $0 \leq x_1 \leq \ell_1$. Data used to numerically solve the problem were: $\Delta x_3' = 0.4$ cm, $\Delta x_1' = 0.4$ cm, $\Delta t = 2$ sec, $V_3' = 0.071$ cm sec^{-1}, $V_1' = 0.071$ cm sec^{-1}, $V_3 = 0.10$ cm sec^{-1}, grid dimensions = 20 x 20, $D_L = 0.01$ $cm^2 sec^{-1}$, $D_T = 0.001$ $cm^2 sec^{-1}$, $\ell_3 = 5.66$ cm, $\ell_1 = 5.66$ cm, and the number of moving points per grid = 4.

Two solutions were obtained for this problem; one solution used the tensorial transformations for the dispersion coefficients, D_L and D_T, given by equations (37) and the other solution used no tensor transformation. With the tensor transformation, the longitudinal dispersion coefficient (D_{33}) is oriented parallel to the velocity vector (V_3) and the lateral dispersion coefficient (D_{11}) is oriented perpendicular to the velocity vector (V_3). For the case with no tensor transformation, the longitudinal dispersion coefficient (D_{33}) is oriented parallel to the x_3' coordinate axis and the lateral dispersion coefficient (D_{11}) is oriented parallel to the x_1' coordinate axis.

The results from the numerical solution of this longitudinal dispersion problem, with and without the tensor transformation, are shown in Figure 23. The analytical solution as given by equation (17) is also plotted. The results indicate an excellent agreement between the numerical and analytical solution when the tensor transformation is used. The solution without the tensor

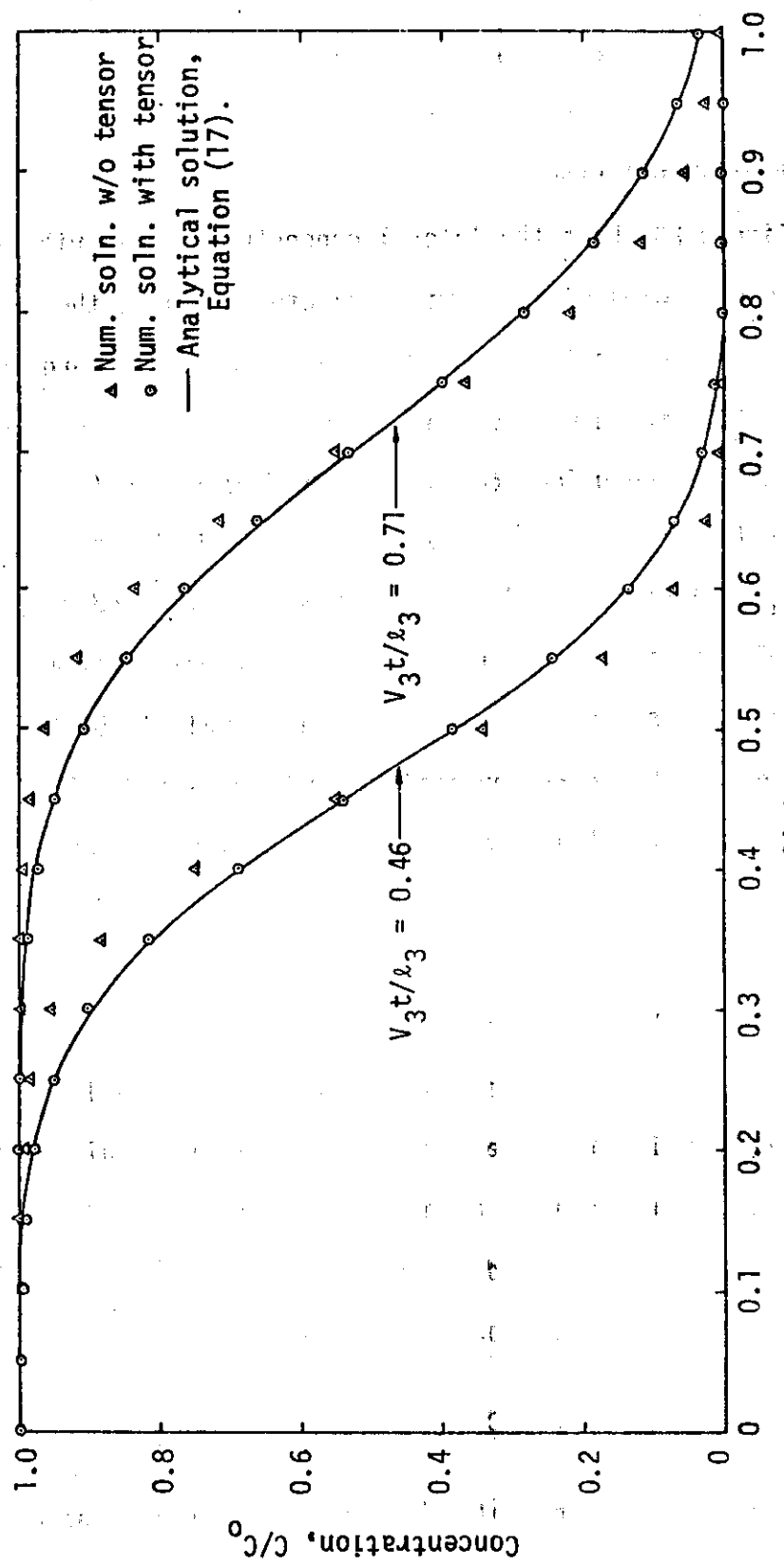

Figure 23. Comparison of longitudinal concentration distribution calculated with and without the tensor transformation

transformation yielded a steeper concentration profile than the analytical solution. Thus, a significant error results in the numerical solution of the dispersion equation when the tensor transformation is not used.

Figure 24 shows the lateral concentration distribution after 0.71 pore volumes of fluid were injected. Again, the numerical solution using the tensor transformation provides more accurate results than those without the tensor transformation. Some error in the numerical solution occurs near the boundaries ($x_1 = 0$ and $x_1 = \ell_1$). This occurs because the straight boundaries of the column in the (x_1, x_3) coordinate system must be approximated by a series of rectangles or squares in the rotated coordinate system (x_1', x_3') (Figure 22). As $\Delta x_1'$ and $\Delta x_3'$ become very small, a better approximation of the boundary conditions can be expected. The numerical results for any value of x_3/ℓ_3 were generally the same for $0.3 \leq x_1/\ell_1 \leq 0.7$. No dispersion (or mass-flow) was allowed to occur across the boundary columns $x_1 = 0$ and $x_1 = \ell_1$. This condition was appoximated numerically by setting the dispersion coefficients equal to zero for all grids on these two boundaries. Reddell and Sunada (1970) reported a better agreement between numerical solutions and analytical solutions when a reflective boundary condition ($\partial C/\partial x_1' = 0$ and $\partial C/\partial x_1' = 0$) was used instead of setting the dispersion coefficients equal to zero along the boundary.

Longitudinal and Lateral Dispersion

A longitudinal and lateral dispersion problem was also solved

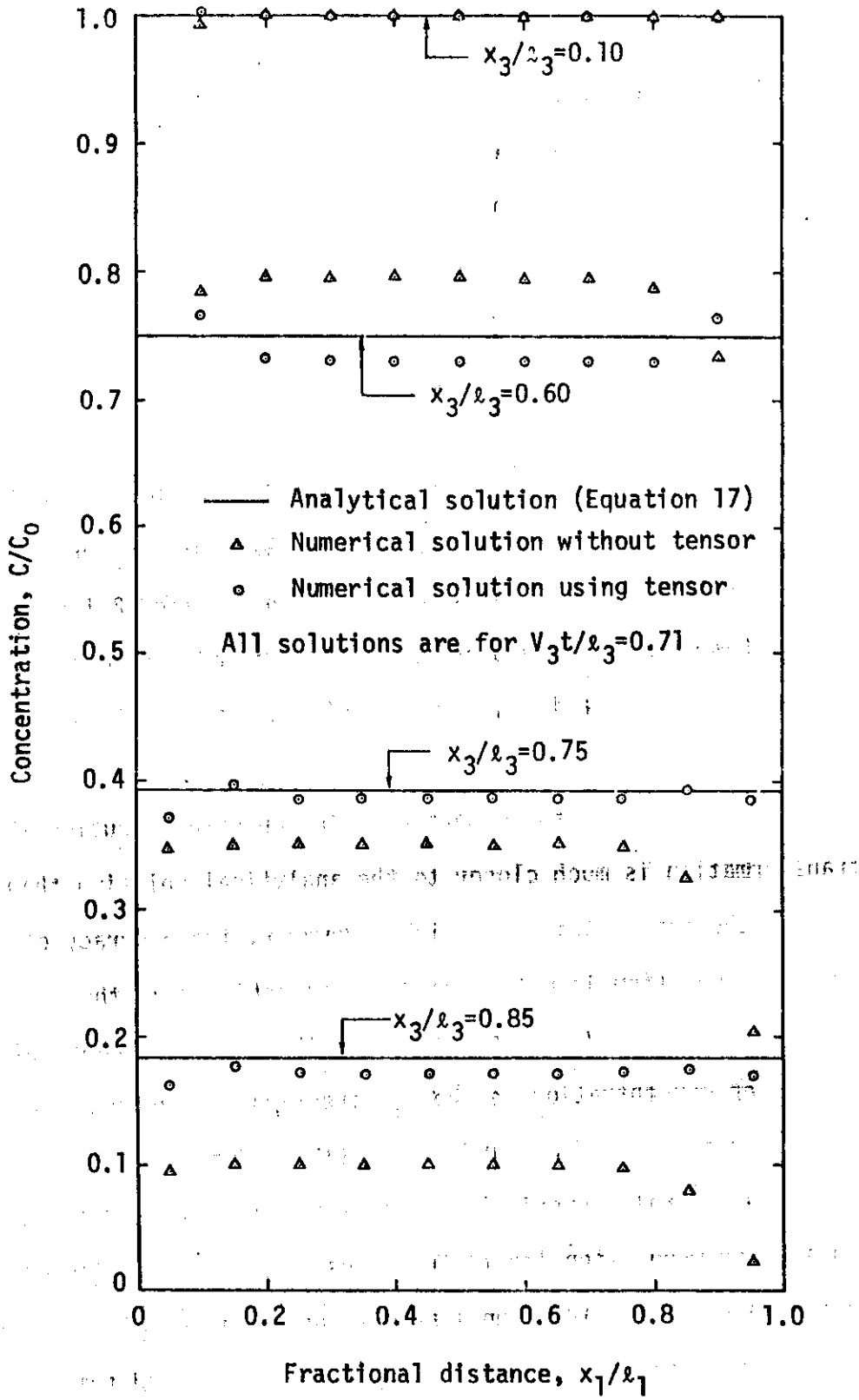

Figure 24. Comparison of lateral concentration distribution with and without the tensor transformation.

numerically in the rotated coordinate system (x_1', x_3') as shown in Figure 25. A fluid with a relative concentration of $C/C_o = 1.0$ was injected over the interval $a \leq x_1 < b$ and fluid with a relative concentration of $C/C_o = 0.0$ was injected over the intervals $0 \leq x_1 \leq a$ and $b \leq x_1 \leq \ell_1$. Data used to numerically solve this problem were the same as for the previously described longitudinal dispersion problem. The dimensions for a and b were 1.98 cm and 3.68 cm respectively.

The results from the numerical solution of the longitudinal and lateral dispersion problem, with and without the tensor transformation, are shown in Figures 26 throguh 29 after 2.1 pore volumes of fluid were injected and an approximate steady state condition was achieved. For comparison, the approximate analytical solution for the steady case as determined from equation (21) is also plotted. Figure 29 shows that the numerical solution obtained using the tensor transformation is much closer to the analytical solution than those without the tensor transformation. However, the accuracy of the numerical solution is not as good as was achieved in the longitudinal dispersion problem described earlier. This occurs because of the very steep concentration in the x_1-direction, which approaches a "step" function. Reddell and Sunada (1970) discussed the problem of achieving accurate numerical solutions along steep concentration profiles or when "step-input" functions are used. They reported that much smaller grid dimensions were necessary in these areas to achieve accurate answers. It must also be remembered that equation (21) is only an approximate analytical solution and not an exact

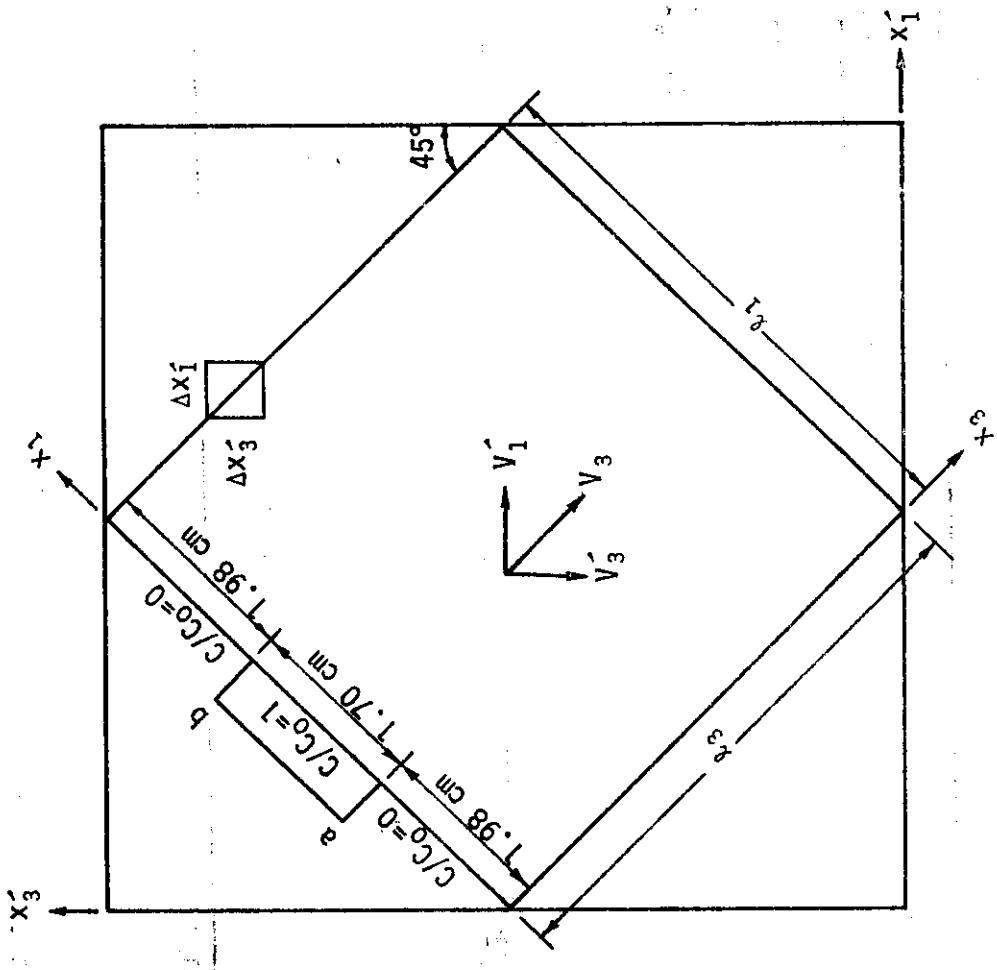

Figure 25. Schematic sketch of coordinate axes rotation used for comparing numerical and analytical solutions of the longitudinal and lateral dispersion problem.

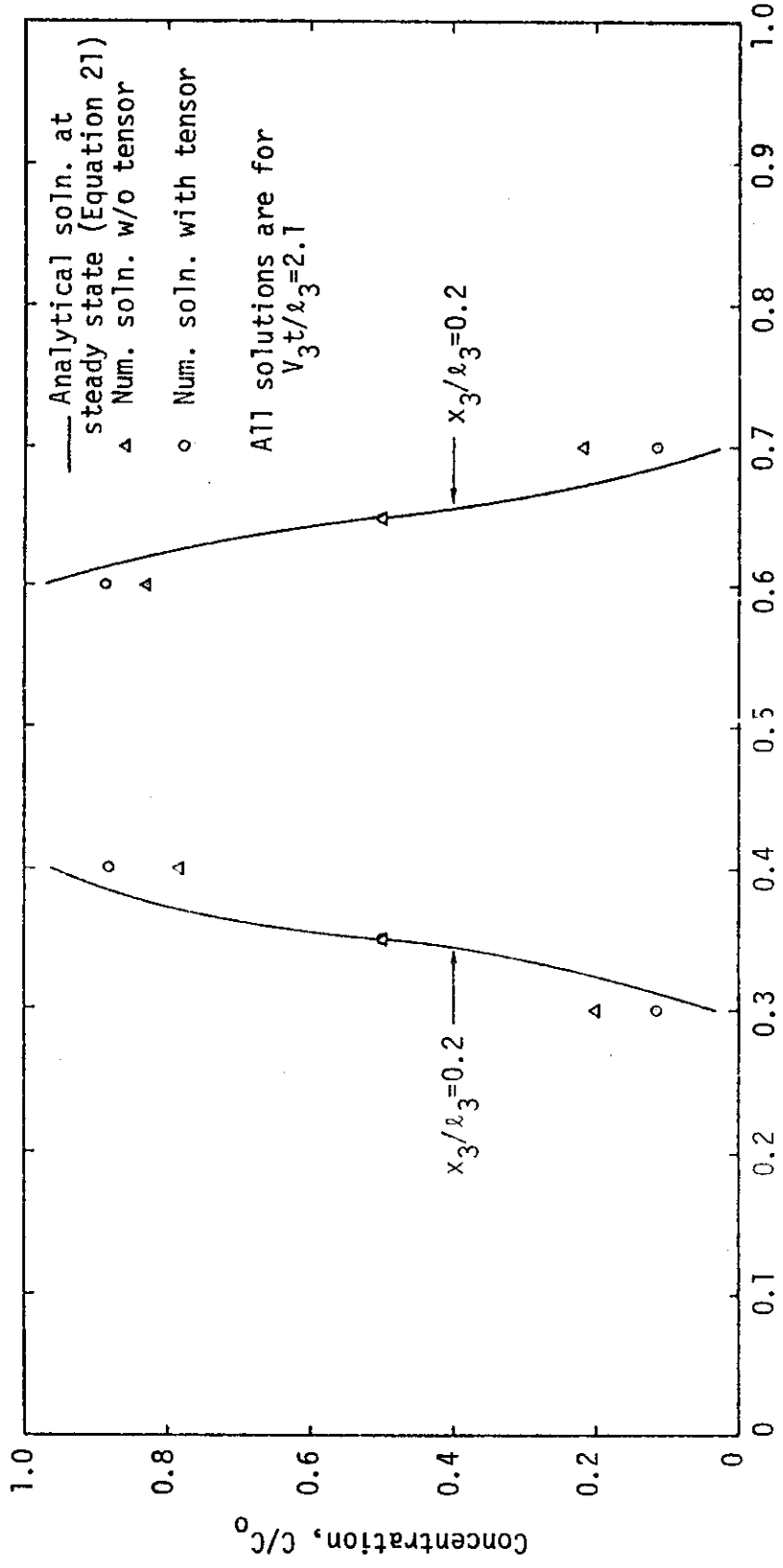

Figure 26. Comparison of lateral concentration distribution at $x_3/\ell_3=0.2$ as calculated by using the tensor transformation, without the tensor transformation, and by an approximate analytical solution for steady state conditions.

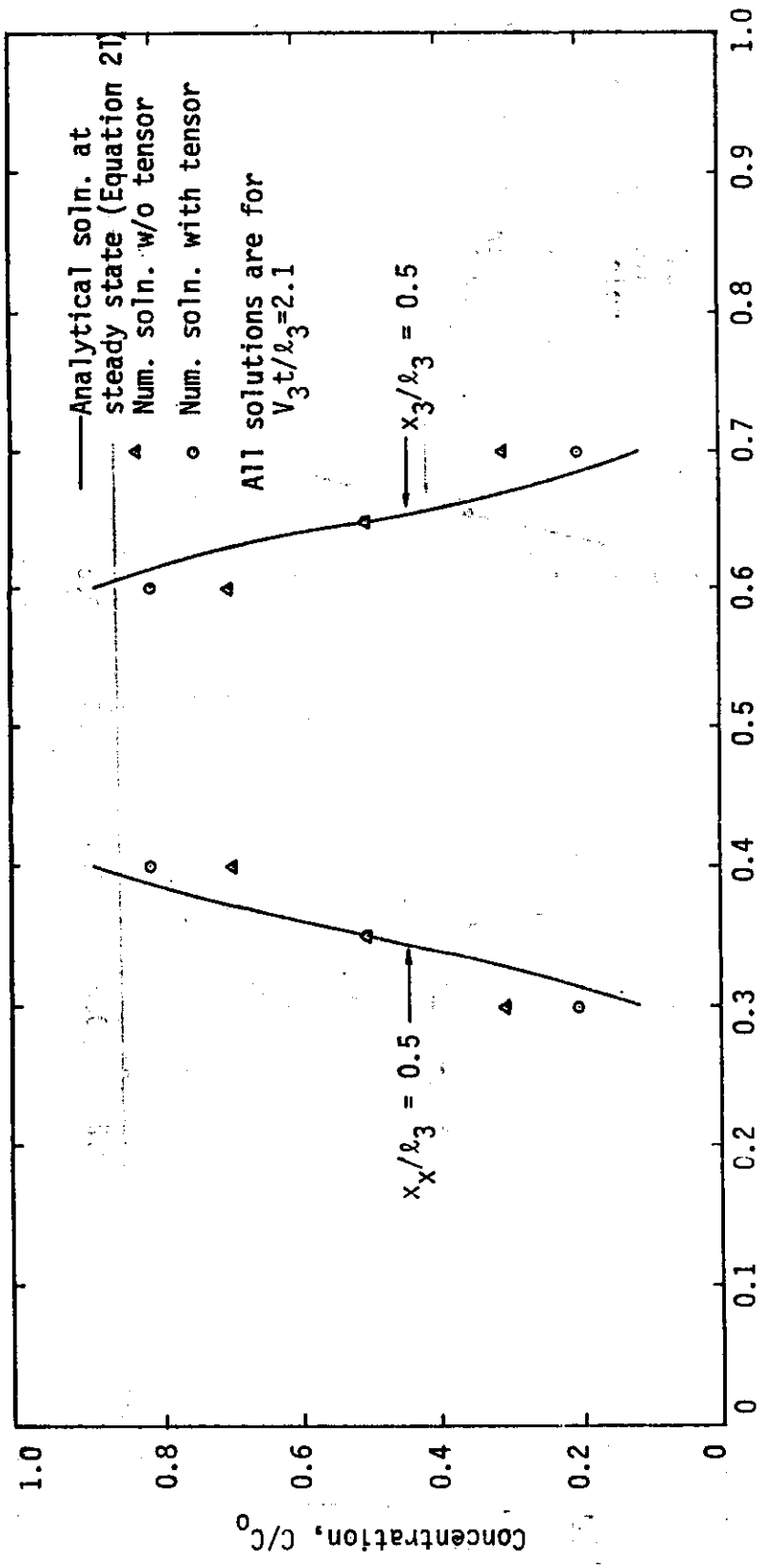

Figure 27. Comparison of lateral concentration distribution at $x_3/\ell_3=0.5$ as calculated by using the tensor transformation, without the tensor transformation, and by an approximate analytical solution for steady state conditions.

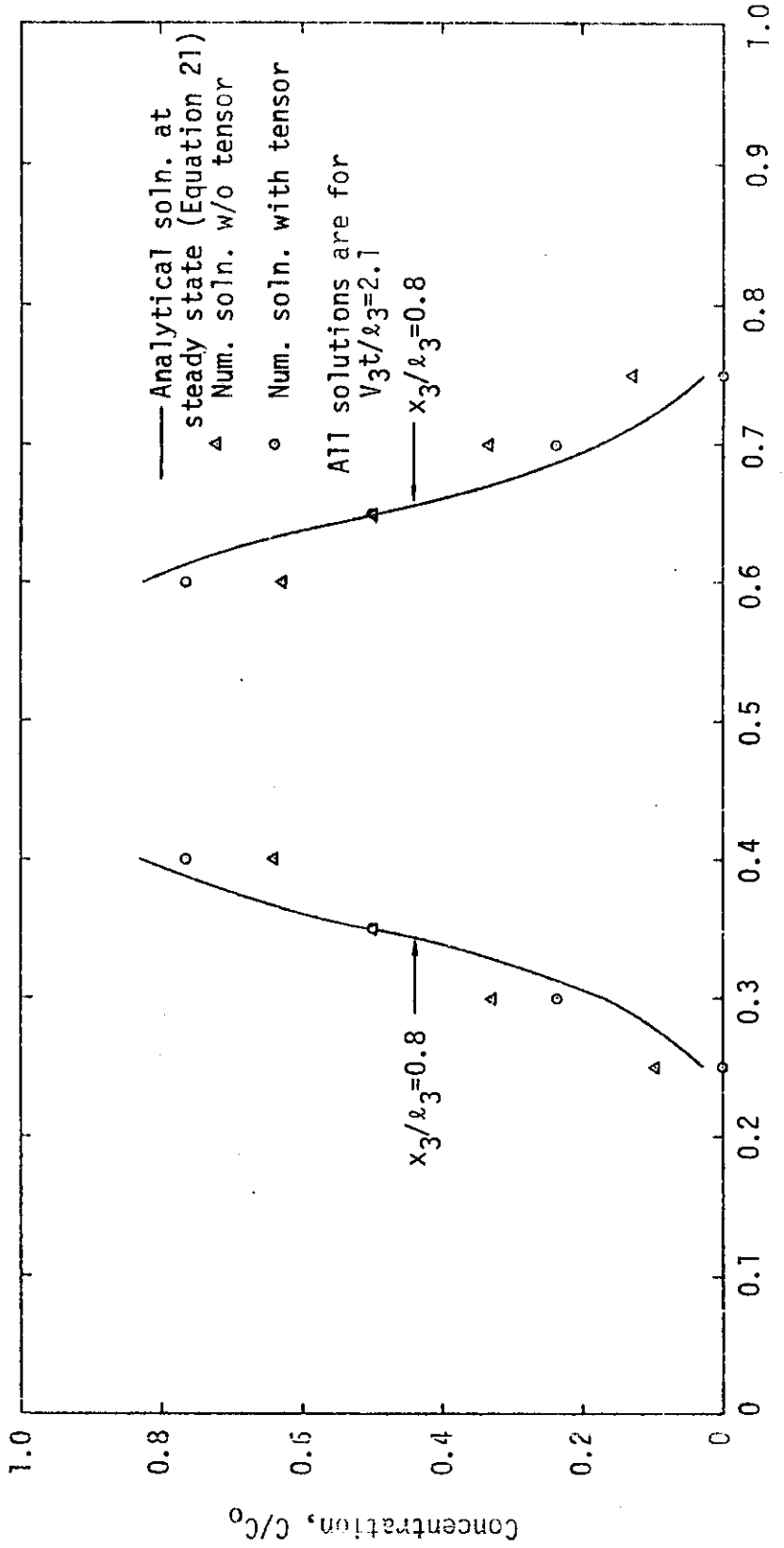

Figure 28. Comparison of lateral concentration distribution at x_3/ℓ_3=0.8 as calculated by using the tensor transformation, without the tensor transformation, and by an approximate analytical solution for steady state conditions.

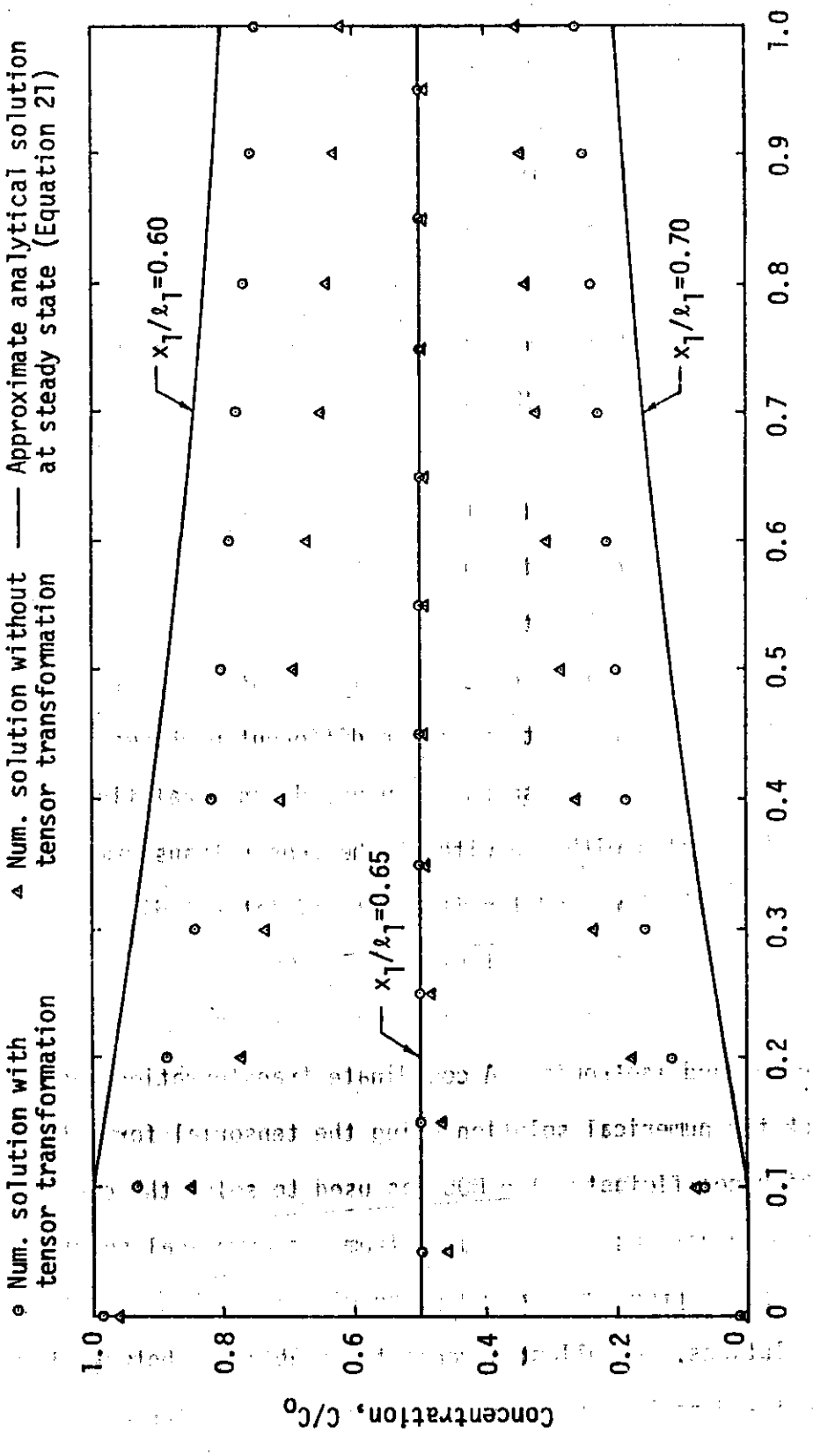

Figure 29. Comparison of longitudinal concentration distribution at steady state as calculated by using the tensor transformation, without the tensor transformation, and by an approximate analytical solution.

analytical solution. Also, equation (21) is a steady state solution, but the numerical solutions are transient. The numerical solutions were terminated after only 2.1 pore volumes were injected and the results were changing only slightly with each additional time step. Nevertheless, the results were still changing some, and a true steady state case had not been achieved.

The concentration profiles as plotted do not show any "overshoot" or "undershoot." However, "overshoot" and "undershoot" did occur; but was generally of the order of 10^{-3} to 10^{-4} C/C_o. Since the numerical solution without the tensor transformation did not produce any "overshoot," the use of the "nine-star" grid pattern to estimate the cross-derivatives for the tensor transformation is believed to be the source of this small amount of "overshoot."

In the preceding section, three different problems were considered: Longitudinal dispersion in one-dimensional flow, longitudinal dispersion with and without the tensor transformation in two-dimensional flow, and longitudinal and lateral dispersion with and without the tensor transformation in two-dimensional flow. A steady, uniform flow field was assumed and the porous medium was homogeneous and isotropic. A coordinate transformation was necessary to check the numerical solution using the tensorial form of the dispersion coefficient. The MOC was used to solve the convective-dispersion equations. The results from the numerical solutions of the dispersion problems were compared with available analytical or exact solutions. Excellent agreement was obtained between the numerical and analytical solutions when the tensor transformation is

used. This provides strong evidence for the accuracy of the proposed numerical tensor transformation and the convective-dispersion segment of the total numerical simulator.

The MOC appears to be capable of solving the longitudinal dispersion as well as the longitudinal and lateral dispersion problems. No problems with "overshoot" occured and no "numerical dispersion" resulted from the numerical process. The small amount of "overshoot" that occured in the numerical solution is believed to be the result of using a "nine-star" grid pattern to estimate the cross-derivatives for the tensor transformation.

A major detriment to the numerical scheme appears to be moving points. A numerical solution was obtained using 2 points per grid for the longitudinal dispersion problem in a steady, uniform, two-dimensional flow field. Even though the tensor transformation was used in both cases, the numerical solution using 4 points per grid showed much closer agreement with the analytical solution than the one using 2 points per grid. This indicates that the number and relative position of the moving points does have an influence on the accuracy of the results. It also indicates that the method of calculating the average grid concentration is an important factor in the numerical scheme. If an adequate scheme for weighting the concentration can be developed based on the concept of "area of influence" of the moving points as a weighting function as suggested by Reddell and Sunada (1970), then a smaller number of moving points per grid may be used. Using this concept, Reddell and Sunada (1970) obtained accurate results for the problems where a steady, uniform

flow field was used. They concluded that if some type of weighted average is not used, then a sufficient number of moving points must be used to guarantee a reasonable estimate of the average. The development of a numerical scheme to determine the "area of influence" for each moving point in a nonuniform, unsteady flow field would be difficult.

The applications of the convective-dispersion model developed in this study are numerous. A few examples are salt-water intrusion into coastal aquifers, underground waste disposal, and infiltration of pollutants from surface sources into aquifers. In the following sections, the convective-dispersion model will be used to solve the simultaneous transport of solutes and water under transient conditions in an integrated saturated-unsaturated porous medium.

Saturated-Unsaturated, Two-Phase Infiltration and Dispersion Problem

All the problems solved so far have bypassed either the dispersion segments or fluid flow segments of the numerical simulator. No known investigator has attempted a combined numerical solution of the fluid flow and the dispersion equations in an integrated saturated-unsaturated flow domain. To study the combined fluid flow-dispersion numerical simulator, a drainage problem was solved in which a constant source of pollution was infiltrated from the land surface.

A schematic diagram of the drainage problem is shown in Figure 30. The flow medium consists of a rectangular soil slab resting on an impermeable base and drained by parallel drains spaced at $2\ell_1$.

The distance ℓ_1 is, therefore, one-half the spacing between the drains. The elevation H_A is the head at one-half the drain spacing and the elevation H_B is the head at the drain. At time $t < 0$, the water table is in hydrostatic equilibrium with the head H_A at one-half the drain spacing. At time $t \geq 0$, an arbitrary time after the commencement of drainage, the water table is represented by cd. The distance oc can be simulated as a no-flow boundary.

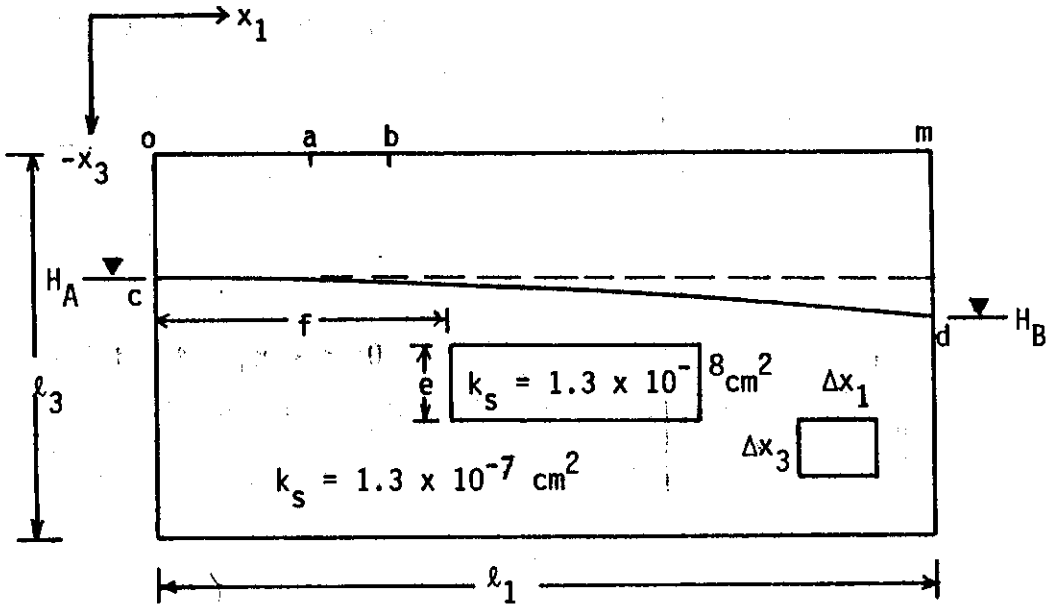

Figure 30. Schematic diagram of the drainage problem.

Data used for analyzing the drainage problem were: Δx_1 = 100 cm, Δx_3 = 50 cm, ϕ = 0.3, number of rows, NR = 13, number of columns, NC = 18, length of model, ℓ_1 = 1800 cm, depth of model, ℓ_3 = 650 cm, moving points per grid = 4, g = 981 cm sec^{-2}, ρ_w = 1 gm cm^{-3}, ρ_a = 0.00122 gm cm^{-3}, μ_w = 0.0115 poise, and μ_a = 0.000191 poise. The dimensions for oa and ab were 400 cm and 100 cm respectively.

Boundary conditions for the problem were:

$$\left.\begin{aligned} &\frac{\partial \psi_w}{\partial x_3} = 0 \quad , \\ &\psi_a = \psi_{atm} = 0, \\ &\frac{\partial C}{\partial x_3} = 0 \quad , \end{aligned}\right\} \qquad \begin{aligned} &0 \le x_1 \le a,\ x_3 = 0\ ,\ t \ge 0 \\ &b < x_1 \le \ell_1,\ x_3 = 0,\ t \ge 0 \end{aligned}$$

$$\left.\begin{aligned} &\psi_w = 0 \quad , \\ &\frac{\partial \psi_a}{\partial x_3} = 0 \quad , \\ &\frac{C}{C_o} = 1 \quad , \end{aligned}\right\} \qquad a \le x_1 \le b,\ x_3 = 0,\ t \ge 0$$

$$\left.\begin{aligned} &\psi_w = H_A - x_3 \ , \\ &\frac{\partial \psi_a}{\partial x_1} = 0 \quad , \\ &\frac{\partial C}{\partial x_1} = 0 \quad , \end{aligned}\right\} \qquad x_1 = 0,\ c < x_3 \le \ell_3,\ t \ge 0$$

$$\left.\begin{aligned} &\psi_w = H_B - x_3 \ , \\ &\frac{\partial \psi_a}{\partial x_1} = 0 \quad , \\ &\frac{\partial C}{\partial x_1} = 0 \quad , \end{aligned}\right\} \qquad x_1 = \ell_1,\ d < x_3 \le \ell_3,\ t \ge 0$$

$$\left.\begin{aligned} &\frac{\partial \psi_w}{\partial x_1} = 0 \quad , \\ &\frac{\partial \psi_a}{\partial x_1} = 0 \quad , \\ &\frac{\partial C}{\partial x_1} = 0 \quad , \end{aligned}\right\} \qquad \begin{aligned} &x_1 = 0,\ 0 \le x_3 \le c,\ t \ge 0 \\ &x_1 = \ell_1,\ m \le x_3 \le d,\ t \ge 0 \end{aligned}$$

$$\left.\begin{aligned} \frac{\partial \psi_w}{\partial x_3} &= 0 \quad , \\ \frac{\partial \psi_a}{\partial x_3} &= 0 \quad , \\ \frac{\partial C}{\partial x_3} &= 0 \quad , \end{aligned}\right\} \qquad 0 \leq x_1 \leq \ell_1,\ x_3 = \ell_3,\ t \geq 0 \tag{72}$$

where H_A and H_B are constant head elevations at one-half the drain spacing and at the drain respectively. The dimensions of H_A and H_B were -250 cm and -300 cm respectively. The initial conditions were those of hydrostatic air and water pressure distributions. The initial condition for the tracer was $C/C_o = 0$ for all grids.

The numerical model can simulate systems with variable permeability. The saturated permeability, k_s, in the unshaded area of the model (Figure 30) was 1.3×10^{-7} cm^2 and in the shaded area 1.3×10^{-8} cm^2. Thus, the saturated permeability in the unshaded area was 10 times greater than in the shaded area. However, all layers were assumed to have the same porosity. The dimensions of e and f (Figure 30) were 150 cm and 600 cm respectively.

Soil hydraulic properties are given in Figures 31 and 32. The longitudinal and lateral dispersion coefficients, D_L and D_T, were obtained as a function of Peclet Number, P_e (Bear, 1972). The resulting relationships are shown in Figure 33. Equations were derived from Figure 33 to represent the functional relationships between dispersion coefficients and Peclet Number. For the longitudinal dispersion coefficient:

$$D_L/D_d = 0.72 \ , \qquad P_e \leq 0.4$$

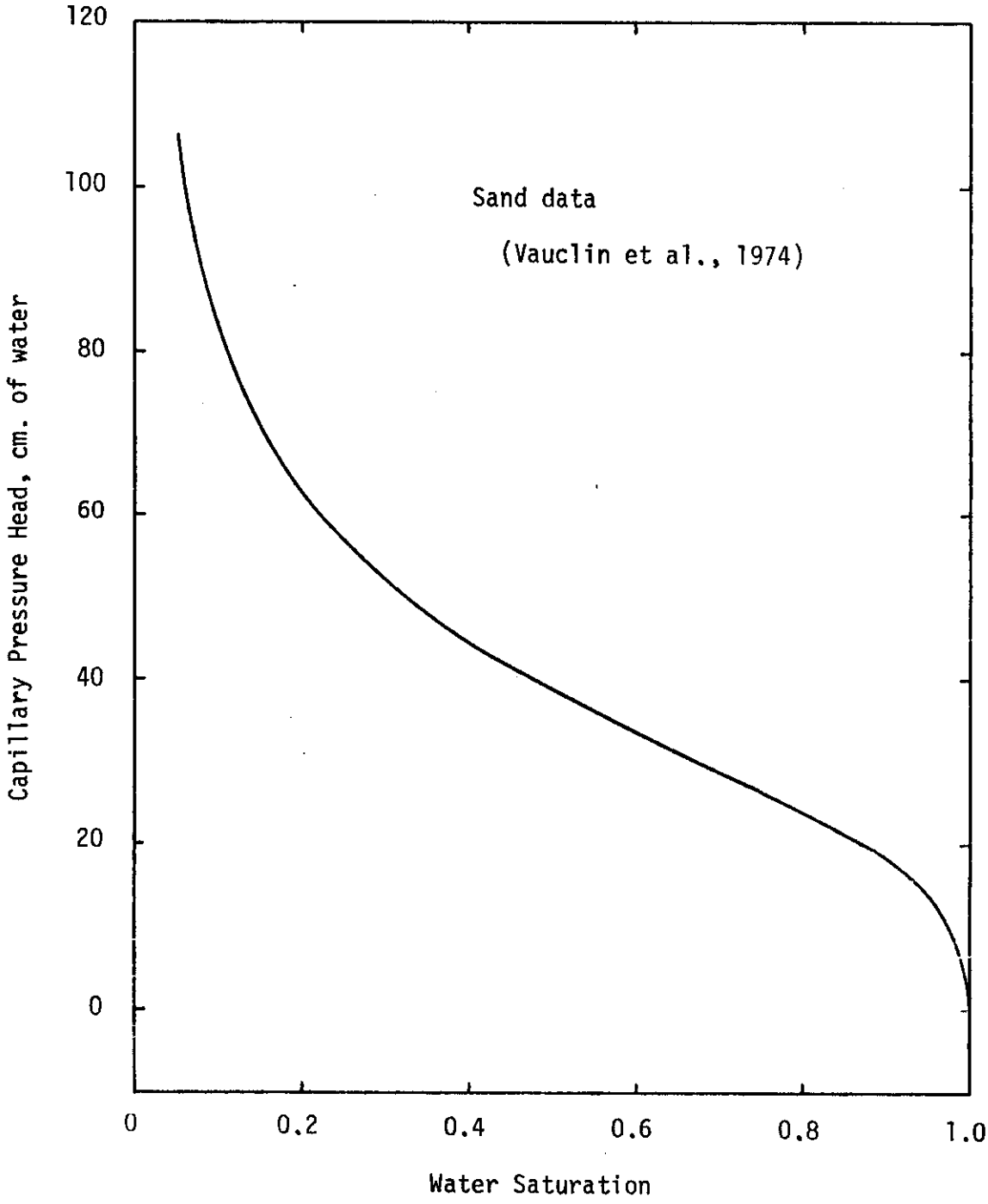

Figure 31. Capillary pressure head as a function of water saturation for the drainage problem.

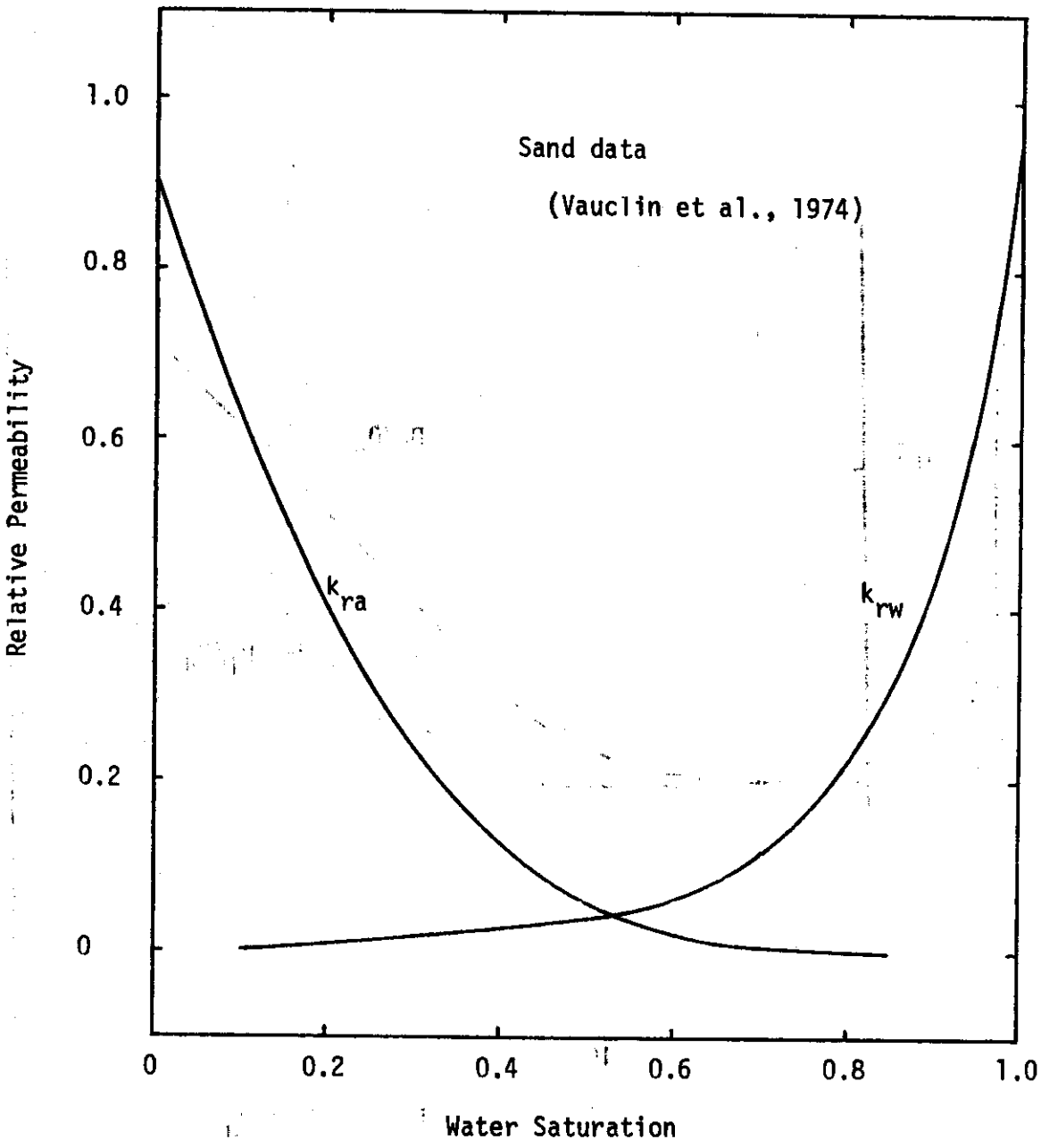

Figure 32. Relative permeabilities for water and air as a function of water saturation for the drainage problem.

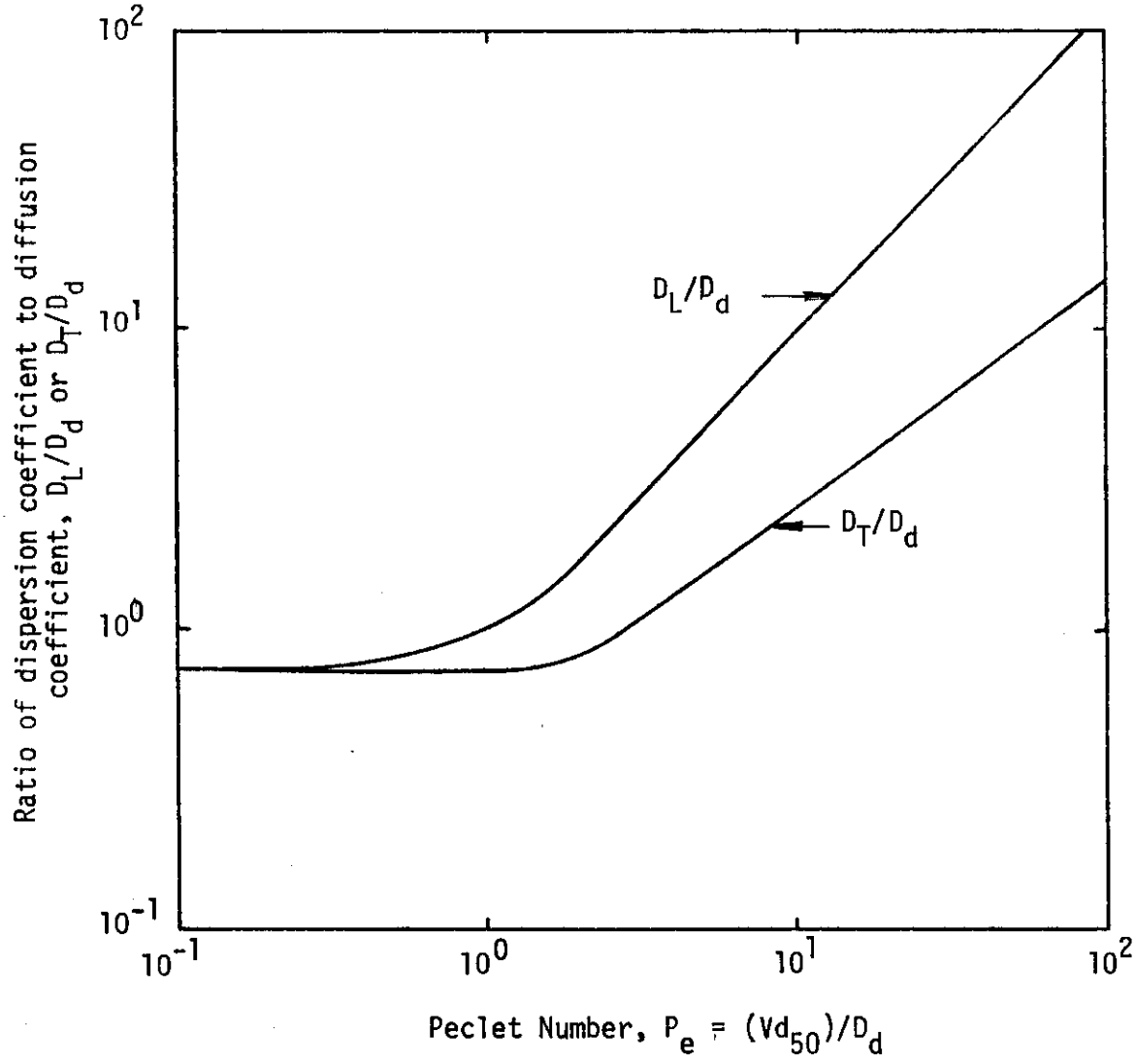

Figure 33. Dispersion coefficients as a function of Peclet number (After Bear, 1972).

$$D_L/D_d = 0.59 \exp(0.53\ P_e), \qquad 0.4 < P_e \leq 2$$

and

$$D_L/D_d = 0.81\ P_e^{1.083} \qquad 2 < P_e \leq 100 \qquad (73)$$

where D_d is the molecular diffusion coefficient (= 1.85×10^{-5} cm^2 sec^{-1}). The mean grain size diameter, d_{50}, was given by Bear (1972) as:

$$d_{50} = \left(\frac{k_s}{6.54 \times 10^{-4}}\right)^{0.5} . \qquad (74)$$

For the transverse or lateral dispersion coefficient:

$$D_T/D_d = 0.72 \quad , \quad P_e \leq 1.5$$

$$D_T/D_d = 0.6\ P_e^{0.499} \quad , \quad 1.5 < P_e \leq 3$$

and

$$D_T/D_d = 0.465\ P_e^{0.746} \quad , \quad 3 < P_e < 100 . \qquad (75)$$

Water pressures were obtained implicitly using equation (40) and water and air saturations were obtained explicitly using equations (44) and (46). The numerical simulation was made for 100 time steps or 57.8 hours. A maximum change in water saturation of only 0.05 was allowed during any one time step. If a change in water saturation greater than 0.05 occurred, the time step size was reduced and the calculations redone. Water pressures and water saturations were changing very slowly towards the end of the simulation. Therefore, the fluid velocities were assumed to have reached steady state. The infiltration rate of water at the land surface at steady state was 0.0234 cm/sec. The total computer time required to run the program for this 13 x 18 grid network was 240 seconds or 2.4 seconds per time step.

Figures 34 and 35 show the equipotential lines and the water table positions at 9.7 hours and 57.8 hours. The continuity of the potential field in the entire flow domain of saturated and unsaturated zones is clearly demonstrated in these figures. The water table position was obtained numerically by interpolating to zero between negative and positive water pressure heads. If the water pressures in a column were all positive, the water table position for that particular column was defined at the soil surface.

The equipotential lines of -240 cm and -250 cm in Figure 34 illustrate the effects of using a layered porous media. These equipotential lines are nearly vertical above the permeability transition. Within the less permeable zone, the slope of these lines changes. If the porous medium was homogeneous, these equipotential lines would be nearly vertical through the entire depth of the medium.

Figure 35 illustrates some of the effects of time upon the infiltration process. As infiltration proceeds, the equipotential curves move forward and their slopes are changed. Figures 34 and 35 also demonstrate that the water movement involves vertical as well as horizontal flow components.

To illustrate the effect of vertical and horizontal flow components, distribution of water fluxes at time t = 57.8 hours is shown in Figure 36 using a vectorial representation. At each grid center, the vertical and horizontal pore-velocities are obtained from the Darcian flux. The resultant velocity vector is then drawn at each grid center with a length proportional to its size. Figure 36 shows the magnitude and direction of the pore-velocities at time

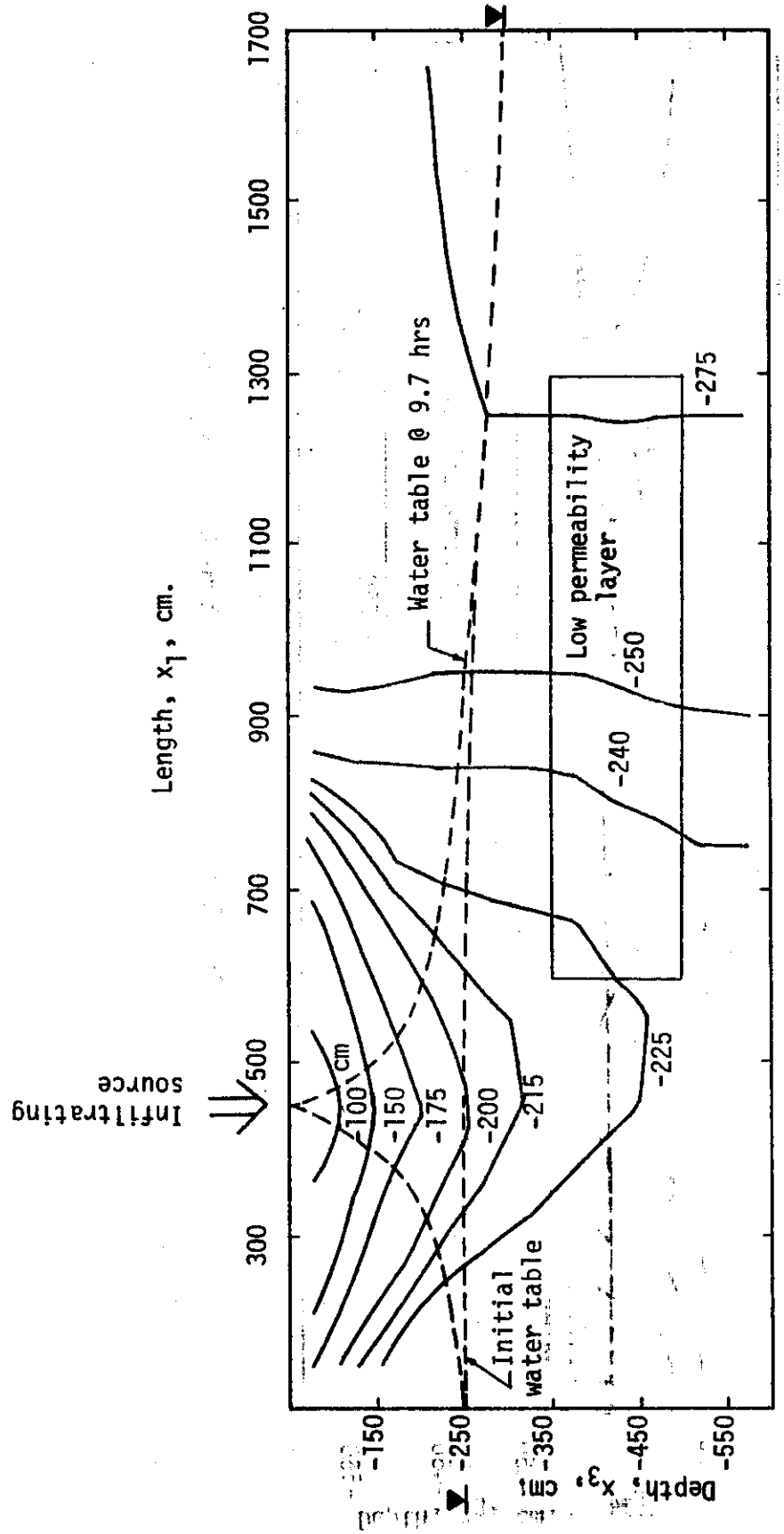

Figure 34. Equipotential map at time t = 9.7 hours

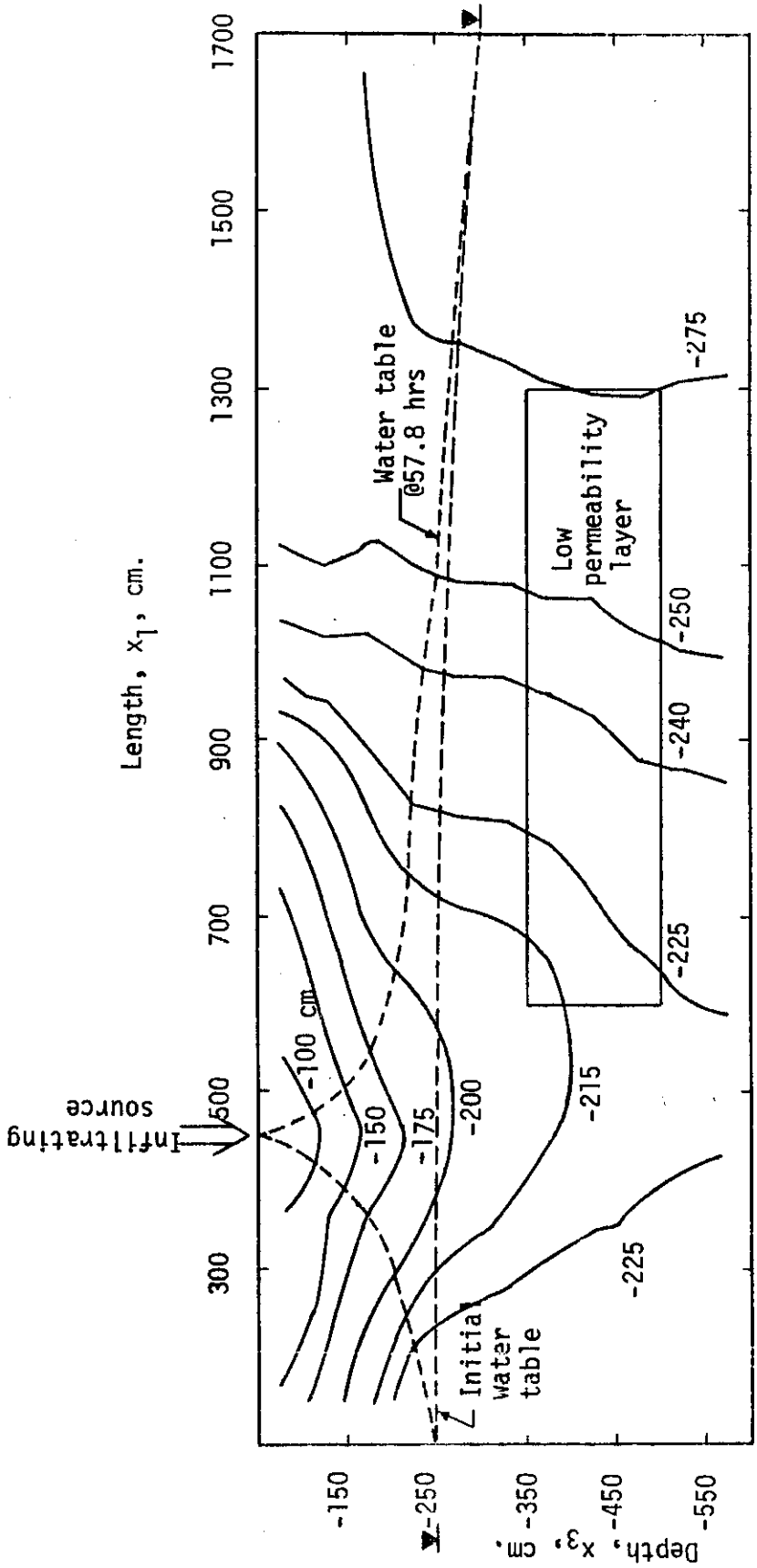

Figure 35. Equipotential map at time t = 57.8 hours

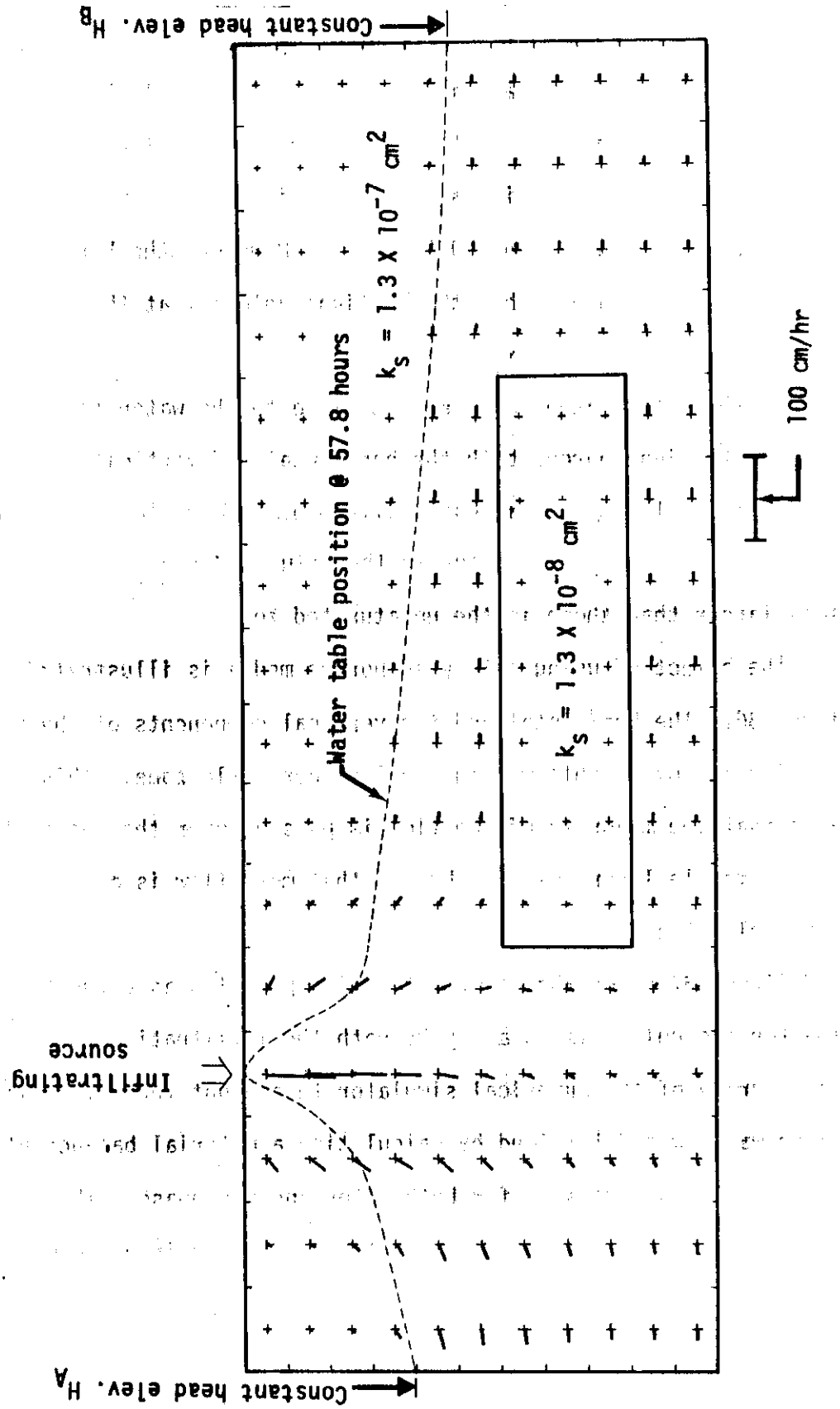

Figure 36. Pore-velocity distribution at time t = 57.80 hours.

t = 57.8 hours. As expected, the vertical component of the pore-velocity is clearly dominant in the column immediately beneath the infiltrating source. The vertical pore-velocity at the grid center immediately below the infiltrating source is 76.0 cm/hr while the horizontal component is only 0.50 cm/hr. However, the horizontal velocity is much larger than the vertical velocity at the two outflow faces at $x_1 = 0$ and $x_1 = \ell_1$.

In the unsaturated zone, except close to the water table and the infiltrating source, both the horizontal and vertical components of the pore-velocity are almost negligible compared to those in the saturated zone. The velocities in the saturated zone are several times larger than those in the unsaturated zone.

The effect of using a layered porous media is illustrated in Figure 36. The horizontal and the vertical components of the pore-velocity are negligible within the less permeable zone. This indicates that the majority of the flow is passing over the top of the less permeable layer. It is obvious that more flow is also taking place below the less permeable layer.

Figure 37 shows the water saturation profiles as a function of time for the column immediately beneath the infiltrating source. The accuracy of the numerical simulator to account for all infiltrated water was determined by calculating a material balance at the end of each time step for both water and air phase. The cumulative material balance error for either water or air phase was defined as:

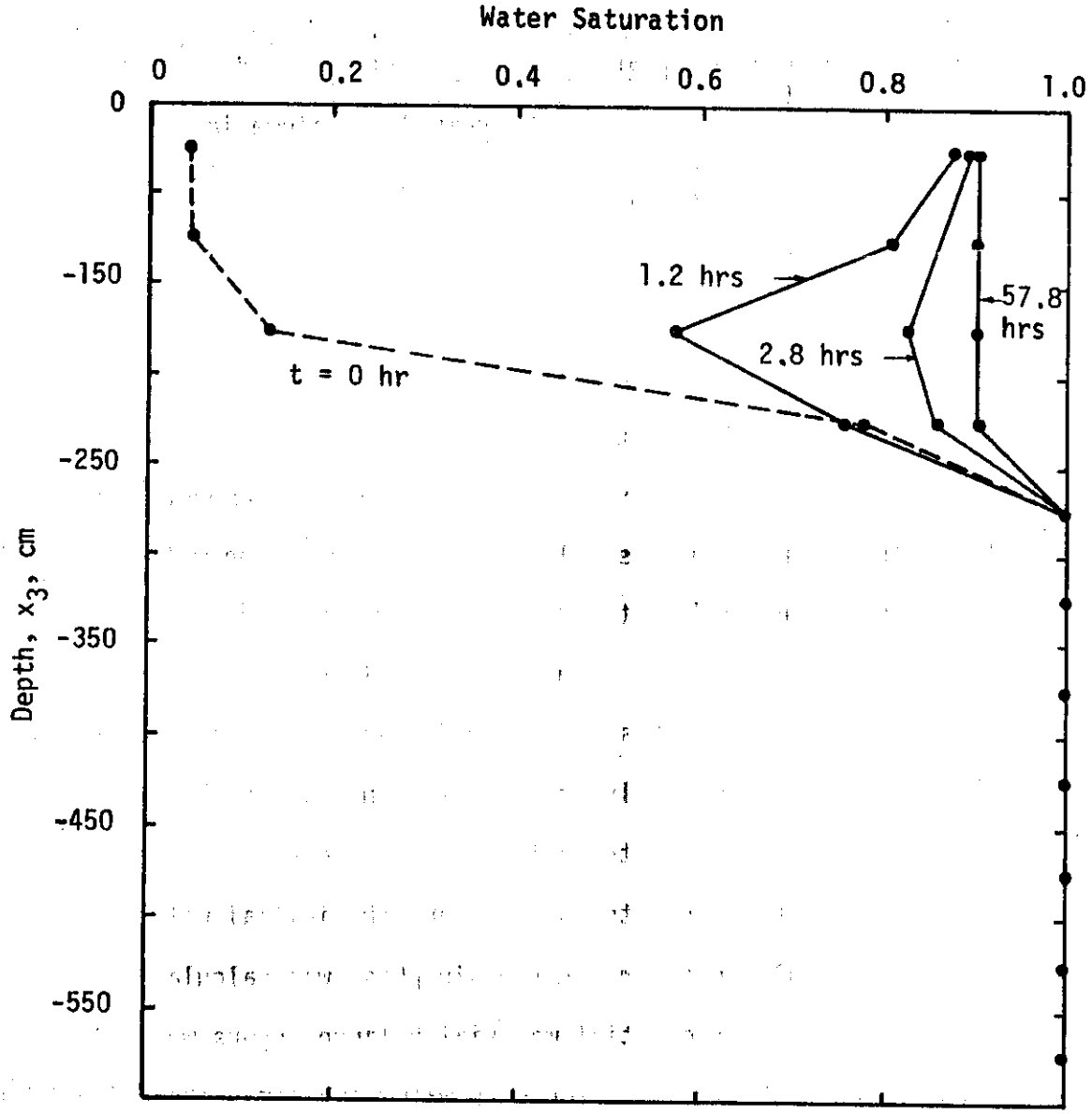

Figure 37. Water saturation profiles for the column beneath the infiltrating source (x_1 = 450 cm) at various times.

$$\text{Cumulative material balance error (\%)} = \left\{ \frac{\text{Change in volume storage} - \text{Total volume infiltrated} + \text{Total volume leaving}}{\text{Total volume infiltrated} + \text{Total initial volume in system}} \right\} \times 100 \qquad (76)$$

The total amount of water infiltrated into the system was calculated by integrating the volume of water over the appropriate inflow boundaries at $x_3 = 0$. The total amount of water leaving the system was calculated by integrating the volume of water over the outflow boundaries at $x_1 = 0$ and $x_1 = \ell_1$. The cumulative amount of water in the system at any time was calculated by summing the water saturation at each grid node and multiplying the resulting sum by the total pore volume of the system. The initial volume of water in the system was calculated by summing the initial water saturation at each grid node and multiplying the resulting sum by the total pore volume. The change in water volume was defined as the difference between the cumulative water storage and the initial water storage. The material balance error for the air phase was calculated in a similar manner. Differential material balance errors were also computed for each time step for both water and air. The definition of the differential error is analogous to the cumulative material balance error.

Cumulative and differential errors were of the order of 10^{-3} percent for the water phase using "single precision" for all the variables and constants in the computer program. A "single precision" number can represent a precision of at most seven digits after the decimal whereas, using "double precision," over 16 significant digits

can be recorded. While the term "double precision" implies a doubling of precision, in actual practice, more than a doubling is achieved. Cumulative and differential errors were of the order of 10^{-8} percent using "double precision" for all the variables and constants in the computer program. However, "double precision" numbers occupy double the physical space in the computer's memory and the computations require longer execution times. "Single precision" was, therefore, used in the entire computer program. The differential error for the air phase was of the order of 10^{-2} percent towards the end of simulation. The cumulative error for the air phase was about 1.0 to 1.5 percent. This was due to the fact that the air saturation at the end of each time step was obtained by subtracting the water saturation from one. This resulted in some error which accumulated over time. This could be improved by iterating within each time step, that is, updating the fluid flow coefficients and resolving the water pressures and saturations. This would increase the computation time considerably. Nevertheless, a cumulative error of 1.0 to 1.5 percent for the air phase at the end of 57.8 hours of simulation was considered very reasonable and no further attempts were made to improve it.

Besides the material balance error, an independent check on the accuracy of the two-phase numerical simulator is provided by calculating the saturation error for each grid node at each time step. The saturation error, as discussed in Chapter IV, is the error resulting from the sum of water and air saturations being different from one at the end of a time step. A tolerance of 0.01 was allowed

for the saturation error. If the sum of water and air saturations does not converge to unity, an iteration of the fluid flow equations is necessary. This was, however, seldom needed for this problem.

All previous investigators working with an integrated saturated-unsaturated flow domain experienced difficulties in simulating the moving water table boundary between the two flow regions. This study was no exception. In the initial phase of this study, considerable difficulties were encountered when a grid changed from a negative to a positive water pressure head or vice-versa. Most of these difficulties, as discovered later, were due to an erroneous assumption. The air pressures were wrongly assumed to be zero at all times in the saturated flow region. This created a discontinuity in the capillary pressure and resulted in error in the numerical solution. The problem was overcome by maintaining a continuous air pressure distribution in both the saturated and unsaturated flow regions.

Also, the method of calculating the flow coefficients does have an influence on the accuracy of the numerical solution. The use of the "upstream mobility" concept, as discussed in the petroleum literature (Brutsaert, 1971), to calculate the fluid flow coefficients resulted in more accurate numerical results. To compute the fluid flow coefficient between any two grids, the "upstream mobility" concept uses the relative permeability of water or air of the grid from which the fluid emanates. This concept is particularly useful when a grid is desaturating, that is, changing from positive to negative water pressures or when a grid is saturating, that is,

changing from negative to positive water pressures.

The water and air saturations, in this numerical simulator, were obtained explicitly. An explicit scheme has stability criterion and, for the numerical solution to be stable, the time step size has to be limited. The time step size in this study was limited by not allowing the water saturation at any one time step to be greater than 0.05. However, as the grids saturated, the explicit nature of the numerical scheme resulted in "overshoot" in the water saturations at some time steps and the water saturations for several grids exceeded one. The "overshoot" was usually of the order of 10^{-2}. Such an "overshoot" accumulates over time and gets larger. To overcome this problem, a scan was made of all the grid saturations at each time step and the small amount of "overshoot" was distributed over all unsaturated grids. This created no new problems and the "overshoot" problem was not a major obstacle to the numerical scheme.

Figure 38 shows the relative concentration of displaced fluid as a function of time. The relative concentration of the displaced fluid was defined as the ratio of the total tracer outflow volume to the total water outflow volume. The infiltrating tracer mass did not reach the outflow boundary at $x_1 = \ell_1$ for a simulation time of 57.8 hours. Therefore, the trace mass leaving the system at the outflow face at $x_1 = 0$ is only represented in the tracer outflow volume. For a simulation time of 57.8 hours, the relative concentration of the displaced fluid reached a maximum of $C/C_0 = 0.64$. Longitudinal concentration profiles at various times immediately

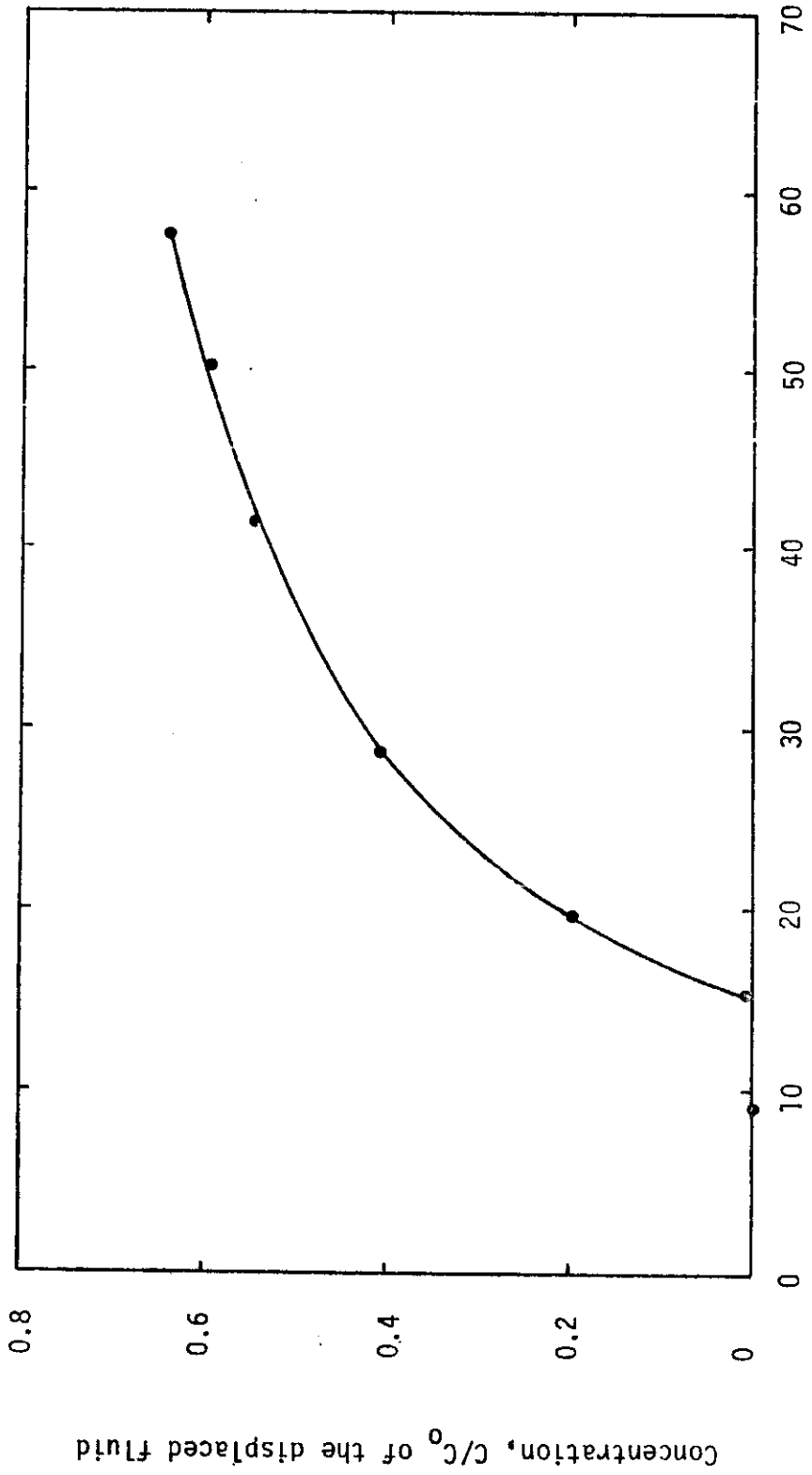

Figure 38. Concentration of displaced fluid as a function of time.

beneath the infiltrating source are depicted in Figure 39. Lateral concentration profiles at time t = 5.7 hours are shown in Figure 40. These figures indicate the relative concentrations are very close to either one or zero. This is because the flow velocities are very small for this problem, and therefore dispersion is also very small.

Instead of using the concentration profiles shown in Figures 39 and 40, a better form of illustration is to plot the concentrations of the moving points at various times. Such a plot locates a moving point with its coordinates and concentration and when all the points are plotted, a concentration map is generated. Figures 41 through 44 show concentration maps of the moving points at various times. As discussed earlier in Chapter IV, grid concentrations are obtained by averaging the concentrations of all moving points within a grid at the end of a time step. Such an averaging scheme is sometimes misleading, particularly when the concentration of the moving points in a grid are either $C/C_0 = 1$ or $C/C_0 = 0$. A more efficient computational scheme would be one which uses the coordinates of the moving points to obtain a weighted average for the grid concentration. Reddell and Sunada (1970) developed such a computational scheme for a steady, uniform flow field. A similar scheme would be very difficult to program for the non-uniform, transient velocity field developed in this problem. In the absence of a more efficient averaging scheme, it appears desirable to plot a moving points' concentration map instead of a grid concentration map.

As the moving points exit the system at $x_1 = 0$ or $x_1 = \ell_1$, they are reintroduced at the appropriate inflow boundary. The

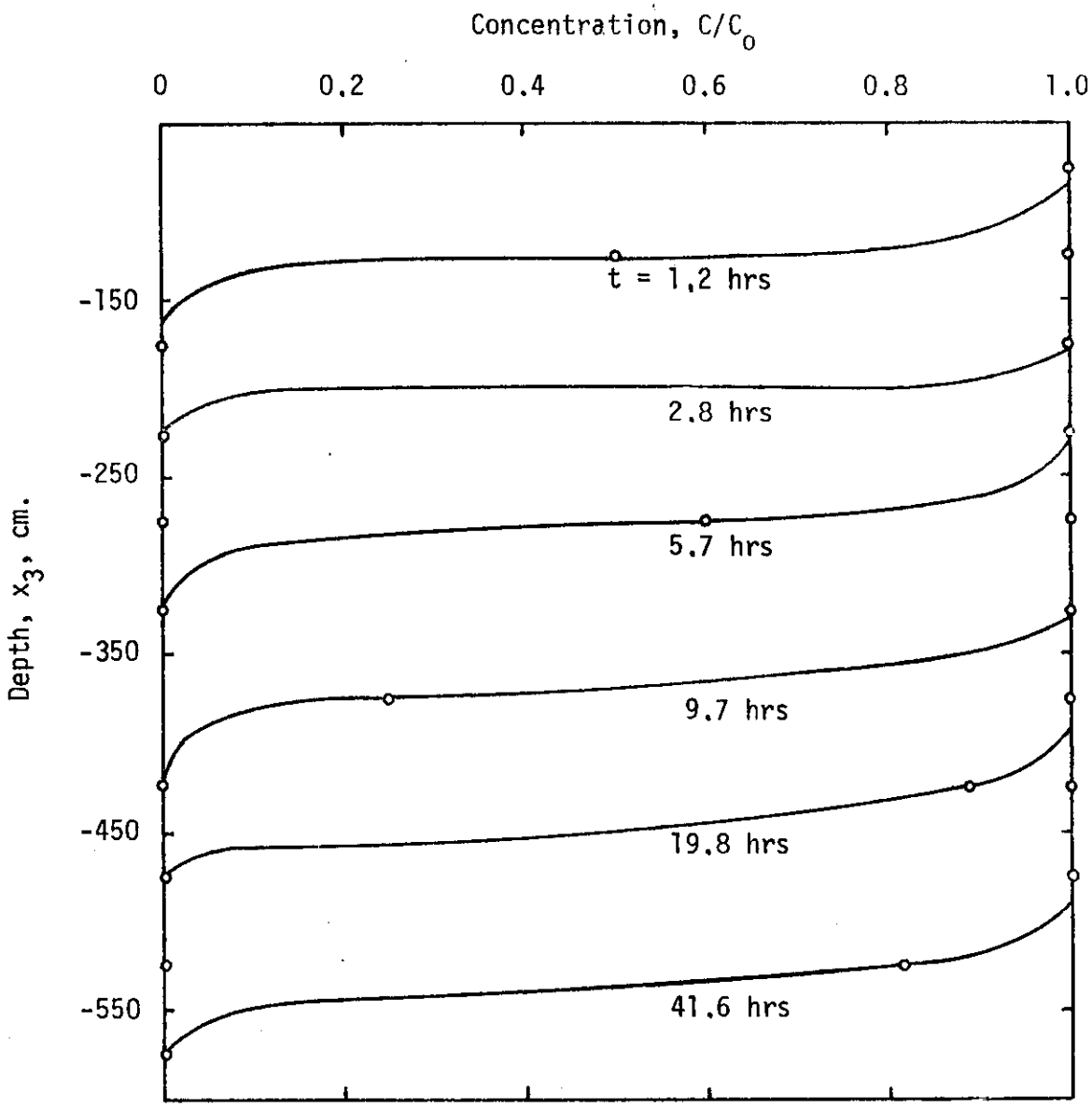

Figure 39. Longitudinal concentration profiles for the column beneath the infiltrating source (x_1 = 450 cm) at various times.

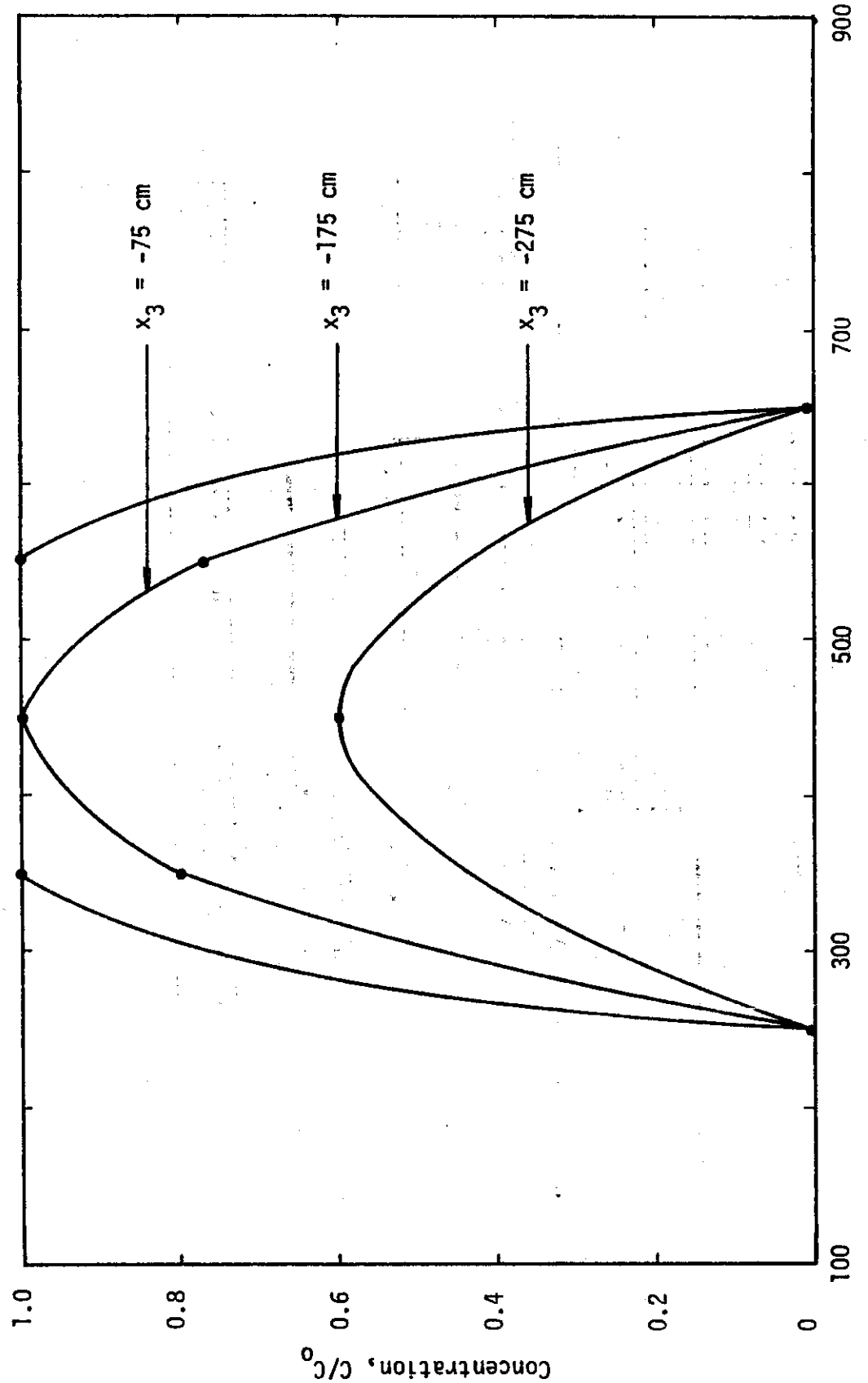

Figure 40. Lateral concentration distribution at time t = 5.7 hours.

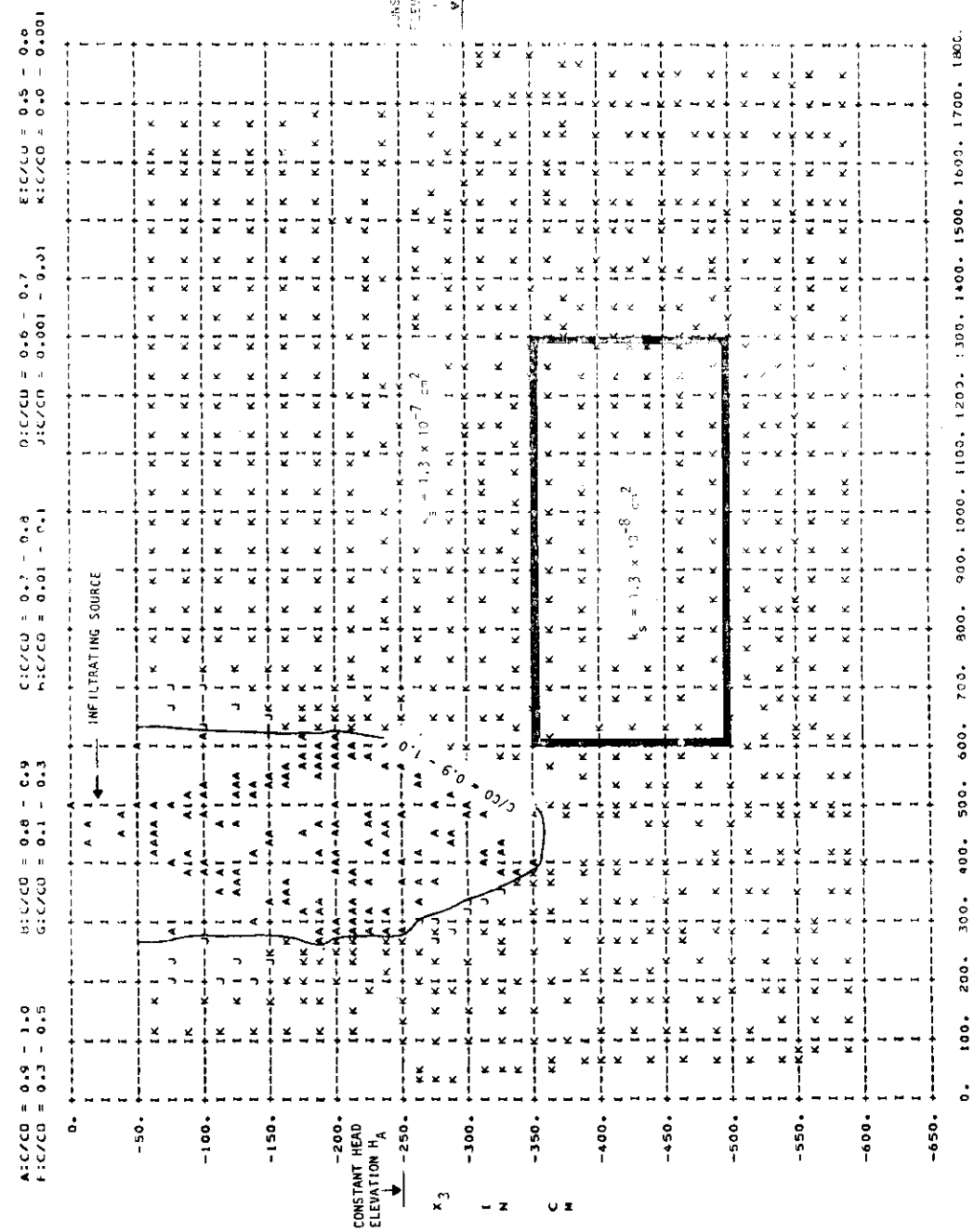

Figure 41. Moving points' concentration map at time t = 9.70 hours.

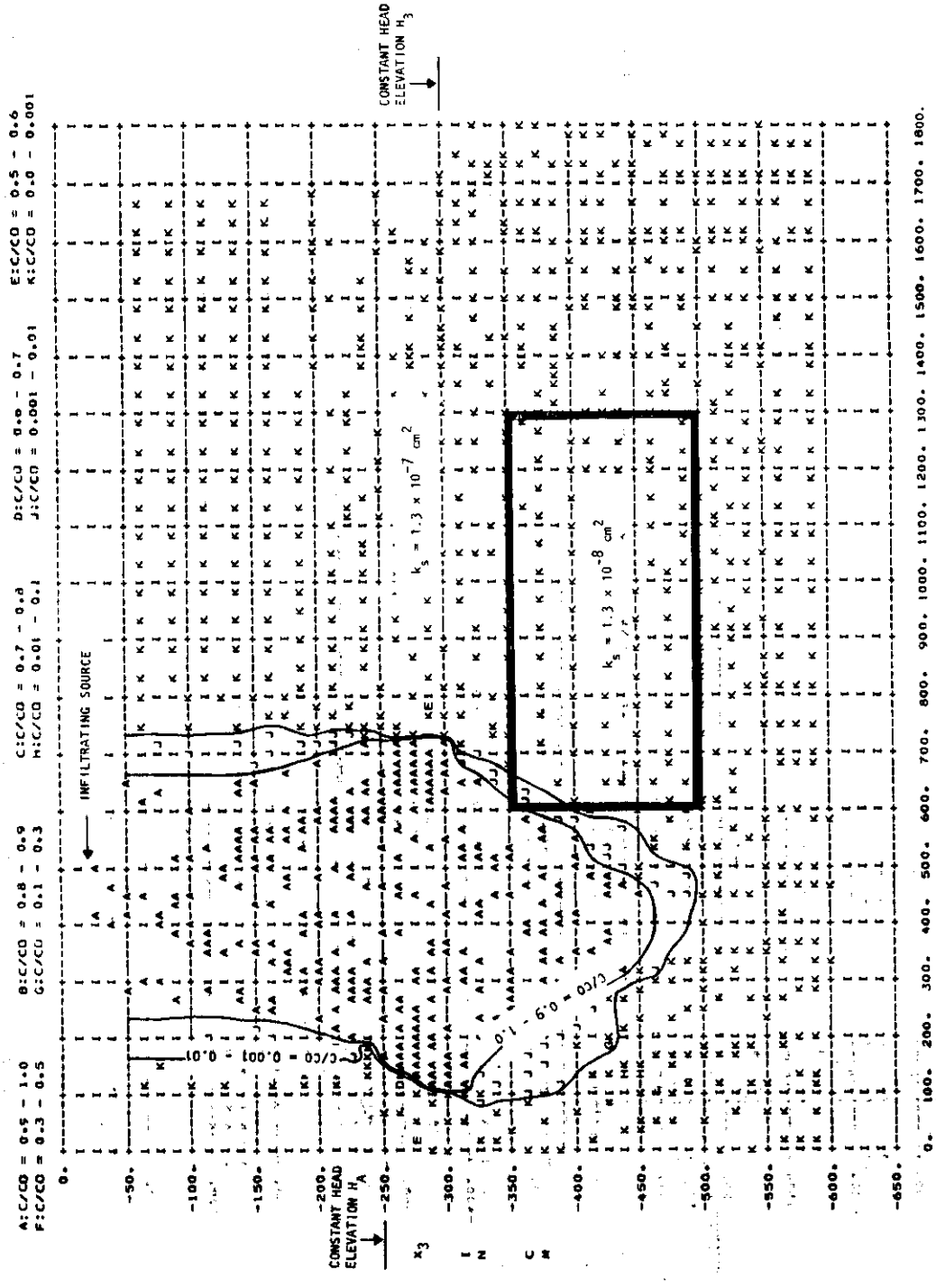

Figure 42. Moving points' concentration map at time t = 19.80 hours.

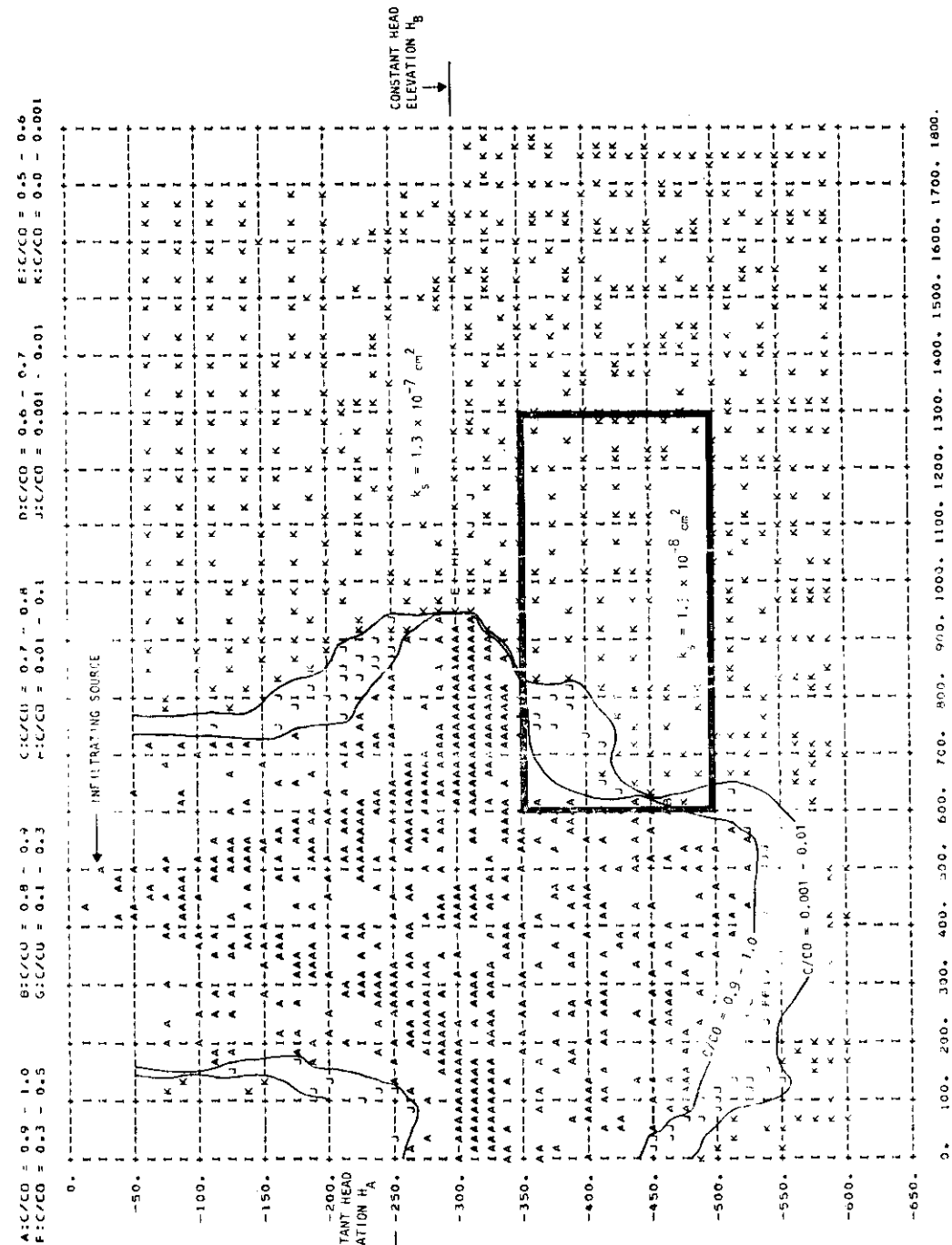

Figure 43. Moving points' concentration map at time t = 41.60 hours.

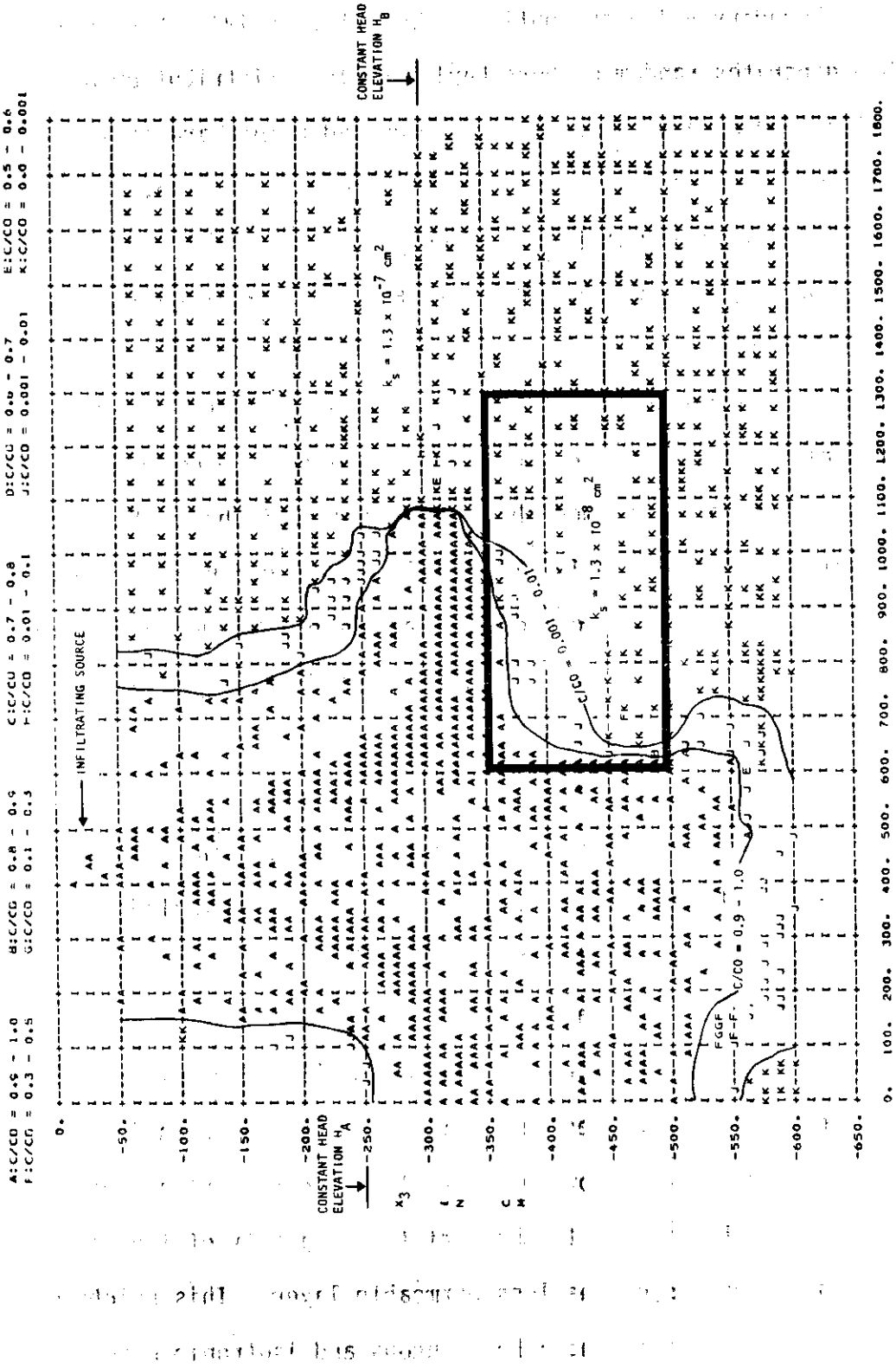

Figure 44. Moving points' concentration map at time t = 57.80 hours.

coordinates of the reintroduced points are randomly assigned at the inflow boundary using subroutine RANDU (Chapter IV). Subroutine RANDU generates random numbers having uniform distribution and ranging from zero to one. The reintroduced points are assigned the concentration of the appropriate inflow boundary. Also, if the number of moving points in a grid drops below a specified minimum number, new points are introduced in that grid to bring it to a minimum number. Subroutine RANDU is again used to assign the coordinates of the new moving points and the grid or grids the fluid is emanating is taken into account in assigning the coordinates. The new points are assigned the concentration of the grid or grids the fluid is emanating. Initially, the new or old points were introduced with the same coordinates as the initial moving points in that grid. As a result, the reintroduced points traced essentially the same flow paths as the original moving points. This generated no new flow paths and no new knowledge. Discontinuities in the concentration distribution were also established. These problems were corrected by reintroducing or adding points with their coordinates assigned randomly using subroutine RANDU.

The effect of using a layered porous media is illustrated in Figures 43 and 44. As expected, the grids above the permeability transition zone accumulated moving points with concentrations close to $C/C_o = 1$ and grids below the transition had concentrations close to $C/C_o = 0$. This is due to the fact that majority of the flow is passing over the top of the less permeable layer. This points out the limitations of assuming a homogeneous and isotropic porous

media which have been used in many previously developed models. The times of travel of the moving points are inversely proportional to the saturated permeability. Freeze (1972) showed that with about the same length of flow paths, the time of travel in one case was less than half of the other. This was due to the nonhomogeneous and anisotropic nature of real aquifers. The flow path with least travel time traversed high permeability layers and avoided the low gradient, low permeability layers.

Material balance errors were computed at the end of each time step for the tracer. The cumulative material balance error for the tracer was defined as:

$$\text{Cumulative tracer material balance error (\%)} = \left[\frac{\text{Tracer storage change} - \text{Total tracer injected} + \text{Total tracer leaving}}{\text{Total tracer injected} + \text{Total initial tracer in system}}\right] \times 100 \qquad (77)$$

The total amount of tracer injected into the system was calculated by integrating the infiltrated water volume multiplied by the relative concentration, C/C_o, of the infiltrating tracer. The above integration was carried out over the appropriate inflow boundaries at $x_3 = 0$. The total amount of tracer leaving the system was calculated by integrating the water volume leaving the system over the outflow boundaries at $x_1 = 0$ and $x_1 = \ell_1$ and multiplying it by the relative concentration, C/C_o, of the outgoing tracer. The cumulative amount of tracer in the system at any time was calculated by summing the average grid concentration over all grid nodes in the system. The initial amount of tracer in the system was calculated by

summing the average initial grid concentration over all grid nodes in the system. The change in tracer storage was defined as the difference between the cumulative and initial tracer storage. Differential material balance error was also computed for each time step. The expression for the differential error is analogous to that of the cumulative error.

The material balance error for the tracer is very much dependent on the numerical scheme of MOC. In the first few minutes of simulation, no moving points with the concentration of $C/C_0 = 1$ have moved into the system. However, the amount of tracer injected into the system was calculated by integrating the infiltrated water volume multiplied by its tracer concentration of $C/C_0 = 1$. Since in the initial few minutes of simulation, the tracer storage change and the tracer leaving the system are essentially zero, the cumulative error, using equation (77), is calculated as 100 percent. But as time progresses, moving points move into the system and the material balance error begins to decrease. This decay in the material balance error with time is illustrated in Figure 45. The cumulative tracer material balance error near the end of 57.8 hours of simulation was on the order of 2.0 to 2.5 percent. Much better results could be obtained if the cumulative tracer storage was calculated based on the area occupied by the isochlors (Figure 44) instead of using the average grid concentration. Differential tracer material balance errors were also computed for each time step. They ran about 5 to 10 percent near the end of simulation. Because of the nature of MOC, it was difficult to keep a check on the differential tracer

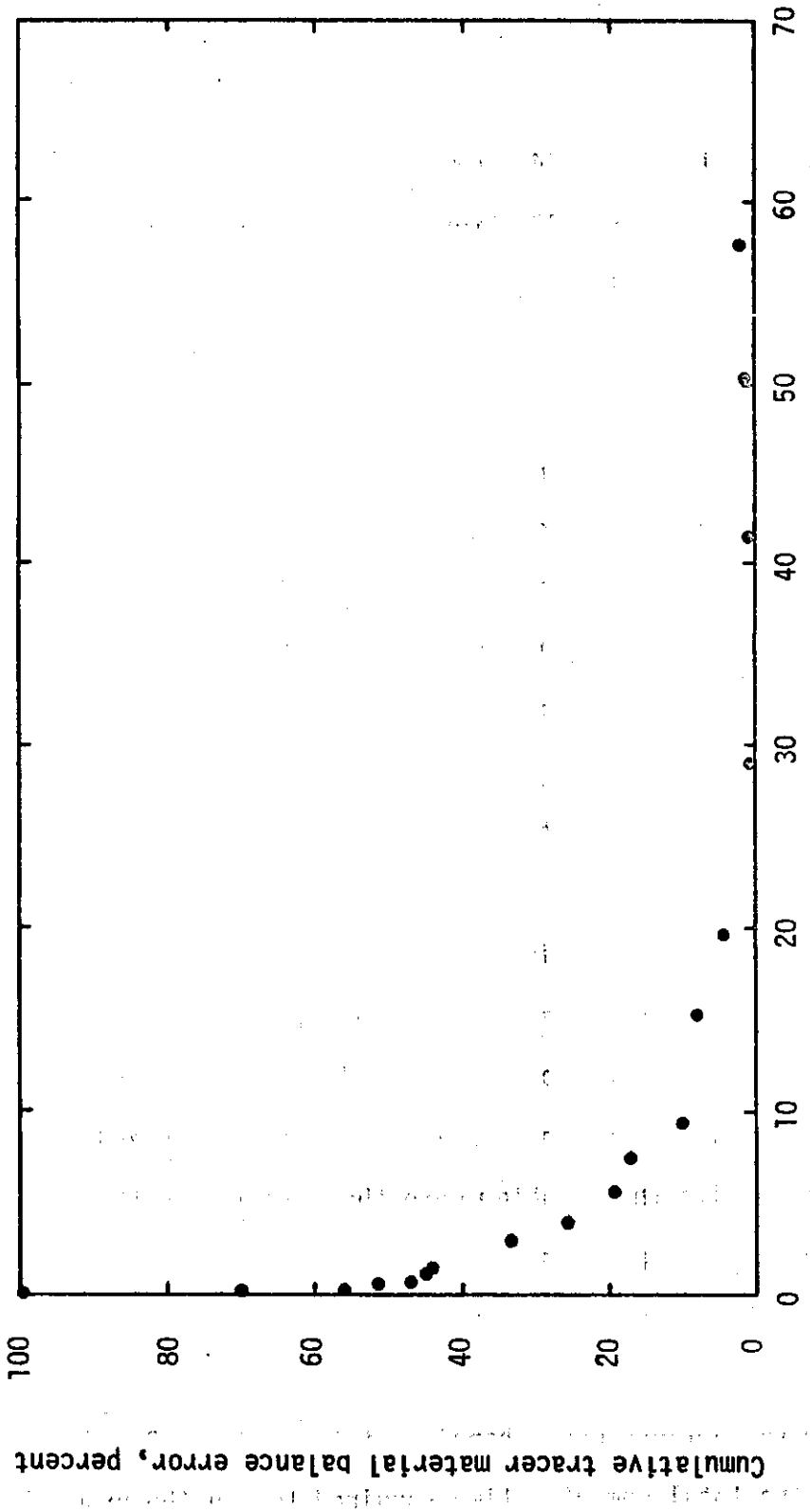

Figure 45. Cumulative tracer material balance error as a function of time.

material balance errors. However, the cumulative tracer errors obtained near the end of simulation were considered to be very reasonable.

Figures 41 through 44 show the isochlor, C/C_o = 0.9 - 1.0, at various times. Figures 42 through 44 also show the isochlor, C/C_o = 0.001 - 0.01, at various times. There were very few points which had concentrations between the ranges of A and K, indicating that the concentration profiles are extremely steep.

The above drainage problem was on a small scale. A problem describing the migration of septic-tank wastes around the perimeter of a lake was considered and solved using the total numerical simulator of fluid flow and dispersion equations. A schematic diagram of the septic-tank problem is similar to Figure 30 of the drainage problem. The elevation H_B represents the constant head at the lake. The polluting source is at ab (Figure 30) and seeps through the unsaturated region and into the saturated region.

Data used for analyzing the septic-tank problem were: Δx_1 = 2000 cm, Δx_3 = 50 cm, NR = 13, NC = 26, ℓ_1 = 520 meters, and ℓ_3 = 650 cm. The dimensions for aa, ab, and f were 80 meters, 20 meters, and 120 meters, respectively. All other dimensions and data used to numerically solve this problem were the same as for the previously described drainage problem.

The numerical simulation was made for 400 time steps or about 42.8 days. A steady state was not reached, and the water pressures and water satuartions were changing at the end of 42.8 days of simulation. The total computer time required to run the program for this

13 x 26 grid network was 1126 seconds of 2.8 seconds per time step.

Figure 46 shows the initial water table position and the water table position at the end of 42.8 days of simulation. A moving points' concentration map at the end of 42.8 days of simulation is shown in Figure 47. Since the vertical dimension of the model was much smaller compared to the horizontal scale, the moving points moved essentially in a vertical direction. The moving points did not reach the outflow face at $x_1 = 0$ at the end of 42.8 days. It would take a much longer period of time for the moving points to reach the outflow face at $x_1 = \ell_1$. The problem, therefore, needs to be run for a longer time to obtain more results. The cumulative material balance error for the water, air, and tracer were of the order of 10^{-3}, 6.0 and 3.5 percent, respectively at the end of simulation.

A typical drainage problem in agriculture and a septic-tank problem were solved using the two-dimensional, two-phase, saturated-unsaturated infiltration and dispersion model developed in this study. The numerical results obtained using the model indicated that the movement of pollutants in an integrated saturated-unsaturated porous medium is a valid and reproducible phenomenon. No analytical solution, numerical solution, or experimental data were available to compare with the numerical results obtained using the total numerical simulator. However, the cumulative and differential material balance errors for the air, water, and tracer provide an independent check on the accuracy of the total simulator. The cumulative and differential errors obtained using the model were reasonable. This suggests that the total numerical simulator was

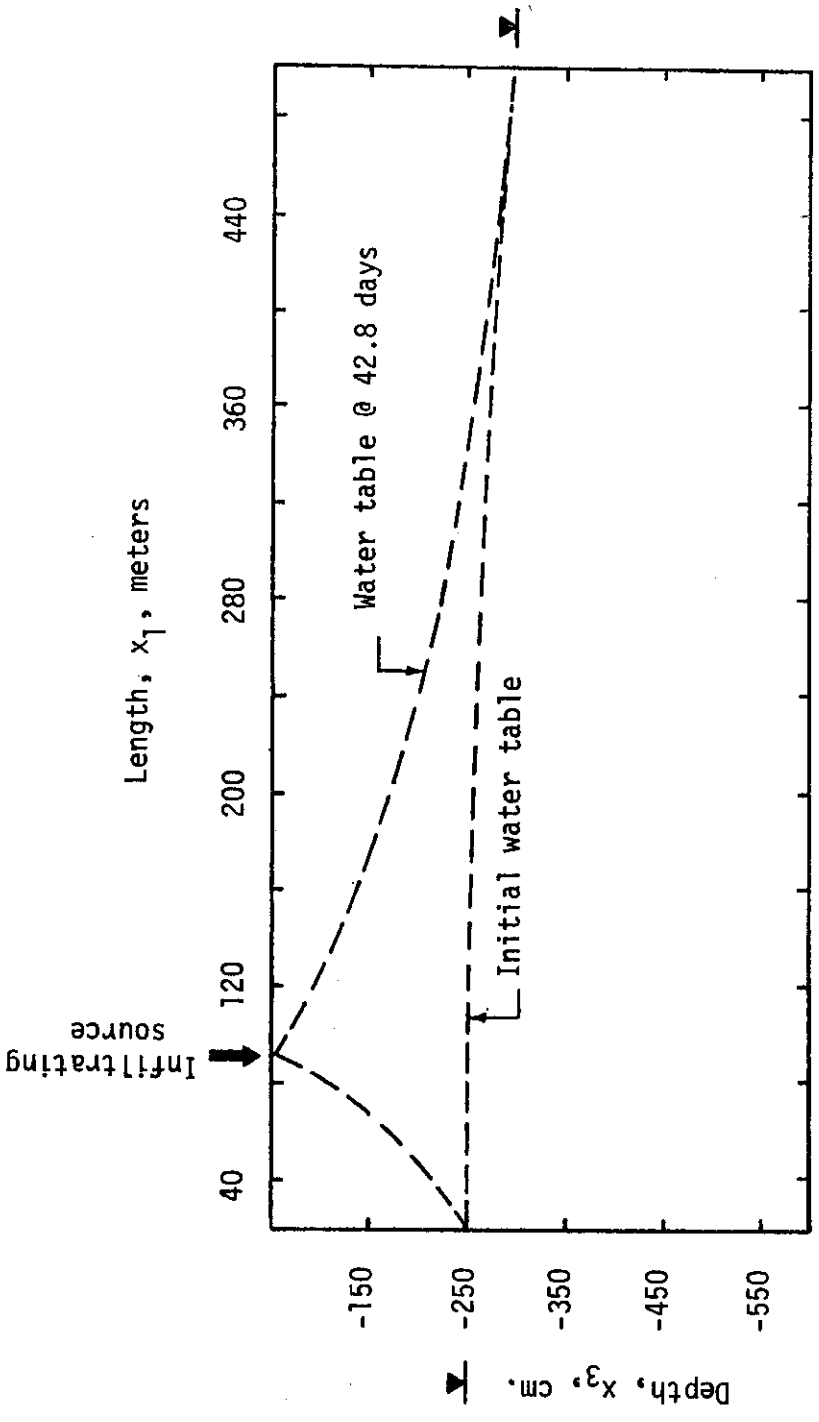

Figure 46. Initial water table and water table position at the end of 42.8 days for the septic-tank problem.

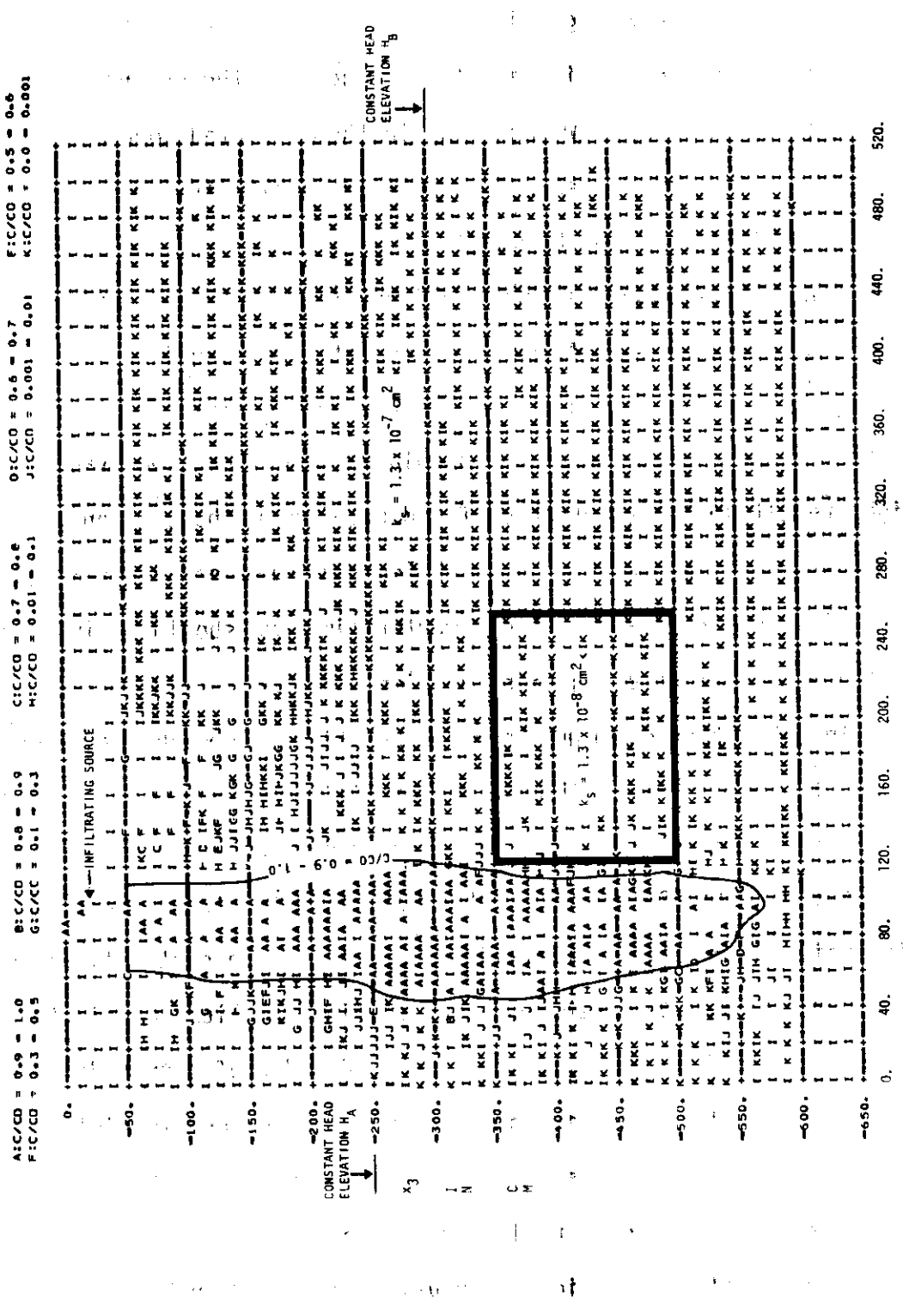

Figure 47. Moving points' concentration map at time t = 42.8 days.

working well.

The model can provide a variety of outputs, such as an equipotential map or a moving points' concentration map at any given time step. The hydrologic results obtained for the drainage problem indicate most of the flow occurring in the saturated zone. The behavior of a nonhomogeneous porous media is illustrated by using a less permeable layer in the model.

Since dispersion was very small and the tracer was moving as a slug flow, the use of a tensor transformation was believed to have little or no influence on the concentration profiles for the two problems solved using the total simulator. However, the error that might result in the solution of field problems without a tensor transformation is unknown. Nevertheless, the use of tensor transformation required very little computer time and should be included in the numerical solution of dispersion problems.

In laboratory experiments using relatively homogeneous porous media, the longitudinal dispersion coefficient is normally found to be greater than the lateral or transverse dispersion coefficient by a factor of 5 to 20. Also, in these experiemnts, the values for the dispersivity are of the order of 10^{-2} to 1 cm. In contrast, values of dispersivity used in the modeling of field problems are in the range of 10 to 100 meters, which is 3 to 6 order of magnitude larger than typical laboratory values. This wide difference in field and laboratory dispersivity estimates is because of the nonhomogeneous and anisotropic nature of real ground water flow systems in contrast to laboratory studies, which are usually performed on homogeneous

materials (Reddell and Sunada, 1970).

The numerical simulator developed in this study can be applied to environmental problems concerning groundwater contamination from waste disposal sites, provided the values of the input parameters, such as the field dispersivities, are known under field conditions.

This work is a first step in developing a numerical simulator for miscible displacement in the entire flow domain of saturated and unsaturated regions. The uniqueness of the model is shown in the following set of properties:

1. The model is three-dimensional. However, only two-dimensional problems were solved using the numerical simulator;

2. The model considers infiltration as a two-phase (air-water) process;

3. The model has its upper boundary at the ground surface. It treats the complete subsurface regime as a unified whole because the flow in the saturated region is integrated with that in the unsaturated region;

4. The model can handle a combination of a variety of realistic boundary conditions;

5. The model recognizes the tensorial nature of the dispersion coefficients;

6. The model can handle transient as well as steady state conditions; and

7. The model allows consideration of nonhomogeneous porous media.

CHAPTER VI

CONCLUSIONS AND RECOMMENDATIONS

A three-dimensional model describing the two-phase (air-water) fluid flow equations in an integrated saturated-unsaturated porous media was developed. Also, a three-dimensional convective-dispersion equation describing the movement of a conservative, noninteracting tracer into a nonhomogeneous, anisotropic, integrated saturated-unsaturated porous medium was derived. Finite difference forms of these two equations were developed. The two models were linked by the pore-velocity term.

Using the two-dimensional form of the total simulator, a computer program was written in FORTRAN IV to solve the two-phase fluid flow and convective-dispersion equations in a nonhomogeneous, isotropic porous media. The computer program was developed to handle a variety of boundary conditions, such as, constant pressure, constant head, constant flux, a time-dependent flux based on rainfall rate, and a no-flow boundary. The two-phase fluid flow equations were solved using an implicit scheme to solve for water or air pressures and an explicit scheme to solve for water and air saturations. A numerical tensor transformation for an isotropic medium developed by Reddell and Sunada (1970) was used to treat the dispersion coefficient as a tensor. The method of characteristics as presented by Garder et al. (1964) was used to solve the convective-dispersion equations.

The fluid flow and convective-dispersion segments of the simulator were tested independently with success. The numerical results obtained from two-phase fluid flow problems were compared with analytical solutions

or experimental data. The method of characteristics (MOC) with numerical tensor transformation was used to test the convective-dispersion segment of the simulator for a uniform flow field and the numerical results were compared with analytical solutions for a homogeneous and isotropic media. A typical two-dimensional drainage problem in agriculture was solved in a nonhomogeneous, integrated saturated-unsaturated medium using the total simulator of fluid flow and convective-dispersion equations. A variety of outputs, such as an equipotential map or a moving points' concentration map showing isochlors were obtained at selected time steps. The limitations of the assumptions of a homogeneous and isotropic medium are illustrated by the accumulation of moving points at a transition from a higher to lower permeability. A field-size problem describing the migration of septic-tank wastes around the perimeter of a lake was also considered and solved using the total simulator.

The following specific conclusions can be drawn as a result of this study:

1. The numerical results obtained by using a two-phase fluid flow model were compared with those using a one-phase model. Excellent agreement was obtained with respect to infiltration rates, cumulative infiltration amounts and water saturation profiles when these results were compared with Philip's (1969) analytical solution. The numerical results indicated no significant differences using one-phase and two-phase flow models since the boundary conditions were such that there was no appreciable air pressure build-up.

2. To investigate the effect of existence of air in the porous medium, a time-dependent boundary condition problem in which the infiltration rate was a function of rainfall, ponding and flux at the soil surface was considered. The infiltration rates obtained were compared with those of Phuc and Morel-Seytoux's (1972) work. Unlike theirs, the infiltration rates did not show any scatter of points but followed a smooth curve. However, immediately after air counterflow starts, the curve behaved differently from theirs and dropped rapidly to a minimum value well below the saturated hydraulic conductivity. As soon as air was released from the medium, the infiltration rate increased to a value below the saturated hydraulic conductivity and continued to remain below after 10 hours of simulation. This is in contrast to one-phase flow in which the saturated hydraulic conductivity is the lower bound of infiltration rate. The infiltration rates, after the initial stage, showed excellent agreement with Phuc and Morel-Seytoux's work.

3. An attempt was made to compare the experimental data obtained by McWhorter (1971) with the numerical results. The boundary condition was that of a constant ponding depth of 0.8 cm. Qualitatively, both the numerical and experimental infiltration rates and air pressure curves behaved in a similar manner before and after air counterflow starts. The deviation between the numerical solution and experimental data, after air is escaping from the medium, was believed to be caused by change in medium properties and the hysteresis effect.

4. The longitudinal dispersion problem considered by Garder et al. (1964) in a uniform flow field was solved using the MOC and excellent agreement with his results was obtained.

5. The proposed numerical tensor transformation by Reddell and Sunada (1970) was tested on dispersion problems in uniform flow field. The longitudinal and lateral concentration profiles obtained with and without tensor transformation were compared with known analytical solutions. Excellent agreement was obtained between the numerical solution with tensor transformation and analytical solution. The solution without the tensor transformation resulted in a steeper concentration distribution curve than the analytical solution. The use of "nine-star" grid pattern to estimate cross-derivatives resulted in a small amount of "overshoot" in the numerical solution.

6. A two-dimensional infiltration problem was solved in a non-homogeneous, integrated saturated-unsaturated medium using the total simulator of fluid flow and convective-dispersion equations. The limitations of the assumptions of a homogeneous and isotropic medium are illustrated by the accumulation of moving points at a transition from higher to lower permeability. No analytical solutions or experimental data are available to compare with numerical solution. Therefore, much of the validity of the numerical solution for this particular problem had to be based on material balance errors. However, laboratory experiments are presently well underway to validate the numerical simulator.

Suggestions for Future Research

Concerning this research, further work is recommended in the following areas.

1. As demonstrated, inclusion of air as a second phase in infiltration problems led to interesting results. The two-phase fluid flow problems should be investigated more under a variety of boundary conditions and for nonhomogeneous, anisotropic porous media. Also hysteresis effect should be included in the numerical solution.

2. Very little experimental data are available on studies involving air-water movement in porous media. Laboratory and field experiments should be performed to study two-phase flow problems.

3. Several other numerical techniques, such as, ADIPIT, SOR need to be investigated in solving the fluid flow equations.

4. A scheme based on coordinates of moving points should be investigated in calculating average grid concentration for transient, nonuniform flow fields.

5. While the method of characteristics is a valid numerical scheme and does not generate numerical dispersion, MOC requires much programming effort especially for transient, two-, or three-dimensional, nonuniform flow field. Numerical techniques developed by Chaudhari (1971) and Tagamets and Sternberg (1974) should be investigated for possible use. Also, the finite element technique (Nalluswami, 1971; Segol et al., 1975; Pickens and Lennox, 1976) should be considered in solving convective-dispersion problems.

6. A study of dispersion in nonhomogeneous, anisotropic porous media should be undertaken.

7. The numerical simulator should be used to solve an actual field problem.

REFERENCES

1. Bear, Jacob. 1961a. On the tensor form of dispersion in porous media. Journal of Geophysical Research 66(4):1185-1198.

2. Bear, Jacob. 1961b. Some experiments in dispersion. Journal of Geophysical Research 66(8):2455-2467.

3. Bear, Jacob. 1972. Dynamics of Fluids in Porous Media. American Elsevier Publishing Co., Inc. New York. 756p.

4. Biggar, J. W. and D. R. Nielsen. 1960. Diffusion effects in miscible displacement occurring in saturated and unsaturated porous materials. Journal of Geophysical Research 65(9):2887-2895.

5. Bredehoeft, J. D. and G. F. Pinder. 1973. Mass transport in flowing groundwater. Water Resources Research 9(1):194-210.

6. Breitenbach, E. A., D. H. Thurnau and H. K. van Poollen. 1968a. The fluid flow simulation equations. Society of Petroleum Engineers of AIME. Preprint SPE 2020. Dallas, Texas. 11p.

7. Breitenbach, E. A., D. H. Thurnau and H. K. van Poollen. 1968b. Solution of the immiscible fluid flow simulation equations. Society of Petroleum Engineers of AIME. Preprint SPE 2021. Dallas, Texas. 13p.

8. Bresler, Eshel. 1973. Simultaneous transport of solutes and water under transient unsaturated flow conditions. Water Resources Research 9(4):975-986.

9. Bresler, E. and R. J. Hanks. 1969. Numerical method for estimating simultaneous flow of water and salt in unsaturated soils. Soil Science Society of America Proceedings 33(6):827-832.

10. Bresler, E., W. D. Kemper and R. J. Hanks. 1969. Infiltration, redistribution, and subsequent evaporation of water from soil as affected by wetting rate and hysteresis. Soil Science Society of America Proceedings 33(6):832-840.

11. Brooks, R. H. and A. T. Corey. 1966. Properties of porous media affecting fluid flow. Proceedings, American Society of Civil Engineers, Irrigation and Drainage Div. 92(IR2):61-88.

12. Bruch, J. C. 1970. Two-dimensional dispersion experiments in a porous medium. Water Resources Research 6(3):791-800.

13. Bruch, J. C. and R. L. Street. 1967. Two-dimensional dispersion. Proceedings, American Society of Civil Engineers, Sanitary Engineering Div. 93(SA6):17-39.

14. Brustkern, R. L. and H. J. Morel-Seytoux. 1970. Analytical treatment of two-phase infiltration. Proceedings, American Society of Civil Engineers, Hydraulics Div. 96(HY12):2535-2548.

15. Brutsaert, W. F., E. A. Breitenbach and D. K. Sunada. 1971. Computer analysis of free surface well flow. Proceedings, American Society of Civil Engineers, Irrigation and Drainage Div. 97(IR3): 405-420.

16. Brutsaert, W. F. 1971. A functional iteration technique for solving the Richards equation applied to two-dimensional infiltration problems. Water Resources Research 7(6):1583-1596.

17. Cavendish, J. C., H. S. Price and R. S. Varga. 1973. Galerkin methods for the numerical solution of boundary value problems, p. 31-47. In:Numerical Simulation. SPE Reprint Series 11. Society of Petroleum Engineers of AIME. Dallas, Texas.

18. Chaudhari, N. M. 1971. An improved numerical technique for solving multidimensional miscible displacement equations. Society of Petroleum Engineers Journal 11(3):277-284.

19. de Josselin de Jong, G. 1958. Longitudinal and transverse diffusion in granular deposits. Transactions, American Geophysical Union 39(1):67-74.

20. de Josselin de Jong, G. and M. J. Bossen. 1961. Tensor form of dispersion in porous media --- discussion. Journal of Geophysical Research 66(10):3623-3624.

21. DeWiest, R. 1969. Flow Through Porous Media. Academic Press. New York. 530p.

22. Dixon, R. M. and D. R. Linden. 1972. Soil air pressure and water infiltration under border irrigation. Soil Science Society of America Proceedings 36(6):948-953.

23. Ebach, E. A. and R. R. White. 1958. Mixing of fluids flowing through beds of packed solids. American Institute of Chemical Engineers Journal 4(2):161-169.

24. Free, G. R. and V. J. Palmer. 1940. Interrelationship of infiltration, air movement, and pore size in graded silica sand. Soil Science Society of America Proceedings 5:390-398.

25. Freeze, R. A. 1969. The mechanism of natural groundwater recharge and discharge, 1. One-dimensional, vertical, unsteady, unsaturated flow above a recharging or discharging groundwater flow system. Water Resources Research 5(1):153-171.

26. Freeze, R. A. 1971. Three-dimensional, transient, saturated-unsaturated flow in a groundwater basin. Water Resources Research 7(2):347-366.

27. Freeze, R. A. 1972. Subsurface hydrology at waste disposal sites. IBM Journal of Research and Development 16(2):117-129.

28. Garder, A. O. Jr., D. W. Peaceman and A. L. Pozzi, Jr. 1964. Numerical calculation of multidimensional miscible displacement by the method of characteristics. Society of Petroleum Engineers Journal 4(1):26-36.

29. Green, D. W., Hassan Dabiri and C. F. Weinaug. 1970. Numerical modeling of unsaturated groundwater flow and comparison of the model to a field experiment. Water Resources Research 6(3):362-374.

30. Gupta, S. P. and R. A. Greenkorn. 1973. Dispersion during flow in porous media with bilinear adsorption. Water Resources Research 9(5):1357-1368.

31. Gupta, S. P. and R. A. Greenkorn. 1976. Solution for radial flow with nonlinear adsorption. Proceedings, American Society of Civil Engineers, Environmental Engineering Div. 102(EE1):87-94.

32. Hanks, R. J. and S. A. Bowers. 1962. Numerical solution of the moisture flow equation for infiltration into layered soils. Soil Science Society of America Proceedings 26(6):530-534.

33. Hanks, R. J., A. Klute and E. Bresler. 1969. A numeric method for estimating infiltration, redistribution, drainage, and evaporation of water from soil. Water Resources Research 5(5):1064-1069.

34. Harleman, D. R. F. and R. R. Rumer. 1963. Longitudinal and lateral dispersion in an isotropic porous medium. Journal of Fluid Mechanics 16:385-394.

35. Hiler, E. A. and S. I. Bhuiyan. 1971. Dynamic simulation of unsteady flow of water in unsaturated soils and its application to subirrigation system design. Technical Report No. 40. Texas Water Resources Institute. 94p.

36. Hoopes, J. A. and D. R. F. Harleman. 1965. Wastewater recharge and dispersion in porous media. Massachusetts Institute of Technology Hydrodynamics Laboratory, Technical Report 75. 166p.

37. Hoopes, J. A. and D. R. F. Harleman. 1967. Dispersion in radial flow from a recharge well. Journal of Geophysical Research 72(14): 3595-3607.

38. Horton, R. E. 1940. An approach toward a physical interpretation of infiltration capacity. Soil Science Society of America Proceedings 5:399-417.

39. Konikow, L. F. and J. D. Bredehoeft. 1974. Modeling flow and chemical quality changes in an irrigated stream-aquifer system. Water Resources Research 10(3):546-562.

40. Lantz, R. B. 1971. Quantitative evaluation of numerical diffusion (truncation error). Society of Petroleum Engineers Journal 11(3): 315-320.

41. Lau, L. K., W. J. Kaufman and D. K. Todd. 1957. Studies of dispersion in a radial flow system. University of California at Berkeley Sanitary Engineering Research Laboratory, Canal seepage Research Progress Report 3. 44p.

42. Linden, D. R. and R. M. Dixon. 1973. Infiltration and water table effects of soil air pressure under border irrigation. Soil Science Society of America Proceedings 37(1):94-98.

43. Linden, D. R. and R. M. Dixon. 1975. Water table position as affected by soil air pressure. Water Resources Research 11(1):139-143.

44. Luthin, J. N., Akin Orhun and G. S. Taylor. 1975. Coupled saturated-unsaturated transient flow in porous media: experimental and numerical model. Water Resources Research 11(6):973-978.

45. McWhorter, D. B. 1971. Infiltration affected by flow of air. Colorado State University, Hydrology Papers, No. 49. 43p.

46. Morel-Seytoux, H. J. 1973. Systematic treatment of infiltration with applications. Colorado State University, Completion Report Series, No. 50. 64p.

47. Nalluswami, M. 1971. Numerical simulation of general hydrodynamic dispersion in porous medium. Colorado State University, Unpublished Ph.D. Thesis. Fort Collins, Colorado.

48. Ogata, A. and R. B. Banks. 1961. A solution of the differential equation of longitudinal dispersion in porous media. U.S. Geological Survey Professional Paper 411-A. U.S. Govt. Printing Office. Washington D. C. 7p.

49. Parlange, J. V. 1971a. Theory of water movement in soils:1. One-dimensional absorption. Soil Science 111(2):134-137.

50. Parlange, J. V. 1971b. Theory of water movement in soils:2. One-dimensional infiltration. Soil Science 111(3):170-174.

51. Parlange, J. V. 1975. Theory of water movement in soils:11. conclusion and discussion of some recent developments. Soil Science 119(2):158-161.

52. Peaceman, D. W. and H. H. Rachford, Jr. 1962. Numerical calculation of multidimensional miscible displacement. Society of Petroleum Engineers Journal 2(4):327-339.

53. Peck, A. J. 1965. Moisture profile development and air compression during water uptake by bounded porous bodies:3. vertical columns. Soil Science 100(1):44-51.

54. Philip, J. R. 1969. Theory of infiltration, p. 215-296. In: Ven T. Chow, (ed.) Advances in Hydroscience. Vol. 5. Academic Press. New York.

55. Phuc, Le van and H. J. Morel-Seytoux. 1972. Effect of soil air movement and compressibility on infiltration rates. Soil Science Society of America Proceedings 36(2):237-241.

56. Pickens, J. F. and W. C. Lennox. 1976. Numerical simulation of waste movement in steady groundwater flow systems. Water Resources Research 12(2):171-180.

57. Pikul, M. F., R. L. Street and Irwin Remson. 1974. A numerical model based on coupled one-dimensional Richards and Boussinesq equations. Water Resources Research 10(2):295-302.

58. Pinder, G. F. 1973. A Galerkin-finite element simulation of groundwater contamination on Long Island, New York. Water Resources Research 9(6):1657-1669.

59. Pinder, G. F. and H. H. Cooper, Jr. 1970. A numerical technique for calculating the transient position of the saltwater front. Water Resources Research 6(3):875-882.

60. Poreh, Michael. 1965. The dispersivity tensor in isotropic and axisymmetric mediums. Journal of Geophysical Research 70(16): 3909-3913.

61. Reddell, D. L. and D. K. Sunada. 1970. Numerical simulation of dispersion in groundwater aquifers. Colorado State University, Hydrology Papers, No. 41. 79p.

62. Remson, Irwin, G. M. Hornberger and F. J. Molz. 1971. Numerical Methods in Subsurface Hydrology. Wiley-Interscience, Inc. New York. 389p.

63. Richards, L. A. 1931. Capillary conduction of liquids through porous mediums. Physics 1:318-333.

64. Rubin, J. 1968. Theoretical analysis of two-dimensional, transient flow of water in unsaturated and partly unsaturated soils. Soil Science Society of America Proceedings 32(5):607-615.

65. Saffman, P. G. 1959. A theory of dispersion in a porous medium. Journal of Fluid Mechanics 6(3):321-349.

66. Saftman, P. G. 1960. Dispersion due to molecular diffusion and macroscopic mixing in flow through a network of capillaries. Journal of Fluid Mechanics 7(2):194-208.

67. Scheidegger, A. E. 1954. Statistical hydrodynamics in porous media. Journal of Applied Physics 25(8):994-1001.

68. Scheidegger, A. E. 1961. General theory of dispersion in porous media. Journal of Geophysical Research 66(10):3273-3278.

69. Segol, G. and G. F. Pinder. 1976. Transient simulation of saltwater intrusion in southeastern Florida. Water Resources Research 12(1):65-70.

70. Segol, G., G. F. Pinder and W. G. Gray. 1975. A Galerkin-finite element technique for calculating the transient position of the saltwater front. Water Resources Research 11(2):343-347.

71. Shamir, U. Y. and D. R. F. Harleman. 1966. Numerical and analytical solutions of dispersion problems in homogeneous and layered aquifers. Massachusetts Institute of Technology Hydrodynamics Laboratory, Technical Report 89. Cambridge, Massachusetts. 206p.

72. Shamir, U. Y. and D. R. F. Harleman. 1967. Dispersion in layered porous media. Proceedings, American Society of Civil Engineers, Hydraulics Div. 93(HY5):237-260.

73. Skaggs, R. W. and Y. K. Tang. 1976. Saturated and unsaturated flow to parallel drains. Proceedings, American Society of Civil Engineers, Irrigation and Drainage Div. 102(IR2):221-238.

74. Smajstrla, A. G., D. L. Reddell and E. A. Hiler. 1975. Simulation of miscible displacement in soils using the method of characteristics. Transactions, American Society of Agricultural Engineers 18(2):281-287,292.

75. Smith, R. E. and D. A. Woolhiser. 1971. Mathematical simulation of infiltrating watersheds. Colorado State University, Hydrology Papers, No. 47. 44p.

76. Sonu, J. 1973. Water and air movement in bounded layered soil. Ph.D. dissertation, Civil Engineering Department, Colorado State University, Fort Collins. Dissertation No. 73-29,061. Xerox University Microfilms, Ann Arbor, Michigan.

77. Staple, W. J. 1966. Infiltration and redistribution of water in vertical columns of loam soil. Soil Science Society of America Proceedings 30(5):553-558.

78. Staple, W. J. 1969. Comparison of computed and measured moisture distribution following infiltration. Soil Science Society of America Proceedings 33(6):840-847.

79. Stone, H. L. and P. L. T. Brian. 1963. Numerical solution of convective transport problems. American Institute of Chemical Engineers Journal 9(5):681-688.

80. Tagamets, T. and Y. M. Sternberg. 1974. A predictor-corrector method for solving the convection-dispersion equation for adsorption in porous media. Water Resources Research 10(5):1003-1011.

81. Thurnau, D. H. 1963. Algorithm 195, Bandsolve. Communications of the Association for Computing Machinery 6(8):441.

82. Vachaud, G., M. Vauclin and R. Haverkamp. 1974. Towards a physically based analysis of transient water table flow problems. Paper presented at the IFIP working conference on modeling and simulation of water resource systems. Ghent, France. 22p.

83. Vauclin, M., G. Vachaud and J. Khanji. 1974. Two-dimensional numerical analysis of transient water transfer in saturated-unsaturated soils. Paper presented at the IFIP working conference on modeling and simulation of water resource systems. Ghent, France. 30p.

84. Warrick, A. W., J. W. Biggar and D. R. Nielsen. 1971. Simultaneous solute and water transfer for an unsaturated soil. Water Resources Research 7(5):1216-1225.

85. Warrick, A. W., J. H. Kichen and J. L. Thames. 1972. Solutions for miscible displacement of soil water with time-dependent velocity and dispersion coefficients. Soil Science Society of America Proceedings 36(6):863-867.

86. Whisler, F. D. and A. Klute. 1965. The numerical analysis of infiltration considering hysteresis, into a vertical soil column at equilibrium under gravity. Soil Science Society of America Proceedings 29(5):489-494.

87. Whisler, F. D. and A. Klute. 1967. Rainfall infiltration into a vertical soil column. Transactions, American Society of Agricultural Engineers 10(3):391-395.

APPENDIX A

DERIVATION OF FLOW EQUATIONS

A set of fundamental flow equations are derived describing the behavior of the two fluid phases, water and air, that are present in the saturated as well as in the unsaturated zone. The nonlinear, partial differential equations for transient, saturated-unsaturated, three-dimensional flow through porous media are obtained by combining the continuity principle for each fluid phase, Darcy's law for each phase, a fluid conservation equation, an equation defining the capillary pressure, and an equation of state for air.

Continuity Equation

The principle of conservation of mass when applied to a differential volume element of porous media fixed in space may be stated as:

(Rate of mass inflow) - (Rate of mass outflow) =

(Rate of change of mass inside the volume element).

Applying this principle to the volume element shown in Figure A-1 results in

$$M_{x_1-\Delta x_1/2} - M_{x_1+\Delta x_{1/2}} + M_{x_2-\Delta x_{2/2}} - M_{x_2+\Delta x_{2/2}} +$$

$$M_{x_3-\Delta x_3/2} - M_{x_3+\Delta x_{3/2}} = \frac{\partial M_{VE}}{\partial t} + M_p \quad , \qquad \text{(A-1)}$$

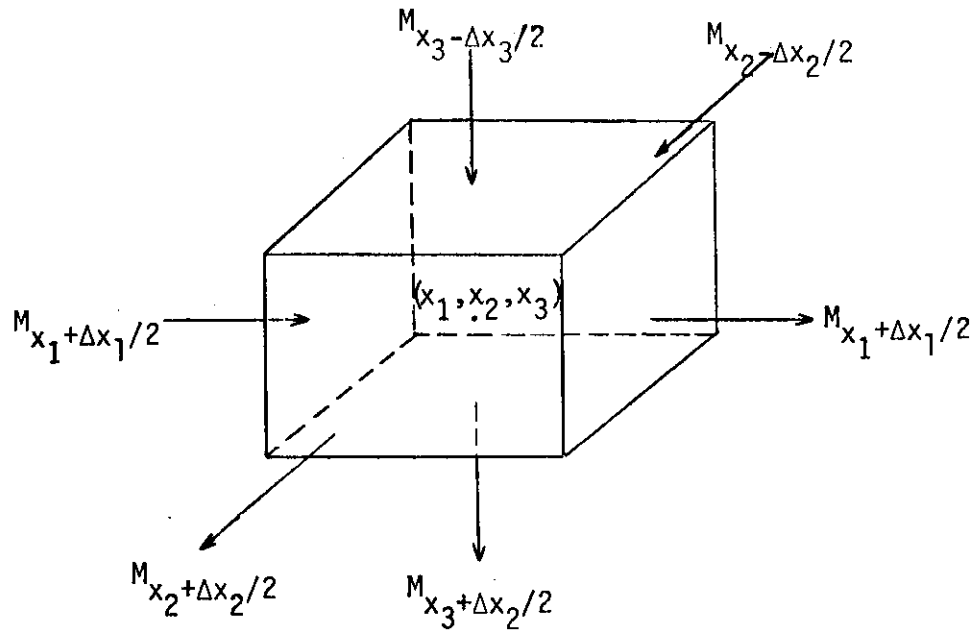

Figure A-1. Volume element of a porous medium used for developing continuity equation.

where $M_{x_1-\Delta x_1/2}$, $M_{x_2-\Delta x_2/2}$, $M_{x_3-\Delta x_3/2}$ are rates of mass inflow across faces $x_1-\Delta x_1/2$, $x_2-\Delta x_2/2$ and $x_3-\Delta x_3/2$ respectively,

$M_{x_1+\Delta x_1/2}$, $M_{x_2+\Delta x_2/2}$ and $M_{x_3+\Delta x_3/2}$ are rates of mass outflow across faces $x_1+\Delta x_1/2$, $x_2+\Delta x_2/2$ and $x_3+\Delta x_3/2$ respectively,

M_{VE} is the mass contained inside the volume element, and

M_p is a mass source or sink term which is negative for a source and positive for a sink.

Applying Taylor series expansion about a point (x_1, x_2, x_3) of Figure A-1 gives:

$$M_{x_i-\Delta x_i/2} = M_{x_i} - \frac{\partial M_{x_i}}{\partial x_i}\frac{\Delta x_i}{2} + \frac{1}{2!}\frac{\partial^2 M_{x_i}}{\partial x_i^2}\left(\frac{\Delta x_i}{2}\right)^2 - \ldots ; \quad i = 1, 2, 3$$

and

$$M_{x_i+\Delta x_i/2} = M_{x_i} + \frac{\partial M_{x_i}}{\partial x_i}\frac{\Delta x_i}{2} + \frac{1}{2!}\frac{\partial^2 M_{x_i}}{\partial x_i^2}\left(\frac{\Delta x_i}{2}\right)^2 + \ldots ;$$

$$i = 1, 2, 3. \quad \text{(A-2)}$$

Neglecting second order terms and higher, the following relationships are obtained from equation (A-2):

$$M_{x_i-\Delta x_i/2} - M_{x_i+\Delta x_i/2} = -\frac{\partial M_{x_i}}{\partial x_i}\Delta x_i, \qquad i = 1, 2, 3. \quad \text{(A-3)}$$

Substituting equation (A-3) into equation (A-1) gives:

$$\sum_{i=1}^{3}\frac{\partial M_{x_i}}{\partial x_i}\Delta x_i = \frac{\partial M_{VE}}{\partial t} - M_p \quad \text{(A-4)}$$

Expressing individual mass flow components in terms of the fluid density, the dimensions of the volume element and the volume flux

$$M_{x_i} = \rho q_i \Delta A_i; \qquad i = 1, 2, 3 \quad \text{(A-5a)}$$

$$M_{VE} = \rho\phi S\Delta\overline{V}, \text{ and} \quad \text{(A-5b)}$$

$$M_p = \rho_p Q \quad \text{(A-5c)}$$

where ρ = mass density of the solution (ML^{-3}),

q_i = the volume flux component in the i-th direction (LT^{-1}),

ϕ = porosity of the medium,

S = saturation of the fluid,

ΔA_i = area (L^2) of the volume element perpendicular to q_i, the volume flux in the i-th direction such as, $\Delta A_1 = \Delta x_2 \Delta x_3$ and so on,

$\Delta \bar{V} = \Delta x_1 \Delta x_2 \Delta x_3$, ($L^3$),

Q = production rate (L^3T^{-1}), and

ρ_p = mass density of fluid passed in the source or sink (ML^{-3}).

Substituting equation (A-5) into equation (A-4) and using short hand tensor notation gives

$$\frac{\partial}{\partial x_i} (\rho q_i \Delta A_i) \Delta x_i = - \frac{\partial}{\partial t} (\rho \phi S \Delta \bar{V}) - \rho_p Q \qquad \text{(A-6)}$$

where $i = 1, 2, 3$ is a cartesian coordinate system (x_1, x_2, x_3).

Fundamental Flow Equations

To develop the flow equations, an expression for the volume flux terms is required. Assuming the axes of the coordinate system (x_1, x_2, x_3) to coincide with the axes of the permeability tensor, the volume flux terms are given by Darcy's law as:

$$q_i = - \frac{k_{x_i} k_r}{\mu} \left(\frac{\partial P}{\partial x_i} + \rho g \frac{\partial h}{\partial x_i} \right) \quad , \quad i = 1, 2, 3 \qquad \text{(A-7)}$$

where k_{x_i} = absolute permeability in the i-th direction (L^2),

k_r = relative permeability to fluid,

μ = dynamic viscosity of fluid ($ML^{-1}T^{-1}$),

P = fluid pressure ($ML^{-1}T^{-2}$),

g = acceleration of gravity (LT^2), and

h = elevation of the volume element above an arbitrary datum which is perpendicular to the direction of gravity (L).

Substituting equation (A-7) into equation (A-6) results in

$$\frac{\partial}{\partial x_i}\left[\frac{\bar{\rho} k_{x_i} k_r}{\mu}\left(\frac{\partial P}{\partial x_i} + \rho g \frac{\partial h}{\partial x_i}\right)\Delta A_i\right] \Delta x_i = \frac{\partial}{\partial t}(\rho \phi S \Delta \bar{V}) + \rho_p Q. \qquad \text{(A-8)}$$

By analogy, equations similar to equation (A-8) may be written for both water and air phases. For the water phase:

$$\frac{\partial}{\partial x_i}\left[\frac{\bar{\rho}_w k_{x_i} k_{rw}}{\mu_w}\left(\frac{\partial P_w}{\partial x_i} + \rho_w g \frac{\partial h}{\partial x_i}\right)\Delta A_i\right] \Delta x_i =$$

$$\frac{\partial}{\partial t}(\rho_w \phi S_w \Delta \bar{V}) + \rho_p Q_w \quad , \qquad \text{(A-9a)}$$

and for the air phase:

$$\frac{\partial}{\partial x_i}\left[\frac{\bar{\rho}_a k_{x_i} k_{ra}}{\mu_a}\left(\frac{\partial P_a}{\partial x_i} + \rho_a g \frac{\partial h}{\partial x_i}\right)\Delta A_i\right] \Delta x_i =$$

$$\frac{\partial}{\partial t}(\rho_a \phi S_a \Delta \bar{V}) + \rho_p Q_a \qquad \text{(A-9b)}$$

where the subscript 'w' refers to the wetting phase or water and the subscript 'a' refers to the nonwetting phase or air.

The fluid conservation equation states

$$S_w + S_a = 1 \qquad \text{(A-10a)}$$

Differentiating equation (A-10a)

$$\frac{\partial S_a}{\partial t} = -\frac{\partial S_w}{\partial t} \quad . \qquad \text{(A-10b)}$$

From the definition of capillary pressure

$$P_c = P_a - P_w = P_c (S_w) \ . \qquad \text{(A-11a)}$$

Differentiating equation (A-11a)

$$\frac{\partial P_a}{\partial x_i} = \frac{\partial P_c}{\partial x_i} + \frac{\partial P_w}{\partial x_i} \ ; \qquad i = 1, 2, 3 \qquad \text{(A-11b)}$$

The six dependent variables are:

$$k_{rw} = k_{rw} (S_w) \ , \qquad \text{(A-12a)}$$

$$k_{ra} = k_{ra} (S_a) = k_{ra} (1 - S_w) \ , \qquad \text{(A-12b)}$$

$$\rho_a = \rho_a (P_a) \ , \qquad \text{(A-12c)}$$

$$\rho_w = \rho_w (P_w) \ , \qquad \text{(A-12d)}$$

$$\mu_a = \mu_a (P_a) \ , \qquad \text{(A-12e)}$$

and

$$\mu_w = \mu_w (P_w) \ . \qquad \text{(A-12f)}$$

Using product rule of differentiation, the first term on the right hand side of equation (A-9a) yields:

$$\frac{\partial}{\partial t} (\rho_w \phi S_w \Delta\overline{V}) = (\rho_w \phi \Delta\overline{V}) \frac{\partial S_w}{\partial t} + (\rho_w S_w) \frac{\partial}{\partial t} (\phi \Delta\overline{V}) +$$

$$(\phi \Delta\overline{V} S_w) \frac{\partial \rho_w}{\partial t} \ . \qquad \text{(A-13)}$$

Substituting equation (A-13) into equation (A-9a) and dividing throughout by $(\rho_w \phi \Delta\overline{V})$ gives:

$$\left(\frac{1}{\rho_w \phi \Delta \bar{V}}\right) \frac{\partial}{\partial x_i} \left[\frac{\bar{\rho}_w k_{x_i} k_{rw}}{\mu_w} \left(\frac{\partial P_w}{\partial x_i} + \rho_w g \frac{\partial h}{\partial x_i}\right) \Delta A_i\right] \Delta x_i -$$

$$\frac{\rho_P Q_w}{\rho_w \phi \Delta \bar{V}} - \frac{S_w}{\phi \Delta \bar{V}} \frac{\partial}{\partial t} (\phi \Delta \bar{V}) - \frac{S_w}{\rho_w} \frac{\partial \rho_w}{\partial t} = \frac{\partial S_w}{\partial t} . \qquad \text{(A-14)}$$

Using the product of differentiation for the first term on the right hand side of equation (A-9b), substituting equation (A-11b) into equation (A-9b), and dividing throughout by $(\rho_a \phi \Delta \bar{V})$ yields:

$$\left(\frac{1}{\rho_a \phi \Delta \bar{V}}\right) \frac{\partial}{\partial x_i} \left[\frac{\bar{\rho}_a k_{x_i} k_{ra}}{\mu_a} \left(\frac{\partial P_c}{\partial x_i} + \frac{\partial P_w}{\partial x_i} + \rho_a g \frac{\partial h}{\partial x_i}\right) \Delta A_i\right] \Delta x_i -$$

$$\frac{\rho_P Q_a}{\rho_a \phi \Delta \bar{V}} - \frac{S_a}{\phi \Delta \bar{V}} \frac{\partial}{\partial t} (\phi \Delta \bar{V}) - \frac{S_a}{\rho_a} \frac{\partial \rho_a}{\partial t} = - \frac{\partial S_w}{\partial t} . \qquad \text{(A-15)}$$

Adding equations (A-14) and (A-15) and rearranging yields:

$$\left(\frac{1}{\rho_w \phi \Delta \bar{V}}\right) \frac{\partial}{\partial x_i} \left[\frac{\bar{\rho}_w k_{x_i} k_{rw} \Delta A_i}{\mu_w} \frac{\partial P_w}{\partial x_i}\right] \Delta x_i +$$

$$\left(\frac{1}{\rho_a \phi \Delta \bar{V}}\right) \frac{\partial}{\partial x_i} \left[\frac{\bar{\rho}_a k_{x_i} k_{ra} \Delta A_i}{\mu_a} \frac{\partial P_w}{\partial x_i}\right] \Delta x_i =$$

$$- \left(\frac{1}{\rho_a \phi \Delta \bar{V}}\right) \frac{\partial}{\partial x_i} \left[\frac{\bar{\rho}_a k_{x_i} k_{ra} \Delta A_i}{\mu_a} \frac{\partial P_c}{\partial x_i}\right] \Delta x_i$$

$$\left(\frac{1}{\rho_w \phi \Delta \bar{V}}\right) \frac{\partial}{\partial x_i} \left[\frac{\bar{\rho}_w^2 g k_{x_i} k_{rw} \Delta A_i}{\mu_w} \frac{\partial h}{\partial x_i}\right] \Delta x_i -$$

$$\left(\frac{1}{\rho_a \phi \Delta \bar{V}}\right) \frac{\partial}{\partial x_i} \left[\frac{\rho_a^2 g k_{x_i} k_{ra} \Delta A_i}{\mu_a} \frac{\partial h}{\partial x_i}\right] \Delta x_i \quad +$$

$$\frac{S_w}{\phi \Delta \bar{V}} \frac{\partial}{\partial t} (\phi \Delta \bar{V}) + \frac{S_w}{\rho_w} \frac{\partial \rho_w}{\partial t} + \frac{S_a}{\phi \Delta \bar{V}} \frac{\partial}{\partial t} (\phi \Delta \bar{V}) + \frac{S_a}{\rho_a} \frac{\partial \rho_a}{\partial t} +$$

$$\frac{\rho_p Q_w}{\rho_w \phi \Delta \bar{V}} + \frac{\rho_p Q_a}{\rho_a \phi \Delta \bar{V}} \quad . \tag{A-16}$$

Defining all pressures in terms of pressure head of water:

$$\psi_w = \frac{P_w}{\rho_w g} \quad ,$$

$$\psi_a = \frac{P_a}{\rho_w g} \quad ,$$

and

$$\psi_c = \frac{P_c}{\rho_w g} \quad . \tag{A-17}$$

Substituting equations (A-17) into equation (A-16) and factoring out the acceleration of gravity g:

$$\left(\frac{1}{\rho_w \phi \Delta \bar{V}}\right) \frac{\partial}{\partial x_i} \left[\frac{\rho_w^2 k_{x_i} k_{rw} \Delta A_i}{\mu_w} \frac{\partial \psi_w}{\partial x_i}\right] \Delta x_i \quad +$$

$$\left(\frac{1}{\rho_a \phi \Delta \bar{V}}\right) \frac{\partial}{\partial x_i} \left[\frac{\rho_a \rho_w k_{x_i} k_{ra} \Delta A_i}{\mu_a} \frac{\partial \psi_w}{\partial x_i}\right] \Delta x_i = -$$

$$\left(\frac{1}{\rho_a \phi \Delta \bar{V}}\right) \frac{\partial}{\partial x_i} \left[\frac{\rho_a \rho_w k_{x_i} k_{ra} \Delta A_i}{\mu_a} \frac{\partial \psi_c}{\partial x_i}\right] \Delta x_i \quad -$$

$$\left(\frac{1}{\rho_w \phi \Delta \bar{V}}\right) \frac{\partial}{\partial x_i} \left[\frac{\rho_w^2 k_{x_i} k_{rw} \Delta A_i}{\mu_w} \frac{\partial h}{\partial x_i}\right] \Delta x_i -$$

$$\left(\frac{1}{\rho_a \phi \Delta \bar{V}}\right) \frac{\partial}{\partial x_i} \left[\frac{\rho_a^2 k_{x_i} k_{ra} \Delta A_i}{\mu_w} \frac{\partial h}{\partial x_i}\right] \Delta x_i + \frac{S_w}{\phi \Delta \bar{V} g} \frac{\partial}{\partial t} (\phi \Delta \bar{V}) + \frac{S_w}{\rho_w g} \frac{\partial \rho_w}{\partial t}$$

$$+ \frac{S_a}{\phi \Delta \bar{V} g} \frac{\partial}{\partial t} (\phi \Delta \bar{V}) + \frac{S_a}{\rho_a g} \frac{\partial \rho_a}{\partial t} + \frac{\rho_p Q_w}{\rho_w \phi \Delta \bar{V} g} + \frac{\rho_p Q_a}{a \phi \Delta \bar{V} g} . \qquad \text{(A-18)}$$

Equation (A-18) henceforth will be called the Water Pressure Equation.

Expressing equation (A-14) in terms of pressure head of water and factoring out "g":

$$\frac{\partial S_w}{\partial t} = \frac{g}{(\rho_w \phi \Delta \bar{V})} \frac{\partial}{\partial x_i} \left[\frac{\rho_w^2 k_{x_i} k_{rw} \Delta A_i}{\mu_w} \frac{\partial \psi_w}{\partial x_i}\right] \Delta x_i +$$

$$\frac{g}{(\rho_w \phi \Delta \bar{V})} \frac{\partial}{\partial x_i} \left[\frac{\rho_w^2 k_{x_i} k_{rw} \Delta A_i}{\mu_w} \frac{\partial h}{\partial x_i}\right] \Delta x_i - \frac{\rho_p Q_w}{\rho_w \phi \Delta \bar{V}} -$$

$$\frac{S_w}{\phi \Delta \bar{V}} \frac{\partial}{\partial t} (\phi \Delta \bar{V}) - \frac{S_w}{\rho_w} \frac{\partial \rho_w}{\partial t} . \qquad \text{(A-19)}$$

Equation (A-19) will be called Water Saturation Equation.

Similarly, equation (A-15) may be expressed in terms of pressure head of water as

$$\frac{\partial S_a}{\partial t} = \frac{g}{(\rho_a \phi \Delta \bar{V})} \frac{\partial}{\partial x_i} \left[\frac{\rho_a \rho_w k_{x_i} k_{ra} \Delta A_i}{\mu_a} \frac{\partial \psi_a}{\partial x_i}\right] \Delta x_i +$$

$$\frac{g}{(\rho_a \phi \Delta \bar{V})} \frac{\partial}{\partial x_i} \left[\frac{\rho_a^2 k_{x_i} k_{ra} \Delta A_i}{\mu_a} \frac{\partial h}{\partial x_i}\right] \Delta x_i - \frac{\rho_p Q_a}{\rho_a \phi \Delta \bar{V}} - \frac{S_a}{\phi \Delta \bar{V}} \frac{\partial}{\partial t} (\phi \Delta \bar{V}) -$$

$$\frac{S_a}{\rho_a}\frac{\partial \rho_a}{\partial t} \quad . \quad \ldots \qquad \text{(A-20)}$$

Equation (A-20) will be called Air Saturation Equation.

The Air Pressure Equation can be derived using a similar procedure as employed in obtaining the Water Pressure Equation (A-18):

$$\left(\frac{1}{\rho_w \phi \Delta \bar{V}}\right) \frac{\partial}{\partial x_i}\left[\frac{\rho_w^2 k_{x_i} k_{rw} \Delta A_i}{\mu_w}\frac{\partial \psi_a}{\partial x_i}\right] \Delta x_i +$$

$$\left(\frac{1}{\rho_a \phi \Delta \bar{V}}\right) \frac{\partial}{\partial x_i}\left[\frac{\rho_a \rho_w k_{x_i} k_{rw} \Delta A_i}{\mu_a}\frac{\partial \psi_a}{\partial x_i}\right] \Delta x_i =$$

$$\left(\frac{1}{\rho_w \phi \Delta \bar{V}}\right) \frac{\partial}{\partial x_i}\left[\frac{\rho_w^2 k_{x_i} k_{rw} \Delta A_i}{\mu_w}\frac{\partial \psi_c}{\partial x_i}\right] \Delta x_i -$$

$$\left(\frac{1}{\rho_w \phi \Delta \bar{V}}\right) \frac{\partial}{\partial x_i}\left[\frac{\rho_w^2 k_{x_i} k_{rw} \Delta A_i}{\mu_w}\frac{\partial h}{\partial x_i}\right] \Delta x_i -$$

$$\left(\frac{1}{\rho_a \phi \Delta \bar{V}}\right) \frac{\partial}{\partial x_i}\left[\frac{\rho_a^2 k_{x_i} k_{ra} \Delta A_i}{\mu_a}\frac{\partial h}{\partial x_i}\right] \Delta x_i + \frac{S_w}{\phi \Delta \bar{V} g}\frac{\partial}{\partial t}(\phi \Delta \bar{V}) +$$

$$\frac{S_w}{\rho_w g}\frac{\partial \rho_w}{\partial t} + \frac{S_a}{\phi \Delta \bar{V} g}\frac{\partial}{\partial t}(\phi \Delta \bar{V}) + \frac{S_a}{\rho_a g}\frac{\partial \rho_a}{\partial t} + \frac{\rho_p Q_w}{\rho_w \phi \Delta \bar{V} g} + \frac{\rho_p Q_a}{\rho_a \phi \Delta \bar{V} g} \quad . \qquad \text{(A-21)}$$

Equation (A-21) will be called the Air Pressure Equation.

Air is assumed to behave as a perfect gas and equation (A-12c) for density of air as a function of air pressure is given by the

perfect gas law:

$$\rho_a = \frac{P_a}{RT}, \qquad \text{(A-22)}$$

where P_a = air pressure in dynes cm^{-2},

R = gas constant = 2.71×10^6 dyne-cm $gm^{-1}(°K)^{-1}$

T = temperature in °K.

The gas constant, R, may also be given as:

$$R = 8.3144 \times 10^7 \text{ erg (gm mole)}^{-1} (°K)^{-1},$$

where 1 erg = 9.86923×10^7 cu cm - atm,

1 atm = 1033.26 cm of water at 4°C, and

1 gm mole of air = 28.9 gm.

Therefore, R can also be given as:

$$R = 2.9337 \times 10^3 \text{ (cu cm)(gm)}^{-1}\text{(cm water)}(°K)^{-1}.$$

If the air pressure is in cm. of water, then equation (A-22) may be written as:

$$\rho_a = \frac{\psi_a + \psi_{atm}}{RT}, \quad \ldots \qquad \text{(A-23)}$$

where ψ_a = air pressure in cm of water,

ψ_{atm} = atmospheric pressure = 1033.3 cm of water,

R = gas constant = 2.9337×10^3 (cu cm)$(gm)^{-1}$(cm water) $(°K)^{-1}$,

T = temperature in °K.

Using chain rule:

$$\frac{\partial \rho_a}{\partial t} = \frac{\partial \rho_a}{\partial \psi_a} \cdot \frac{\partial \psi_a}{\partial t} = \frac{1}{RT} \frac{\partial \psi_a}{\partial t} \qquad \text{(A-24)}$$

The term $\left(\frac{S_a}{\rho_a g} \frac{\partial \rho_a}{\partial t}\right)$ on the right hand side of equation (A-21), after substituting equations (A-23) and (A-24), becomes:

$$\frac{S_a}{\rho_a g}\frac{\partial \rho_a}{\partial t} = \frac{S_a}{(\psi_a + \psi_{atm})g}\frac{\partial \psi_a}{\partial t} \qquad \text{(A-25)}$$

The Water Pressure Equation (A-18), the Air Pressure Equation (A-21), the Water Saturation Equation (A-19), and the Air Saturation Equation (A-20), combined together will be called Fluid Flow Equations.

APPENDIX B

Finite Difference Equations for Flow Equations

The Water Pressure Equation (A-18), the Air Pressure Equation (A-21), the Water Saturation Equation (A-19) and the Air Saturation Equation (A-20) are rewritten. The Water Pressure Equation is:

$$\left(\frac{1}{\rho_w \phi \Delta \overline{V}}\right) \frac{\partial}{\partial x_i} \left[\frac{\rho_w^2 k_{x_i} k_{rw} \Delta A_i}{\mu_w} \frac{\partial \psi_w}{\partial x_i}\right] \Delta x_i + \left(\frac{1}{\rho_a \phi \Delta \overline{V}}\right) \frac{\partial}{\partial x_i} \left[\frac{\rho_a \rho_w k_{x_i} k_{ra} \Delta A_i}{\mu_a} \frac{\partial \psi_w}{\partial x_i}\right] \Delta x_i$$

$$= - \left(\frac{1}{\rho_a \phi \Delta \overline{V}}\right) \frac{\partial}{\partial x_i} \left[\frac{\rho_a \rho_w k_{x_i} k_{ra} \Delta A_i}{\mu_a} \frac{\partial \psi_c}{\partial x_i}\right] \Delta x_i$$

$$- \left(\frac{1}{\rho_w \phi \Delta \overline{V}}\right) \frac{\partial}{\partial x_i} \left[\frac{\rho_w^2 k_{x_i} k_{r_w} \Delta A_i}{\mu_w} \frac{\partial h}{\partial x_i}\right] \Delta x_i$$

$$- \left(\frac{1}{\rho_a \phi \Delta \overline{V}}\right) \frac{\partial}{\partial x_i} \left[\frac{\rho_a^2 k_{x_i} k_{ra} \Delta A_i}{\mu_a} \frac{\partial h}{\partial x_i}\right] \Delta x_i + \frac{S_w}{\phi \Delta \overline{V} g} \frac{\partial}{\partial t} (\phi \Delta \overline{V})$$

$$+ \frac{S_w}{\rho_w g} \frac{\partial \rho_w}{\partial t} + \frac{S_a}{\phi \Delta \overline{V} g} \frac{\partial}{\partial t} (\phi \Delta \overline{V}) + \frac{S_a}{\rho_a g} \frac{\partial \rho_a}{\partial t} + \frac{\rho_p Q_w}{\rho_w \phi \Delta \overline{V} g}$$

$$+ \frac{\rho_p Q_a}{\rho_a \phi \Delta \overline{V} g} , \qquad \text{(B-1)}$$

where $x_i (i = 1, 2, 3)$ indicates a cartesian coordinate system.

The Air Pressure Equation is:

$$\left(\frac{1}{\rho_w \phi \Delta \overline{V}}\right) \frac{\partial}{\partial x_i} \left[\frac{\rho_w^2 k_{x_i} k_{rw} \Delta A_i}{\mu_w} \frac{\partial \psi_a}{\partial x_i}\right] \Delta x_i$$

$$+ \left(\frac{1}{\rho_a \phi \Delta \overline{V}}\right) \frac{\partial}{\partial x_i} \left[\frac{\rho_a \rho_w k_{x_i} k_{rw} \Delta A_i}{\mu_a} \frac{\partial \psi_a}{\partial x_i}\right] \Delta x_i$$

$$= \left(\frac{1}{\rho_w \phi \Delta \overline{V}}\right) \frac{\partial}{\partial x_i} \left[\frac{\rho_w^2 k_{x_i} k_{rw} \Delta A_i}{\mu_w} \frac{\partial \psi_c}{\partial x_i}\right] \Delta x_i$$

$$- \left(\frac{1}{\rho_w \phi \Delta \overline{V}}\right) \frac{\partial}{\partial x_i} \left[\frac{\rho_w^2 k_{x_i} k_{rw} \Delta A_i}{\mu_w} \frac{\partial h}{\partial x_i}\right] \Delta x_i$$

$$- \left(\frac{1}{\rho_a \phi \Delta \overline{V}}\right) \frac{\partial}{\partial x_i} \left[\frac{\rho_a^2 k_{x_i} k_{ra} \Delta A_i}{\mu_a} \frac{\partial h}{\partial x_i}\right] \Delta x_i$$

$$+ \frac{S_w}{\phi \Delta \overline{V} g} \frac{\partial}{\partial t} (\phi \Delta \overline{V}) + \frac{S_w}{\rho_w g} \frac{\partial \rho_w}{\partial t} + \frac{S_a}{\phi \Delta \overline{V} g} \frac{\partial}{\partial t} (\phi \Delta \overline{V})$$

$$+ \frac{S_a}{\rho_a g} \frac{\partial \rho_a}{\partial t} + \frac{\rho_p Q_w}{\rho_w \phi \Delta \overline{V} g} + \frac{\rho_p Q_w}{\rho_a \phi \Delta \overline{V} g} . \qquad \text{(B-2)}$$

The Water Saturation Equation is:

$$\frac{\partial S_w}{\partial t} = \left(\frac{g}{\rho_w \phi \Delta \overline{V}}\right) \frac{\partial}{\partial x_i} \left[\frac{\rho_w^2 k_{x_i} k_{rw} \Delta A_i}{\mu_w} \frac{\partial \psi_w}{\partial x_i}\right] \Delta x_i$$

$$+ \left[\frac{g}{\rho_w \phi \Delta \bar{V}}\right] \frac{\partial}{\partial x_i} \left[\frac{\rho_w^2 k_{x_i} k_{rw} \Delta A_i}{\mu_w} \frac{\partial h}{\partial x_i}\right] \Delta x_i$$

$$- \frac{\rho_p Q_w}{\rho_w \phi \Delta \bar{V}} - \frac{S_w}{\phi \Delta \bar{V}} \frac{\partial}{\partial t} (\phi \Delta \bar{V}) - \frac{S_w}{\rho_w} \frac{\partial \rho_w}{\partial t} . \qquad \text{(B-3)}$$

The Air Saturation Equation is:

$$\frac{\partial S_a}{\partial t} = \left[\frac{g}{\rho_a \phi \Delta \bar{V}}\right] \frac{\partial}{\partial x_i} \left[\frac{\rho_a \rho_w k_{x_i} k_{ra} \Delta A_i}{\mu_a} \frac{\partial \psi_a}{\partial x_i}\right] \Delta x_i$$

$$+ \left[\frac{g}{\rho_a \phi \Delta \bar{V}}\right] \frac{\partial}{\partial x_i} \left[\frac{\rho_a^2 k_{x_i} k_{ra} \Delta A_i}{\mu_a} \frac{\partial h}{\partial x_i}\right] \Delta x_i$$

$$- \frac{\rho_p Q_a}{\rho_a \phi \Delta \bar{V}} - \frac{S_a}{\phi \Delta \bar{V}} \frac{\partial}{\partial t} (\phi \Delta \bar{V}) - \frac{S_a}{\rho_a} \frac{\partial \rho_a}{\partial t} . \qquad \text{(B-4)}$$

The finite difference grid system used for equations (B-1) through (B-4) is shown in Figure B-1.

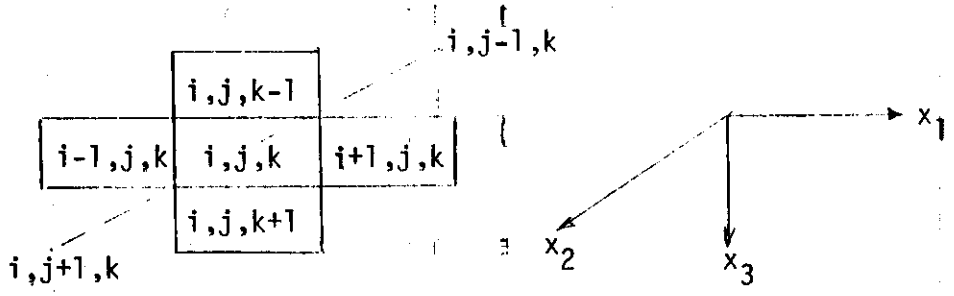

Figure B-1. Central grid and six adjacent grids with the Subscripting used in the finite difference equations.

Because of the symmetry of the spatial derivatives in equations (B-1) through (B-4), only a detailed description of the finite difference equations in the x_1-direction will be given.

The spatial derivative at a point on the boundary between the grids (i, j, k) and (i+1, j, k) may be approximated by

$$\left(\frac{\partial \psi_w}{\partial x_1}\right)_{i+\frac{1}{2},j,k} = \frac{\psi_{w_{i+1,j,k}} - \psi_{w_{i,j,k}}}{0.5[(\Delta x_1)_{i+1,j,k} + (\Delta x_1)_{i,j,k}]}, \tag{B-5a}$$

$$\left(\frac{\partial \psi_c}{\partial x_1}\right)_{i+\frac{1}{2},j,k} = \frac{\psi_{c_{i+1,j,k}} - \psi_{c_{i,j,k}}}{0.5[(\Delta x_1)_{i+1,j,k} + (\Delta x_1)_{i,j,k}]}, \tag{B-5b}$$

$$\left(\frac{\partial h}{\partial x_1}\right)_{i+\frac{1}{2},j,k} = \frac{h_{i+1,j,k} - h_{i,j,k}}{0.5[(\Delta x_1)_{i+1,j,k} + (\Delta x_1)_{i,j,k}]}. \tag{B-5c}$$

Likewise for a point on the boundary between the grids (i -1, j,k) and (i, j, k):

$$\left(\frac{\partial \psi_w}{\partial x_1}\right)_{i-\frac{1}{2},j,k} = \frac{\psi_{w_{i,j,k}} - \psi_{w_{i-1,j,k}}}{0.5[(\Delta x_1)_{i,j,k} + (\Delta x_1)_{i-1,j,k}]}, \tag{B-5d}$$

$$\left(\frac{\partial \psi_c}{\partial x_1}\right)_{i-\frac{1}{2},j,k} = \frac{\psi_{c_{i,j,k}} - \psi_{c_{i-1,j,k}}}{0.5[(\Delta x_1)_{i,j,k} + (\Delta x_1)_{i-1,j,k}]}, \tag{B-5e}$$

$$\left(\frac{\partial h}{\partial x_1}\right)_{i-\frac{1}{2},j,k} = \frac{h_{i,j,k} - h_{i-1,j,k}}{0.5[(\Delta x_1)_{i,j,k} + (\Delta x_1)_{i-1,j,k}]}. \tag{B-5f}$$

The x_1-component on the left hand side of equation (B-1) may be appxoimated by:

$$[\ell hs]_{x_1} = \left(\frac{\Delta x_1}{\rho_w \phi \Delta \overline{V}}\right)_{i,j,k} \frac{\partial}{\partial x_1} \left[\frac{\rho_w^2 k_{x_1} k_{rw} \Delta A_1}{\mu_w} \left(\frac{\partial \psi_w}{\partial x_1}\right)\right]_{i,j,k}$$

$$+ \left(\frac{\Delta x_1}{\rho_w \phi \Delta \bar{V}}\right)_{i,j,k} \frac{\partial}{\partial x_1} \left[\frac{\rho_a \rho_w k_{x_1} k_{ra} \Delta A_1}{\mu_a} \left(\frac{\partial \psi_w}{\partial x_1}\right)\right]_{i,j,k}$$

$$= \left(\frac{\Delta x_1}{\rho_w \phi \Delta \bar{V}}\right)_{i,j,k} \left(\frac{1}{\Delta x_1}\right)_{i,j,k} \left\{\left[\frac{\rho_w^2 k_{x_1} k_{rw} \Delta A_1}{\mu_w} \left(\frac{\partial \psi_w}{\partial x_1}\right)\right]_{i+\frac{1}{2},j,k}\right.$$

$$\left. - \left[\frac{\rho_w^2 k_{x_1} k_{rw} \Delta A_1}{\mu_w} \left(\frac{\partial \psi_w}{\partial x_1}\right)\right]_{i-\frac{1}{2},j,k}\right\}$$

$$+ \left(\frac{\Delta x_1}{\rho_a \phi \Delta \bar{V}}\right)_{i,j,k} \left(\frac{1}{\Delta x_1}\right)_{i,j,k} \left\{\left[\frac{\rho_a \rho_w k_{x_1} k_{ra} \Delta A_1}{\mu_a} \left(\frac{\partial \psi_w}{\partial x_1}\right)\right]_{i+\frac{1}{2},j,k}\right.$$

$$\left. - \left[\frac{\rho_a \rho_w k_{x_1} k_{ra} \Delta A_1}{\mu_a} \left(\frac{\partial \psi_w}{\partial x_1}\right)\right]_{i-\frac{1}{2},j,k}\right\} . \qquad \text{(B-6)}$$

Defining the following notations:

$$\Delta x_1^+ = 0.5[(\Delta x_1)_{i+1,j,k} + (\Delta x_1)_{i,j,k}] , \qquad \text{(B-7a)}$$

$$\Delta x_1^- = 0.5[(\Delta x_1)_{i-1,j,k} + (\Delta x_1)_{i,j,k}] , \qquad \text{(B-7b)}$$

$$\Delta x_2^+ = 0.5[(\Delta x_2)_{i,j+1,k} + (\Delta x_2)_{i,j,k}] , \qquad \text{(B-7c)}$$

$$\Delta x_2^- = 0.5[(\Delta x_2)_{i,j-1,k} + (\Delta x_2)_{i,j,k}] , \qquad \text{(B-7d)}$$

$$\Delta x_3^+ = 0.5[(\Delta x_3)_{i,j,k+1} + (\Delta x_3)_{i,j,k}] , \qquad \text{(B-7e)}$$

$$\Delta x_3^- = 0.5[(\Delta x_3)_{i,j,k-1} + (\Delta x_3)_{i,j,k}] . \qquad \text{(B-7f)}$$

Also the following notations are used:

$$(\Delta A_1)_{i,j,k} = (\Delta x_2 \Delta x_3)_{i,j,k} = (\Delta x_2)_{i,j,k} (\Delta x_3)_{i,j,k} \quad , \tag{B-7g}$$

$$(\Delta A_2)_{i,j,k} = (\Delta x_1 \Delta x_3)_{i,j,k} = (\Delta x_1)_{i,j,k} (\Delta x_3)_{i,j,k} \quad , \tag{B-7h}$$

$$(\Delta A_3)_{i,j,k} = (\Delta x_1 \Delta x_2)_{i,j,k} = (\Delta x_1)_{i,j,k} (\Delta x_2)_{i,j,k} \quad , \tag{B-7i}$$

$$(\Delta \bar{V})_{i,j,k} = (\Delta x_1 \Delta x_2 \Delta x_3)_{i,j,k} = (\Delta x_1)_{i,j,k} (\Delta x_2)_{i,j,k} (\Delta x_3)_{i,j,k} . \tag{B-7j}$$

Substituting equations (B-5) into equation (B-6) and using equations (B-7):

$$[\ell hs]_{x_1} = \left(\frac{\Delta x_1}{\rho_w \phi \Delta \bar{V}}\right)_{i,j,k} \left(\frac{1}{\Delta x_1}\right)_{i,j,k} \left\{ \left(\frac{\rho_w^2 k_{x_1} k_{rw} \Delta A_1}{\mu_w}\right)_{i+\frac{1}{2},j,k} \left(\frac{\psi_{w_{i+1,j,k}} - \psi_{w_{i,j,k}}}{0.5\Delta x_1^+}\right) - \left(\frac{\rho_w^2 k_{x_1} k_{rw} \Delta A_1}{\mu_w}\right)_{i-\frac{1}{2},j,k} \left(\frac{\psi_{w_{i,j,k}} - \psi_{w_{i-1,j,k}}}{0.5\Delta x_1^-}\right) \right\} + \left(\frac{\Delta x_1}{\rho_a \phi \Delta \bar{V}}\right)_{i,j,k} \left(\frac{1}{\Delta x_1}\right)_{i,j,k} \left\{ \left(\frac{\rho_a \rho_w k_{x_1} k_{ra} \Delta A_1}{\mu_a}\right)_{i+\frac{1}{2},j,k} \left(\frac{\psi_{w_{i+1,j,k}} - \psi_{w_{i,j,k}}}{0.5\Delta x_1^+}\right) - \left(\frac{\rho_a \rho_w k_{x_1} k_{ra} \Delta A_1}{\mu_a}\right)_{i-\frac{1}{2},j,k} \left(\frac{\psi_{w_{i,j,k}} - \psi_{w_{i-1,j,k}}}{0.5\Delta x_1^-}\right) \right\} . \tag{B-8}$$

The concept of "upstream mobility" will be used in calculating the flow coefficients. According to "upstream mobility" concept, the relative permeability of the grid from which the fluid emanates is

used in calculating the fluid flow coefficients. Therefore, using the harmonic mean concept and the concept of "upstream mobility," the flow coefficients at grid interfaces may be calculated as:

$$\left(\frac{\rho_w^2 k_{x_1} k_{rw} \Delta A_1}{\mu_w}\right)_{i+\frac{1}{2},j,k}$$

$$= \frac{2(\rho_w^2 k_{x_1} \Delta A_1)_{i,j,k} (\rho_w^2 k_{x_1} \Delta A_1)_{i+1,j,k}}{(\rho_w^2 k_{x_1} \Delta A_1)_{i,j,k} (\mu_w)_{i+1,j,k} + (\rho_w^2 k_{x_1} \Delta A_1)_{i+1,j,k} (\mu_w)_{i,j,k}} (k_{rw})_u \tag{B-9}$$

where $(k_{rw})_u$ is the relative permeability of the grid from which the fluid emanates. Also the following notations are implied for combination of variables such as:

$$(\rho_w^2 k_{x_1} \Delta A_1)_{i,j,k} = (\rho_w^2)_{i,j,k} (k_{x_1})_{i,j,k} (\Delta A_1)_{i,j,k} , \tag{B-10a}$$

and

$$(\rho_w \phi \Delta \overline{V})_{i,j,k} = (\rho_w)_{i,j,k} (\phi)_{i,j,k} (\Delta \overline{V})_{i,j,k} . \tag{B-10b}$$

Defining the following terms:

$$N^+_{x_1 w} = \left(\frac{\Delta x_1}{\rho_w \phi \Delta \overline{V}}\right)_{i,j,k} \left(\frac{1}{\Delta x_1}\right)_{i,j,k} \left(\frac{\rho_w^2 k_{x_1} k_{rw} \Delta A_1}{\mu_w}\right)_{i+\frac{1}{2},j,k} \left(\frac{1}{\Delta x_1^+}\right)$$

$$= \frac{(\Delta x_1)_{i,j,k}}{(\rho_w \phi \Delta \overline{V})_{i,j,k}} \left(\frac{1}{\Delta x_1}\right)_{i,j,k} \left(\frac{1}{\Delta x_1^+}\right)$$

$$\left[\frac{2(\rho_w^2 k_{x_1} \Delta A_1)_{i,j,k} (\rho_w^2 k_{x_1} \Delta A_1)_{i+1,j,k}}{(\rho_w^2 k_{x_1} \Delta A_1)_{i,j,k} (\mu_w)_{i+1,j,k} + (\rho_w^2 k_{x_1} \Delta A_1)_{i+1,j,k} (\mu_w)_{i,j,k}} (k_{rw})_u\right]$$

$$= \left[\frac{2(\rho_w^2 k_{x_1} \Delta A_1)_{i,j,k} \, (\rho_w^2 k_{x_1} \Delta A_1)_{i+1,j,k}}{(\rho_w^2 k_{x_1} \Delta A_1)_{i,j,k} \, (\mu_w)_{i+1,j,k} + (\rho_w^2 k_{x_1} \Delta A_1)_{i+1,j,k} \, (\mu_w)_{i,j,k}} (k_{rw})_u\right]$$

$$/[(\rho_w \phi \Delta \bar{V})_{i,j,k} \, \Delta x_1^+] \, , \qquad \text{(B-11a)}$$

$$N_{x_1 w}^- = \left[\frac{2(\rho_w^2 k_{x_1} \Delta A_1)_{i,j,k} (\rho_w^2 k_{x_1} \Delta A_1)_{i-1,j,k}}{(\rho_w^2 k_{x_1} \Delta A_1)_{i,j,k} \, (\mu_w)_{i-1,j,k} + (\rho_w^2 k_{x_1} \Delta A_1)_{i-1,j,k} \, (\mu_w)_{i,j,k}}\right.$$

$$\left.(k_{rw})_u\right] \, / \, [(\rho_w \phi \Delta \bar{V})_{i,j,k} \, \Delta x_1^-] \, , \qquad \text{(B-11b)}$$

$$N_{x_1 a}^+ = \left[\frac{2(\rho_a \rho_w k_{x_1} \Delta A_1)_{i,j,k} \, (\rho_a \rho_w k_{x_1} \Delta A_1)_{i+1,j,k}}{(\rho_a \rho_w k_{x_1} \Delta A_1)_{i,j,k} \, (\mu_a)_{i+1,j,k} + (\rho_a \rho_w k_{x_1} \Delta A_1)_{i+1,j,k} (\mu_a)_{i,j,k}}\right.$$

$$\left.(k_{ra})_u\right] \, / \, [(\rho_a \phi \Delta \bar{V})_{i,j,k} \, \Delta x_1^+] \, , \qquad \text{(B-11c)}$$

$$N_{x_1 a}^- = \left[\frac{2(\rho_a \rho_w k_{x_1} \Delta A_1)_{i,j,k} (\rho_a \rho_w k_{x_1} \Delta A_1)_{i-1,j,k}}{(\rho_a \rho_w k_{x_1} \Delta A_1)_{i,j,k} \, (\mu_a)_{i-1,j,k} + (\rho_a \rho_w k_{x_1} \Delta A_1)_{i-1,j,k} (\mu_a)_{i,j,k}}\right.$$

$$\left.(k_{ra})_u\right] \, / \, [(\rho_a \phi \Delta \bar{V})_{i,j,k} \, \Delta x_1^-] \, , \qquad \text{(B-11d)}$$

$$N_{x_2 w}^+ = \left[\frac{2(\rho_w^2 k_{x_2} \Delta A_2)_{i,j,k} \, (\rho_w^2 k_{x_2} \Delta A_2)_{i,j+1,k}}{(\rho_w^2 k_{x_2} \Delta A_2)_{i,j,k} \, (\mu_w)_{i,j+1,k} + (\rho_w^2 k_{x_2} \Delta A_2)_{i,j+1,k} \, (\mu_w)_{i,j,k}}\right.$$

$$(k_{rw})_u \Big] \; / \; [(\rho_w \phi \Delta \bar{V})_{i,j,k} \, \Delta x_2^+] \,, \tag{B-11e}$$

$$N_{x_2 w}^- = \left[\frac{2(\rho_w^2 k_{x_2} \Delta A_2)_{i,j,k} \, (\rho_w^2 k_{x_2} \Delta A_2)_{i,j-1,k}}{(\rho_w^2 k_{x_2} \Delta A_2)_{i,j,k} \, (\mu_w)_{i,j-1,k} + (\rho_w^2 k_{x_2} \Delta A_2)_{i,j-1,k} \, (\mu_w)_{i,j,k}} \right.$$

$$(k_{rw})_u \Big] \; / \; [(\rho_w \phi \Delta \bar{V})_{i,j,k} \, \Delta x_2^-] \,, \tag{B-11f}$$

$$N_{x_2 a}^+ = \left[\frac{2(\rho_a \rho_w \, k_{x_2} \Delta A_2)_{i,j,k} \, (\rho_a \rho_w k_{x_2} \Delta A_2)_{i,j+1,k}}{(\rho_a \rho_w k_{x_2} \Delta A_2)_{i,j,k} (\mu_a)_{i,j+1,k} + (\rho_a \rho_w k_{x_2} \Delta A_2)_{i,j+1,k} (\mu_a)_{i,j,k}} \right.$$

$$(k_{ra})_u \Big] \; / \; [(\rho_a \phi \Delta \bar{V})_{i,j,k} \Delta x_2^+] \,, \tag{B-11g}$$

$$N_{x_2 a}^- = \left[\frac{2(\rho_a \rho_w k_{x_2} \Delta A_2)_{i,j,k} \, (\rho_a \rho_w k_{x_2} \Delta A_2)_{i,j-1,K}}{(\rho_a \rho_w k_{x_2} \Delta A_2)_{i,j,k} (\mu_a)_{i,j-1,k} + (\rho_a \rho_w k_{x_2} \Delta A_2)_{i,j-1,k} (\mu_a)_{i,j,k}} \right.$$

$$(k_{ra})_u \Big] \; / \; [(\rho_a \phi \Delta \bar{V})_{i,j,k} \, \Delta x_2^-] \,, \tag{B-11h}$$

$$N_{x_3 w}^+ = \left[\frac{2(\rho_w^2 k_{x_3} \Delta A_3)_{i,j,k} \, (\rho_w^2 k_{x_3} \Delta A_3)_{i,j,k+1}}{(\rho_w^2 k_{x_3} \Delta A_3)_{i,j,k} (\mu_w)_{i,j,k+1} + (\rho_w^2 k_{x_3} \Delta A_3)_{i,j,k+1} (\mu_w)_{i,j,k}} \right.$$

$$(k_{rw})_u \Big] \; / \; [(\rho_w \phi \Delta \bar{V})_{i,j,k} \, \Delta x_3^+] \,, \tag{B-11i}$$

$$N^{-}_{x_3 w} = \left[\frac{2(\rho_w^2 k_{x_3} \Delta A_3)_{i,j,k} \, (\rho_w^2 k_{x_3} \Delta A_3)_{i,j,k-1}}{(\rho_w^2 k_{x_3} \Delta A_3)_{i,j,k} (\mu_w)_{i,j,k-1} + (\rho_w^2 k_{x_3} \Delta A_3)_{i,j,k-1} (\mu_w)_{i,j,k}} \right.$$

$$\left. (k_{rw})_u \right] \; / \; [(\rho_w \phi \Delta \bar{V})_{i,j,k} \, \Delta x_3^{-}] \; , \qquad \text{(B-11j)}$$

$$N^{+}_{x_3 a} = \left[\frac{2(\rho_a \rho_w k_{x_3} \Delta A_3)_{i,j,k} \, (\rho_a \rho_w k_{x_3} \Delta A_3)_{i,j,k+1}}{(\rho_a \rho_w k_{x_3} \Delta A_3)_{i,j,k} (\mu_a)_{i,j,k+1} + (\rho_a \rho_w k_{x_3} \Delta A_3)_{i,j,k+1} (\mu_a)_{i,j,k}} \right.$$

$$\left. (k_{ra})_u \right] \; / \; [(\rho_a \phi \Delta \bar{V})_{i,j,k} \, \Delta x_3^{+}] \; , \qquad \text{(B-11k)}$$

$$N^{-}_{x_3 a} = \left[\frac{2(\rho_a \rho_w k_{x_3} \Delta A_3)_{i,j,k} \, (\rho_a \rho_w k_{x_3} \Delta A_3)_{i,j,k-1}}{(\rho_a \rho_w k_{x_3} \Delta A_3)_{i,j,k} (\mu_a)_{i,j,k-1} + (\rho_a \rho_w k_{x_3} \Delta A_3)_{i,j,k-1} (\mu_a)_{i,j,k}} \right.$$

$$\left. (k_{ra})_u \right] \; / \; [(\rho_a \phi \Delta \bar{V})_{i,j,k} \, \Delta x_3^{-}] \; , \qquad \text{(B-11}\ell\text{)}$$

$$N^{++}_{x_1 a} = \left[\frac{2(\rho_a^2 k_{x_1} \Delta A_1)_{i,j,k} \, (\rho_a^2 k_{x_1} \Delta A_1)_{i+1,j,k}}{(\rho_a^2 k_{x_1} \Delta A_1)_{i,j,k} (\mu_a)_{i+1,j,k} + (\rho_a^2 k_{x_1} \Delta A_1)_{i+1,j,k} (\mu_a)_{i,j,k}} \right.$$

$$\left. (k_{ra})_u \right] \; / \; [(\rho_a \phi \Delta \bar{V})_{i,j,k} \, \Delta x_1^{+}] \; , \qquad \text{(B-11m)}$$

$$N^{--}_{x_1 a} = \left[\frac{2(\rho_a^2 k_{x_1} \Delta A_1)_{i,j,k} \, (\rho_a^2 k_{x_1} \Delta A_1)_{i-1,j,k}}{(\rho_a^2 k_{x_1} \Delta A_1)_{i,j,k} (\mu_a)_{i-1,j,k} + (\rho_a^2 k_{x_1} \Delta A_1)_{i-1,j,k} (\mu_a)_{i,j,k}} \right.$$

$$\left. (k_{ra})_u \right] \Big/ \left[(\rho_a \phi \Delta \bar{V})_{i,j,k} \, \Delta x_1^- \right] , \qquad \text{(B-11n)}$$

$$N^{++}_{x_2 a} = \left[\frac{2(\rho_a^2 k_{x_2} \Delta A_2)_{i,j,k} \, (\rho_a^2 k_{x_2} \Delta A_2)_{i,j+1,k}}{(\rho_a^2 k_{x_2} \Delta A_2)_{i,j,k} (\mu_a)_{i,j+1,k} + (\rho_a^2 k_{x_2} \Delta A_2)_{i,j+1,k} (\mu_a)_{i,j,k}} \right.$$

$$\left. (k_{ra})_u \right] \Big/ \left[(\rho_a \phi \Delta \bar{V})_{i,j,k} \, \Delta x_2^+ \right] , \qquad \text{(B-11o)}$$

$$N^{--}_{x_2 a} = \left[\frac{2(\rho_a^2 k_{x_2} \Delta A_2)_{i,j,k} \, (\rho_a^2 k_{x_2} \Delta A_2)_{i,j-1,k}}{(\rho_a^2 k_{x_2} \Delta A_2)_{i,j,k} (\mu_a)_{i,j-1,k} + (\rho_a^2 k_{x_2} \Delta A_2)_{i,j-1,k} (\mu_a)_{i,j,k}} \right.$$

$$\left. (k_{ra})_u \right] \Big/ \left[(\rho_a \phi \Delta \bar{V})_{i,j,k} \, \Delta x_2^- \right] \qquad \text{(B-11p)}$$

$$N^{++}_{x_3 a} = \left[\frac{2(\rho_a^2 k_{x_3} \Delta A_3)_{i,j,k} \, (\rho_a^2 k_{x_3} \Delta A_3)_{i,j,k+1}}{(\rho_a^2 k_{x_3} \Delta A_3)_{i,j,k} (\mu_a)_{i,j,k+1} + (\rho_a^2 k_{x_3} \Delta A_3)_{i,j,k+1} (\mu_a)_{i,j,k}} \right.$$

$$\left. (k_{ra})_u \right] \Big/ \left[(\rho_a \phi \Delta \bar{V})_{i,j,k} \, \Delta x_3^+ \right] \qquad \text{(B-11q)}$$

$$N^{--}_{x_3 a} = \left[\frac{2(\rho_a^2 k_{x_3} \Delta A_3)_{i,j,k} \, (\rho_a^2 k_{x_3} \Delta A_3)_{i,j,k-1}}{(\rho_a^2 k_{x_3} \Delta A_3)_{i,j,k} (\mu_a)_{i,j,k-1} + (\rho_a^2 k_{x_3} \Delta A_3)_{i,j,k-1} (\mu_a)_{i,j,k}} \right.$$

$$\left. (k_{ra})_u \right] \Big/ \left[(\rho_a \phi \Delta \bar{V})_{i,j,k} \, \Delta x_3^- \right] . \qquad \text{(B-11r)}$$

Defining the following notations:

$$\Delta h^+_{x_1} = h_{i+1,j,k} - h_{i,j,k} , \qquad \text{(B-12a)}$$

$$\Delta h^-_{x_1} = h_{i-1,j,k} - h_{i,j,k} , \qquad \text{(B-12b)}$$

$$\Delta h^+_{x_2} = h_{i,j+1,k} - h_{i,j,k} , \qquad \text{(B-12c)}$$

$$\Delta h^-_{x_2} = h_{i,j-1,k} - h_{i,j,k} , \qquad \text{(B-12d)}$$

$$\Delta h^+_{x_3} = h_{i,j,k+1} - h_{i,j,k} , \qquad \text{(B-12e)}$$

$$\Delta h^-_{x_3} = h_{i,j,k-1} - h_{i,j,k} . \qquad \text{(B-12f)}$$

The derivatives with respect to time are evaluated as follows:

$$\frac{\partial}{\partial t} (\phi \Delta \bar{V}) = \frac{(\phi \Delta \bar{V})^t_{i,j,k} - (\phi \Delta \bar{V})^{t-1}_{i,j,k}}{\Delta t_{old}} , \qquad \text{(B-13a)}$$

$$\frac{\partial \rho_w}{\partial t} = \frac{\rho^t_{w_{i,j,k}} - \rho^{t-1}_{w_{i,j,k}}}{\Delta t_{old}} , \qquad \text{(B-13b)}$$

$$\frac{\partial \rho_a}{\partial t} = \frac{\rho^t_{a_{i,j,k}} - \rho^{t-1}_{a_{i,j,k}}}{\Delta t_{old}} . \qquad \text{(B-13c)}$$

Where Δt_{old} is the time increment used in the preceding time step.

Combining equations (B-11), (B-12) and (B-13), an implicit finite difference representation of the Water Pressure equation (B-1) is:

$$(N^{+}_{x_1 w} + N^{+}_{x_1 a})\,\psi^{t+1}_{w_{i+1,j,k}} + (N^{-}_{x_1 w} + N^{-}_{x_1 a})\,\psi^{t+1}_{w_{i-1,j,k}}$$

$$+ (N^{+}_{x_2 w} + N^{+}_{x_2 a})\,\psi^{t+1}_{w_{i,j+1,k}} + (N^{-}_{x_2 w} + N^{-}_{x_2 a})\,\psi^{t+1}_{w_{i,j-1,k}}$$

$$+ (N^{+}_{x_3 w} + N^{-}_{x_3 a})\,\psi^{t+1}_{w_{i,j,k+1}} + (N^{-}_{x_3 w} + N^{-}_{x_3 a})\,\psi^{t+1}_{w_{i,j,k-1}}$$

$$- (N^{+}_{x_1 w} + N^{+}_{x_1 a} + N^{-}_{x_1 w} + N^{-}_{x_1 a} + N^{+}_{x_2 w} + N^{+}_{x_2 a} + N^{-}_{x_2 w} + N^{-}_{x_2 a} + N^{+}_{x_3 w}$$

$$+ N^{+}_{x_3 a} + N^{-}_{x_3 w} + N^{-}_{x_3 a})\,\psi^{t+1}_{w_{i,j,k}}$$

$$= -[N^{+}_{x_1 a}\,\psi^{t}_{c_{i+1,j,k}} + N^{-}_{x_1 a}\,\psi^{t}_{c_{i-1,j,k}} + N^{+}_{x_2 a}\,\psi^{t}_{c_{i,j+1,k}} + N^{-}_{x_2 a}\,\psi^{t}_{c_{i,j-1,k}}$$

$$+ N^{+}_{x_3 a}\,\psi^{t}_{c_{i,j,k+1}} + N^{-}_{x_3 a}\,\psi^{t}_{c_{i,j,k-1}} - (N^{+}_{x_1 a} + N^{-}_{x_1 a} + N^{+}_{x_2 a} + N^{-}_{x_2 a}$$

$$N^{+}_{x_3 a} + N^{-}_{x_3 a})\,\psi^{t}_{c_{i,j,k}} + (N^{+}_{x_1 w} + N^{++}_{x_1 a})\,\Delta h^{+}_{x_1} + (N^{-}_{x_1 w} + N^{--}_{x_1 a})\,\Delta h^{-}_{x_1}$$

$$+ (N^{+}_{x_2 w} + N^{++}_{x_2 a})\,\Delta h^{+}_{x_2} + (N^{-}_{x_2 w} + N^{--}_{x_2 a})\,\Delta h^{-}_{x_2} + (N^{+}_{x_3 w} + N^{++}_{x_3 a})\,\Delta h^{+}_{x_3}$$

$$+ (N^{-}_{x_3 w} + N^{--}_{x_3 a})\,\Delta h^{-}_{x_3}]$$

$$+ \frac{1}{g(\phi\Delta\bar{V})^{t}_{i,j,k}} \frac{(\phi\Delta\bar{V})^{t}_{i,j,k} - (\phi\Delta\bar{V})^{t-1}_{i,j,k}}{\Delta t_o} + \frac{(S^{t}_{w})_{i,j,k}}{g(\rho^{t}_{w})_{i,j,k}}$$

$$\frac{(\rho_w)^{t}_{i,j,k} - (\rho_w)^{t-1}_{i,j,k}}{\Delta t_{old}}$$

$$+ \frac{(S_a^t)_{i,j,k}}{g(\rho_a^t)_{i,j,k}} \frac{(\rho_a)^t_{i,j,k} - (\rho_a)^{t-1}_{i,j,k}}{\Delta t_{old}} + \frac{(\rho_p^t)_{i,j,k}}{g(\phi\Delta\bar{V})^t_{i,j,k}} \left[\left[\frac{Q_w}{\rho_w}\right]^t_{i,j,k}\right.$$

$$\left. + \left[\frac{Q_a}{\rho_a}\right]^t_{i,j,k}\right] . \qquad \text{(B-14)}$$

The equation (B-14) is solved implicitly for water pressures at time t+1. These pressures are then used in equations (B-3) and (B-4) to solve for water saturation and air saturation, respectively.

An explicit form for water saturation equation (B-3) is:

$$(\Delta S_w)^+_{i,j,k} = g\Delta t \left[N^+_{x_1w} \psi^{t+1}_{w_{i+1,j,k}} + N^-_{x_1w} \psi^{t+1}_{w_{i-1,j,k}}\right.$$

$$+ N^+_{x_2w} \psi^{t+1}_{w_{i,j+1,k}} + N^-_{x_2w} \psi^{t+1}_{w_{i,j-1,k}} + N^+_{x_3w} \psi^{t+1}_{w_{i,j,k+1}}$$

$$\left. + N^-_{x_3w} \psi^{t+1}_{w_{i,j,k-1}}\right] - (N^+_{x_1w} + N^-_{x_1w} + N^+_{x_2w} + N^-_{x_2w} + N^+_{x_3w}$$

$$+ N^-_{x_3w}) \psi^{t+1}_{w_{i,j,k}} + N^+_{x_1w} \Delta h^+_{x_1} + N^-_{x_1w} \Delta h^-_{x_1} + N^+_{x_2w} \Delta h^+_{x_2} + N^-_{x_2w} \Delta h^-_{x_2}$$

$$+ N^+_{x_3w} \Delta h^+_{x_3} + N^-_{x_3w} \Delta h^-_{x_3}] - \left[\left[\frac{\rho_p Q_w}{\rho_w \phi\Delta\bar{V}}\right]^t_{i,j,k} - (S_w)^t_{i,j,k}\right.$$

$$\left. \frac{\{(\phi\Delta\bar{V})^t_{i,j,k} - (\phi\Delta\bar{V})^{t-1}_{i,j,k}\}}{(\phi\Delta\bar{V})^t_{i,j,k}\, \Delta t_{old}} - \left[\frac{S_w}{\rho_w}\right]^t_{i,j,k} \frac{(\rho_w)^t_{i,j,k} - (\rho_w)^{t-1}_{i,j,k}}{\Delta t_{old}}\right] \Delta t \qquad \text{(B-15)}$$

where $(\Delta S_w)^t_{i,j,k} = (S_w)^{t+1}_{i,j,k} - (S_w)^t_{i,j,k}$.

Similarly, an explicit form for air saturation equation (B-4) is:

$$(\Delta S_a)^{+}_{i,j,k} = g\Delta t \left[N^{+}_{x_1 a}\, \psi^{t+1}_{a_{i+1,j,k}} + N^{-}_{x_1 a}\, \psi^{t+1}_{a_{i-1,j,k}} + N^{+}_{x_2 a}\, \psi^{t+1}_{a_{i,j+1,k}}\right.$$

$$+ N^{-}_{x_2 a}\, \psi^{t+1}_{a_{i,j-1,k}} + N^{+}_{x_3 a}\, \psi^{t+1}_{a_{i,j,k+1}} + N^{-}_{x_3 a}\, \psi^{t+1}_{a_{i,j,k-1}} - (N^{+}_{x_1 a}$$

$$+ N^{-}_{x_1 a} + N^{+}_{x_2 a} + N^{-}_{x_2 a} + N^{+}_{x_3 a} + N^{-}_{x_3 a})\, \psi^{t+1}_{a_{i,j,k}} + N^{++}_{x_1 a}$$

$$\Delta h^{+}_{x_1} + N^{--}_{x_1 a}\, \Delta h^{-}_{x_1} + N^{++}_{x_2 a}\, \Delta h^{+}_{x_2} + N^{--}_{x_2 a}\, \Delta h^{-}_{x_2} + N^{++}_{x_3 a}\, \Delta h^{+}_{x_3}$$

$$\left. + N^{--}_{x_3 a}\, \Delta h^{-}_{x_3}\right] - \left[\left(\frac{\rho_p Q_a}{\rho_a \phi \Delta \bar{V}}\right)^{t}_{i,j,k} - (S_a)^{t}_{i,j,k}\, \frac{\{(\phi\Delta\bar{V})^{t}_{i,j,k} - (\phi\Delta\bar{V})^{t-1}_{i,j,k}\}}{(\phi\Delta\bar{V})^{t}_{i,j,k}\, \Delta t_{old}}\right.$$

$$\left. - \left(\frac{S_w}{\rho_w}\right)^{t}_{i,j,k} \frac{(\rho_w)^{t}_{i,j,k} - (\rho_w)^{t-1}_{i,j,k}}{\Delta t_{old}}\right] \Delta t \qquad \text{(B-16)}$$

where $(\Delta S_a)^{+}_{i,j,k} = (S_a)^{t+1}_{i,j,k} - (S_a)^{t}_{i,j,k}$ and

$$(\psi_a)^{t+1}_{i,j,k} = (\psi_c)^{t}_{i,j,k} + (\psi_w)^{t+1}_{i,j,k}$$

The finite difference form of equation (A-25) is:

$$\frac{S_a}{(\psi_a + \psi_{atm})g}\, \frac{\partial \psi_a}{\partial t} = \frac{S^{t}_{a_{i,j,k}}}{(\psi^{t}_{a_{i,j,k}} + 1033.3)g}\, \frac{(\psi_a)^{t+1}_{i,j,k} - (\psi_a)^{t}_{i,j,k}}{\Delta t} \qquad \text{(B-17)}$$

The finite difference form of the Air Pressure Equation (B-2) when combined with equation (B-17) is:

$$(N^{+}_{x_1 w} + N^{+}_{x_1 a})\, \psi^{t+1}_{a_{i+1,j,k}} + (N^{-}_{x_1 w} + N^{-}_{x_1 a})\, \psi^{t+1}_{a_{i-1,j,k}}$$

$$+ (N^{+}_{x_2 w} + N^{+}_{x_2 a})\, \psi^{t+1}_{a_{i,j+1,k}} + (N^{-}_{x_2 w} + N^{-}_{x_2 a})\, \psi^{t+1}_{a_{i,j-1,k}}$$

$$+ (N^{+}_{x_3w} + N^{+}_{x_3a})\,\psi^{t+1}_{a_{i,j,k+1}} + (N^{-}_{x_3w} + N^{-}_{x_3a})\,\psi^{t+1}_{a_{i,j,k-1}}$$

$$- (N^{+}_{x_1w} + N^{+}_{x_1a} + N^{-}_{x_1w} + N^{-}_{x_1a} + N^{+}_{x_2w} + N^{+}_{x_2a} + N^{-}_{x_2w}$$

$$+ N^{-}_{x_2a} + N^{+}_{x_3w} + N^{+}_{x_3a} + N^{-}_{x_3w} + N^{-}_{x_3a} + \frac{S^{t}_{a_{i,j,k}}}{(\psi^{t}_{a_{i,j,k}} + 1033.3)\Delta tg})$$

$$\psi^{t+1}_{a_{i,j,k}} = N^{+}_{x_1w}\,\psi^{t}_{c_{i+1,j,k}} + N^{-}_{x_1w}\,\psi^{t}_{c_{i-1,j,k}} + N^{+}_{x_2w}\,\psi^{t}_{c_{i,j+1,k}}$$

$$+ N^{-}_{x_2w}\,\psi^{t}_{c_{i,j-1,k}} + N^{+}_{x_3w}\,\psi^{t}_{c_{i,j,k+1}} + N^{-}_{x_3w}\,\psi^{t}_{c_{i,j,k-1}} - (N^{+}_{x_1w}$$

$$+ N^{-}_{x_1w} + N^{+}_{x_2w} + N^{-}_{x_2w} + N^{+}_{x_3w} + N^{-}_{x_3w})\,\psi^{t}_{c_{i,j,k}} - (N^{+}_{x_1w}$$

$$+ N^{++}_{x_1a})\,\Delta h^{+}_{x_1} - (N^{-}_{x_1w} + N^{--}_{x_1a})\,\Delta h^{-}_{x_1} - (N^{+}_{x_2w} + N^{++}_{x_2a})\,\Delta h^{+}_{x_2}$$

$$- (N^{-}_{x_2w} + N^{--}_{x_2a})\,\Delta h^{-}_{x_2} - (N^{+}_{x_3w} + N^{++}_{x_3a})\,\Delta h^{+}_{x_3} - (N^{-}_{x_3w} + N^{--}_{x_3a})$$

$$\Delta h^{-}_{x_3} + \frac{1}{g(\phi\Delta\bar{V})_{i,j,k}}\,\frac{\{(\phi\Delta\bar{V})^{t}_{i,j,k} - (\phi\Delta\bar{V})^{t-1}_{i,j,k}\}}{\Delta t_o} + \frac{S^{t}_{w_{i,j,k}}}{g(\rho_w)^{t}_{i,j,k}}$$

$$\frac{(\rho^{t}_{w_{i,j,k}} - \rho^{t-1}_{w_{i,j,k}})}{\Delta t_o} + \frac{(\rho_p)_{i,j,k}}{g(\phi\Delta\bar{V})_{i,j,k}}\left[\left(\frac{Q_w}{\rho_w}\right)_{i,j,k} + \left(\frac{Q_a}{\rho_a}\right)_{i,j,k}\right] . \tag{B-18}$$

If equation (B-18) is used to solve air pressures implicitly at time t+1, the water pressures at time t+1 is obtained as:

$$(\psi_w)^{t+1}_{i,j,k} = (\psi_a)^{t+1}_{i,j,k} - (\psi_c)^{t}_{i,j,k} .$$

APPENDIX C

DERIVATION OF THE DISPERSION EQUATION

In deriving the dispersion equation, the concept of representative elementary volume (REV) is used. The REV at a point in the porous medium is defined with respect to some medium properties such as porosity: it is the smallest volume element containing that point, such that when several channels are added or subtracted, the global variation of volume leaves the porosity invariant.

The derivation is conducted in three steps: (1) derivation of the continuity equation for the dispersing tracer, (2) development of microscopic mass flux equations, and (3) development of macroscopic mass flux equation by averaging the microscopic equations in a REV of the medium. It is assumed that only the water phase contains the tracer.

Continuity Equation for the Tracer

The continuity equation for the tracer is given as:

(Rate of mass inflow of tracer) -
(Rate of mass outflow of tracer) =
(Rate of change of tracer mass inside the REV).

When applied to a REV of porous media with the dimensions of Δx_1, Δx_2, and Δx_3, as shown in Figure C-1, the results are:

$$(M_t)_{x_1-\Delta x_1/2} - (M_t)_{x_1+\Delta x_1/2} + (M_t)_{x_2-\Delta x_2/2} -$$

$$(M_t)_{x_2+\Delta x_2/2} + (M_t)_{x_3-\Delta x_3/2} - (M_t)_{x_3+\Delta x_3/2} = \frac{\partial M_{tREV}}{\partial t} + M_{tp} , \qquad (C\text{-}1)$$

where $(M_t)_{x_i-\Delta x_i/2}$ = rates of mass inflow of tracer (i = 1, 2, and 3),

$(M_t)_{x_i+\Delta x_i/2}$ = rates of mass outflow of tracer (i = 1, 2, and 3),

M_{tREV} = mass of tracer contained inside the REV, and

M_{tp} = tracer mass flow rate of source or sink which is positive when a sink and negative when a source.

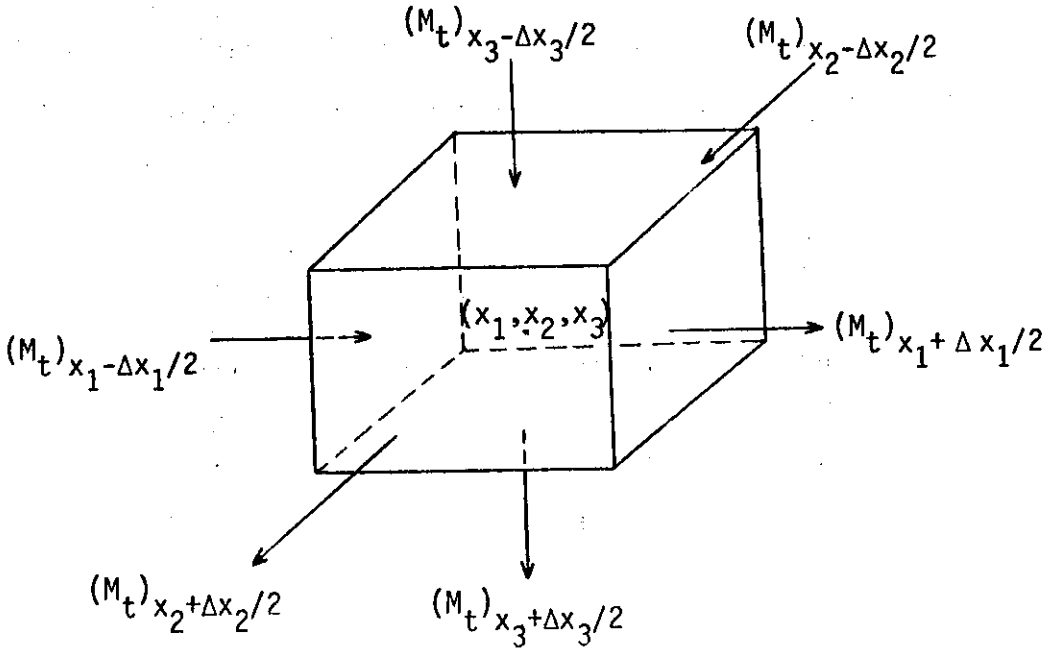

Figure C-1. Representative elementary volume (REV) of a porous medium to develop continuity equation for tracer.

Expanding each one of the mass flow rate terms in a Taylor series about the point (x_1, x_2, x_3) of Figure C-1 gives:

$$(M_t)_{x_i-\Delta x_i/2} = (M_t)_{x_i} - \frac{\partial}{\partial x_i}(M_t)_{x_i}\frac{\Delta x_i}{2} + \frac{1}{2!}\frac{\partial^2 (M_t)_{x_i}}{\partial x_i^2}\left(\frac{\Delta x_i}{2}\right)^2 - \ldots;$$

$$i = 1, 2, 3,$$

and

$$(M_t)_{x_i+\Delta x_i/2} = (M_t)_{x_i} + \frac{\partial}{\partial x_i}(M_t)_{x_i}\frac{\Delta x_i}{2} + \frac{1}{2!}\frac{\partial^2 (M_t)_{x_i}}{\partial x_i^2}\left(\frac{\Delta x_i}{2}\right)^2 + \ldots;$$

$$i = 1, 2, 3. \qquad \text{(C-2)}$$

The tracer mass flow rates may be expressed in terms of the tracer mass flux, the dimensions of the volume element, and the porous media properties, that is,

$$(M_t)_{x_i} = J_i^* \phi S_w \Delta A_i \; ; \quad i = 1, 2, \text{ and } 3 \qquad \text{(C-3a)}$$

$$M_{tRVE} = \phi S_w \Delta \overline{V} C, \qquad \text{(C-3b)}$$

and

$$M_{tp} = C_P Q_w \qquad \text{(C-3c)}$$

where

C = average tracer concentration in the REV, mass of tracer per volume of solution (ML^{-3}),

J_i^* = macroscopic tracer mass flux components in the i-th direction $(ML^{-2}T^{-1})$,

ϕ = porosity,

S_w = saturation of water phase containing tracer,

Q_w = production rate (L^3T^{-1}),

C_p = tracer concentration of production fluid (ML^{-3})

ΔA_i = cross-sectional area (L^2), perpendicular to the mass flux component, J_i^*, and

$\Delta \overline{V} = \Delta x_1 \Delta x_2 \Delta x_3$ = volume of the REV (L^3).

J_i^*'s (i = 1, 2, and 3) are defined as the mass flow rate per unit pore area. The reason for choosing a flux per unit pore area is because the microscopic fluid elements will be averaged over a cross-section of the volume element to yield J_i^*. Since the fluid elements exist only in the pores, the results are a flux in terms of the pore area rather than gross area.

Substituting equations (C-3) and (C-2) into equation (C-1) and neglecting the second order terms in equation (C-2), and using shorthand tensor notation:

$$\frac{\partial}{\partial x_i}(J_i^* \phi S_w \Delta A_i)\Delta x_i = -\frac{\partial}{\partial t}(\phi S_w \Delta \overline{V} C) - C_p Q_w \qquad \text{(C-4)}$$

where i = 1, 2, and 3 corresponds to x_1, x_2, and x_3 coordinates.

Microscopic Analysis

The diffusive volumetric flux with respect to volume-averaged velocity, assuming no volume changes upon mixing is (Bear, 1972; p. 69).

$$\vec{J} = \hat{C}(\vec{\hat{V}}_t - \vec{\hat{V}}) = -D_d \nabla \hat{C} \qquad \text{(C-5)}$$

where $\vec{J}$ = diffusive mass flux of the tracer ($ML^{-2}T^{-1}$),

$\hat{C}$ = concentration of tracer in fluid element (ML^{-3}),

$\vec{\hat{V}}_t$ = velocity of tracer in fluid element with respect to a fixed coordinate system (LT^{-1}),

$\vec{V}$ = volume-averaged velocity of fluid element (LT^{-1}), and

D_d = coefficient of molecular diffusion (L^2T^{-1}).

Let the tortuous path followed by a fluid element in porous media be represented by the axis of channel as shown in Figure C-2. The diffusive mass flux may be written as

$$\vec{J} = - D_d \frac{d\hat{C}}{d\sigma} \tag{C-6}$$

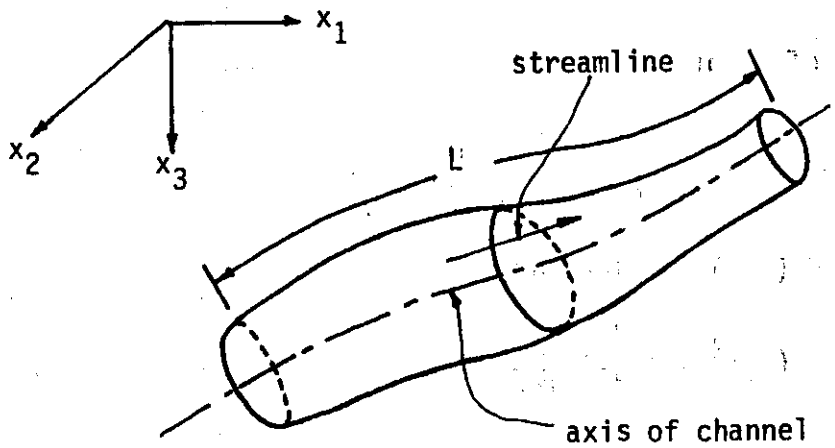

σ = length along axis of channel

ξ = length along streamline

Figure C-2. Model of tortuous path of a fluid element.

Using chain rule, equation (C-6) may be written as:

$$\vec{J} = - D_d \frac{d\hat{C}}{d\xi} \frac{d\xi}{d\sigma} \tag{C-7}$$

To obtain the components of $\vec{J}$ in the x_i ($i = 1, 2, 3$) coordinate system, a transformation is needed. This transformation is carried out in two steps. First the flux $\vec{J}$ as given by equation (C-7) is projected on the direction of the streamline, ξ and then in the direction of the x_i coordinate system. The result is

$$J_i = \left(\left(- D_d \frac{d\hat{C}}{d\xi} \frac{d\xi}{d\sigma} \right) \frac{d\xi}{d\sigma} \right) \frac{dx_i}{d\xi} \quad . \tag{C-8}$$

By the definition of a total derivative,

$$\frac{d\hat{C}}{d\xi} = \frac{\partial \hat{C}}{\partial x_1} \frac{dx_1}{d\xi} + \frac{\partial \hat{C}}{\partial x_2} \frac{dx_2}{d\xi} + \frac{\partial \hat{C}}{\partial x_3} \frac{dx_3}{d\xi} \quad . \tag{C-9}$$

Equations (C-8) and (C-9) combine to give

$$J_i = - D_d \left(\frac{d\xi}{d\sigma}\right)^2 \frac{dx_i}{d\xi} \frac{dx_j}{d\xi} \frac{d\hat{C}}{dx_j} \tag{C-10}$$

where the double summation convention of tensor notation has been invoked. The term $(dx_i/d\xi)(dx_j/d\xi)$ represents a matrix whose nine elements (for $i,j = 1, 2, 3$) are products of cosines of angles between the direction of a streamline at a point and the coordinate axis. The term $(d\xi/d\sigma)^2$ $(dx_i/d\xi)(dx_j/d\xi)$ is analogous to the reciprocal of a term commonly referred to as tortuosity, and is a tensor of rank two which "deflects" or "twists" the gradient of concentration to form a new vector oriented in a different direction. By definition, let

$$\hat{T}_{ij} = \left(\frac{d\xi}{d\sigma}\right)^2 \frac{dx_i}{d\xi} \frac{dx_j}{d\xi} \quad . \tag{C-11}$$

Substituting equations (C-10) and (C-11) into equation (C-5):

$$\hat{C}\,\hat{V}_{t_i} = \hat{C}\,\hat{V}_i - D_d\,\hat{T}_{ij}\,\frac{\partial \hat{C}}{\partial x_j} \quad . \tag{C-12}$$

Macroscopic Analysis

The objective here is to obtain a relationship for the components, J_i^*, of the tracer mass flux vector corresponding to the REV shown in Figure C-1. The value of a variable, $\hat{g}$, at a point in the porous medium may be represented as the sum of the average value of the REV and a local deviation:

$$\hat{g} = g + \overset{o}{g}, \qquad \overline{\overset{o}{g}} = 0 \tag{C-13}$$

where g is the averaged value of the variable over the cross-sectional area, ΔA_i and $\overset{o}{g}$ is the deviation of the variable at a point from the cross-sectional averages.

The average, g of $\hat{g}$ over a cross-sectional area, ΔA_i of the REV is expressed for a point in the porous medium by:

$$g = \frac{1}{\phi S_w \Delta A_i} \int_{\phi S_w \Delta A_i} \hat{g}\, dA_i \quad , \tag{C-14}$$

where $(\phi S_w \Delta A_i)$ is the pore area through which the fluid moves and g is defined in accordance with the continuum approach of REV described at the beginning of this appendix. We assume that for the properties $\hat{g}$ considered here, g is differentiable up to second order.

Using the equation (C-13) for $\hat{C}$, $\hat{V}_i$, and $\hat{T}_{ij}$ and introducing them

into right hand side of equation (C-12)

$$\begin{aligned} rhs &= (C+\overset{\circ}{C})\ (V_i+\overset{\circ}{V}_i) - D_d\ (T_{ij}+\overset{\circ}{T}_{ij})\ \nabla\ (C+\overset{\circ}{C}) \\ &= CV_i + \overset{\circ}{C}V_i + C\overset{\circ}{V}_i + \overline{\overset{\circ}{C}\overset{\circ}{V}_i} - D_d\ T_{ij}\ \nabla\ C - D_d\ T_{ij}\ \nabla\overset{\circ}{C} \\ &\quad - D_d\ \overset{\circ}{T}_{ij}\ \nabla C - D_d\ \overline{\overset{\circ}{T}_{ij}\ \nabla\overset{\circ}{C}}\ . \end{aligned} \tag{C-15}$$

Multiplying each term of equation (C-15) by ΔA_i, integrating over $(\phi S_w \Delta A_i)$ and dividing the result by $(\phi S_w \Delta A_i)$, an average for each term over the REV is obtained. Multiplying the left hand side of equation (C-12) by ΔA_i, integrating over $(\phi S_w \Delta A_i)$ and dividing the result by $(\phi S_w \Delta A_i)$ gives the tracer mass flux, J_i^* for the REV:

$$J_i^* = \frac{1}{\phi S_w \Delta A_i} \int_{\phi S_w \Delta A_i} \hat{C}\ \hat{V}_{t_i}\ \Delta A_i \quad . \tag{C-16}$$

Assuming that 1) $\overline{\overset{\circ}{C}} = \overline{\overset{\circ}{V}_i} = \overline{\overset{\circ}{T}_{ij}} = 0$,

2) average of a gradient = gradient of the average, and

3) there is no correlation between $\nabla\overset{\circ}{C}$ and $\overset{\circ}{T}_{ij}$,

equation (C-15) results in:

$$rhs = C\ V_i + \overset{\circ}{C}\ \overset{\circ}{V}_i - D_d\ T_{ij}\ \nabla C\ . \tag{C-17}$$

Equating equations (C-16) and (C-17):

$$J_i^* = C\ V_i + \overline{\overset{\circ}{C}\ \overset{\circ}{V}_i} - D_d\ T_{ij}\ \nabla C \tag{C-18}$$

Thus, the averaged mass flux of the tracer over a cross-sectional area of the REV is composed of three different flux terms. The first is a flux, CV_i, due to convection with the average velocity of the fluid.

The second is the dispersive flux, $\overline{\overset{o}{C}\overset{o}{V}_i}$, and it expresses the rate at which the mass is transported due to velocity variations in the void space of the REV, where the solute's concentration distribution may be taken instantaneously as stationary, i.e., $\partial C/\partial t = 0$. The third is the diffusive flux, $D_d T_{ij} \nabla C$, due to molecular diffusion.

The dispersive flux, $\overline{\overset{o}{C}\overset{o}{V}_i}$, in analogy to diffusive fluxes in general, may be expressed as (Bear, 1972, p. 605):

$$\overline{\overset{o}{C}\overset{o}{V}_i} = - D_{ij} \frac{\partial C}{\partial x_j} \quad , \tag{C-19}$$

where D_{ij} is a second rank tensor called the coefficient of mechanical dispersion.

Introducing equation (C-19) into equation (C-18) gives

$$J_i^* = CV_i - (D_{ij} + D_d T_{ij}) \frac{\partial C}{\partial x_j} \quad . \tag{C-20}$$

Dispersion Equation

The results of the flux determination given in equation (C-20) are now introduced into equation (C-4) to yield

$$\frac{\partial}{\partial t} (\phi S_w \Delta \overline{V} C) = \frac{\partial}{\partial x_i} \left[(D_{ij} + D_d T_{ij}) \frac{\partial C}{\partial x_j} \phi S_w \Delta A_i \right] \Delta x_i -$$

$$\frac{\partial}{\partial x_i} (CV_i \phi S_w \Delta A_i) \Delta x_i - C_p Q_w \quad , \tag{C-21}$$

Equation (C-21) is the general form of the dispersion equation. The volume flux for water flowing through a porous medium may be expressed as

$$q_{w_i} = V_i \phi S_w \quad , \tag{C-22}$$

where q_{w_i} is the volume flux for water, in the i-th direction.

Substituting equation (C-22) into equation (C-21) and chaining out the derivatives of concentration results in

$$\frac{1}{\Delta\bar{V}} \frac{\partial}{\partial x_i}\left[(q_{w_i}\Delta A_i)\Delta x_i + \frac{\partial}{\partial t}(\phi S_w \Delta\bar{V})\right] = \frac{1}{C\Delta\bar{V}} \frac{\partial}{\partial x_i}\left[D^*_{ij} \frac{\partial C}{\partial x_j} \phi S_w \Delta A_i\right] \Delta x_i -$$

$$\frac{\phi S_w}{C} \frac{\partial C}{\partial t} - \frac{q_{w_i}}{C} \frac{\partial C}{\partial x_i} - \frac{C_p}{C} \frac{Q_w}{\Delta\bar{V}} \quad , \tag{C-23}$$

where $D^*_{ij} = D_{ij} + D_d T_{ij}$.

From Appendix A, equation (A-9a) for the water flow equation is

$$\frac{\partial}{\partial x_i}(\rho_w q_{w_i} \Delta A_i)\Delta x_i = -\frac{\partial}{\partial t}(\rho_w \phi S_w \Delta\bar{V}) - \rho_p Q_w \quad . \tag{C-24}$$

Chaining out the derivatives of density in equation (C-24) gives

$$\frac{1}{\Delta\bar{V}} \frac{\partial}{\partial x_i}\left[(q_{w_i}\Delta A_i)\Delta x_i + \frac{\partial}{\partial t}(\phi S_w \Delta\bar{V})\right] = -\frac{\phi S_w}{\rho_w} \frac{\partial \rho_w}{\partial t} - \frac{q_{w_i}}{\rho_w} \frac{\partial \rho_w}{\partial x_i} - \frac{\rho_p}{\rho_w} \frac{Q_w}{\Delta\bar{V}} \quad . \tag{C-25}$$

The left hand sides of equations (C-23) and (C-25) are equal. Thus, the right hand sides must be equal also, i.e.,

$$-\frac{\phi S_w}{\rho_w} \frac{\partial \rho_w}{\partial t} - \frac{q_{w_i}}{\rho_w} \frac{\partial \rho_w}{\partial x_i} - \frac{\rho_p}{\rho_w} \frac{Q_w}{\Delta\bar{V}} = \frac{1}{C\Delta\bar{V}} \frac{\partial}{\partial x_i}\left[D^*_{ij} \frac{\partial C}{\partial x_j} \phi S_w \Delta A_i\right] \Delta x_i -$$

$$\frac{\phi S_w}{C} \frac{\partial C}{\partial t} - \frac{q_{w_i}}{C} \frac{\partial C}{\partial x_i} - \frac{C_p}{C} \frac{Q_w}{\Delta\bar{V}} \quad . \tag{C-26}$$

Collecting like terms gives

$$\phi S_w \left(\frac{\partial C}{\partial t} - \frac{C}{\rho_w} \frac{\partial \rho_w}{\partial t} \right) = \frac{1}{\Delta \bar{V}} \frac{\partial}{\partial x_i} \left[D^*_{ij} \frac{\partial C}{\partial x_j} \phi S_w \Delta A_i \right] \Delta x_i -$$

$$q_{w_i} \left(\frac{\partial C}{\partial x_i} - \frac{C}{\rho_w} \frac{\partial \rho_w}{\partial x_i} \right) - \left(C_p - \frac{\rho_p C}{\rho_w} \right) \frac{Q_w}{\Delta \bar{V}} \quad . \tag{C-27}$$

Assuming homogeneous fluid, i.e., ρ_w = constant, μ_w = constant, and using $q_{w_i} = V_i \phi S_w$, equation (C-27) yields

$$\frac{\partial C}{\partial t} = \frac{1}{(\phi S_w \Delta A_i)} \frac{\partial}{\partial x_i} \left[D_{ij}^* \frac{\partial C}{\partial x_j} \phi S_w \Delta A_i \right] - V_i \frac{\partial C}{\partial x_i} - \left(C_p - \frac{\rho_p C}{\rho_w} \right) \frac{Q_w}{\Delta \bar{V}} \quad . \tag{C-28}$$

APPENDIX D

FINITE DIFFERENCE EQUATION FOR THE DISPERSION EQUATION

The dispersion equation as given by equation (C-28) is reproduced

$$\frac{\partial C}{\partial t} = \frac{1}{\phi S_w \Delta A_i} \frac{\partial}{\partial x_i} \left[D^*_{ij} \phi S_w \Delta A_i \frac{\partial C}{\partial x_j} \right] - V_i \frac{\partial C}{\partial x_i} \quad , \tag{D-1}$$

where $D^*_{ij} = D_{ij} + D_d T_{ij}$.

A numerical solution to the dispersion equation will be obtained by the method of characteristics. Following the development of Garder et al. (1964), the second order terms of equation (D-1) are regarded as given functions of x_1, x_2, x_3, and t, and equation (D-1) treated as a first-order equation. Such an equation will have four characteristic curves which are the solutions to the following ordinary differential equations:

$$\frac{dx_1}{dt} = V_1 \quad , \tag{D-2}$$

$$\frac{dx_2}{dt} = V_2 \quad , \tag{D-3}$$

$$\frac{dx_3}{dt} = V_3 \quad , \text{ and} \tag{D-4}$$

$$\frac{dC}{dt} = \frac{1}{\phi S_w \Delta A_i} \frac{\partial}{\partial x_i} \left[D^*_{ij} \phi S_w \Delta A_i \frac{\partial C}{\partial x_j} \right] \quad . \tag{D-5}$$

In addition to the usual division of the flow region into a grid system, a set of moving points is introduced into this numerical solution. Each one of the moving points has associated with it a concentration, which varies with time. Within each time interval, the moving points are relocated using the finite difference equations,

$$x_{1_\ell}^{t+1} = x_{1_\ell}^{t} + \Delta t V_{1_\ell}^{t+1} \quad , \tag{D-6}$$

$$x_{2_\ell}^{t+1} = x_{2_\ell}^{t} + \Delta t \, V_{2_\ell}^{t+1} \quad , \tag{D-7}$$

and

$$x_{3_\ell}^{t+1} = x_{3_\ell}^{t} + \Delta t \, V_{3_\ell}^{t+1} \tag{D-8}$$

where t+1 is the new time level and t is the old time level. Each cell in the grid system is assigned a concentration equal to the average of the concentrations of the moving points located inside the cell at time t+1. The concentration of the cell is then modified for dispersion by solving the explicit form of Equation (D-5).

Because of symmetry, only a detailed description of the finite difference form of Equation (D-5) in the x_1 - direction will be given. Expanding the x_1-derivative on the right hand side of Equation (D-5) gives

$$(rhs)_{x_1} = \frac{1}{(\phi S_w \Delta x_2 \Delta x_3)} \frac{\partial}{\partial x_1} \left[D_{11}^{*} \phi S_w \Delta x_2 \Delta x_3 \frac{\partial C}{\partial x_1} + D_{12}^{*} \phi S_w \Delta x_2 \Delta x_3 \frac{\partial C}{\partial x_2} + \right.$$

$$\left. D_{13}^{*} \phi S_w \Delta x_2 \Delta x_3 \frac{\partial C}{\partial x_3} \right] \quad . \tag{D-9}$$

As can be seen, Equation (D-9) involves three cross-derivatives and six second-order derivatives of concentration.

To develop a finite difference form of Equation (D-9), consider the cell (i, j, k) as shown in Figure D-1 and the 18 indicated adjacent cells. The spatial derivative at a point on the boundary between cells (i, j, k) and (i+1, j, k) may be approximated by

$$\left(\frac{\partial C}{\partial x_1}\right)_{i+1/2,j,k} = \frac{C_{i+1,j,k} - C_{i,j,k}}{\Delta x_1} , \qquad \text{(D-10a)}$$

$$\left(\frac{\partial C}{\partial x_2}\right)_{i+1/2,j,k} = \frac{C_{i+1/2,j+1,k} - C_{i+1/2,j-1,k}}{2\Delta x_2} , \qquad \text{(D-10b)}$$

and

$$\left(\frac{\partial C}{\partial x_3}\right)_{i+1/2,j,k} = \frac{C_{i+1/2,j,k+1} - C_{i+1/2,j,k-1}}{2\Delta x_3} . \qquad \text{(D-10c)}$$

Using a linear interpolation scheme,

$$C_{i+1/2,j+1,k} = \frac{C_{i,j+1,k} + C_{i+1,j+1,k}}{2} , \qquad \text{(D-11a)}$$

$$C_{i+1/2,j-1,k} = \frac{C_{i,j-1,k} + C_{i+1,j-1,k}}{2} , \qquad \text{(D-11b)}$$

$$C_{i+1/2,j,k+1} = \frac{C_{i,j,k+1} + C_{i+1,j,k+1}}{2} , \qquad \text{(D-11c)}$$

and

$$C_{i+1/2,j,k-1} = \frac{C_{i,j,k-1} + C_{i+1,j,k-1}}{2} . \qquad \text{(D-11d)}$$

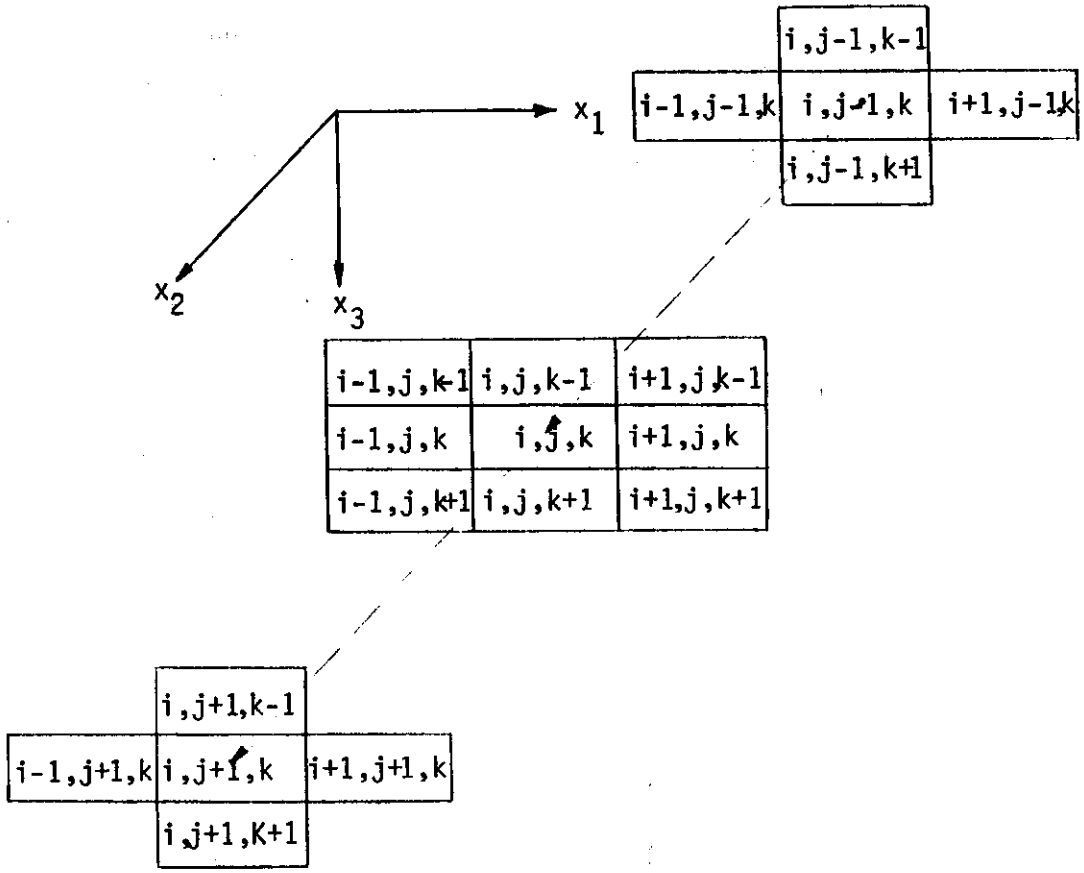

Figure D-1. Three-dimensional grid system with subscripting used to develop the finite difference form of dispersion equation.

Substituting equations (D-11) into equations (D-10) gives

$$\left(\frac{\partial C}{\partial x_1}\right)_{i+1/2,j,k} = \frac{C_{i+1,j,k} - C_{i,j,k}}{\Delta x_1} \quad , \tag{D-12a}$$

$$\left(\frac{\partial C}{\partial x_2}\right)_{i+1/2,j,k} = \frac{C_{i,j+1,k} + C_{i+1,j+1,k} - C_{i,j-1,k} - C_{i+1,j-1,k}}{4\Delta x_2} \quad , \tag{D-12b}$$

and

$$\left(\frac{\partial C}{\partial x_3}\right)_{i+\frac{1}{2},j,k} = \frac{C_{i,j,k+1} + C_{i+1,j,k+1} - C_{i,j,k-1} - C_{i+1,j,k-1}}{4\Delta x_3} \quad . \tag{D-12c}$$

Similarly, for a point on the boundary between cells (i,j,k) and (i-1,j,k), the spatial derivatives are

$$\left(\frac{\partial C}{\partial x_1}\right)_{i-1/2,j,k} = \frac{C_{i,j,k} - C_{i-1,j,k}}{\Delta x_1} \quad , \tag{D-13a}$$

$$\left(\frac{\partial C}{\partial x_2}\right)_{i-1/2,j,k} = \frac{C_{i,j+1,k} + C_{i-1,j+1,k} - C_{i,j-1,k} - C_{i-1,j-1,k}}{4\Delta x_2} \quad , \tag{D-13b}$$

and

$$\left(\frac{\partial C}{\partial x_3}\right)_{i-1/2,j,k} = \frac{C_{i,j,k+1} + C_{i-1,j,k+1} - C_{i,j,k-1} - C_{i-1,j,k-1}}{4\Delta x_3} \quad . \tag{D-13c}$$

By using a central finite difference scheme, equation (D-9) may be written as

$$(rhs)_{x_1} = \frac{1}{(\phi S_w \Delta x_2 \Delta x_3)_{i,j,k}} \left\{ \frac{(D^*_{11} \phi S_w \Delta x_2 \Delta x_3 \frac{\partial C}{\partial x_1})_{i+\frac{1}{2},j,k}}{\Delta x_1} - \right.$$

$$\frac{(D^*_{11} \phi S_w \Delta x_2 \Delta x_3 \frac{\partial C}{\partial x_1})_{i-1/2,j,k}}{\Delta x_1} + \frac{(D^*_{12} \phi S_w \Delta x_2 \Delta x_3 \frac{\partial C}{\partial x_2})_{i+1/2,j,k}}{\Delta x_1} -$$

$$\left. \frac{(D^*_{12} \phi S_w \Delta x_2 \Delta x_3 \frac{\partial C}{\partial x_2})_{i-1/2,j,k}}{\Delta x_1} + \frac{(D^*_{13} \phi S_w \Delta x_2 \Delta x_3 \frac{\partial C}{\partial x_3})_{i+1/2,j,k}}{\Delta x_1} - \right.$$

$$\left.\frac{(D^*_{13}\phi S_w \Delta x_2 \Delta x_3 \frac{\partial c}{\partial x_3})_{i-\frac{1}{2},j,k}}{\Delta x_1}\right\} . \qquad \text{(D-14)}$$

Introducing Equations (D-12) and (D-13) into equation (D-14) gives

$$(rhs)_{x_1} = \frac{1}{(\phi S_w \Delta x_2 \Delta x_3)_{i,j,k}} \left\{ \frac{(D^*_{11}\phi S_w \Delta x_2 \Delta x_3)_{i+\frac{1}{2},j,k}(C_{i+1,j,k} - C_{i,j,k})}{(\Delta x_1)^2} \right.$$

$$- \frac{(D^*_{11}\phi S_w \Delta x_2 \Delta x_3)_{i-\frac{1}{2},j,k}(C_{i,j,k} - C_{i-1,j,k})}{(\Delta x_1)^2} +$$

$$\frac{(D^*_{12}\phi S_w \Delta x_2 \Delta x_3)_{i+\frac{1}{2},j,k}(C_{i,j+1,k} + C_{i+1,j+1,k} - C_{i,j-1,k} - C_{i+1,j-1,k})}{4\Delta x_1 \Delta x_2}$$

$$- \frac{(D^*_{12}\phi S_w \Delta x_2 \Delta x_3)_{i-\frac{1}{2},j,k}(C_{i,j+1,k} + C_{i-1,j+1,k} - C_{i,j-1,k} - C_{i-1,j-1,k})}{4\Delta x_1 \Delta x_2}$$

$$+ \frac{(D^*_{13}\phi S_w \Delta x_2 \Delta x_3)_{i+\frac{1}{2},j,k}(C_{i,j,k+1} + C_{i+1,j,k+1} - C_{i,j,k-1} - C_{i+1,j,k-1})}{4\Delta x_1 \Delta x_3}$$

$$\left. - \frac{(D^*_{13}\phi S_w \Delta x_2 \Delta x_3)_{i-\frac{1}{2},j,k}(C_{i,j,k+1} + C_{i-1,j,k+1} - C_{i,j,k-1} - C_{i-1,j,k-1})}{4\Delta x_1 \Delta x_3} \right\} . \qquad \text{(D-15)}$$

Coefficients of the form $(D^*_{11}\phi S_w \Delta x_2 \Delta x_3)_{i+\frac{1}{2},j,k}$ will be calculated using arithmetic mean, i.e.:

$$(D^*_{11}\phi S_w \Delta x_2 \Delta x_3)_{i+\frac{1}{2},j,k} = 0.5[(D^*_{11}\phi S_w \Delta x_2 \Delta x_3)_{i+1,j,k} + (D^*_{11}\phi S_w \Delta x_2 \Delta x_3)_{i,j,k}]. \qquad \text{(D-16)}$$

Thus, the coefficients of concentration in Equation (D-15) are of the form

$$\frac{(D^*_{11}\phi S_w \Delta x_2 \Delta x_3)_{i+\frac{1}{2},j,k}}{(\phi S_w \Delta x_2 \Delta x_3)_{i,j,k}} = \frac{[(D^*_{11}\phi S_w)_{i+1,j,k} + (D^*_{11}\phi S_w)_{i,j,k}]}{2(\phi S_w)_{i,j,k}} . \qquad \text{(D-17)}$$

In a completely analogous development to that used in equations

(D-10) through (D-16), the x_2-derivative and x_3-derivative on the right hand side of equation (D-15) may be obtained. An explicit form of the left hand side of equation (D-5) is

$$\frac{dC}{dt} = \frac{C^{t+1}_{i,j,k} - C^{t}_{i,j,k}}{\Delta t} \quad . \tag{D-18}$$

To simplify notations, the following definitions are made:

$$E^{+}_{x_1x_1} = \frac{[(D^{*}_{11}\phi S_w)_{i+1,j,k} + (D^{*}_{11}\phi S_w)_{i,j,k}]\,\Delta t}{2\Delta x_1^2(\phi S_w)_{i,j,k}} \quad , \tag{D-19a}$$

$$E^{-}_{x_1x_1} = \frac{[(D^{*}_{11}\phi S_w)_{i-1,j,k} + (D^{*}_{11}\phi S_w)_{i,j,k}]\,\Delta t}{2\Delta x_1^2(\phi S_w)_{i,j,k}} \quad , \tag{D-19b}$$

$$E^{+}_{x_2x_2} = \frac{[(D^{*}_{22}\phi S_w)_{i,j+1,k} + (D^{*}_{22}\phi S_w)_{i,j,k}]\,\Delta t}{2\Delta x_2^2(\phi S_w)_{i,j,k}} \quad , \tag{D-19c}$$

$$E^{-}_{x_2x_2} = \frac{[(D^{*}_{22}\phi S_w)_{i,j-1,k} + (D^{*}_{22}\phi S_w)_{i,j,k}]\,\Delta t}{2\Delta x_2^2(\phi S_w)_{i,j,k}} \quad , \tag{D-19d}$$

$$E^{+}_{x_3x_3} = \frac{[(D^{*}_{33}\phi S_w)_{i,j,k+1} + (D^{*}_{33}\phi S_w)_{i,j,k}]\,\Delta t}{2\Delta x_3^2(\phi S_w)_{i,j,k}} \quad , \tag{D-19e}$$

$$E^{-}_{x_3x_3} = \frac{[(D^{*}_{33}\phi S_w)_{i,j,k-1} + (D^{*}_{33}\phi S_w)_{i,j,k}]\,\Delta t}{2\Delta x_3^2(\phi S_w)_{i,j,k}} \quad , \tag{D-19f}$$

$$F^{+}_{x_1x_2} = \frac{[(D^{*}_{12}\phi S_w)_{i+1,j,k} + (D^{*}_{12}\phi S_w)_{i,j,k}]\,\Delta t}{8\Delta x_1\Delta x_2(\phi S_w)_{i,j,k}} \quad , \tag{D-19g}$$

$$F^{-}_{x_1x_2} = \frac{[(D^{*}_{12}\phi S_w)_{i-1,j,k} + (D^{*}_{12}\phi S_w)_{i,j,k}]\,\Delta t}{8\Delta x_1\Delta x_2(\phi S_w)_{i,j,k}} \quad , \tag{D-19h}$$

$$F^{+}_{x_2x_1} = \frac{[(D^{*}_{21}\phi S_w)_{i,j+1,k} + (D^{*}_{21}\phi S_w)_{i,j,k}]\,\Delta t}{8\Delta x_1\Delta x_2(\phi S_w)_{i,j,k}}, \qquad \text{(D-19i)}$$

$$F^{-}_{x_2x_1} = \frac{[(D^{*}_{21}\phi S_w)_{i,j-1,k} + (D^{*}_{21}\phi S_w)_{i,j,k}]\,\Delta t}{8\Delta x_1\Delta x_2(\phi S_w)_{i,j,k}}, \qquad \text{(D-19j)}$$

$$G^{+}_{x_1x_3} = \frac{[(D^{*}_{13}\phi S_w)_{i+1,j,k} + (D^{*}_{13}\phi S_w)_{i,j,k}]\,\Delta t}{8\Delta x_1\Delta x_3(\phi S_w)_{i,j,k}}, \qquad \text{(D-19k)}$$

$$G^{-}_{x_1x_3} = \frac{[(D^{*}_{13}\phi S_w)_{i-1,j,k} + (D^{*}_{13}\phi S_w)_{i,j,k}]\,\Delta t}{8\Delta x_1\Delta x_3(\phi S_w)_{i,j,k}}, \qquad \text{(D-19}\ell\text{)}$$

$$G^{+}_{x_3x_1} = \frac{[(D^{*}_{31}\phi S_w)_{i,j,k+1} + (D^{*}_{31}\phi S_w)_{i,j,k}]\,\Delta t}{8\Delta x_1\Delta x_3(\phi S_w)_{i,j,k}}, \qquad \text{(D-19m)}$$

$$G^{-}_{x_3x_1} = \frac{[(D^{*}_{31}\phi S_w)_{i,j,k-1} + (D^{*}_{31}\phi S_w)_{i,j,k}]\,\Delta t}{8\Delta x_1\Delta x_3(\phi S_w)_{i,j,k}}, \qquad \text{(D-19n)}$$

$$H^{+}_{x_2x_3} = \frac{[(D^{*}_{23}\phi S_w)_{i,j+1,k} + (D^{*}_{23}\phi S_w)_{i,j,k}]\,\Delta t}{8\Delta x_2\Delta x_3(\phi S_w)_{i,j,k}}, \qquad \text{(D-19o)}$$

$$H^{-}_{x_2x_3} = \frac{[(D^{*}_{23}\phi S_w)_{i,j-1,k} + (D^{*}_{23}\phi S_w)_{i,j,k}]\,\Delta t}{8\Delta x_2\Delta x_3(\phi S_w)_{i,j,k}}, \qquad \text{(D-19p)}$$

$$H^{+}_{x_3x_2} = \frac{[(D^{*}_{32}\phi S_w)_{i,j,k+1} + (D^{*}_{32}\phi S_w)_{i,j,k}]\,\Delta t}{8\Delta x_2\Delta x_3(\phi S_w)_{i,j,k}}, \qquad \text{(D-19q)}$$

and

$$H^{-}_{x_3x_2} = \frac{[(D^{*}_{32}\phi S_w)_{i,j,k-1} + (D^{*}_{32}\phi S_w)_{i,j,k}]\,\Delta t}{8\Delta x_2\Delta x_3(\phi S_w)_{i,j,k}}. \qquad \text{(D-19r)}$$

Using equation (D-18), the notation of equations (D-19) and substituting finite difference approximations for all concentration

derivatives, the explicit form of equation (D-5) becomes:

$$C^{t+1}_{i,j,k} = C^{t}_{i,j,k} + E^{+}_{x_1x_1}(C^{t}_{i+1,j,k} - C^{t}_{i,j,k}) -$$

$$E^{-}_{x_1x_1}(C^{t}_{i,j,k} - C^{t}_{i-1,j,k}) + E^{+}_{x_2x_2}(C^{t}_{i,j+1,k} - C^{t}_{i,j,k}) -$$

$$E^{-}_{x_2x_2}(C^{t}_{i,j,k} - C^{t}_{i,j-1,k}) + E^{+}_{x_3x_3}(C^{t}_{i,j,k+1} - C^{t}_{i,j,k}) -$$

$$E^{-}_{x_3x_3}(C^{t}_{i,j,k} - C^{t}_{i,j,k-1}) + F^{+}_{x_1x_2}(C^{t}_{i,j+1,k} + C^{t}_{i+1,j+1,k} -$$

$$C^{t}_{i,j-1,k} - C^{t}_{i+1,j-1,k}) - F^{-}_{x_1x_2}(C^{t}_{i,j+1,k} + C^{t}_{i-1,j+1,k} -$$

$$C^{t}_{i,j-1,k} - C^{t}_{i-1,j-1,k}) + F^{+}_{x_2x_1}(C^{t}_{i+1,j,k} + C^{t}_{i+1,j+1,k} -$$

$$C^{t}_{i-1,j,k} - C^{t}_{i-1,j+1,k}) - F^{-}_{x_2x_1}(C^{t}_{i+1,j,k} + C^{t}_{i+1,j-1,k} -$$

$$C^{t}_{i-1,j,k} - C^{t}_{i-1,j-1,k}) + G^{+}_{x_1x_3}(C^{t}_{i,j,k+1} + C^{t}_{i+1,j,k+1} -$$

$$C^{t}_{i,j,k-1} - C^{t}_{i+1,j,k-1}) - G^{-}_{x_1x_3}(C^{t}_{i-1,j,k+1} + C^{t}_{i,j,k+1} -$$

$$C^{t}_{i,j,k-1} - C^{t}_{i-1,j,k-1}) + G^{+}_{x_3x_1}(C^{t}_{i+1,j,k+1} + C^{t}_{i+1,j,k} -$$

$$C^{t}_{i-1,j,k+1} - C^{t}_{i-1,j,k}) - G^{-}_{x_3x_1}(C^{t}_{i+1,j,k} + C^{t}_{i+1,j,k-1} -$$

$$C^{t}_{i-1,j,k} - C^{t}_{i-1,j,k-1}) + H^{+}_{x_2x_3}(C^{t}_{i,j,k+1} + C^{t}_{i,j+1,k+1} -$$

$$C^{t}_{i,j,k-1} - C^{t}_{i,j+1,k-1}) - H^{-}_{x_2x_3}(C^{t}_{i,j-1,k+1} + C^{t}_{i,j,k+1} -$$

$$C^{t}_{i,j-1,k-1} - C^{t}_{i,j,k-1}) + H^{+}_{x_3x_2}(C^{t}_{i,j+1,k+1} + C^{t}_{i,j+1,k} -$$

$$C^{t}_{i,j-1,k+1} - C^{t}_{i,j-1,k}) - H^{-}_{x_3x_2}(C^{t}_{i,j+1,k} + C^{t}_{i,j+1,k-1} -$$

$$c^t_{i,j-1,k} - c^t_{i,j-1,k-1}). \qquad \text{(D-20)}$$

APPENDIX E

FLOW CHART OF PROGRAM

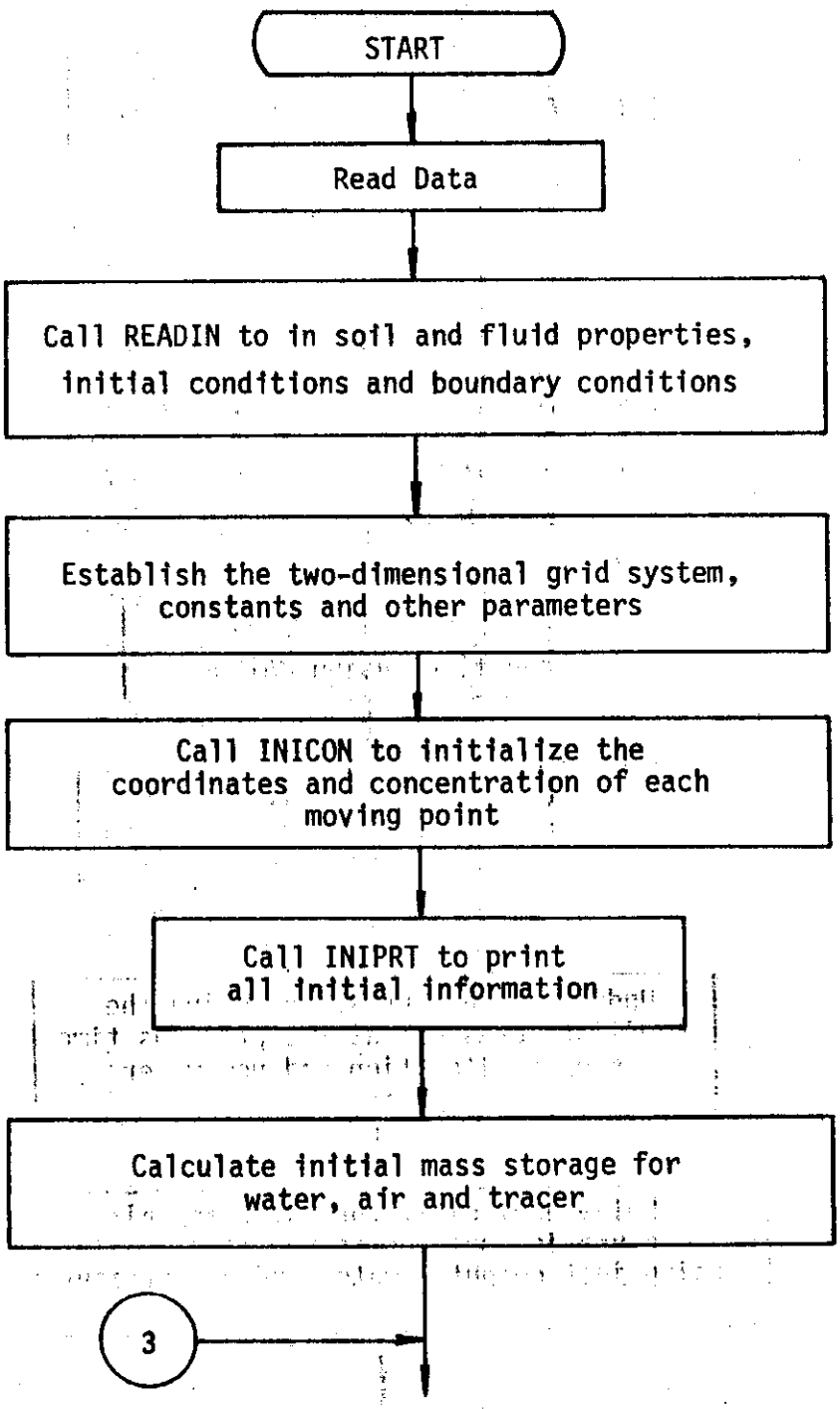

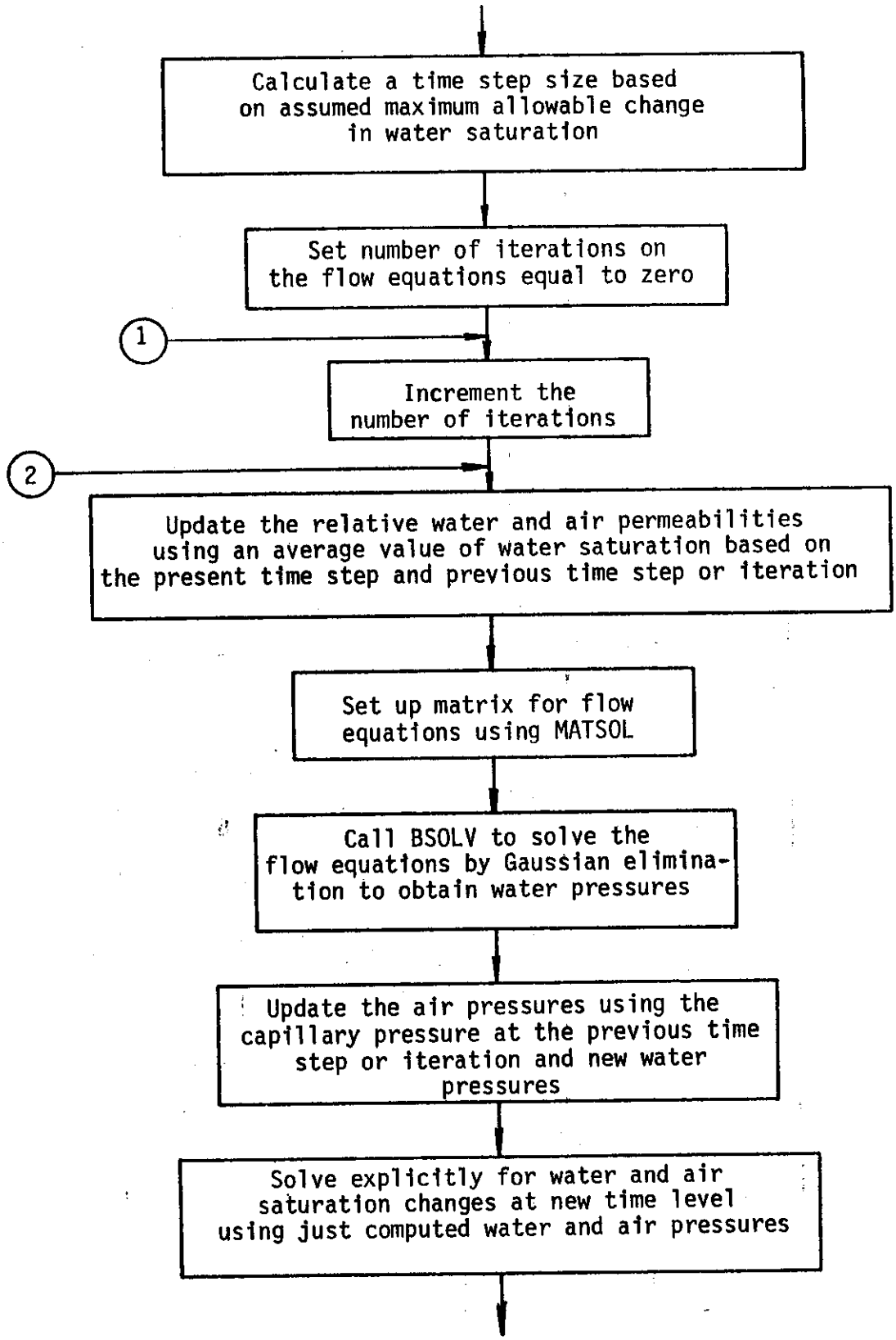
Calculate a time step size based on assumed maximum allowable change in water saturation
Set number of iterations on the flow equations equal to zero
1
Increment the number of iterations
2
Update the relative water and air permeabilities using an average value of water saturation based on the present time step and previous time step or iteration
Set up matrix for flow equations using MATSOL
Call BSOLV to solve the flow equations by Gaussian elimination to obtain water pressures
Update the air pressures using the capillary pressure at the previous time step or iteration and new water pressures
Solve explicitly for water and air saturation changes at new time level using just computed water and air pressures

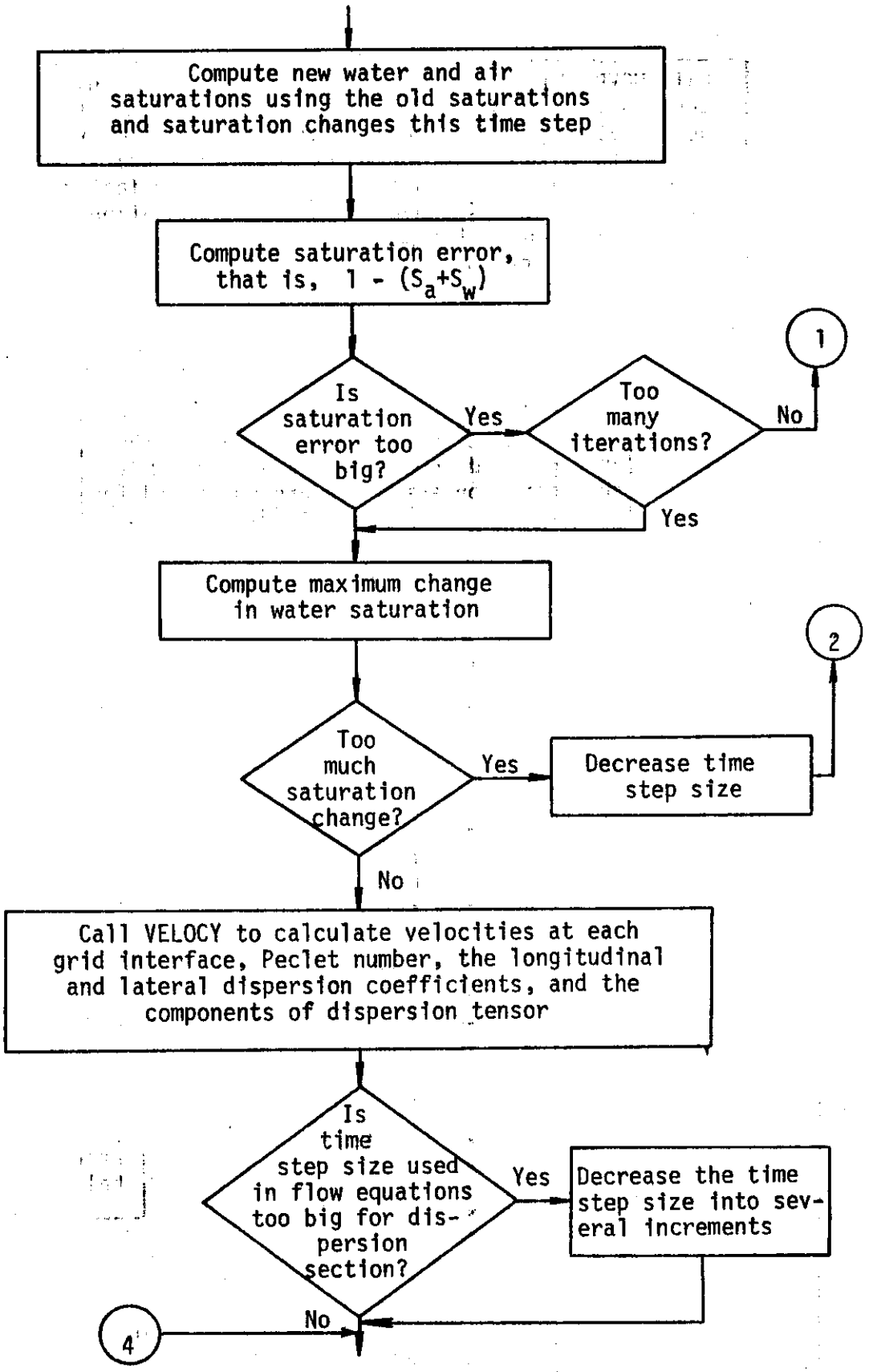
Compute new water and air saturations using the old saturations and saturation changes this time step
Compute saturation error, that is, 1 - (Sa+Sw)
Is saturation error too big?
Yes
Too many iterations?
No
1
Yes
Compute maximum change in water saturation
Too much saturation change?
Yes
Decrease time step size
2
No
Call VELOCY to calculate velocities at each grid interface, Peclet number, the longitudinal and lateral dispersion coefficients, and the components of dispersion tensor
Is time step size used in flow equations too big for dispersion section?
Yes
Decrease the time step size into several increments
No
4

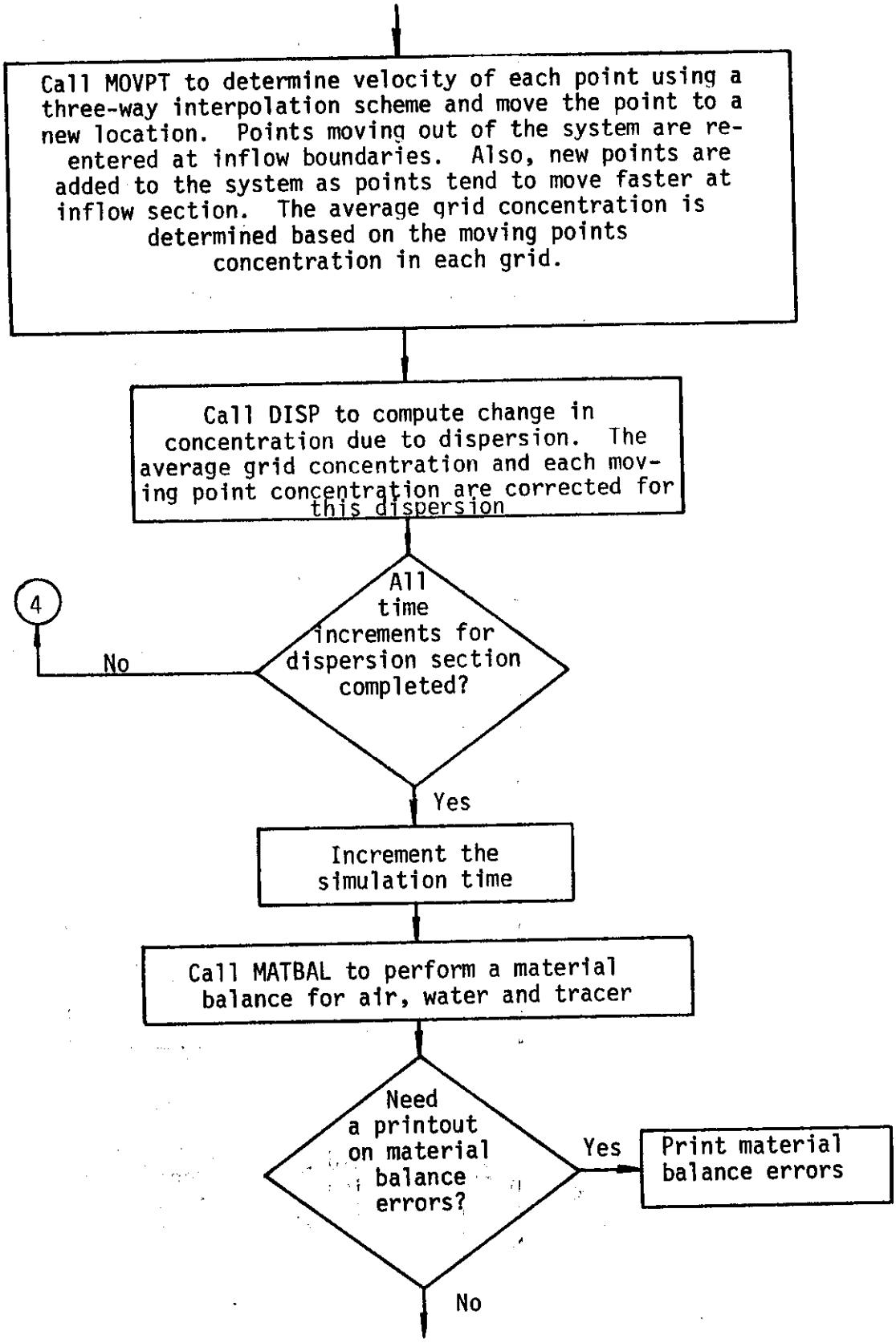
Call MOVPT to determine velocity of each point using a three-way interpolation scheme and move the point to a new location. Points moving out of the system are re-entered at inflow boundaries. Also, new points are added to the system as points tend to move faster at inflow section. The average grid concentration is determined based on the moving points concentration in each grid.
Call DISP to compute change in concentration due to dispersion. The average grid concentration and each moving point concentration are corrected for this dispersion
4
All time increments for dispersion section completed?
No
Yes
Increment the simulation time
Call MATBAL to perform a material balance for air, water and tracer
Need a printout on material balance errors?
Yes
Print material balance errors
No

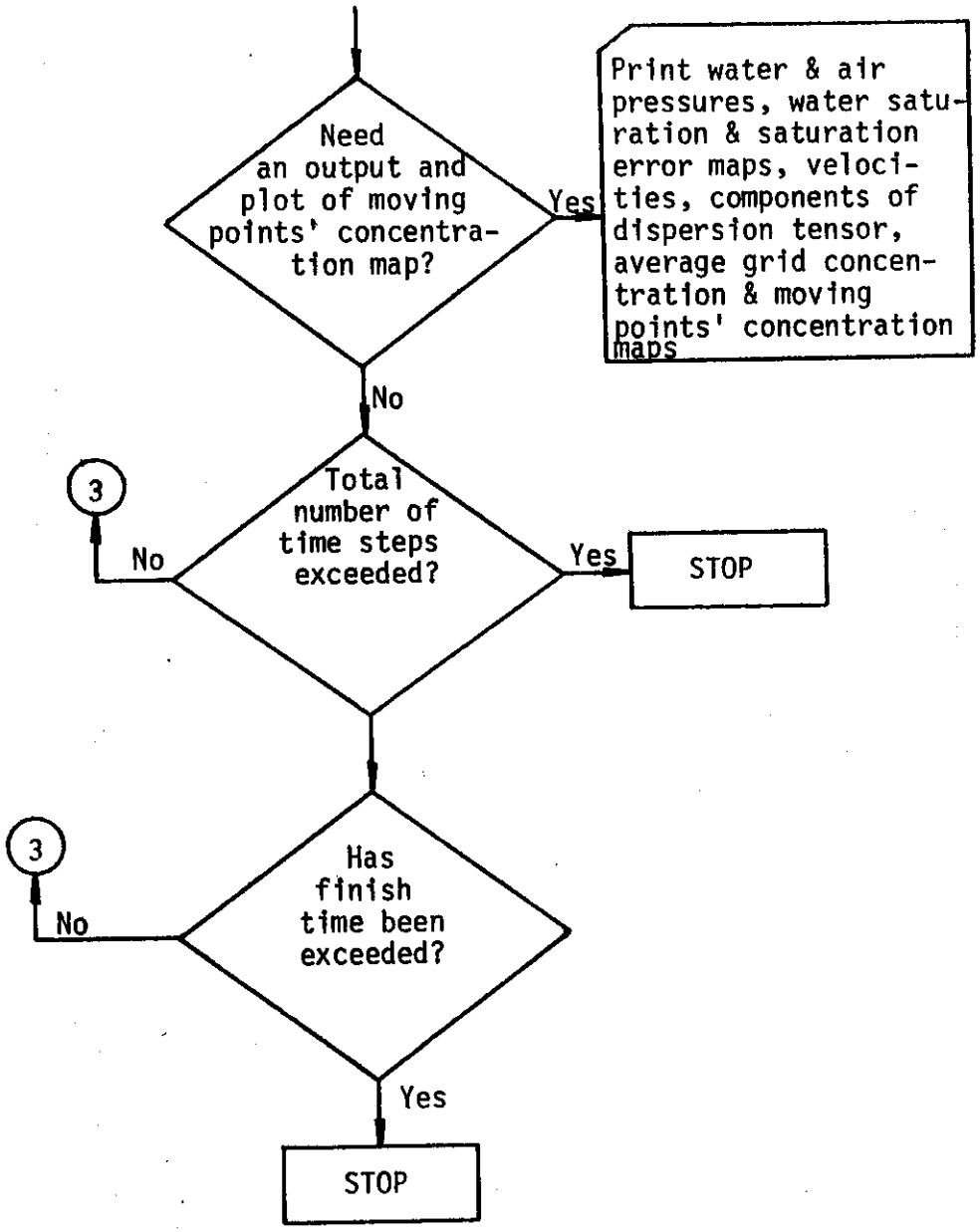
Need an output and plot of moving points' concentration map?
Yes
Print water & air pressures, water saturation & saturation error maps, velocities, components of dispersion tensor, average grid concentration & moving points' concentration maps
No
3
Total number of time steps exceeded?
No
Yes
STOP
3
Has finish time been exceeded?
No
Yes
STOP

APPENDIX F

FORTRAN IV COMPUTER PROGRAM

```
C*************************************************************************
C                                                                        *
C                                                                        *
C          NUMERICAL SIMULATION OF TWO-PHASE FLOW  AND DISPERSION        *
C                  IN SATURATED-UNSATURATED POROUS MEDIA                 *
C                                                                        *
C                                                                        *
C          THIS PROGRAM SIMULATES TWO-DIMENSIONAL, TWO-PHASE             *
C          (AIR-WATER) FLOW AND MISCIBLE DISPLACEMENT OF TRACER          *
C          IN A SATURATED-UNSATURATED, NONHOMOGENEOUS,ISOTROPIC          *
C          POROUS MEDIA WITH A HOMOGENEOUS FLUID. THE BOUNDARY           *
C          CONDITIONS ARE: INFILTRATING SOURCE ON THE UPPER              *
C          BOUNDARY OF ONE OR MORE OF SURFACE GRIDS; CONSTANT            *
C          HEAD RESERVOIRS ON THE LEFT & RIGHT HAND SIDES OF             *
C          THE MODEL. THE INITIAL CONDITIONS ARE: NON-UNIFORM            *
C          WATER PRESSURE & CONSTANT ATMOSPHERIC PRESSURE AND A          *
C          NON-DIMENSIONALIZED TRACER DISTRIBUTION. THE MAIN             *
C          PROGRAM IS THE CONTROL PROGRAM AND DIRECTS THE                *
C          SEQUENCE OF OPERATIONS FOR SOLVING TWO-PHASE FLOW             *
C          EQUATIONS AND THE DISPERSION EQUATION. APPROPRIATE            *
C          SUBROUTINES ARE CALLED AS NEEDED TO MAKE THE NECESSARY        *
C          CALCULATIONS.                                                 *
C                                                                        *
C          THE PROGRAM LISTING THAT FOLLOWS AND THE DIMENSION            *
C          STATEMENTS ARE SPECIFIC TO THE DRAINAGE PROBLEM               *
C          DESCRIBED IN CHAPTER V. FOR A DETAILED DESCRIPTION OF         *
C          THE INITIAL AND BOUNDARY CONDITIONS, REFER TO CHAPTER V.      *
C          THE PROGRAM WRITTEN IN FORTRAN LANGUAGE WAS RUN ON            *
C          AMDAHL 470V/6 AT TEXAS A&M UNIVERSITY DATA PROCESSING         *
C                          CENTER                                        *
C                                                                        *
C     ******** THE FOLLOWING VARIABLES ARE USED THROUGHOUT THE MAIN &     *
C          SUBROUTINES  **********                                       *
C                                                                        *
C              NC     = NUMBER OF COLUMNS                               *
C              NR     = NUMBER OF ROWS                                  *
C              DELZ   = SPATIAL INCREMENT IN Z-DIRECTION (CM)           *
C              DELX   = SPATIAL INCREMENT IN X-DIRECTION (CM)           *
C              DELT   = TIME INCREMENT (SEC)                            *
C              DELMLT = MULTIPLYING FACTOR FOR TIME STEP SIZE           *
C              DSWMX  = MAXIMUM ALLOWABLE WATER SATURATION CHANGE       *
C                       IN ONE TIME STEP                                *
C              TSTEP  = NUMBER OF TIME STEPS                            *
C              ITER   = ITERATION NUMBER IN A TIME STEP                 *
C              MAXIT  = MAXIMUM NUMBER OF ITERATIONS PER TIME STEP      *
C              MAXST  = MAXIMUM ALLOWABLE NUMBER OF TIME STEPS          *
C                       IN THE SIMULATION                               *
C              PW     = WATER PRESSURE (CM OF WATER) AT THE             *
C                       PRESENT TIME LEVEL                              *
C              PA     = AIR PRESSURE (CM OF WATER) AT THE               *
C                       PRESENT TIME LEVEL                              *
C              PC     = CAPILLARY PRESSURE (CM OF WATER) AT THE         *
C                       PRESENT TIME LEVEL                              *
C              PSAVE  = WATER PRESSURE (CM OF WATER) AT THE             *
C                       PREVIOUS TIME STEP OR ITERATION                 *
C              SW     = WATER SATURATION AT PRESENT TIME STEP           *
```

```
C              SA      = AIR SATURATION AT THE PRESENT TIME STEP                *
C              SS      = WATER SATURATION AT PREVIOUS TIME STEP OR              *
C                        PREVIOUS ITERATION                                     *
C              FINTIM  = TOTAL SIMULATION TIME (SEC)                            *
C              TIME    = CUMULATIVE SIMULATION TIME (SEC)                       *
C              HOURS   = CUMULATIVE SIMULATION TIME (HOURS)                     *
C              WKTAB   = TABULATED REL. WATER PERMEABILITY VALUES (.)           *
C              AKTAB   = TABULATED REL. AIR PERMEABILITY VALUES (.)             *
C              PCTAB   = TABULATED CAPILLARY PRESSURE (CM OF WATER)             *
C              SWTAB   = TABULATED WATER SATURATION VALUES (.)                  *
C              WK      = RELATIVE WATER PERMEABILITY (.)                        *
C              AK      = RELATIVE AIR PERMEABILITY (.)                          *
C              VISW    = WATER VISCOSITY (GM/CM/SEC)                            *
C              VISA    = AIR VISCOSITY (GM/CM/SEC)                              *
C              RHOW    = WATER DENSITY (GM/CM**3)                               *
C              RHOA    = AIR DENSITY (GM/CM**3)                                 *
C              SATPER  = SATURATED OR ABSOLUTE PERMEABILITY (CM/SEC)            *
C              SATP    = SATURATED PERMEABILITY (CM/SEC) . 2-D ARRAY            *
C              G       = ACCELERATION OF GRAVITY (CM/SEC**2)                    *
C              PHI     = POROSITY                                               *
C              PSOURC  = WATER PRESSURE OF INFILTRATING SOURCE (CM)             *
C              NC1     = BEGINNING COL. NO. OF UPPER SURFACE BOUNDARY           *
C              NC2     = ENDING COL. NO. OF UPPER SURFACE BOUNDARY              *
C              IPRINT  = COUNTER TO WRITE OUTPUT                                *
C              IFAC    = INTERVAL AT WHICH SUBROUTINE OUTPUT IS CALLED          *
C              ITENSR  = 0 FOR NO TENSOR TRANSFORMATION                         *
C                        1 WITH TENSOR TRANSFORMATION                           *
C              ISK     = NUMBER OF DATA POINTS IN SOIL PROP. TABLE              *
C              DELMAX  = MAXIMUM ALLOWABLE TIME STEP SIZE (SEC)                 *
C              DELMIN  = MINIMUM ALLOWABLE TIME STEP SIZE (SEC)                 *
C              TOLRNC  = CONVERGENCE CRITERION                                  *
C              HA      = LEFT HAND CONSTANT HEAD RESERVOIR ELEV. (CM)           *
C              HB      = RIGHT HAND CONSTANT HEAD RESERVOIR ELEV. (CM)          *
C              NR2     = STARTING ROW NO. FOR LEFT RESERVOIR                    *
C              NR3     = STARTING ROW NO. FOR RIGHT RESERVOIR                   *
C              ZZ      = ELEVATION HEAD AT CENTER OF GRID (CM)                  *
C                                                                               *
C*******************************************************************************
C                                                                               *
C                        M A I N   P R O G R A M                                *
C                                                                               *
C*******************************************************************************
C
      INTEGER TSTEP
      DIMENSION PCTAB(22),SWTAB(22),WKTAB(22),AKTAB(22),PC(17,12),PW(17,
     112),PSAVE(17,12),PA(17,12),SW(17,12),SS(17,12),SA(17,12),WK(17,12)
     2,AK(17,12),VISW(17,12),VISA(17,12),RHOW(17,12),RHOA(17,12),SATP(17
     3,12),AW(17,12),BW(17,12),WT(17),SERROR(17,12),ZZ(17,12),STAB(22),C
     4ONST1(17,2),CONST2(17,2),CONST(17,12)
      DIMENSION VX(19,13),VZ(18,14),X(4500),Z(4500),C(4500),SUMC(18,13),
     1COUNT(18,13),CAVG(18,13),DX(17,12),DZ(17,12),DXZ(17,12),DELC(18,13
     2)
      DIMENSION CAVGSV(18,13)
      COMMON      PCTAB,SWTAB,WKTAB,AKTAB,PC,PW,PSAVE,PA,SW,SS,SA,WK,AK,V
     1            ISW,VISA,RHOW,RHOA,SATP,AW,BW,WT,SERROR,ZZ,CONST1,CONST
     2            2,X,Z,C,VX,VZ,SUMC,COUNT,DELC,CAVG,DX,DZ,DXZ,STAB,DELX,
     3            DELZ,DELT,SATPER,PHI,G,CRHC,PSOURC,HA,HB,DELMLT,TOLRNC,
     4            DSWMX,DSWMAX,AX,AZ,AXZ,ALENX,ALENZ,CONST,ONE,TWO,FOUR,H
     5            ALF,ZERO,DELT1, DELT2,DIA,DIFF,SOLNC,ISAT,NRM1,NCM1,NRM
     6            2,NCM2,NR2,NR3,NC1,NC2,NDELT,IS1,IPRINT,IFAC,LOG,ITER,I
     7            A,IB,IC,ID,IE,IBM1,IDP1,NWM1,TSTEP,IPC,ISK,ISW,ITENSR,I
```

```
     8            CHECK,ISWICH,IRES,ISTEDY,IFPLOT,IWRITE,NN,IVEL,ICLOG
      DATA  TAIN,TAOUT,TAUT,TWIN,TWOUT,TWEN,TWUT,TSIN,TSOUT,WS,AS,CS,WIS
     1            ,AIS,SIS / 0.0,0.0,0.0,0.0,0.0,0.0,0.0,0.0,0.0,0.0,0.0,0.0,0.0,0.0,0.0,0.0,0.0,0.0,0.0,0.0,
     2            0.0,0.0,0.0,0.0,0.0, 0.0 /
      READ (5,1) NR, NC
      READ (5,2) DELX, DELZ
      READ (5,2) ALPHA
      NRM1=NR-1
      NCM1=NC-1
      NRM2=NR-2
      NCM2=NC-2
      NCP1=NC+1
      NRP1=NR+1
      NG=NRM2*NCM2
      IF (NC .GE. NR) GO TO 60
      NW=2*NCM2+1
      IC=NCM2+1
      GO TO 21
   60 NW=2*NRM2+1
      IC=NRM2+1
   21 IB=IC-1
      ID=IC+1
      IA=1
      IE=NW
      NWM1=NW-1
      IBM1=IE-1
      IDP1=ID+1
      ONE=1.0
      TWO=2.0
      ZERO=0.0
      FOUR=4.0
      HALF=0.5
      CALL READIN (NC, NR, MAXIT, MAXST, TIME, FINTIM, DELMAX, DELMIN)
      AX=TWO/DELX/DELX
      AZ=TWO/DELZ/DELZ
      AXZ=HALF/DELX/DELZ/FOUR
      DO 101 I=2,NCM1
  101 ZZ(I,2)=HALF*DELZ
      DO 102 I=2,NCM1
      DO 102 K=3,NRM1
  102 ZZ(I,K)=ZZ(I,K-1)+DELZ
      TSTEP=0
      FINTIM=FINTIM*3600.
      CALL INICON (NC, NR, NCP1, NRP1, NPZ, NPX, CAVGSV)
      CALL INIPRT (NC, NR, NG, NW,MAXIT, MAXST, NPZ, NPX,TIME, FINTIM, D
     1             ELMAX, DELMIN)
      AR=DELX*DELZ*ONE*PHI
C
C  .......  COMPUTES THE INITIAL MATERIAL BALANCE FOR AIR, WATER
C           AND TRACER   ..................
      DO 430 K=2,NRM1
      DO 430 I=2,NCM1
      SA(I,K)=ONE-SW(I,K)
      SIS=SIS+CAVG(I,K)*SW(I,K)
      WIS=WIS+SW(I,K)
  430 AIS=AIS+SA(I,K)
      WIS=WIS*AR
      AIS=AIS*AR
      SIS=SIS*AR
      DSWMAX=ZERO
      DELT=DELMIN/DELMLT
```

```
      SAREA=DELX*DELZ*G
 1000 CONTINUE
      TSTEP=TSTEP+1
      DETOLD=DELT
C
C  .......  SELECTS A TIME STEP SIZE  ............
      DELT=DELT*DELMLT
      IF (DS*MAX*DELT/DETOLD .GT. DSWMX) DELT=DELT*DS*MX*0.9/(DELMLT*DS*
     $MAX)
      IF (DELT .LT. DELMIN) DELT=DELMIN
      IF (DELT .GT. DELMAX) DELT=DELMAX
      IF (DELT+TIME .GT. FINTIM) DELT=FINTIM-TIME
      TAEN=TAIN
      TAUT=TACUT
      TWEN=TWIN
      TWUT=TWOUT
      WS1=WS
      AS1=AS
      CS1=CS
      ITER=0
      DO 66 K=2,NRM1
      DO 66 I=2,NCM1
      PSAVE(I,K)=PW(I,K)
   66 SS(I,K)=SW(I,K)
   52 ITER=ITER+1
      ISW=0
      CALL        MATSOL (NC, NR, NG, NW, ALPHA)
      IF (ITER .GE.  MAXIT) GO TO 500
      IF (ISW .EQ. 1) GO TO 52
  500 CONTINUE
      DTSAVE=DELT
      DWIN=ZERO
      DWOUT=ZERO
      DAIN=ZERO
      DAOUT=ZERO
      DSIN=ZERO
      DSOUT=ZERO
      NDELT=1
      CALL VELOCY (NC, NR, NCP1, NRP1)
      DO 5000 KKKK=1,NDELT
      IF (ISTEDY .EQ. 1) GO TO 650
      DO 541 K=1,NR
      DO 541 I=1,NC
      CAVGSV(I,K)=CAVG(I,K)
      SUMC(I,K)=0.0
  541 COUNT(I,K)=0.0
      IF (NDELT .EQ. 1) GO TO 656
      IF (KKKK .EQ. 1) DELT=DELT1
      IF (KKKK .GE. 2) DELT=DELT2
  656 CONTINUE
      CALL        MOVPT (NC, NR, NCP1,NRP1, NPZ, NPX)
      CALL DISP (NC, NR)
  650 CALL MATEAL (NC, NR, TAOUT, TAUT, TWIN, TWOUT, TWEN, TWUT, TSIN,
     1              TSOUT, WS, AS, CS, WS1, AS1, CS1, WIS, AIS, SIS, SARE
     2              A, AR, TAIN,  DAIN, DAOUT, DWIN, DWOUT, DSIN, DSOUT,
     3              KKKK, DTSAVE, TIME, CAVGSV, TAEN)
 5000 CONTINUE
      WRITE (6,155) TSTEP, LOG
      WRITE (6,425) NDELT
C
C  .......  CHECKS IF A PRINTOUT IS NEEDED  ............
```

```
      IF (TSTEP .NE. IPRINT*IFAC) GO TO 900
      IPRINT=IPRINT+1
      CALL OUTPUT (NC, NR, NCP1, NRP1)
  900 CONTINUE
      IF (TSTEP .EQ. MAXST) STOP
      IF (TIME .LT. FINTIM) GO TO 1000
      STOP
    1 FORMAT (4I10)
    2 FORMAT (2F10.3)
  199 FORMAT (/1X,      'TOTAL NUMBER OF MOVING POINTS IN THE SYSTEM AT T
     $HE END OF TIME STEP',I5, ' IS =', I5 )
  425 FORMAT ( 1X, ' NUMBER OF TIME INTERVALS ON DISPERSION SECTION IN D
     $ELTA-T =', I4/)
      END
C
C*************************************************************************
C                                                                        *
C         S U B R O U T I N E     R E A D I N                            *
C                                                                        *
C*************************************************************************
C                                                                        *
C            THIS SUBROUTINE READS IN THE PHYSICAL DATA NEEDED TO        *
C            SOLVE THE PROBLEM                                           *
C                                                                        *
      SUBROUTINE READIN (NC, NR, MAXIT, MAXST, TIME, FINTIM, DELMAX, DEL
     1                   MIN)
      INTEGER TSTEP
      DIMENSION PCTAB(22),SWTAB(22),WKTAB(22),AKTAB(22),PC(17,12),PW(17,
     112),PSAVE(17,12),PA(17,12),SW(17,12),SS(17,12),SA(17,12),WK(17,12)
     2,AK(17,12),VISW(17,12),VISA(17,12),RHOW(17,12),RHOA(17,12),SATP(17
     3,12),AW(17,12),BW(17,12),WT(17),SERROR(17,12),ZZ(17,12),STAB(22),C
     4ONST1(17,2),CONST2(17,2),CONST(17,12)
      DIMENSION VX(19,13),VZ(18,14),X(4500),Z(4500),C(4500),SUMC(18,13),
     1COUNT(18,13),CAVG(18,13),DX(17,12),DZ(17,12),DXZ(17,12),DELC(18,13
     2)
      COMMON      PCTAB,SWTAB,WKTAB,AKTAB,PC,PW,PSAVE,PA,SW,SS,SA,WK,AK,V
     1            ISW,VISA,RHOW,RHOA,SATP,AW,BW,WT,SERROR,ZZ,CONST1,CONST
     2            2,X,Z,C,VX,VZ,SUMC,COUNT,DELC,CAVG,DX,DZ,DXZ,STAB,DELX,
     3            DELZ,DELT,SATPER,PHI,G,CRHC,PSOURC,HA,HB,DELMLT,TOLRNC,
     4            DSWMX,DSWMAX,AX,AZ,AXZ,ALENX,ALENZ,CONST,ONE,TWO,FOUR,H
     5            ALF,ZERO,DELT1, DELT2,DIA,DIFF,SOLNC, ISAT,NRM1,NCM1,NRM
     6            2,NCM2,NR2,NR3,NC1,NC2,NDELT,IS1,IPRINT,IFAC,LOG,ITER,I
     7            A,IB,IC,ID,IE,IBM1,IDP1,NWM1,TSTEP,IPC,ISK,ISW,ITENSR,I
     8            CHECK,ISWICH,IRES,ISTEDY, IFPLOT,IWRITE,NN,IVEL,ICLOG
      READ (5,1) IPRINT, IFAC, ITENSR,IRES, ISTEDY, IFPLOT, IWRITE
      READ (5,2) PHI, G, PSOURC, NN, IVEL, ICLOG, ICHECK, ISWICH
      READ (5,1)  IPC, ISK, NC1, NC2
      READ (5,3) TIME, FINTIM, DELMAX, DELMIN
      READ (5,1) MAXIT, MAXST
      READ (5,4) TOLRNC
      READ (5,11) HA, HB, NR2, NR3, DSWMX, DELMLT
      READ (5,9) (SWTAB(I),WKTAB(I),AKTAB(I),PCTAB(I), I=1,ISK)
      DO 12 K=2,NRM1
   12 READ (5,10) (PW(I,K), I=2,NCM1)
      DO 14 K=2,NRM1
   14 READ (5,4) (SATP(I,K), I=2,NCM1)
      RETURN
    1 FORMAT (7I10)
    2 FORMAT (3F10.3, 5I10)
    3 FORMAT (4F10.3)
    4 FORMAT (8E10.3)
```

```
    5 FORMAT(F16.5)
    9 FORMAT (4F10.4)
   10 FORMAT (8F10.0)
   11 FORMAT (2F10.2,2I10,2F10.5)
      END
C
C*****************************************************************************
C                                                                             *
C          S U B R O U T I N E     I N I C O N                                *
C                                                                             *
C*****************************************************************************
C                                                                             *
C            THIS SUBROUTINE DETERMINES THE INITIAL X-Z COORDINATES           *
C            OF THE MOVING POINTS AND ASSIGNS AN INITIAL CONCENTRATION        *
C            TO EACH OF THE MOVING POINTS. THE MOVING POINTS ARE              *
C            INITIALLY UNIFORMLY DISTRIBUTED THROUGHOUT THE GRID              *
C            SYSTEM, INCLUDING THE BOUNDARY GRIDS.                            *
C                                                                             *
C                ISI    = RANDOM SEED NUMBER                                  *
C                DIFF   = MOLECULAR DIFFUSION COEFFICIENT (CM**2/SEC)         *
C                DIA    = MEDIAN GRAIN SIZE DIAMETER (CM)                     *
C                SCONC  = NON-DIMENSIONALIZED CONCENTRATION OF THE            *
C                         INFILTRATING SOLUTION                               *
C                X      = X-COORDINATE OF MOVING POINT                        *
C                Z      = Z-COORDINATE OF MOVING POINT                        *
C                C      = NON-DIMENSIONALIZED CONCENTRATION OF                *
C                         MOVING POINT                                        *
C                NPX    = NUMBER OF MOVING POINTS PER GRID IN                 *
C                         X-DIRECTION                                         *
C                NPZ    = NUMBER OF MOVING POINTS PER GRID IN                 *
C                         Z-DIRECTION                                         *
C                         NPX*NPZ IS THE NUMBER OF MOVING POINTS PER          *
C                         GRID INITIALLY                                      *
C                PX     = FLOATING POINT DESIGNATION OF NPX                   *
C                PZ     = FLOATING POINT DESIGNATION OF NPZ                   *
C                NP1    = NUMBER OF MOVING POINTS IN Z-DIRECTION              *
C                NP2    = NUMBER OF MOVING POINTS IN X-DIRECTION.             *
C                         NP1*NP2 IS THE TOTAL NUMBER OF MOVING               *
C                         POINTS INITIALLY IN THE SYSTEM                      *
C                SUMC   = SUMMATION OF CONCENTRATION OF MOVING POINTS         *
C                         IN A GRID                                           *
C                CCUNT  = A COUNT OF NUMBER OF MOVING POINTS IN A GRID        *
C                CAVG   = AVERAGE NON-DIMENSIONALIZED CONCENTRATION           *
C                         OF TRACER = SUMC/CCUNT                              *
C                CAVGSV = CAVG AT PREVIOUS TIME STEP                          *
C                DELC   = CHANGE IN CONCENTRATION DUE TO DISPERSION           *
C                NI1    = COLUMN NUMBER OF GRID IN WHICH THE MOVING           *
C                         POINT IS LOCATED                                    *
C                NI2    = ROW NUMBER OF GRID IN WHICH THE MOVING              *
C                         POINT IS LOCATED                                    *
C
      SUBROUTINE INICON (NC, NR, NCP1, NRP1, NPZ, NPX, CAVGSV)
      INTEGER TSTEP
      DIMENSION FCTAB(22),SWTAB(22),WKTAB(22),AKTAB(22),PC(17,12),PW(17,
     112),PSAVE(17,12),PA(17,12),SW(17,12),SS(17,12),SA(17,12),WK(17,12)
     2,AK(17,12),VISW(17,12),VISA(17,12),RHOW(17,12),RHOA(17,12),SATP(17
     3,12),AW(17,12),BW(17,12),WT(17),SERROR(17,12),ZZ(17,12),STAB(22),C
     4ONST1(17,2),CONST2(17,2),CONST(17,12)
      DIMENSION VX(19,13),VZ(18,14),X(4500),Z(4500),C(4500),SUMC(18,13),
     1COUNT(18,13),CAVG(18,13),DX(17,12),DZ(17,12),DXZ(17,12),DELC(18,13
     2)
```

```
      DIMENSION CAVGSV(18,13)
      COMMON     PCTAE,SWTAE,WKTAB,AKTAB,PC,PW,PSAVE,PA,SW,SS,SA,WK,AK,V
     1           ISW,VISA,RHOW,RHOA,SATP,AW,BW,WT,SERRCR,ZZ,CONST1,CONST
     2           2,X,Z,C,VX,VZ,SUMC,CCUNT,DELC,CAVG,DX,DZ,DXZ,STAB,DELX,
     3           DELZ,DELT,SATPER,PHI,G,CRHO,PSOURC,HA,HB,DELMLT,TOLRNC,
     4           DSWMX,DSWMAX,AX,AZ,AXZ,ALENX,ALENZ,CONST,ONE,TWO,FOUR,H
     5           ALF,ZERO,DELT1, DELT2,DIA,DIFF,SOLNC,ISAT,NRM1,NCM1,NRM
     6           2,NCM2,NR2,NR3,NC1,NC2,NDELT,IS1,IPRINT,IFAC,LOG,ITER,I
     7           A,IB,IC,ID,IE,IBM1,IDP1,NWM1,TSTEP,IPC,ISK,ISW,ITENSR,I
     8           CHECK,ISWICH,IRES,ISTEDY,IFPLOT,IWRITE,NN,IVEL,ICLOG
      READ (5,1) NPZ, NPX, IS1
      READ (5,2)  DIFF, SOLNC
      NP1=NPZ*NR
      NP2=NPX*NC
      LOG=1-NP1
      NOG=0
      PX=NPX
      PZ=NPZ
      ADISZ=DELZ/PZ
      ADISX=DELX/PX
      ALENX=DELX*NC
      ALENZ=DELZ*NR
      DO 37 K=1,NR
      DO 37 I=1,NC
      SUMC(I,K)=0.
      COUNT(I,K)=0.
   37 DELC(I,K)=0.
      DO 90 I=1,NP2
      DOG=I-1
      XD=ADISX*(HALF +DOG)
      LOG=LOG+NP1
      NOG=NOG+NP1
      DO 90 K=LOG,NOG
      DOG=K-LOG
      Z(K)=ADISZ*(HALF +DOG)
      X(K)=XD
      IF (X(K) .LT. (  NC1-1 )*DELX) GO TO 35
      IF (Z(K) .GT. DELZ) GO TO 35
      IF (X(K) .GT.     NC2*DELX) GO TO 35
      C(K)=1.0
      GO TO 36
   35 C(K)=0.0
   36 CONTINUE
      NI1=X(K)/DELX+1.
      NI2=Z(K)/DELZ+1.
      SUMC(NI1,NI2)=SUMC(NI1,NI2)+C(K)
      CCUNT(NI1,NI2)=COUNT(NI1,NI2)+1.
   90 CONTINUE
      DO 30 K=1,NR
      DO 30 I=1,NC
      IF (COUNT(I,K) .EQ. 0.0) COUNT(I,K)=1.0
      CAVG(I,K)=SUMC(I,K)/COUNT(I,K)
   30 CAVGSV(I,K)=CAVG(I,K)
      LOG=NP1+NP2
      RETURN
    1 FORMAT (3I10)
    2 FORMAT ( E10.5, F10.2)
      END
```

```
C*****************************************************************************
C                                                                             *
C         S  U  B  R  O  U  T  I  N  E      I  N  I  P  R  T                 *
C                                                                             *
C*****************************************************************************
C                                                                             *
C            THIS SUBROUTINE WRITES OUT ALL OF THE INITIAL DATA               *
C            BY USE OF SUBROUTINE MATROP                                      *
C
      SUBROUTINE INIPRT (NC, NR, NG, NW,MAXIT, MAXST, NPZ, NPX,TIME, FIN
     1              TIM, DELMAX, DELMIN)
      INTEGER TSTEP
      DIMENSION PCTAB(22),SWTAB(22),WKTAB(22),AKTAB(22),PC(17,12),PW(17,
     112),PSAVE(17,12),PA(17,12),SW(17,12),SS(17,12),SA(17,12),WK(17,12)
     2,AK(17,12),VISW(17,12),VISA(17,12),RHOW(17,12),RHOA(17,12),SATP(17
     3,12),AW(17,12),BW(17,12),WT(17),SERROR(17,12),ZZ(17,12),STAB(22),C
     4ONST1(17,2),CONST2(17,2),CONST(17,12)
      DIMENSION VX(19,13),VZ(18,14),X(4500),Z(4500),C(4500),SUMC(18,13),
     1COUNT(18,13),CAVG(18,13),DX(17,12),DZ(17,12),DXZ(17,12),DELC(18,13
     2)
      COMMON      PCTAB,SWTAB,WKTAB,AKTAB,PC,PW,PSAVE,PA,SW,SS,SA,WK,AK,V
     1            ISW,VISA,RHOW,RHOA,SATP,AW,BW,WT,SERROR,ZZ,CONST1,CONST
     2            2,X,Z,C,VX,VZ,SUMC,COUNT,DELC,CAVG,DX,DZ,DXZ,STAB,DELX,
     3            DELZ,DELT,SATPER,PHI,G,CRHC,PSOURC,HA,HB,DELMLT,TOLRNC,
     4            DSWMX,DSWMAX,AX,AZ,AXZ,ALENX,ALENZ,CONST,ONE,TWO,FOUR,H
     5            ALF,ZERO,DELT1, DELT2,DIA,DIFF,SOLNC,ISAT,NRM1,NCM1,NRM
     6            2,NCM2,NR2,NR3,NC1,NC2,NDELT,IS1,IPRINT,IFAC,LOG,ITER,I
     7            A,IB,IC,ID,IE,IBM1,IDP1,NWM1,TSTEP,IPC,ISK,ISW,ITENSR,I
     8            CHECK,ISWICH,IRES,ISTEDY,IFPLOT,IWRITE,NN,IVEL,ICLOG
      WRITE (6,1)
      WRITE (6,2) NR,NC,NG,NW,ITENSR,IRES,ISTEDY,IFPLOT,IWRITE
      WRITE (6,3) DELX,DELZ,NC1,NC2,NN,IVEL,ICLOG
      WRITE (6,4)  PHI, G, PSOURC
      WRITE (6,5) TIME, FINTIM,DELMAX, DELMIN
      WRITE (6,6) MAXIT, MAXST,  TOLRNC
      WRITE (6,12) HA, HB, NR2, NR3, DSWMX, DELMLT
      WRITE (6,10) NPZ, NPX, IS1,  DIFF, SOLNC
      DO 30 K=2,NRM1
      DO 30 I=2,NCM1
      PA(I,K)=ZERO
      IF (PW(I,K) .GE. ZERO) GO TO 87
      PC(I,K)=-PW(I,K)
      GO TO 30
   87 SW(I,K)=0.999
      PC(I,K)=ZERO
   30 CONTINUE
      CALL SLEROP (NC, NR, 0, 1)
      DO 40 K=2,NRM1
      DO 40 I=2,NCM1
      PA(I,K)=PC(I,K)+PW(I,K)
      SS(I,K)=SW(I,K)
      VISW(I,K)=1.15E-02
      RHOW(I,K)=0.9957
      VISA(I,K)=1.91E-04
   40 RHOA(I,K)=0.001224
      CALL SLEROP (NC, NR, 1, 0)
      WRITE (6,21)
      WRITE (6,18) (I,SWTAB(I),WKTAB(I),AKTAB(I),PCTAB(I), I=1,ISK)
      WRITE (6,22)
      CALL MATROP (NCM1, NRM1, PW)
      WRITE (6,11)
      CALL MATROP (NCM1, NRM1, PA)
      WRITE (6,7)
```

```
      CALL MATROP (NCM1, NRM1, PC)
      WRITE (6,8)
      CALL MATROP (NCM1, NRM1, SW)
      WRITE (6,9)
      CALL MATROP (NCM1, NRM1, WK)
      WRITE (6,13)
      CALL MATROP (NCM1, NRM1, AK)
      WRITE (6,14)
      CALL MATROP (NCM1, NRM1, VISW)
      WRITE (6,15)
      CALL MATROP (NCM1, NRM1, VISA)
      WRITE (6,16)
      CALL MATROP (NCM1, NRM1, RHOW)
      WRITE (6,17)
      CALL MATROP (NCM1, NRM1, RHOA)
      WRITE (6,25)
      CALL MATROP (NCM1, NRM1, SATP)
      RETURN
    1 FORMAT (1H1, 36X, '  **********TWO-DIMENSIONAL,TWO-PHASE VERTICAL
     $FLOW PROBLEM********** '//)
    2 FORMAT (1X, 'NR=',I5,5X,'NC=',I5,5X,'NGRIDS=',I5,5X,'NWIDTH=',I5,
     $4X,'ITENSOR =',I3,3X,'IRES =',I3,3X,'ISTEDY =',I3,3X,'IPPLOT =',I3
     $,3X,'IWRITE =',I3/)
    3 FORMAT (1X, 'DELTA-X (CM) =',F8.0,4X,'DELTA-Z (CM) =',F8.0,4X,'NC1
     $ =',I4,4X,'NC2 =',I4,3X,'NN =',I3,3X,'IVEL =',I3,3X,'ICLOG =',I3/)
    4 FORMAT (1X,'POROSITY =',F8.5,4X,'G =',F10.3,4X,'PSOURC =',E10.3)
    5 FORMAT (1X,'TIME (SEC)=',F10.1,3X,'FINTIM(SEC)=',E12.5,3X,'DELMAX
     *(SEC)=',F10.1,3X,'DELMIN (SEC) =',F10.1/)
    6 FORMAT (1X, 'MAXIT=', I5,5X,'MAXST=',I5,5X,'TOLRNC=',E10.4/)
    7 FORMAT (/45X, 'INITIAL CAPILLARY PRESSURE (CM) MAP'/)
    8 FORMAT (/45X, 'INITIAL WATER SATURATION MAP'/)
    9 FORMAT (/45X, 'INITIAL REL. WATER PERMEABILITY MAP'/)
   10 FORMAT (1X,'NPZ =',I3,3X,'NPX =',I3,3X,'RANDOM SEED NO  (SI =',  I
     19,//1X,                          'DIFF, =',E14.5,' (CM**2)/SEC',3X,
     2'C/CC IN =', F5.2/)
   11 FORMAT (/45X, 'INITIAL AIR PRESSURE (CM)'/)
   12 FORMAT (1X, 'HA (CM) =', F10.3,5X, 'HB (CM) =', F10.3,5X,'NR2=',I5
     $,5X, 'NR3=',I5,5X,'DSMAX=', F10.5,3X,'DELMLT=',F5.2/)
   13 FORMAT (/1X, 45X, 'INITIAL REL. AIR PERMEABILITY MAP'/)
   14 FORMAT (/45X, 'INITIAL WATER VISCOSITY MAP- GM/(CM-SEC)')
   15 FORMAT (/45X, 'INITIAL  AIR  VISCOSITY MAP- GM/(CM-SEC)')
   16 FORMAT (/45X, 'INITIAL WATER DENSITY MAP - GM/(CM**3)'/)
   17 FORMAT (/45X, 'INITIAL  AIR  DENSITY MAP - GM/(CM**3)'/)
   18 FORMAT (5X,I5,4E16.7)
   19 FORMAT (5X,I5,2E16.7)
   20 FORMAT (/10X,'WATER SATURATION - CAPILLARY PRESSURE (CM.)'/)
   21 FORMAT (/1X,  'WATER SATURATION - REL. WATER PERMEABILITY - REL .
     $AIR PERMEABILITY - CAPILLARY PRESSURE (CM)'/)
   22 FORMAT (/45X, 'INITIAL WATER PRESSURE (CM) MAP'/)
   25 FORMAT (/45X, 'SATURATED PERMEABILITY MAP - CM**2'/)
      END
C
C*****************************************************************************
C                                                                             *
C        S U B R O U T I N E     M A T S O L                                  *
C                                                                             *
C*****************************************************************************
C                                                                             *
C          THIS SUBROUTINE SETS UP THE COEFFICIENT MATRIX AND                 *
C          THE RIGHT HAND SIDE COLUMN VECTOR. IT ALSO CALLS                   *
C          SUBROUTINE BSOLVE TO SOLVE FOR THE FLOW EQUATIONS.                 *
```

```
C                                                                       *
C               CMATRX = ELEMENTS OF COEFFICIENT MATRIX OF SIZE NG*NW   *
C               NG     = NUMBER OF GRIDS = (NR-2)*(NC-2)                *
C               NW     = BANDWIDTH OF BANDED COEFFICIENT MATRIX         *
C               RHS    = ELEMENTS OF RIGHT HAND SIDE COLUMN VECTOR      *
C               DSW    = WATER SATURATION CHANGES IN TIME DELTA-T        *
C               DSA    = AIR SATURATION CHANGES IN TIME DELTA-T          *
C               SERROR = SATURATION ERROR = 1. - (SW+SA)                *
C               RHOWS  = WATER DENSITY IN PREVIOUS TIME STEP            *
C               RHOAS  = AIR DENSITY IN PREVIOUS TIME STEP              *
C               ISTEDY =1 ; STEADY STATE PROBLEM BEING SOLVED.          *
C                      = 0 ; TRANSIENT STATE PROBLEM BEING SOLVED       *
C               IRES   = 0; NO CONSTANT HEAD RESERVOIR ON L.H.S. OF     *
C                        MODEL.                                         *
C                      = 1; CONSTANT HEAD RESERVOIR ON L.H.S.           *
C               ALPHA  = CONSTANT RELATING RHOW TO CAVG                 *
C               PSURFC = WATER PRESSURE HEAD (CM OF WATER) AT THE       *
C                        UPPER SURFACE BOUNDARY OF THE INFILTRATING      *
C                        SOURCE. THIS VARIABLE IS SAME AS PSOURC        *
C
      SUBROUTINE MATSOL (NC, NR, NG, NW, ALPHA)
      INTEGER TSTEP
      DIMENSION PCTAB(22),SWTAB(22),WKTAB(22),AKTAB(22),PC(17,12),PW(17,
     112),PSAVE(17,12),PA(17,12),SW(17,12),SS(17,12),SA(17,12),WK(17,12)
     2,AK(17,12),VISW(17,12),VISA(17,12),RHOW(17,12),RHOA(17,12),SATP(17
     3,12),AW(17,12),BW(17,12),WT(17),SERROR(17,12),ZZ(17,12),STAB(22),C
     4ONST1(17,2),CONST2(17,2),CONST(17,12)
      DIMENSION CMATRX(176,23), RHS(176)
      DIMENSION DW(17,12),EW(17,12),AA(17,12),DA(17,12),BA(17,12),EA(17,
     112),DSW(17,12),DSA(17,12),RHOAS(17,12),RHOWS(17,12)
      DIMENSION VX(19,13),VZ(18,14),X(4500),Z(4500),C(4500),SUMC(18,13),
     1COUNT(18,13),CAVG(18,13),DX(17,12),DZ(17,12),DXZ(17,12),DELC(18,13
     2)
      COMMON      PCTAB,SWTAB,WKTAB,AKTAB,PC,PW,PSAVE,PA,SW,SS,SA,WK,AK,V
     1            ISW,VISA,RHOW,RHOA,SATP,AW,BW,WT,SERROR,ZZ,CONST1,CONST
     2            2,X,Z,C,VX,VZ,SUMC,COUNT,DELC,CAVG,DX,DZ,DXZ,STAB,DELX,
     3            DELZ,DELT,SATPER,PHI,G,CRHC,PSOURC,HA,HB,DELMLT,TOLRNC,
     4            DSWMX,DSWMAX,AX,AZ,AXZ,ALENX,ALENZ,CONST,ONE,TWO,FOUR,H
     5            ALF,ZERO,DELT1, DELT2,DIA,DIFF,SOLNC,ISAT,NRM1,NCM1,NRM
     6            2,NCM2,NR2,NR3,NC1,NC2,NDELT,IS1,IPRINT,IFAC,LOG,ITER,I
     7            A,IB,IC,ID,IE,IBM1,IDP1,NWM1,TSTEP,IPC,ISK,ISW,ITENSR,I
     8            CHECK,ISWICH,IRES,ISTEDY,IFPLOT,IWRITE,NN,IVEL,ICLOG
  900 CONTINUE
      DO 64 J=1,NG
      DO 63 L=2,IBM1
   63 CMATRX(J,L)=ZERO
      DO 66 L=IDP1,NWM1
   66 CMATRX(J,L)=ZERO
   64 CONTINUE
      DO 16 K=2,NRM1
      DO 16 I=2,NCM1
      RHOW(I,K)=RHCW(I,K) + ALPHA*CAVG(I,K)
      RHOWS(I,K)=RHOW(I,K)
   16 RHOAS(I,K)=RHCA(I,K)
      PSURFC=ZERO
      DO 10 K=2,NRM1
      DO 10 I=2,NCM1
      SW(I,K)=  HALF *(SW(I,K)+SS(I,K))
   10 CONTINUE
      CALL SLFROP (NC, NR, 1, 1)
      IF (ISTEDY .EQ. 1) GO TO 15
```

```
      K=2
      DO 65 I=NC1,NC2
      DHZW=PSCLRC-PW(I,K)+HALF*DELZ
      IF (DHZW .GT. ZERO) GO TO 81
      AVKRW=WK(I,K)
      GO TO 65
   81 AVKRW=ONE
   65 CONST2(I,K)=RHOW(I,K)/VISW(I,K)*SATP(I,K)*TWO/DELZ/DELZ*AVKRW
   15 CONTINUE
      IF (IRES .EQ. 0) GO TO 14
      I=2
      DO 11 K=NR2,NRM1
      DHXW=HA*ZZ(I,K)-PW(I,K)
      IF (DHXW .GT. ZERO) GO TO 82
      AVKRW=WK(I,K)
      GO TO 11
   82 AVKRW=ONE
   11 CONST (I,K)=RHOW(I,K)/VISW(I,K)*SATP(I,K)*TWO/DELX/DELX*AVKRW
   14 CONTINUE
      I=NCM1
      DO 12 K=NR3,NRM1
      DHXW=PW(I,K)-(HB*ZZ(I,K))
      IF (DHXW .GT. ZERO) GO TO 83
      AVKRW=ONE
      GO TO 12
   83 AVKRW=WK(I,K)
   12 CONST (I,K)=RHOW(I,K)/VISW(I,K)*SATP(I,K)*TWO/DELX/DELX*AVKRW
C
C  .......  INITIALLY, MATSOL SETS UP THE BOUNDARY CONDITIONS AROUND THE
C           BOUNDARY GRIDS FOR NO-FLOW CONDITIONS.  APPROPRIATE BOUNDARY
C           CONDITIONS ARE THEN INTRODUCED AND THE COEFFICIENT MATRIX,
C           CMATRX AND THE RIGHT HAND SIDE MATRIX, RHS ARE UPDATED  ....
      DO 52 I=2,NCM1
      AW(I,2)=ZERO
      AA(I,2)=ZERO
      EA(I,NRM1)=ZERO
   52 EW(I,NRM1)=ZERO
      DO 53 K=2,NRM1
      BW(2,K)=ZERO
      BA(2,K)=ZERO
      DA(NCM1,K)=ZERO
   53 DW(NCM1,K)=ZERO
      DO 301 K=J,NRM1
      DO 301 I=2,NCM1
      CRHO=RHOW(I,K)/RHOA(I,K)
      KM=K-1
      DHZW=PW(I,KM)-PW(I,K)+DELZ
      DHZA=PA(I,KM)-PA(I,K)+DELZ/CRHO
      IF (DHZW .GT. ZERO) GO TO 41
      AVKRW=WK(I,K)
      GO TO 42
   41 AVKRW=WK(I,KM)
   42 AW(I,K)=RHOW(I,K)*RHOW(I,KM)*SATP(I,K)*SATP(I,KM)/((VISW(I,K)*RHOW
     $(I,KM)*SATP(I,KM)) + (VISW(I,KM)*RHOW(I,K)*SATP(I,K)))*AZ*AVKRW
      EW(I,KM)=AW(I,K)
      IF (DHZA .GT. ZERO) GO TO 43
      AVKRA=AK(I,K)
      GO TO 44
   43 AVKRA=AK(I,KM)
   44 AA(I,K)=RHOA(I,K)*RHOA(I,KM)*SATP(I,K)*SATP(I,KM)/((VISA(I,K)*RHOA
     $(I,KM)*SATP(I,KM)) + (VISA(I,KM)*RHOA(I,K)*SATP(I,K)))*AZ*AVKRA*
```

```
     $CRHO
      EA(I,KM)=AA(I,K)
  301 CONTINUE
      DO 302 K=2,NRM1
      DO 302 I=3,NCM1
      CRHO=RHOW(I,K)/RHOA(I,K)
      IM=I-1
      DHXW=PW(IM,K)-PW(I,K)
      DHXA=PA(IM,K)-PA(I,K)
      IF (DHXW .GT. ZERO) GO TO 45
      AVKRW=WK(I,K)
      GO TO 46
   45 AVKRW=WK(IM,K)
   46 BW(I,K)=RHOW(I,K)*RHOW(IM,K)*SATP(I,K)*SATP(IM,K)/((VISW(I,K)*RHOW
     $(IM,K)*SATP(IM,K)) + (VISW(IM,K)*RHOW(I,K)*SATP(I,K)))*AX*AVKRW
      DW(IM,K)=BW(I,K)
      IF (DHXA .GT. ZERO) GO TO 47
      AVKRA=AK(I,K)
      GO TO 48
   47 AVKRA=AK(IM,K)
   48 BA(I,K)=RHOA(I,K)*RHOA(IM,K)*SATP(I,K)*SATP(IM,K)/((VISA(I,K)*RHOA
     *(IM,K)*SATP(IM,K)) + (VISA(IM,K)*RHOA(I,K)*SATP(I,K)))*AX*AVKRA*
     $CRHO
      DA(IM,K)=EA(I,K)
  302 CONTINUE
      IF (NC .LE. NR) GO TO 300
      J=0
      IM=2
      DO 240 I=2,NCM1
      KM=2
      IF (I .GT. 2) IM=I-1
      IF (I .LT. NCM1) IP=I+1
      DO 250 K=2,NRM1
      IF (K .GT. 2) KM=K-1
      IF (K .LT. NRM1) KP=K+1
      J=J+1
      CRHO=RHOW(I,K)/RHOA(I,K)
      CMATRX(J,IA)=BW(I,K)+BA(I,K)
      CMATRX(J,IB)=AW(I,K)+AA(I,K)
      CMATRX(J,ID)=EW(I,K)+EA(I,K)
      CMATRX(J,IE)=DW(I,K)+DA(I,K)
      CMATRX(J,IC)=-(CMATRX(J,IA)+CMATRX(J,IB)+CMATRX(J,ID)+CMATRX(J,IE)
     $)
      IF (K .EQ. 2 .AND. ISTEDY .EQ. 1) GO TO 421
      IF (K .EQ. 2 .AND. I .LT. NC1 .OR. K .EQ. 2 .AND. I .GT. NC2) GO T
     $O 421
      IF ( K .EQ. 2) GO TO 422
      RHS(J)=-(EA(I,K)*PC(I,KP)+AA(I,K)*PC(I,KM)+BA(I,K)*PC(IM,K)+DA(I,K
     *)*PC(IP,K) - (AA(I,K)+EA(I,K)+BA(I,K)+DA(I,K))*PC(I,K) + (AW(I,K)+
     *AA(I,K)/CRHO-EW(I,K)-EA(I,K)/CRHO)*DELZ)+ SW(I,K)/RHOW(I
     $,K)/G/DELT*PHI*(RHOW(I,K)-RHOWS(I,K)) + (ONE-SW(I,K))/RHOA(I,K)/G/
     $DELT*PHI*(RHOA(I,K)-RHOAS(I,K))
      IF ( I .EQ. 2 .AND. K .GE. NR2) GO TO 108
      IF ( I .EQ. NCM1 .AND. K .GE. NR3) GO TO 109
      GO TO 250
C
C  ....... INCORPORATES THE B.C. FOR AIR AT THE SOIL SURFACE .........
  421 RHS(J)=-(EA(I,K)*PC(I,KP)+BA(I,K)*PC(IM,K)+DA(I,K)*PC(IP,K) -(CONS
     $T1(I,K)+EA(I,K)+EA(I,K)+DA(I,K))*PC(I,K) + (( HALF*CONST1(I,K)-EA(
     $I,K))/CRHO-EW(I,K))*DELZ)-CONST1(I,K)*PSURFC+SW(I,K)/RHOW(I,K)/G/D
     $ELT*PHI*(RHOW(I,K)-RHOWS(I,K)) +(ONE-SW(I,K))/RHOA(I,K)/G/DELT*PHI
```

```
     $*(RHCA(I,K)-RHCAS(I,K))
      CMATRX(J,IC)=CMATRX(J,IC)-CONST1(I,K)
      GO TO 250
C
C  .......  INCORPORATES THE B.C. FOR WATER AT THE INFILTRATING SOURCE
  422 RHS(J)=-(EA(I,K)*PC(I,KP)+AA(I,K)*PC(I,KM)+BA(I,K)*PC(IM,K)+DA(I,K
     $)*PC(IP,K) - (AA(I,K)+EA(I,K)+BA(I,K)+DA(I,K))*PC(I,K) + ( HALF*CO
     $NST2(I,K)+AA(I,K)/CRHO-EW(I,K)-EA(I,K)/CRHO)*DELZ)+SW(I,K)/RHOW(I,
     $K)/G/DELT*PHI*(RHOW(I,K)-RHOWS(I,K))+(1.-SW(I,K))/RHOA(I,K)/G/DELT
     $*PHI*(RHCA(I,K)-RHOAS(I,K))
      CMATRX(J,IC)=CMATRX(J,IC)-CONST2(I,K)
      GO TO 250
C
C  .......  INCORPORATES THE CONSTANT HEAD B. C. ON THE L.H.S. OF MODEL
  108 RHS(J)=RHS(J)-CONST (I,K)*(HA+ZZ(I ,K))
      CMATRX(J,IC)=CMATRX(J,IC)-CONST (I,K)
      GO TO 250
C
C  .......  INCORPORATES THE CONSTANT HEAD B. C. ON THE R.H.S. OF MODEL
  109 RHS(J)=RHS(J)-CONST (I,K)*(HB+ZZ(I ,K))
      CMATRX(J,IC)=CMATRX(J,IC)-CONST (I,K)
  250 CONTINUE
  240 CONTINUE
C
C  .......  CALLS SUBROUTINE BSOLV & SOLVES FOR WATER PRESSURES  .......
      CALL BSOLV (CMATRX,NG,NW,RHS)
      J=0
      DO 310 I=2,NCM1
      DO 310 K=2,NRM1
      J=J+1
      PW(I,K)=RHS(J)
C
C  .......  COMPUTES NEW AIR PRESSURES  ............
      PA(I,K)=PC(I,K)+PW(I,K)
  310 CONTINUE
      GO TO 400
  300 CONTINUE
      J=0
      KM=2
      DO 350 K=2,NRM1
      IM=2
      IF (K .GT. 2) KM=K-1
      IF (K .LT. NRM1) KP=K+1
      DO 340 I=2,NCM1
      IF (I .GT. 2) IM=I-1
      IF (I .LT. NCM1) IP=I+1
      J=J+1
      CRHO=RHOW(I,K)/RHOA(I,K)
      CMATRX(J,IA)=AW(I,K)+AA(I,K)
      CMATRX(J,IB)=EW(I,K)+BA(I,K)
      CMATRX(J,IC)=DW(I,K)+DA(I,K)
      CMATRX(J,ID)=EW(I,K)+EA(I,K)
      CMATRX(J,IC)=-(CMATRX(J,IA)+CMATRX(J,IB)+CMATRX(J,ID)+CMATRX(J,IE)
     $)
      IF (K .EQ. 2 .AND. ISTEDY .EQ. 1) GO TO 321
      IF (K .EQ. 2 .AND. I .LT. NC1 .OR. K .EQ. 2 .AND. I .GT. NC2) GO T
     $O 321
      IF ( K .EQ. 2) GO TO 322
      RHS(J)=-(EA(I,K)*PC(I,KP)+AA(I,K)*PC(I,KM)+BA(I,K)*PC(IM,K)+DA(I,K
     *)*PC(IP,K) - (AA(I,K)+EA(I,K)+BA(I,K)+DA(I,K))*PC(I,K) + (AW(I,K)+
     *AA(I,K)/CRHO-EW(I,K)-EA(I,K)/CRHO)*DELZ)+ SW(I,K)/RHOW(I
```

```
     $,K)/G/DELT*PHI*(RHOW(I,K)-RHOWS(I,K)) + (ONE-SW(I,K))/RHOA(I,K)/G/
     $DELT*PHI*(RHCA(I,K)-RHOAS(I,K))
      IF ( I .EQ. 2 .AND. K .GE. NR2) GO TO 308
      IF ( I .EQ. NCM1 .AND. K .GE. NR3) GO TO 309
      GO TO 340
C
C  ....... INCORPORATES THE B.C. FOR AIR AT THE SOIL SURFACE .........
  321 RHS(J)=-(EA(I,K)*PC(I,KP)+BA(I,K)*PC(IM,K)+DA(I,K)*PC(IP,K) -(CONS
     $T1(I,K)+EA(I,K)+EA(I,K)+DA(I,K))*PC(I,K) + (( HALF*CONST1(I,K)-EA(
     $I,K))/CRHC-EW(I,K))*DELZ)-CONST1(I,K)*PSURFC+SW(I,K)/RHOW(I,K)/G/D
     $ELT*PHI*(RHOW(I,K)-RHOWS(I,K)) +(ONE-SW(I,K))/RHOA(I,K)/G/DELT*PHI
     $*(RHOA(I,K)-RHCAS(I,K))
      CMATRX(J,IC)=CMATRX(J,IC)-CONST1(I,K)
      GO TO 340
C
C  ....... INCORPORATES THE B.C. FOR WATER AT THE INFILTRATING SOURCE
  322 RHS(J)=-(EA(I,K)*PC(I,KP)+AA(I,K)*PC(I,KM)+BA(I,K)*PC(IM,K)+CA(I,K
     $)*PC(IP,K) - (AA(I,K)+EA(I,K)+BA(I,K)+DA(I,K))*PC(I,K) + ( HALF*CO
     $NST2(I,K)+AA(I,K)/CRHO-EW(I,K)-EA(I,K)/CRHO)*DELZ)+SW(I,K)/RHOW(I,
     $K)/G/DELT*PHI*(RHOW(I,K)-RHOWS(I,K))+(1.-SW(I,K))/RHOA(I,K)/G/DELT
     $*PHI*(RHCA(I,K)-RHOAS(I,K))
      CMATRX(J,IC)=CMATRX(J,IC)-CONST2(I,K)
      GO TO 340
C
C  ....... INCORPORATES THE CONSTANT HEAD B. C. ON THE L.H.S. OF MODEL
  308 RHS(J)=RHS(J)-CONST (I,K)*(HA+ZZ(I ,K))
      CMATRX(J,IC)=CMATRX(J,IC)-CONST (I,K)
      GO TO 340
C
C  ....... INCORPORATES THE CONSTANT HEAD B. C. ON THE R.H.S. OF MODEL
  309 RHS(J)=RHS(J)-CONST (I,K)*(HB+ZZ(I ,K))
      CMATRX(J,IC)=CMATRX(J,IC)-CONST (I,K)
  340 CONTINUE
  350 CONTINUE
C
C  ....... CALLS SUBROUTINE BSOLV & SOLVES FOR WATER PRESSURES .......
      CALL BSOLV (CMATRX,NG,NW,RHS)
      J=0
      DO 410 K=2,NRM1
      DO 410 I=2,NCM1
      J=J+1
      PW(I,K)=RHS(J)
C
C  ....... COMPUTES NEW AIR PRESSURES ............
      PA(I,K)=PC(I,K)+PW(I,K)
  410 CONTINUE
  400 CONTINUE
      DSWMAX=ZERO
C
C  ....... SOLVES EXPLICITLY FOR THE WATER & AIR SATURATIONS. THEN
C          COMPUTES THE SATURATION ERROR. .................
      KM=2
      DO 72 K=2,NRM1
      IM=2
      IF (K .GT. 2) KM=K-1
      IF (K .LT. NRM1) KP=K+1
      DO 72 I=2,NCM1
      IF (I .GT. 2) IM=I-1
      IF (I .LT. NCM1) IP=I+1
      CRHO=RHCW(I,K)/RHOA(I,K)
      IF (K .EQ. 2 .AND. ISTEDY .EQ. 1) GO TO 70
```

```
      IF (K .EQ. 2) GO TO 96
      IF (K .GE. NR2 .AND. I .EQ. 2) GO TO 75
      IF (K .GE. NR3 .AND. I .EQ.NCM1) GO TO 76
      GO TO 70
   96 IF (I-NC1) 70,74,69
   69 IF (I-NC2) 74,74,70
   70 DSW(I,K) =       DELT*G/PHI*(AW(I,K)*PW(I,KM)+EW(I,K)*PW(I,KP)+BW(I
     $,K)*PW(IM,K)+CW(I,K)*PW(IP,K)-(AW(I,K)+EW(I,K)+BW(I,K)+DW(I,K))*PW
     $(I,K) + (AW(I,K)-EW(I,K))*DELZ) - SS(I,K)/RHOW(I,K)*(RHOW(I,K)-RHO
     $WS(I,K))
      GO TO 77
C
C ........  B.C. FOR WATER AT THE INFILTRATING SOURCE  ..............
   74 DSW(I,K)=       DELT*G/PHI*(CONST2(I,K) *PSURFC+EW(I,K)*PW(I,KP)+BW
     $(I,K)*PW(IM,K)+CW(I,K)*PW(IP,K)- (CONST2(I,K)+EW(I,K)+BW(I,K)+DW(I
     $,K))*PW(I,K) + (CONST2(I,K)* HALF-EW(I,K))*DELZ)-SS(I,K)/RHOW(I,K)
     $*(RHOW(I,K)-RHOWS(I,K))
      GO TO 77
C
C  ........  CONSTANT HEAD B. C. AT THE L.H.S. OF MODEL  ..............
   75 DSW(I,K)=DELT*G/PHI*(AW(I,K)*PW(I,KM)+EW(I,K)*PW(I,KP)+CONST (I,K)
     $ *(HA+ZZ(I,K))+CW(I,K)*PW(IP,K)-(AW(I,K)+EW(I,K)+CONST (I,K)+DW(I,
     $K))*PW(I,K) + (AW(I,K)-EW(I,K))*DELZ) - SS(I,K)/RHOW(I,K)*(RHOW(I,
     $K)-RHOWS(I,K))
      GO TO 77
C
C  ........  CONSTANT HEAD B. C. AT THE R.H.S. OF MODEL  ..............
   76 DSW(I,K) =       DELT*G/PHI*(AW(I,K)*PW(I,KM)+EW(I,K)*PW(I,KP)+BW(I
     $,K)*PW(IM,K)+CONST (I,K)*(HB+ZZ(I ,K))-(AW(I,K)+EW(I,K)+BW(I,K)+CO
     $NST (I,K))*PW(I,K)+ (AW(I,K)-EW(I,K))*DELZ) - SS(I,K)/RHOW(I,K)*(R
     $HOW(I,K)-RHOWS(I,K))
   77 CONTINUE
      IF (K .EQ. 2 .AND. ISTEDY .EQ. 1) GO TO 208
      IF (K .EQ. 2 .AND. I .LT. NC1 .OR. K .EQ. 2 .AND. I .GT. NC2) GO T
     $O 208
      DSA(I,K) =       DELT/PHI*G*(AA(I,K)*PA(I,KM)+EA(I,K)*PA(I,KP)+BA(I
     $,K)*PA(IM,K)+DA(I,K)*PA(IP,K) - (AA(I,K)+EA(I,K)+BA(I,K)+DA(I,K))*
     $PA(I,K) + (AA(I,K)-EA(I,K))/CRHO*DELZ) - (ONE-SS(I,K))/RHOA(I,K)*(
     $RHOA(I,K)-RHOAS(I,K))
      GO TO 209
C
C  ........  B. C. FOR AIR AT THE UPPER SURFACE BOUNDARY  ..............
  208 DSA(I,K) =       DELT*G/PHI*(CONST1(I,K)*PSURFC+EA(I,K)*PA(I,KP)+BA
     $(I,K)*PA(IM,K)+DA(I,K)*PA(IP,K) - (CONST1(I,K)+EA(I,K)+BA(I,K)+DA(
     $I,K))*PA(I,K) + ( HALF  *CONST1(I,K)-EA(I,K))/CRHO*DELZ) - (ONE-SS
     $(I,K))/RHOA(I,K)*(RHOA(I,K)-RHOAS(I,K))
  209 CONTINUE
      SERROR(I,K)=DSW(I,K) + DSA(I,K)
      IF (SERROR(I,K) .GT. TOLRNC) ISW=1
      XXX=DSW(I,K)+SS(I,K)
      XX =  TWO *SW(I,K)-SS(I,K)
      IF ( ABS(XX-XXX) .GT. TOLRNC) ISW=1
      IF ( ABS(DSW(I,K)) .LT. DSWMAX) GO TO 58
      DSWMAX= ABS(DSW(I,K))
      II=I
      KK=K
   58 CONTINUE
   72 CONTINUE
C
C  ........  CHECKS IF DSWMAX EXCEEDS 1.25*DSWMX.  IF SO REDUCE THE TIME
C            STEP SIZE & RESOLVE THE FLUID FLOW EQUATIONS  ..............
```

```
      IF (DSWMAX .LT. 1.25*DSWMX) GO TO 59
      XXXX=DSWMX*0.9/DSWMAX
      DO 61 K=2,NRM1
      DO 61 I=2,NCM1
      PW(I,K)=PSAVE(I,K)
   61 SW(I,K)=SS(I,K)
      YYY=DELT
      DELT=DELT*XXXX
      ITER=ITER+1
      WRITE (6,701)
      WRITE (6,710) II,KK,DSW(II,KK),YYY,DELT
      IF (ITER .GT. 2) GO TO 59
      GO TO 500
   59 CONTINUE
C
C  .......  FROM HERE THRU STATEMENT 97:CHECKS IF SATURATION OF ANY
C           GRIDS EXCEEDS ONE.  IF SO, THE EXCESS WATER SATURATION IS
C           DISTRIBUTED OVER ALL UNSATURATED GRIDS  .....................
      ISAT=0
      DELSW=ZERO
      DO 92 K=2,NRM1
      DO 92 I=2,NCM1
      SW(I,K)=SS(I,K)+DSW(I,K)
      SA(I,K)=ONE-SW(I,K)
      SWSAVE=SW(I,K)
      IF (SW(I,K) .GT. ONE) GO TO 93
      GO TO 92
   93 SW(I,K)=ONE
      SA(I,K)=ZERO
      ISAT=1
      DELSW=DELSW+SWSAVE-SW(I,K)
   92 CONTINUE
      IF (ISAT .EQ. 0) GO TO 100
      NCOUNT=0
      DO 97 K=2,NRM1
      DO 97 I=2,NCM1
      IF (SW(I,K) .LT. ONE) NCOUNT=NCOUNT+1
   97 CONTINUE
      DELSW=DELSW/NCOUNT
      DO 98 K=2,NRM1
      DO 98 I=2,NCM1
      IF (SW(I,K) .GE. ONE) GO TO 98
      SW(I,K)=SW(I,K)+DELSW
      SA(I,K)=ONE-SW(I,K)
   98 CONTINUE
  100 CONTINUE
      RETURN
  701 FORMAT (/2X,'===== TIME STEP REDUCTION DUE TO DSW TOO BIG =====')
  710 FORMAT (2X, 'DSW(', I2,',',I2,') =', E14.6,5X,'OLD DELT = ',E14.6,
     $5X,'NEW DELT =',E14.6//)
      END
C
C*************************************************************************
C                                                                        *
C         S U B R O U T I N E     S L P R O P                            *
C                                                                        *
C*************************************************************************
C                                                                        *
C           THIS SUBROUTINE CALCULATES THE SOIL PROPERTIES               *
C                                                                        *
      SUBROUTINE SLPROP (NC, NR, IXN, ICP)
```

```
      INTEGER TSTEP
      DIMENSION PCTAB(22),SWTAB(22),WKTAB(22),AKTAB(22),PC(17,12),PW(17,
     112),PSAVE(17,12),PA(17,12),SW(17,12),SS(17,12),SA(17,12),WK(17,12)
     2,AK(17,12),VISW(17,12),VISA(17,12),RHOW(17,12),RHOA(17,12),SATP(17
     3,12),AW(17,12),BW(17,12),WT(17),SERROR(17,12),ZZ(17,12),STAB(22),C
     4ONST1(17,2),CONST2(17,2),CONST(17,12)
      DIMENSION VX(19,13),VZ(18,14),X(4500),Z(4500),C(4500),SUMC(18,13),
     1COUNT(18,13),CAVG(18,13),DX(17,12),DZ(17,12),DXZ(17,12),DELC(18,13
     2)
      COMMON      PCTAB,SWTAB,WKTAB,AKTAB,PC,PW,PSAVE,PA,SW,SS,SA,WK,AK,V
     1            ISW,VISA,RHOW,RHOA,SATP,AW,BW,WT,SERROR,ZZ,CONST1,CONST
     2            2,X,Z,C,VX,VZ,SUMC,COUNT,DELC,CAVG,DX,DZ,DXZ,STAB,DELX,
     3            DELZ,DELT,SATPER,PHI,G,CRHC,PSOURC,HA,HB,DELMLT,TOLRNC,
     4            DSWMX,DSWMAX,AX,AZ,AXZ,ALENX,ALENZ,CONST,ONE,TWO,FOUR,H
     5            ALF,ZERO,DELT1, DELT2,DIA,DIFF,SOLNC,ISAT,NRM1,NCM1,NRM
     6            2,NCM2,NR2,NR3,NC1,NC2,NDELT,IS1,IPRINT,IFAC,LOG,ITER,I
     7            A,IE,IC,ID,IE,IBM1,IDP1,NWM1,TSTEP,IPC,ISK,ISW,ITENSR,I
     8            CHECK,ISWICH,IRES,ISTEDY,IFPLOT,IWRITE,NN,IVEL,ICLOG
      IF (IXN .EQ. 0) GO TO 55
      SINC=SWTAB(1)-SWTAB(2)
C
C  .......  FROM HERE THRU STATEMENT 60, WK, AK & PC ARE COMPUTED AS
C           FUNCTION OF SW USING LINEAR INTERPOLATION  ................
      DO 60 K=2,NRM1
      DO 60 I=2,NCM1
      IF (SW(I,K) .GE. ONE) GO TO 61
      IN=(SWTAB(1)-SW(I,K))/SINC+2
      IF (IN .LT. 2) IN=2
      IF (IN .GT. ISK) IN=ISK
      INM1=IN-1
      ZMC=(SW(I,K)-SWTAB(IN))/SINC
      WK(I,K)=WKTAB(IN)+ZMC*(WKTAB(INM1)-WKTAB(IN))
      AK(I,K)=AKTAB(IN)+ZMC*(AKTAB(INM1)-AKTAB(IN))
      XX      =SW(I,K)*2.D+00-SS(I,K)
      IN=(SWTAB(1)-  XX    )/SINC+2
      IF (IN .LT. 2) IN=2
      IF (IN .GT. ISK) IN=ISK
      INM1=IN-1
      ZMC=(   XX    -SWTAB(IN))/SINC
      PC(I,K)=PCTAB(IN)+ZMC*(PCTAB(INM1)-PCTAB(IN))
      GO TO 60
   61 WK(I,K)=WKTAB(1)
      AK(I,K)=AKTAB(1)
      PC(I,K)=PCTAB(1)
   60 CONTINUE
      IF (ICP .EQ. 0) GO TO 500
      K=2
      PSURFC=0.0D+00
C
C  .......  FROM HERE THRU STATEMENT 59, THE UPPER BOUNDARY CONDITION
C           ON AIR IS TREATED AND SWSURF, AKSURF ARE OBTAINED AS A
C           FUNCTION OF PCSURF, THAT IS, PC AT THE SURFACE  ............
      DO 59 I=2,NCM1
C
C  .......  PCSURF IS OBTAINED COMBINING THE DEFINITION OF CAPILLARY
C           PRESSURE WITH THE NO-FLOW B.C. FOR WATER FOR THESE GRIDS ...
      PCSURF=PSURFC-PW(I,K)+0.5D+0C*DELZ
      SWSURF=SWTAB(1)
      IF (PCSURF .LT. PCTAB(1)) GO TO 102
      DO 11 J=2,ISK
      N=J
```

```
      IF (PCSURF  .LT. PCTAB(J)) GO TO 51
      IF (PCSURF  .EQ. PCTAB(J)) GO TO 101
   11 CONTINUE
   51 CONTINUE
      SWSURF=SWTAB(N-1)+ ABS((PCSURF-PCTAB(N-1))/(PCTAB(N)-PCTAB(N-1)))*
     $(SWTAB(N)-SWTAB(N-1))
      GO TO 102
  101 SWSURF=SWTAB(J)
  102 CONTINUE
      IN=(SWTAB(1)-SWSURF )/SINC+2
      IF (IN .LT. 2) IN=2
      IF (IN .GT. ISK) IN=ISK
      INM1=IN-1
      ZMC=(SWSURF-SWTAB(IN))/SINC
      AKSURF=AKTAB(IN)+ZMC*(AKTAB(INM1)-AKTAB(IN))
      CONST1(I,K)=RHOA(I,K)/VISA(I,K)*SATP(I,K)*AKSURF*TWO/DELZ/DELZ*RHO
     $W(I,K)/RHOA(I,K)
   59 CONTINUE
      GO TO 500
   55 CONTINUE
C  ******* THE FOLLOWING SEGMENT OF SLPROP IS USED ONLY INITIALLY TO
C          OBTAIN SW AS A FUNCTION OF PC  ***************
      DO 56 K=2,NRM1
      DO 56 I=2,NCM1
      IF (TSTEP .EQ. 0 .AND. PW(I,K) .GE. ZERO) GO TO 56
      SW(I,K)=SWTAB(1)
      IF (PC(I,K) .LT. PCTAB(1)) GO TO 56
      DO 10 J=2,ISK
      N=J
      IF (PC(I,K) .LT. PCTAB(J)) GO TO 50
      IF (PC(I,K) .EQ. PCTAB(J)) GO TO 100
   10 CONTINUE
   50 CONTINUE
      SW(I,K)=SWTAB(N-1)+ ABS((PC(I,K)-PCTAB(N-1))/(PCTAB(N)-PCTAB(N-1))
     $)*(SWTAB(N)-SWTAB(N-1))
      GO TO 56
  100 SW(I,K)=SWTAB(J)
   56 CONTINUE
  500 RETURN
      END
C
C*****************************************************************************
C                                                                             *
C          S U B R O U T I N E     V E L C C Y                                *
C                                                                             *
C*****************************************************************************
C                                                                             *
C            THIS SUBROUTINE CALCULATES THE SEEPAGE VELOCITIES AT             *
C            EACH GRID INTERFACE, THE LONGITUDINAL AND LATERAL                *
C            DISPERSION COEFFICIENTS AS A FUNCTION OF PECLET NUMBER           *
C            AND THE COMPONENTS OF DISPERSION TENSOR USING THE                *
C            APPROPRIATE TRANSFORMATIONS.                                     *
C                                                                             *
C               VX     = VELOCITY IN X-DIRECTION (CM/SEC)                     *
C               VZ     = VELOCITY IN Z-DIRECTION (CM/SEC)                     *
C               VXX    = X-VELOCITY AT CENTER OF GRID                         *
C               VZZ    = Z-VELOCITY AT CENTER OF GRID                         *
C               DL     = LONGITUDINAL DISPERSION COEFFICIENT                  *
C               DT     = LATERAL DISPERSION COEFFICIENT                       *
C               PE     = PECLET NUMBER                                        *
C               DX     = COMPONENT OF DISPERSION COEFFICIENT TENSOR           *
```

```
C               DZ      = COMPONENT OF DISPERSION COEFFICIENT TENSOR      *
C               DXZ     = COMPONENT OF DISPERSION COEFFICIENT TENSOR      *
C
      SUBROUTINE VELOCY (NC, NR, NCP1, NRP1)
      INTEGER TSTEP
      DIMENSION PCTAB(22),SWTAB(22),WKTAB(22),AKTAB(22),PC(17,12),PW(17,
     112),PSAVE(17,12),PA(17,12),SW(17,12),SS(17,12),SA(17,12),WK(17,12)
     2,AK(17,12),VISW(17,12),VISA(17,12),RHOW(17,12),RHOA(17,12),SATP(17
     3,12),AW(17,12),BW(17,12),WT(17),SERROR(17,12),ZZ(17,12),STAB(22),C
     4ONST1(17,2),CONST2(17,2),CONST(17,12)
      DIMENSION VX(19,13),VZ(18,14),X(4500),Z(4500),C(4500),SUMC(18,13),
     1CCOUNT(18,13),CAVG(18,13),DX(17,12),DZ(17,12),DXZ(17,12),DELC(18,13
     2)
      COMMON      PCTAB,SWTAB,WKTAB,AKTAB,PC,PW,PSAVE,PA,SW,SS,SA,WK,AK,V
     1            ISW,VISA,RHOW,RHOA,SATP,AW,BW,WT,SERROR,ZZ,CONST1,CONST
     2            2,X,Z,C,VX,VZ,SUMC,CCOUNT,DELC,CAVG,DX,DZ,DXZ,STAB,DELX,
     3            DELZ,DELT,SATPER,PHI,G,CRHO,PSOURC,HA,HB,DELMLT,TOLRNC,
     4            DSMAX,DSWMAX,AX,AZ,AXZ,ALENX,ALENZ,CONST,ONE,TWO,FOUR,H
     5            ALF,ZERO,DELT1, DELT2,DIA,DIFF,SOLNC,ISAT,NRM1,NCM1,NRM
     6            2,NCM2,NR2,NR3,NC1,NC2,NDELT,ISI,IPRINT,IFAC,LOG,ITER,I
     7            A,IB,IC,ID,IE,IBM1,IDP1,NWM1,TSTEP,IPC,ISK,ISW,ITENSR,I
     8            CHECK,ISWICH,IRES,ISTEDY,IPPLOT,IWRITE,NN,IVEL,ICLOG
      DO 91 K=1,NR
      IM=2
      DO 98 I=2,NC
      IF (I .GT. 2) IM=I-1
      IF (K .EQ. 1 .OR. K .EQ. NR) GO TO 94
      IF (I .EQ. 2 .AND. K .GE. NR2 .AND. K .LE. NRM1)  GO TO 92
      IF (I .EQ. NC    .AND. K .GE. NR3 .AND. K .LE. NRM1) GO TO 93
      IF ( I .EQ. 2 .OR. I .EQ. NC) GO TO 94
C
C  .......  WATER SATURATION OF THE GRID THE FLUID IS EMANATING FROM
C           IS USED IN COMPUTING PORE-VELOCITY  ................
      DHXW=PW(IM,K)-PW(I,K)
      IF (DHXW .GT. ZERO) GO TO 45
      SWAVG=SW(I,K)
      GO TO 46
   45 SWAVG=SW(IM,K)
   46 VX(I,K)=EW(I,K)*DELX*G*DHXW/(PHI*SWAVG)
      GO TO 98
   92 DHXW=HA+ZZ(I,K)-PW(I,K)
      IF (DHXW .GT. ZERO) GO TO 82
      SWAVG=SW(I,K)
      GO TO 11
   82 SWAVG=ONE
   11 VX(I,K)=CONST(I,K)*DELX*G*DHXW/(PHI*SWAVG)
      GO TO 98
   93 DHXW=PW(IM,K)-(HB+ZZ(NCM1,K))
      IF (DHXW .GT. ZERO) GO TO 83
      SWAVG=ONE
      GO TO 12
   83 SWAVG=SW(IM,K)
   12 VX(I,K)=CONST(NCM1,K)*DELX*G*DHXW/(PHI*SWAVG)
      GO TO 98
   94 VX(I,K)=ZERO
   98 CONTINUE
      VX(1,K)=VX(2,K)
      VX(NCP1,K)=VX(NC,K)
   91 CONTINUE
      DO 95 I=1,NC
      KM=2
```

```
      DO 99 K=2,NR
      IF (K .GT. 2) KM=K-1
      IF ( I .EQ. 1 .OR. I .EQ. NC) GO TO 97
      IF (K .EC. 2) GO TO 96
      IF (K .EC. NR) GO TO 97
      DHZW=PW(I,KM)-PW(I,K)+DELZ
      IF (DHZW .GT. ZERO) GC TO 41
      SWAVG=SW(I,K)
      GO TO 42
   41 SWAVG=SW(I,KM)
   42 VZ(I,K)=AW(I,K)*DELZ*G*DHZW/(PHI*SWAVG)
      GO TC 99
   96 IF (ISTECY .EQ. 1) GO TO 97
      IF (I .LT. NC1) GO TO 97
      IF (I .GT. NC2) GO TO 97
      DHZW=PSCLRC-PW(I,K)+HALF*DELZ
      IF (DHZW .GT. ZERO) GO TO 81
      SWAVG=SW(I,K)
      GO TO 65
   81 SWAVG=CNE
   65 VZ(I,K)=CONST2(I,K)*DELZ*G*DHZW/(PHI*SWAVG)
      GO TC 99
   97 VZ(I,K)=ZERO
   99 CONTINUE
      VZ(I,1)=VZ(I,2)
      VZ(I,NRP1)=VZ(I,NR)
   95 CONTINUE
      IF (ISTECY .EQ. 1) GO TO 655
      DSTMAX=0.00
      DO 822 K=1,NR
      DO 822 I=1,NC
      VXX=VX(I,K)- HALF*(VX(I,K)-VX(I+1,K))
      VZZ=VZ(I,K)- HALF*(VZ(I,K)-VZ(I,K+1))
      IF (K .EQ. 1 .OR. K .EQ. NR .OR. I .EQ. 1 .OR. I .EQ. NC) GO TO
     $826
      VXXSQ=VXX*VXX
      VZZSQ=VZZ*VZZ
      VEL= SQRT(VXXSQ+VZZSQ)
C
C  ........ FORM DIMENSIONLESS PECLET NUMBER  ..............
      DIA= SQRT(SATP(I,K)/6.54E-04)
      PE=VEL*DIA/DIFF
C
C  .......  CALCULATE LONGITUDINAL DISPERSION COEFFICIENT  ..............
      IF (PE .GT. 0.400) GO TO 720
      DL=DIFF*0.72
      GO TO 724
  720 IF (PE .GT. 2.00) GO TO 722
      DL=DIFF*0.5900* EXP(0.5300*PE)
      GO TO 724
  722 DL=DIFF*0.8100*PE**1.08274
  724 CONTINUE
C
C  .......  CALCULATE TRANSVERSE DISPERSION COEFFICIENT  ................
      IF (PE .GT. 1.500) GO TO 726
      DT=DIFF*0.72
      GO TO 728
  726 IF (PE .GT. 3.00) GO TO 730
      DT=DIFF*0.6000*PE**0.4991
      GO TO 728
  730 DT=DIFF*0.4650*PE**0.7464
```

```
  728 CONTINUE
      IF (ITENSR .EQ. 0) GO TO 825
      IF (VXXSQ .EQ. ZERO .AND. VZZSQ .EQ. ZERO) GO TO 824
      VELSQ=VEL*VEL
C
C  .......  TRANSFORM DL & DT TO GENERATE DISPERSION TENSORS  ..........
      DX(I,K)=DL*VXXSQ/VELSQ+DT*VZZSQ/VELSQ
      DZ(I,K)=DT*VXXSQ/VELSQ+DL*VZZSQ/VELSQ
      DXZ(I,K)=(DL-DT)*VXX*VZZ/VELSQ
      GO TO 826
  825 DZ(I,K)=DL
      DX(I,K)=DT
      DXZ(I,K)=ZERO
      GO TO 826
  824 DX(I,K)=ZERO
      DZ(I,K)=ZERO
      DXZ(I,K)=ZERO
  826 CONTINUE
      IF ( ABS(DELT*VXX) .LT. DSTMAX) GO TO 745
      DSTMAX= ABS(DELT*VXX)
      VSAVE=VXX
      DSAVE=0.1*DELX
  745 IF ( ABS(DELT*VZZ) .LT. DSTMAX) GO TO 822
      DSTMAX= ABS(DELT*VZZ)
      VSAVE=VZZ
      DSAVE=0.1*DELZ
  822 CONTINUE
      IF (DSTMAX .LT. DSAVE) GO TO 655
      DTINC=DSAVE/VSAVE
      DELTN=DSTMAX/DSAVE
      NDELT=DELTN
      DELT1=(DELTN-NDELT)*DTINC
      DELT2=DTINC
      NDELT=NDELT+1
  655 CONTINUE
      RETURN
      END
C
C*****************************************************************************
C                                                                             *
C         S U B R O U T I N E     M O V P T                                   *
C                                                                             *
C*****************************************************************************
C                                                                             *
C           THIS SUBROUTINE DETERMINES THE VELOCITY OF EACH MOVING            *
C           POINT AND MOVES THE MOVING POINTS ACCORDINGLY.  THE               *
C           VELOCITIES ARE DETERMINED USING A THREE-WAY INTERPO-              *
C           LATION SCHEME. POINTS MOVING OUT OF THE MODEL ARE RE-             *
C           ENTERED AT APPROPRIATE INFLOW BOUNDARY. AN ADDITIONAL             *
C           STORAGE IS CREATED FOR MOVING POINTS. AN ATTEMPT IS               *
C           MADE TO KEEP A MINIMUM NUMBER OF MOVING POINTS IN EACH            *
C           GRID.      POINTS ENTERING THE SYSTEM WITH A NEW NUMBER           *
C           ARE ASSIGNED COORDINATES RANDOMLY WITHIN A GRID USING             *
C           RANDOM NUMBER GENERATOR RANDU. THEIR CONCENTRATIONS ARE           *
C           ASSIGNED USING  A THREE-WAY INTERPOLATION SCHME. A RECORD         *
C           OF SUMC AND COUNT IS MAINTAINED AND CAVG RECALCULATED             *
C           FOR EACH GRID.                                                    *
C                                                                             *
C              LOG    = LOG OF MOVING POINTS IN SYSTEM                        *
C              VXX    = X-VELOCITY COMPONENT OF MOVING POINT                  *
C              VZZ    = Z-VELOCITY COMPONENT OF MOVING POINT                  *
```

```
C                IVEL   = 0 IF VXX & VZZ OBTAINED USING STANDARD LINEAR  *
C                         INTERPOLATION;                                 *
C                       = 1 IF A THREE-WAY INTERPOLATION SCHEME USED      *
C                ICLOG  = 0 IF THE CONCENTRATION OF THE NEWLY INTRODUCED *
C                         POINTS ARE BASED ON THE GRID THE FLUID IS      *
C                         EMANATING FROM;                                *
C                       = 1 IF BASED ON A THREE-WAY INTERPOLATION SCHEME *
C                                                                        *
      SUBROUTINE MOVPT (NC, NR, NCP1,NRP1, NPZ, NPX)
      INTEGER TSTEP
      DIMENSION PCTAE(22),SWTAE(22),WKTAB(22),AKTAB(22),PC(17,12),PW(17,
     112),PSAVE(17,12),PA(17,12),SW(17,12),SS(17,12),SA(17,12),WK(17,12)
     2,AK(17,12),VISW(17,12),VISA(17,12),RHOW(17,12),RHOA(17,12),SATP(17
     3,12),AW(17,12),BW(17,12),WT(17),SERROR(17,12),ZZ(17,12),STAE(22),C
     40NST1(17,2),CONST2(17,2),CONST(17,12)
      DIMENSION VX(19,13),VZ(18,14),X(4500),Z(4500),C(4500),SUMC(18,13),
     1COUNT(18,13),CAVG(18,13),DX(17,12),DZ(17,12),DXZ(17,12),DELC(18,13
     2)
      COMMON       PCTAE,SWTAE,WKTAB,AKTAB,PC,PW,PSAVE,PA,SW,SS,SA,WK,AK,V
     1             ISW,VISA,RHOW,RHOA,SATP,AW,BW,WT,SERROR,ZZ,CONST1,CONST
     2             2,X,Z,C,VX,VZ,SUMC,COUNT,DELC,CAVG,DX,DZ,DXZ,STAB,DELX,
     3             DELZ,DELT,SATPER,PHI,G,CRHC,PSOURC,HA,HB,DELMLT,TOLRNC,
     4             DSWMX,DSWMAX,AX,AZ,AXZ,ALENX,ALENZ,CONST,ONE,TWO,FOUR,H
     5             ALF,ZERO,DELT1, DELT2,DIA,DIFF,SOLNC,ISAT,NRM1,NCM1,NRM
     6             2,NCM2,NR2,NR3,NC1,NC2,NDELT,IS1,IPRINT,IFAC,LOG,ITER,I
     7             A,IB,IC,ID,IE,IBM1,IDF1,NWM1,TSTEP,IPC,ISK,ISW,ITENSR,I
     8             CHECK,ISWICH,IRES,ISTEDY,IFPLOT,IWRITE,NN,IVEL,ICLOG
      DO 200 I=1,LOG
      NI1=X(I)/DELX+1.
      NI2=Z(I)/DELZ+1.
      IF (NI1 .GT. NC .OR. NI2  .GT. NR) GO TO 200
      IF (NI1 .LE. 0 .OR. NI2 .LE. 0) GO TO 200
      AL=NI1-1
      ALL=NI2-1
      IF (IVEL .EQ. 0) GO TO 650
      IF (Z(I) .LT. DELZ .OR. X(I) .LT. DELX .OR. X(I) .GT. (ALENX-DELX)
     $.OR. Z(I) .GT. (ALENZ-DELZ)) GO TO 636
      IF (Z(I) .LT. 1.5*DELZ .OR. Z(I) .GT. ALENZ-1.5*DELZ) GO TO 632
      IF (Z(I) .LT. (ALL+0.5)*DELZ) GO TO 630
      A=(Z(I)-(ALL+0.5)*DELZ)/DELZ
      VXXU=VX(NI1,NI2)-A*(VX(NI1,NI2)-VX(NI1,NI2+1))
      VXXD=VX(NI1+1,NI2)-A*(VX(NI1+1,NI2)-VX(NI1+1,NI2+1))
      VXX=VXXU-((X(I)-AL*DELX)/DELX)*(VXXU-VXXD)
      GO TO 634
  630 A=(Z(I)-(ALL-0.5)*DELZ)/DELZ
      VXXU=VX(NI1,NI2-1)-A*(VX(NI1,NI2-1)-VX(NI1,NI2))
      VXXD=VX(NI1+1,NI2-1)-A*(VX(NI1+1,NI2-1)-VX(NI1+1,NI2))
      VXX=VXXU-((X(I)-AL*DELX)/DELX)*(VXXU-VXXD)
      GO TO 634
  632 VXX=VX(NI1,NI2)-(((X(I)-(AL*DELX))/DELX)*(VX(NI1,NI2)-VX(NI1+1,NI2
     6)))
  634 CONTINUE
      IF (X(I) .LT. 1.5*DELX .OR. X(I) .GT. (ALENX-1.5*DELX)) GO TO 638
      IF (X(I) .LT. (AL+0.5)*DELX) GO TO 637
      A=(X(I)-(AL+0.5)*DELX)/DELX
      VZZU=VZ(NI1,NI2)-A*(VZ(NI1,NI2)-VZ(NI1+1,NI2))
      VZZD=VZ(NI1,NI2+1)-A*(VZ(NI1,NI2+1)-VZ(NI1+1,NI2+1))
      VZZ=VZZU-((Z(I)- ALL*DELZ)/DELZ)*(VZZU-VZZD)
      GO TO 640
  637 A=(X(I)-(AL-0.5)*DELX)/DELX
      VZZU=VZ(NI1-1,NI2)-A*(VZ(NI1-1,NI2)-VZ(NI1,NI2))
```

```
      VZZD=VZ(NI1-1,NI2+1)-A*(VZ(NI1-1,NI2+1)-VZ(NI1,NI2+1))
      VZZ=VZZD-((Z(I)- ALL*CELZ)/DELZ)*(VZZU-VZZD)
      GO TO 640
  638 VZZ=VZ(NI1,NI2)-(((Z(I)-(ALL*DELZ))/DELZ)*(VZ(NI1,NI2)-VZ(NI1,NI2+
     $1)))
      GO TO 640
  636 VXX=VX(NI1,NI2)
      VZZ=VZ(NI1,NI2)
  640 CONTINUE
      GO TO 660
  650 VXX=VX(NI1,NI2)-(((X(I)-(AL*DELX))/DELX)*(VX(NI1,NI2)-VX(NI1+1,NI2
     &)))
      VZZ=VZ(NI1,NI2)-(((Z(I)-(ALL*DELZ))/DELZ)*(VZ(NI1,NI2)-VZ(NI1,NI2+
     $1)))
  660 CONTINUE
C
C  .......  FROM HERE THRU STATEMENT 277, B.C.'S ARE CHECKED & MOVING
C           POINTS CLOSE TO THE NO-FLOW BOUNDARY ARE ASSIGNED A ZERO
C           VELOCITY  ...................
      IF (VX(NI1,NI2) .EQ. ZERO .AND. VXX .LT. ZERO) GO TO 270
      GO TO 271
  270 AL=NI1-1
      DISTA=X(I)-AL*DELX
      DISTB= ABS(DELT*VXX)
      IF (DISTB .GT. DISTA) VXX=(-DISTA+0.0100) /DELT
  271 IF (VX(NI1+1,NI2) .EQ. ZERO .AND. VXX .GT. ZERO) GO TO 272
      GO TO 273
  272 AL=NI1
      DISTA=AL*DELX-X(I)
      DISTB= ABS(DELT*VXX)
      IF (DISTB .GT. DISTA) VXX=(DISTA-0.0100)/DELT
  273 IF (VZ(NI1,NI2) .EQ. ZERO .AND. VZZ .LT. ZERO) GO TO 274
      GO TO 275
  274 ALL=NI2-1
      DISTA=Z(I)-ALL*DELZ
      DISTB= ABS(DELT*VZZ)
      IF (DISTB .GT. DISTA) VZZ=(-DISTA+0.0100) /DELT
  275 IF (VZ(NI1,NI2+1) .EQ. ZERO .AND. VZZ .GT. ZERO) GO TO 276
      GO TO 277
  276 ALL=NI2
      DISTA=ALL*DELZ-Z(I)
      DISTB= ABS(DELT*VZZ)
      IF (DISTB .GT. DISTA) VZZ=(DISTA-0.0100)/DELT
  277 CONTINUE
      Z(I)=Z(I)+DELT*VZZ
      X(I)=X(I)+DELT*VXX
C
C  .......  POINTS MOVING OUT  ARE REINTRODUCED AT THE INFLOW BOUNDARY
      IF (X(I) .GT. ALENX .OR. Z(I) .GT. ALENZ) GO TO 280
      IF (X(I) .LT. ZERO .OR. Z(I) .LT. ZERO) GO TO 280
      GO TO 44
  280 CONTINUE
C
C  .......  RANDU IS A LOCAL LIBRARY SUBROUTINE  ...............
      CALL RANDU (IS1, IS, UNP)
      IS1=IS
      X(I)=(NC1-1+UNP)*DELX
      CALL RANDU (IS1, IS, UNP)
      IS1=IS
      Z(I)=UNP*DELZ
      C(I)=SCLNG
```

```
   44 NI1=X(I)/DELX+1.
      NI2=Z(I)/DELZ+1.
      IF (NI1 .GT. NC .OR. NI2  .GT. NR) GO TO 200
      IF (NI1 .LE. 0 .OR. NI2 .LE. 0) GO TO 200
      COUNT(NI1,NI2)=COUNT(NI1,NI2)+1.
  200 CONTINUE
C
C  ....... FROM HERE THRU STATEMENT 46, THE NUMBER OF POINTS PER GRID
C          ARE CHECKED AND IF IT FALLS SHORT OF THE REQUIRED MINIMUM
C          ,NEW POINTS ARE INTRODUCED  ....................
      DO 46 K=1,NR
      ALL=K-1
      DO 46 I=1,NC
      AL=I-1
      ITRIP=0
      IF (COUNT(I,K) .GE. NN) GO TO 46
    8 IF (VX(I+1,K) .LT. ZERO .AND. I .LT. NC1) GO TO 9
    4 IF (VX(I,K) .GT. ZERO .AND. I .GT. NC2) GO TO 7
    6 IF (VZ(I,K) .GT. ZERO) GO TO 5
   14 IF (VX(I,K) .GT. ZERO .AND. I .LT. NC1) GO TO 12
      ITRIP=ITRIP+1
      IF (ITRIP .GT. NN) GO TO 46
      IF (COUNT(I,K) .LT. NN) GO TO 8
    9 LOG=LOG+1
      X(LOG)=I*DELX-0.001
      CALL RANDU (IS1, IS, UNP)
      IS1=IS
      Z(LOG)=(ALL+UNP)*DELZ
      IF (ICLOG .EQ. 0) GO TO 402
      IF (I .EQ. 1 .AND. K .EQ. NR2 .AND. Z(LOG)  .LT. (ALL+0.5)*DELZ)
     $GO TO 501
      IF (Z(LOG) .LT. 1.5*DELZ .OR. Z(LOG) .GT. (ALENZ-1.5*DELZ)) GO TO
     $601
      GO TO 602
  601 C(LOG)=CAVG(I,K)-((X(LOG)-(AL+0.5)*DELX)/DELX)*(CAVG(I,K)-CAVG(I+1
     $,K))
      GO TO 610
  602 IF (Z(LOG) .LT. (ALL+0.5)*DELZ) GO TO 603
      ADN=(Z(LOG)-(ALL+0.5)*DELZ)/DELZ
      C1=CAVG(I,K)-ADN*(CAVG(I,K)-CAVG(I,K+1))
      C2=CAVG(I+1,K)-ADN*(CAVG(I+1,K)-CAVG(I+1,K+1))
      C(LOG)=C1-((X(LOG)-(AL+0.5)*DELX)/DELX)*(C1-C2)
      GO TO 610
  603 AUP=(Z(LOG)-(ALL-0.5)*DELZ)/DELZ
      C1=CAVG(I,K-1)-AUP*(CAVG(I,K-1)-CAVG(I,K))
      C2=CAVG(I+1,K-1)-AUP*(CAVG(I+1,K-1)-CAVG(I+1,K))
      C(LOG)=C1-((X(LOG)-(AL+0.5)*DELX)/DELX)*(C1-C2)
      GO TO 610
  501 C1=CAVG(I,K)
      C2=CAVG(I+1,K-1)-((Z(LOG)-(ALL-0.5)*DELZ)/DELZ)*(CAVG(I+1,K-1)-
     $CAVG(I+1,K))
      C(LOG)=C1-((X(LOG)-(AL+0.5)*DELX)/DELX)*(C1-C2)
  610 CONTINUE
      GO TO 403
  402 C(LOG)=CAVG(I+1,K)
  403 CONTINUE
      COUNT(I,K)=COUNT(I,K)+1.
      IF (COUNT(I,K) .LT. NN) GO TO 4
      GO TO 46
    7 LOG=LOG+1
      CALL RANDU (IS1, IS, UNP)
```

```
      IS1=IS
      Z(LOG)=(ALL+UNP)*DELZ
      X(LOG)=AL*DELX+0.001
      IF ((CLCE .EQ. 0) GO TO 404
      IF (I .EQ. NC .AND. K .EQ. NR3 .AND. Z(LOG) .LT. (ALL+0.5)*DELZ)
     $GO TO 621
      IF (Z(LOG) .LT. 1.5*DELZ .OR. Z(LOG) .GT. (ALENZ-1.5*DELZ)) GO TO
     $605
      GO TO 606
  605 C(LOG)=CAVG(I-1,K)-((X(LOG)-(AL-0.5)*DELX)/DELX)*(CAVG(I-1,K)-CAVG
     $(I,K))
      GO TO 622
  606 IF (Z(LOG) .LT. (ALL+0.5)*DELZ) GO TO 607
      ADN=(Z(LOG)-(ALL+0.5)*DELZ)/DELZ
      C1=CAVG(I-1,K)-ADN*(CAVG(I-1,K)-CAVG(I-1,K+1))
      C2=CAVG(I,K)-ADN*(CAVG(I,K)-CAVG(I,K+1))
      C(LOG)=C1-((X(LOG)-(AL-0.5)*DELX)/DELX)*(C1-C2)
      GO TO 622
  607 AUP=(Z(LOG)-(ALL-0.5)*DELZ)/DELZ
      C1=CAVG(I-1,K-1)-AUP*(CAVG(I-1,K-1)-CAVG(I-1,K))
      C2=CAVG(I,K-1)-AUP*(CAVG(I,K-1)-CAVG(I,K))
      C(LOG)=C1-((X(LOG)-(AL-0.5)*DELX)/DELX)*(C1-C2)
      GO TO 622
  621 C2=CAVG(I,K)
      C1=CAVG(I-1, K-1) - ((Z(LOG)-(ALL-0.5)*DELZ)/DELZ)*(CAVG(I-1,K-1)-
     $CAVG(I-1,K))
      C(LOG)=C1-((X(LOG)-(AL-0.5)*DELX)/DELX)*(C1-C2)
  622 CONTINUE
      GO TO 405
  404 C(LOG)=CAVG(I-1,K)
  405 CONTINUE
      COUNT(I,K)=COUNT(I,K)+1.
      IF (COUNT(I,K) .LT. NN) GO TO 6
      GO TO 46
    5 LOG=LOG+1
      CALL RANDU (IS1, IS, UNP)
      IS1=IS
      X(LOG)=(AL+UNP)*DELX
      Z(LOG)=ALL*DELZ+0.001
      IF (K .EQ. 1) GO TO 387
      IF ((CLCE .EQ. 0) GO TO 401
      IF (K .EQ. 2 .AND. I .EQ. NC1 .AND. X(LOG) .LT. (AL+0.5)*DELX) GO
     $TO 611
      IF (K .EQ. 2 .AND. I .EQ. NC2 .AND. X(LOG) .GT. (AL+0.5)*DELX) GO
     $TO 612
      GO TO 624
  611 C1=SCLNC
      C2=CAVG(I-1,K)-((X(LOG)-(AL-0.5)*DELX)/DELX)*(CAVG(I-1,K)-CAVG(I,K
     $))
      C(LOG)=C1-((Z(LOG)-(ALL-0.5)*DELZ)/DELZ)*(C1-C2)
      GO TO 625
  612 C1=SCLNC
      C2=CAVG(I,K)-((X(LOG)-(AL+0.5)*DELX)/DELX)*(CAVG(I,K)-CAVG(I+1,K))
      C(LOG)=C1-((Z(LOG)-(ALL-0.5)*DELZ)/DELZ)*(C1-C2)
      GO TO 625
  624 IF (X(LOG) .LT. (AL+0.5)*DELX) GO TO 613
      ADN=(X(LOG)-(AL+0.5)*DELX)/DELX
      C1=CAVG(I,K-1)-ADN*(CAVG(I,K-1)-CAVG(I+1,K-1))
      C2=CAVG(I,K)-ADN*(CAVG(I,K)-CAVG(I+1,K))
      C(LOG)=C1-((Z(LOG)-(ALL-0.5)*DELZ)/DELZ)*(C1-C2)
      GO TO 625
```

```
613 AUP=(X(LCG)-(AL-0.5)*DELX)/DELX
    C1=CAVG(I-1,K-1)-AUP*(CAVG(I-1,K-1)-CAVG(I,K-1))
    C2=CAVG(I-1,K)-AUP*(CAVG(I-1,K)-CAVG(I,K))
    C(LOG)=C1-((Z(LCG)-(ALL-0.5)*DELZ)/DELZ)*(C1-C2)
    GO TO 625
387 C(LOG)=SCLNC
625 CONTINUE
    GO TO 648
401 C(LOG)=CAVG(I,K-1)
648 CONTINUE
    CCUNT(I,K)=CCUNT(I,K)+1.
    IF (COUNT(I,K) .LT. NN) GO TO 14
    GO TO 46
 12 LOG=LOG+1
    X(LOG)=AL*DELX+0.001
    CALL RANDU (IS1, IS, UNF)
    IS1=IS
    Z(LOG)=(ALL+UNF)*DELZ
    IF (I .EQ. 1) GO TO 510
    IF (ICLCG .EQ. 0) GO TO 510
    IF (Z(LCG) .LT. 1.5*DELZ .OR. Z(LOG) .GT. (ALENZ-1.5*DELZ)) GO TO
   $511
    GO TO 515
511 C(LOG)=CAVG(I-1,K)-((X(LOG)-(AL-0.5)*DELX)/DELX)*(CAVG(I-1,K)-CAVG
   $(I,K))
    GO TO 520
515 IF (Z(LCG) .LT. (ALL+0.5)*DELZ) GO TO 513
    ADN=(Z(LCG)-(ALL+0.5)*DELZ)/DELZ
    C1=CAVG(I-1,K)-ADN*(CAVG(I-1,K)-CAVG(I-1,K+1))
    C2=CAVG(I,K)-ADN*(CAVG(I,K)-CAVG(I,K+1))
    C(LOG)=C1-((X(LCG)-(AL-0.5)*DELX)/DELX)*(C1-C2)
    GO TO 520
513 AUP=(Z(LCG)-(ALL-0.5)*DELZ)/DELZ
    C1=CAVG(I-1,K-1)-AUP*(CAVG(I-1,K-1)-CAVG(I-1,K))
    C2=CAVG(I,K-1)-AUP*(CAVG(I,K-1)-CAVG(I,K))
    C(LOG)=C1-((X(LOG)-(AL-0.5)*DELX)/DELX)*(C1-C2)
    GO TO 520
510 C(LOG)=CAVG(I,K)
520 CONTINUE
    CCUNT(I,K)=CCUNT(I,K)+1.
    IF (COUNT(I,K) .LT. NN) GO TO 8
 46 CONTINUE
    DO 201 K=1,NR
    DO 201 I=1,NC
201 CCUNT(I,K)=0.
    DO 205 I=1,LOG
    NI1=X(I)/DELX+1.
    NI2=Z(I)/DELZ+1.
    IF (NI1 .GT. NC .OR. NI2  .GT. NR) GO TO 205
    IF (NI1 .LE. 0 .OR. NI2 .LE. 0) GO TO 205
    SUMC(NI1,NI2)=SUMC(NI1,NI2)+C(I)
    COUNT(NI1,NI2)=COUNT(NI1,NI2)+1.
205 CONTINUE
    DO 85 K=1,NR
    DO 85 I=1,NC
    IF (COUNT(I,K) .EQ. 0.0) CCUNT(I,K)=1.0
 85 CAVG(I,K)=SUMC(I,K)/CCUNT(I,K)
    RETURN
    END
```

```
C*************************************************************************
C                                                                        *
C          S  U  B  R  O  U  T  I  N  E      D  I  S  P                 *
C                                                                        *
C*************************************************************************
C                                                                        *
C            THIS SUBROUTINE CALCULATES THE CHANGE IN CONCENTRA-         *
C            TION DUE TO DISPERSION. CAVG IS THEN CORRECTED FOR THIS     *
C            DISPERSION EFFECT.                                          *
C
      SUBROUTINE DISP (NC, NR)
      INTEGER TSTEP
      DIMENSION PCTAB(22),SWTAB(22),WKTAB(22),AKTAB(22),PC(17,12),PW(17,
     112),PSAVE(17,12),PA(17,12),SW(17,12),SS(17,12),SA(17,12),WK(17,12)
     2,AK(17,12),VISW(17,12),VISA(17,12),RHOW(17,12),RHOA(17,12),SATP(17
     3,12),AW(17,12),BW(17,12),WT(17),SERROR(17,12),ZZ(17,12),STAB(22),C
     4ONST1(17,2),CONST2(17,2),CONST(17,12)
      DIMENSION VX(19,13),VZ(18,14),X(4500),Z(4500),C(4500),SUMC(18,13),
     1COUNT(18,13),CAVG(18,13),DX(17,12),DZ(17,12),DXZ(17,12),DELC(18,13
     2)
      COMMON      PCTAB,SWTAB,WKTAB,AKTAB,PC,PW,PSAVE,PA,SW,SS,SA,WK,AK,V
     1            ISW,VISA,RHOW,RHOA,SATP,AW,BW,WT,SERROR,ZZ,CONST1,CONST
     2            2,X,Z,C,VX,VZ,SUMC,COUNT,DELC,CAVG,DX,DZ,DXZ,STAB,DELX,
     3            DELZ,DELT,SATPER,PHI,G,CRHO,PSOURC,HA,HB,DELMLT,TOLRNC,
     4            DSWMX,DSWMAX,AX,AZ,AXZ,ALENX,ALENZ,CONST,ONE,TWO,FOUR,H
     5            ALF,ZERO,DELT1, DELT2,DIA,DIFF,SOLNC,ISAT,NRM1,NCM1,NRM
     6            2,NCM2,NR2,NR3,NC1,NC2,NDELT,IS1,IPRINT,IFAC,LOG,ITER,I
     7            A,IE,IC,ID,IE,IBM1,IDP1,NWM1,TSTEP,IPC,ISK,ISW,ITENSR,I
     8            CHECK,ISWICH,IRES,ISTEDY,IFPLOT,IWRITE,NN,IVEL,ICLOG
C
C  .......  FROM HERE THRU STATEMENT 337, B.C'S ARE CHECKED & CAVG OF
C           THE BOUNDARY GRIDS ARE BASED ON THE APPROPRIATE B.C'S  .....
C
      K=1
      DO 334 I=2,NCM1
      IF (VZ(I,K) .GT. ZERO) GO TO 347
      CAVG(I,K)=CAVG(I,K+1)
      GO TO 334
  347 CAVG(I,K)=SOLNC
  334 CONTINUE
      K=NR
      DO 335 I=2,NCM1
  335 CAVG(I,NR)=CAVG(I,NRM1)
      I=1
      DO 336 K=2,NRM1
      IF (VX(I,K) .GT. ZERO) GO TO 345
      CAVG(I,K)=CAVG(I+1,K)
      GO TO 336
  345 CAVG(I,K)=0.
  336 CONTINUE
      I=NC
      DO 337 K=2,NRM1
      IF (VX(I,K) .LT. ZERO) GO TO 346
      CAVG(I,K)=CAVG(NCM1,K)
      GO TO 337
  346 CAVG(I,K)=0.
  337 CONTINUE
C
C  .......  CAVG OF THE CORNER GRIDS ARE ASSIGNED  ..............
      CAVG(1,1)=CAVG(2,2)
      CAVG(NC,1)=CAVG(NCM1,2)
      CAVG(1,NR)=CAVG(2,NRM1)
```

```
      CAVG(NC,NR)=CAVG(NCM1,NRM1)
C
      KM=2
      DO 332 K=2,NRM1
      IM=2
      IF (K .GT. 2) KM=K-1
      IF (K .LT. NRM1) KP=K+1
      DO 332 I=2,NCM1
      IF (I .GT. 2) IM=I-1
      IF (I .LT. NCM1) IP=I+1
      DCZZA=AZ*(DZ(I,KM)*SW(I,KM)+DZ(I,K)*SW(I,K))*(CAVG(I,K-1)-CAVG(I,K
     $))
      DCZZB=AZ*(DZ(I,KP)*SW(I,KP)+DZ(I,K)*SW(I,K))*(CAVG(I,K+1)-CAVG(I,K
     $))
      DCXXC=AX*(DX(IM,K)*SW(IM,K)+DX(I,K)*SW(I,K))*(CAVG(I-1,K)-CAVG(I,K
     $))
      DCXXD=AX*(DX(IP,K)*SW(IP,K)+DX(I,K)*SW(I,K))*(CAVG(I+1,K)-CAVG(I,K
     $))
      IF (ITENSR .EQ. 0) GO TO 33)
      DCXZA=AXZ*(DXZ(IM,K)*SW(IM,K)+DXZ(I,K)*SW(I,K))*(CAVG(I,K+1)+CAVG(
     $I-1,K+1)-CAVG(I-1,K-1)-CAVG(I,K-1))
      DCXZB=AXZ*(DXZ(IP,K)*SW(IP,K)+DXZ(I,K)*SW(I,K))*(CAVG(I,K+1)+CAVG(
     $I+1,K+1)-CAVG(I+1,K-1)-CAVG(I,K-1))
      DCZXC=AXZ*(DXZ(I,KM)*SW(I,KM)+DXZ(I,K)*SW(I,K))*(CAVG(I+1,K)+CAVG(
     $I+1,K-1)-CAVG(I-1,K)-CAVG(I-1,K-1))
      DCZXD=AXZ*(DXZ(I,KP)*SW(I,KP)+DXZ(I,K)*SW(I,K))*(CAVG(I+1,K+1)+CAV
     $G(I+1,K)-CAVG(I-1,K)-CAVG(I-1,K+1))
      DELC(I,K)=(DCZZA+DCZZB+DCXXC+DCXXD+DCXZB-DCXZA+DCZXD-DCZXC)*DELT
     $/SW(I,K)
      GO TO 332
  330 DELC(I,K)=(DCZZA+DCZZB+DCXXC+DCXXD)*DELT/SW(I,K)
  332 CONTINUE
      DO 326 K=1,NR
      DO 326 I=1,NC
  326 CAVG(I,K)=CAVG(I,K)+DELC(I,K)
      DO 320 I=1,LOG
      NI1=X(I)/DELX+1.
      NI2=Z(I)/DELZ+1.
      C(I)=C(I)+CELC(NI1,NI2)
  320 CONTINUE
      RETURN
      END
C
C*************************************************************************
C                                                                        *
C         S U B R O U T I N E     M A T B A L                            *
C                                                                        *
C*************************************************************************
C                                                                        *
C            THIS SUBROUTINE CALCULATES THE MATERIAL BALANCE FOR THE     *
C            WATER, AIR AND THE TRACER.                                  *
C                                                                        *
C               ICHECK = COUNTER TO PRINT MATBAL ERRORS, INTEGER         *
C               ISWICH = INTERVAL AT WHICH MATBAL  ERRORS ARE PRINTED,   *
C                        INTEGER                                         *
C
      SUBROUTINE MATBAL ( NC, NR, TAOUT, TAUT, TWIN, TWOUT, TWEN, TWUT,
     1                    TSIN, TSOUT,WS, AS, CS, WS1, AS1, CS1, WIS, AIS,
     2                    SIS, SAREA, AR, TAIN,  DAIN, DAOUT, DWIN, DWOUT,
     3                    DSIN, DSOUT, KKKK, DTSAVE, TIME, CAVGSV, TAEN)
      INTEGER TSTEP
```

```
      DIMENSION PCTAE(22),SWTAE(22),WKTAB(22),AKTAB(22),PC(17,12),PW(17,
     112),PSAVE(17,12),PA(17,12),SW(17,12),SS(17,12),SA(17,12),WK(17,12)
     2,AK(17,12),VISW(17,12),VISA(17,12),RHOW(17,12),RHOA(17,12),SATP(17
     3,12),AW(17,12),BW(17,12),WT(17),SERROR(17,12),ZZ(17,12),STAE(22),C
     4ONST1(17,2),CONST2(17,2),CONST(17,12)
      DIMENSION VX(19,13),VZ(18,14),X(4500),Z(4500),C(4500),SUMC(18,13),
     1COUNT(18,13),CAVG(18,13),DX(17,12),DZ(17,12),DXZ(17,12),DELC(18,13
     2)
      DIMENSION CAVGSV(18,13)
      COMMON      PCTAE,SWTAB,WKTAB,AKTAB,PC,PW,PSAVE,PA,SW,SS,SA,WK,AK,V
     1            ISW,VISA,RHOW,RHOA,SATP,AW,BW,WT,SERROR,ZZ,CONST1,CONST
     2            2,X,Z,C,VX,VZ,SUMC,COUNT,DELC,CAVG,DX,DZ,DXZ,STAB,DELX,
     3            DELZ,DELT,SATPER,PHI,G,CRHO,PSOURC,HA,HB,DELMLT,TOLRNC,
     4            DSWMX,DSWMAX,AX,AZ,AXZ,ALENX,ALENZ,CONST,ONE,TWO,FOUR,H
     5            ALF,ZERO,DELT1,  DELT2,DIA,DIFF,SOLNC,ISAT,NRM1,NCM1,NRM
     6            2,NCM2,NR2,NR3,NC1,NC2,NDELT,IS1,IPRINT,IFAC,LOG,ITER,I
     7            A,IE,IC,ID,IE,IBM1,IDP1,NWM1,ISTEP,IPC,ISK,ISW,ITENSR,I
     8            CHECK,ISWICH,IRES,ISTEDY,IFPLOT,IWRITE,NN,IVEL,ICLOG
      TAIN=TAEN
      TACUT =TALT
      TWIN=TWEN
      TWOUT=TWLT
C
C  .......  COMPUTES AIR INFLOW OR OUTFLOW THROUGH THE UPPER BOUNDARY ..
      K=2
      DO 110 I=2,NCM1
      CRHO=RHOW(I,K)/RHOA(I,K)
      IF (ISTEDY .EQ. 1) GO TO 112
      IF (I-NC1) 112,110,113
  113 IF (I-NC2) 110,110,112
  112 QA =          CONST1(I,K)*DELZ*G*(PSOURC-PA(I,K))*DELX*DELT+CONST1(
     $I,K)*DELZ*G/CRHO*(  HALF*DELZ)*DELX*DELT
      IF (QA .GT. ZERO) GO TO 20
      DAOUT=DAOUT-QA
      GO TO 110
   20 DAIN=DAIN+QA
  110 CONTINUE
      IF (ISTEDY .EQ. 1) GO TO 111
C
C  .......  COMPUTES WATER & TRACER INFLOW OR OUTFLOW THROUGH THE
C           UPPER BOUNDARY  ............
      K=2
      DO 114 I=NC1,NC2
      QW=    (PSOURC-PW(I,K)+ HALF*DELZ)*CONST2(I,K)*SAREA*DELT
      IF (QW .GT. ZERO) GO TO 11
      DWOUT=DWOUT-QW
      GO TO 12
   11 DWIN=DWIN+QW
   12 SM=QW*SOLNC
      IF (SM .GT. ZERO) GO TO 19
      DSOUT=DSOUT-SM
      GO TO 114
   19 DSIN=DSIN+SM
  114 CONTINUE
  111 CONTINUE
      IF (IRES .EQ. 0) GO TO 150
C
C  .......  COMPUTES WATER & TRACER INFLOW OR OUTFLOW THROUGH THE
C           L.P.S. OF THE MODEL  ............
      DO 120 K=NR2,NRM1
      QW=      (HA-PW(2,K)+ZZ(2,K))*CONST (2,K)*SAREA*DELT
```

```
      IF (QW .GT. ZERO) GO TO 13
      DWOUT=DWOUT-GW
      GO TO 14
   13 DWIN=DWIN+GW
   14 SM=QW*HALF*(CAVG(2,K)+CAVGSV(2,K))
      IF (SM .GT. ZERO) GO TO 15
      DSOUT=DSOUT-SM
      GO TO 120
   15 DSIN=DSIN+SM
  120 CONTINUE
  150 CONTINUE
C
C  ......... COMPUTES WATER & TRACER INFLOW OR OUTFLOW THROUGH THE
C             R.H.S. OF THE MODEL ...............
      DO 130 K=NR3,NRM1
      QW=      (PW(NCM1,K)-ZZ(NCM1,K)-HB)*CONST (NCM1,K)*SAREA*DELT
      IF (QW .GT. ZERO) GO TO 16
      DWIN=DWIN-GW
      GO TO 17
   16 DWOUT=DWOUT+GW
   17 SM=QW*HALF*(CAVG(NCM1,K)+CAVGSV(NCM1,K))
      IF (SM .GT. ZERO) GO TO 18
      DSIN=DSIN-SM
      GO TO 130
   18 DSOUT=DSOUT+SM
  130 CONTINUE
C
C  .......  COMPUTES CHANGE IN AIR, WATER & TRACER STORAGE  ..............
      IF (KKKK .NE. NDELT) GO TO 500
      WS=ZERO
      AS=ZERO
      CS=ZERO
      DO 140 K=2,NRM1
      DO 140 I=2,NCM1
      CS=CS+SW(I,K)*CAVG(I,K)
      AS=AS+SA(I,K)
  140 WS=WS+SW(I,K)
      WS2=WS*AR
      AS2=AS*AR
      CS2=CS*AR
      WS=WS2-WIS
      AS=AS2-AIS
      CS=CS2-SIS
      DWS=WS-WSI
      DAS=AS-ASI
      DSALT=CS-CSI
      TWIN=TWIN+DWIN
      TWOUT=TWOUT+DWOUT
      TAIN=TAIN+CAIN
      TAOUT=TAOUT+DAOUT
      TSIN=TSIN+DSIN
      TSOUT=TSOUT+DSOUT
      DADIFF=CAIN-CAOUT
      TADIFF=TAIN-TAOUT
      DWDIFF=DWIN-DWOUT
      TWDIFF=TWIN-TWOUT
      DSDIFF=DSIN-DSOUT
      TSDIFF=TSIN-TSOUT
      DERRW=  ABS(DWS-DWDIFF)/(DWOUT+WS2)
      RERRW= ABS(WS-TWDIFF)/(TWOUT+WS2)
      DERRA= ABS(DAS-DADIFF)/(DAOUT+AS2)
```

```
      RERRA= AES(AS-TADIFF)/(TAOUT+AS2)
      IF (ISTEDY .EQ. 1) GO TO 300
      DERRS= AES(CSALT-DSDIFF)/DSIN
      RERRS= AES(CS-TSDIFF)/TSIN
      GO TO 350
  300 CONTINUE
      RERRS=ZERO
      DERRS=ZERO
  350 CONTINUE
      DELT=DTSAVE
      TIME=TIME+DELT
      HOURS=TIME/3600.0
      IF (TSTEP .NE. ICHECK*ISWICH) GO TO 500
      ICHECK=ICHECK+1
      WRITE (6,475)
      WRITE (6,471)
      WRITE (6,472) TSTEP,ITER,DELT,HOURS,DSWMAX
      WRITE (6,473) DWIN,DWOUT,DWDIFF,DWS    ,TWIN,TWOUT,TWDIFF,WS,WIS,WS
     12,DERRW,RERRW
      WRITE (6,474) DAIN,DAOUT,DADIFF,DAS    ,TAIN,TAOUT,TADIFF,AS,AIS,AS
     12,DERRA,RERRA
      WRITE (6,476) DSIN,DSOUT,DSDIFF,DSALT ,TSIN,TSOUT,TSDIFF,CS,SIS,CS
     12,DERRS,RERRS
  500 RETURN
  471 FORMAT (/1X,T30,'* * * * M A T E R I A L  B A L A N C E  E R R O R
     1  A N A L Y S I S * * * *' )
  472 FORMAT ( 1X,'TSTEP =',I4,T30,'ITER =',I4,T60,'DELT (SECS) =',E12.5
     1,T95,'CUM. HOURS =',F10.4,4X,'MAX.',/1X,'WATER SAT. CHNG =',E12.5)
  474 FORMAT (/ 1X,'INC.  AIR  IN =',D11.4,T30,'INC.  AIR  OUT =',D11.4,
     1T60,'INC.  AIR  IN & OUT =',D11.4,T95,'INC.  AIR  STRG. CHANGE =',
     2D11.4,/1X,'CUM.  AIR  IN =',D11.4,T30,'CUM.  AIR  OUT =',D11.4,T60
     3,'CUM.  AIR  IN & OUT =',D11.4,T95,'CUM.  AIR  STRG. CHANGE =',D11
     4.4/1X,'INTL AIR STRG =',D11.4,T30,'CUM. AIR STRG =',D11.4,T60,'INC
     5. AIR  ERROR. 0/0 =',D11.4,T95,'CUM. AIR  ERROR. 0/0 =',D11.4 )
  473 FORMAT (/ 1X,'INC. WATER IN =',D11.4,T30,'INC. WATER OUT =',D11.4,
     1T60,'INC. WATER IN & OUT =',D11.4,T95,'INC. WATER STRG. CHANGE =',
     2D11.4,/1X,'CUM. WATER IN =',D11.4,T30,'CUM. WATER OUT =',D11.4,T60
     3,'CUM. WATER IN & OUT =',D11.4,T95,'CUM. WATER STRG. CHANGE =',D11
     4.4/1X,'INTL WAT STRG =',D11.4,T30,'CUM. WAT STRG =',D11.4,T60,'INC
     5. WAT. ERROR. 0/0 =',D11.4,T95,'CUM. WAT. ERROR. 0/0 =',D11.4 )
  476 FORMAT (/ 1X,'INC. SALT  IN =',D11.4,T30,'INC. SALT  OUT =',D11.4,
     1T60,'INC. SALT  IN & OUT =',D11.4,T95,'INC. SALT  STRG. CHANGE =',
     2D11.4,/1X,'CUM. SALT  IN =',D11.4,T30,'CUM. SALT  OUT =',D11.4,T60
     3,'CUM. SALT  IN & OUT =',D11.4,T95,'CUM. SALT  STRG. CHANGE =',D11
     4.4/1X,'INTL SLT STRG =',D11.4,T30,'CUM. SLT STRG =',D11.4,T60,'INC
     5. SLT. ERROR. 0/0 =',D11.4,T95,'CUM. SLT. ERROR. 0/0 =',D11.4/)
  475 FORMAT (26('=====*'))
      END
C
C*****************************************************************************
C                                                                             *
C         S U B R O U T I N E     B S O L V                                   *
C                                                                             *
C*****************************************************************************
C                                                                             *
C           THIS SUBROUTINE SOLVES THE MATRIX SET UP IN MATSOL BY             *
C           GAUSS ELIMINATION.                                                *
C           CMATRX & RHS NEED TO BE DIMENSIONED AS TO THEIR EXACT             *
C           SIZES                                                             *
C
      SUBROUTINE BSOLV (CMATRX,N,M,RHS)
```

```
      DIMENSION CMATRX(N,M),RHS(N)
      ZERO=0.0
      LR = (N-1)/2
      DO 2 L=1,LR
      IM = LR-L+1
      DO 13 I =1,IM
      DO 1 J=2,M
      CMATRX(L,J-1) = CMATRX(L,J)
    1 CONTINUE
      KN = N-L
      KM = M-1
      CMATRX(L,M) = ZERO
      CMATRX(KN+1, KM+1) = ZERO
   13 CONTINUE
    2 CONTINUE
      LR = LR+1
      IM = N-1
      DO 10 I=1,IM
      NPIV=I
      LS = I+1
      DO 3 L=LS,LR
      IF ( ABS(CMATRX(L,I)) .GT.  ABS(CMATRX(NPIV,I))) NPIV=L
    3 CONTINUE
      IF (NPIV .LE. I) GO TO 6
      DO 5 J=1,M
      TEMP=CMATRX(I,J)
      CMATRX(I,J)=CMATRX(NPIV,J)
      CMATRX(NPIV,J)=TEMP
    5 CONTINUE
      TEMP=RHS(I)
      RHS(I)=RHS(NPIV)
      RHS(NPIV)=TEMP
    6 CONTINUE
      RHS(I) = RHS(I)/CMATRX(I,I)
      DO 7 J=2,M
      CMATRX(I,J) = CMATRX(I,J)/CMATRX(I,I)
    7 CONTINUE
      DO 9 L=LS,LR
      TEMP = CMATRX(L,I)
      RHS(L) = RHS(L) - TEMP*RHS(I)
      DO 8 J=2,M
      CMATRX(L,J-1) = CMATRX(L,J) -TEMP*CMATRX(I,J)
    8 CONTINUE
      CMATRX(L,M) = ZERO
    9 CONTINUE
      IF (LR .LT. N)  LR=LR+1
   10 CONTINUE
      RHS(N) = RHS(N)/CMATRX(N,I)
      JM=2
      DO 12 I=1,IM
      L = N-I
      DO 11 J=2,JM
      KM = L+J
      RHS(L) = RHS(L) - CMATRX(L,J)*RHS(KM-1)
   11 CONTINUE
      IF (JM .LT. M) JM=JM+1
   12 CONTINUE
      RETURN
      END
C
C
```

```
C*************************************************************************
C                                                                        *
C         S  U  B  R  O  U  T  I  N  E      M  A  T  R  O  P           *
C                                                                        *
C*************************************************************************
C                                                                        *
C            THIS SUBROUTINE ORGANIZES THE INITIAL DATA OR OUTPUT        *
C            INTO A SUITABLE FORM FOR PRINTOUT .                         *
C            MATRICES A & B NEED TO BE DIMENSIONED AS TO THEIR           *
C            EXACT SIZES                                                 *
C
      SUBROUTINE MATROP (NA, NB, B)
      DIMENSION B(NA,NB), A(12)
      DO 11 I=2,NA,12
      ILL=0
      IN=I/12
      DO 9 J=2,NB
      IF ((IN+1)*12.GE.NA) GO TO 3
      DO 2 JJ=1,12
      JJJ=IN*12+JJ+1
    2 A(JJ)=B(JJJ,J)
      GO TO 6
    3 LL=(NA-1) - 12*IN
      ILL=1
      IF (LL .EQ. 0) GO TO 5
      DO 4 JJ=1,LL
      JJJ=IN*12+JJ+1
    4 A(JJ)=B(JJJ,J)
    6 CONTINUE
      IF (IN) 77, 77, 88
   77 IF (ILL .EQ. 1) GO TO 7
      WRITE(6,12) J, (A(II),II=1,12),J
      GO TO 9
    7 WRITE(6,17) J, (A(II),II=1,LL)
      GO TO 9
   88 IF (ILL .EQ. 1) GO TO 8
      WRITE(6,12) IN,(A(II),II=1,12),IN
      GO TO 9
    8 WRITE (6,17) IN,(A(II), II=1,LL)
    9 CONTINUE
      IF (NA.LE.(IN+1)*12) GO TO 11
      WRITE(6,13)
   11 CONTINUE
      RETURN
   12 FORMAT (1H,I4,12E10.3,I4)
   13 FORMAT (1HO,//)
   17 FORMAT (1H,I4, 12E10.3)
      END
C
C*************************************************************************
C                                                                        *
C         S  U  B  R  O  U  T  I  N  E      O  U  T  P  U  T           *
C                                                                        *
C*************************************************************************
C                                                                        *
C            THIS SUBROUTINE WRITES OUT ALL NECESSARY OUTPUT USING       *
C            SUBROUTINE MATROP. IT ALSO MAKES APPROPRIATE PLOTS          *
C            USING LOCAL LIBRARY PLOT ROUTINES                           *
C                                                                        *
C               IFPLOT = 0 ; IF NO PLOT NEEDED.                          *
C                      = 1 ; IF PLOT NEEDED                              *
```

```
C               IWRITE = 0; NO SERROR PRINTED.                          *
C                      = 1; SERROR PRINTED                              *
C
      SUBROUTINE OUTPUT (NC, NR, NCP1, NRP1)
      INTEGER TSTEP
      LOGICAL*1 C(10)
      DATA      C  /  'A','B','C','D','E','F','G','H','J','K'/
      DIMENSION IMAGE(4500), LABEL(9), NSCALE(5)
      DIMENSION PCTAE(22),SWTAB(22),WKTAB(22),AKTAB(22),PC(17,12),PW(17,
     112),PSAVE(17,12),PA(17,12),SW(17,12),SS(17,12),SA(17,12),WK(17,12)
     2,AK(17,12),VISW(17,12),VISA(17,12),RHOW(17,12),RHOA(17,12),SATP(17
     3,12),AW(17,12),BW(17,12),WT(17),SERROR(17,12),ZZ(17,12),STAB(22),C
     4ONST1(17,2),CONST2(17,2),CONST(17,12)
      DIMENSION VX(19,13),VZ(18,14),X(4500),Z(4500),C(4500),SUMC(18,13),
     1COUNT(18,13),CAVG(18,13),DX(17,12),DZ(17,12),DXZ(17,12),DELC(18,13
     2)
      DIMENSION CAVGSV(18,13)
      COMMON      PCTAE,SWTAB,WKTAB,AKTAB,PC,PW,PSAVE,PA,SW,SS,SA,WK,AK,V
     1            ISW,VISA,RHOW,RHOA,SATP,AW,BW,WT,SERROR,ZZ,CONST1,CONST
     2            2,X,Z,C,VX,VZ,SUMC,COUNT,DELC,CAVG,DX,DZ,DXZ,STAB,DELX,
     3            DELZ,DELT,SATPER,PHI,G,CRHC,PSCURC,HA,HB,DELMLT,TOLRNC,
     4            DSWMX,DSWMAX,AX,AZ,AXZ,ALENX,ALENZ,CONST,ONE,TWO,FOUR,H
     5            ALF,ZERO,DELT1, DELT2,DIA,DIFF,SOLNC,ISAT,NRM1,NCM1,NRM
     6            2,NCM2,NR2,NR3,NC1,NC2,NDELT,IS1,IPRINT,IFAC,LOG,ITER,I
     7            A,IB,IC,ID,IE,IBM1,IDP1,NWM1,TSTEP,IPC,ISK,ISW,ITENSR,I
     8            CHECK,ISWICH,IRES,ISTEDY,IFPLOT,IWRITE,NN,IVEL,ICLOG
      WRITE (6,71)
      CALL MATROP (NCM1, NRM1, PW)
      DO 111 I=2,NCM1
      DO 111 K=2,NRM2
      IF (PW(I,K) .LT.  ZERO  .AND. PW(I,K+1) .GT. ZERO)
     &WT(I)=PW(I,K)/(PW(I,K)-PW(I,K+1))*DELZ+ZZ(I,K)
  111 CONTINUE
      WRITE (6,49) (WT(I),I=2,NCM1)
      WRITE (6,73)
      CALL MATROP (NCM1, NRM1, PC)
      WRITE (6,74)
      CALL MATROP (NCM1, NRM1, PA)
      WRITE (6,72)
      CALL MATROP (NCM1, NRM1, SW)
      IF (IWRITE .EQ. 0) GO TO 52
      WRITE (6,76)
      CALL MATROP (NCM1, NRM1, SERROR)
   52 CONTINUE
      WRITE (6,413) TSTEP
      CALL MATROP (NCP1, NR, VX)
      WRITE (6,414) TSTEP
      CALL MATROP (NC, NRP1, VZ)
      IF (ISTEDY .EQ. 1) GO TO 350
      IF (IFPLOT .EQ. 0) GO TO 300
      WRITE (6,5)
    5 FORMAT (1H1)
      NSBH=3
      NSBV=5
      NSCALE(1)=1
      NSCALE(2)=0
      NSCALE(3)=0
      NSCALE(4)=0
      NSCALE(5)=0
C
C  ........ THE FOLLOWING SUBROUTINES : PLOT1, PLOT2, PLOT3, PLOT4 ARE
```

```
C           LOCAL LIBRARY SUBROUTINES AND CAN BE USED ONLY IN FORTRAN ..
      CALL PLOT 1 (NSCALE, NRP1, NSBH, NCP1, NSBV)
      CALL PLOT 2 (IMAGE, ALENX, 0.0, 0.0, -ALENZ)
      DO 920 I=1, LOG
      IF (C(I) .EQ. 0.0) GO TO 920
      Z(I)=-Z(I)
      IF (C(I) .GE. 0.9*SOLNC) GO TO 901
      IF (C(I) .GE. 0.8*SOLNC) GO TO 902
      IF (C(I) .GE. 0.7*SOLNC) GO TO 903
      IF (C(I) .GE. 0.6*SOLNC) GO TO 904
      IF (C(I) .GE. 0.5*SOLNC) GO TO 905
      IF (C(I) .GE. 0.3*SOLNC) GO TO 906
      IF (C(I) .GE. 0.1*SOLNC) GO TO 907
      IF (C(I) .GE. 0.01*SOLNC) GO TO 908
      IF (C(I) .GE. 0.001*SOLNC) GO TO 909
      CALL PLOT 3 (Q(10), X(I),  Z(I), 1, 4)
      GO TO 910
  901 CALL PLOT 3 (Q(1), X(I),  Z(I), 1, 4)
      GO TO 910
  902 CALL PLOT 3 (Q(2), X(I),  Z(I), 1, 4)
      GO TO 910
  903 CALL PLOT 3 (Q(3), X(I),  Z(I), 1, 4)
      GO TO 910
  904 CALL PLOT 3 (Q(4), X(I),  Z(I), 1, 4)
      GO TO 910
  905 CALL PLOT 3 (Q(5), X(I),  Z(I), 1, 4)
      GO TO 910
  906 CALL PLOT 3 (Q(6), X(I),  Z(I), 1, 4)
      GO TO 910
  907 CALL PLOT 3 (Q(7), X(I),  Z(I), 1, 4)
      GO TO 910
  908 CALL PLOT 3 (Q(8), X(I),  Z(I), 1, 4)
      GO TO 910
  909 CALL PLOT 3 (Q(9), X(I),  Z(I), 1, 4)
  910 Z(I)=-Z(I)
  920 CONTINUE
      CALL PLOT 4 (9, 9HX  IN  CM)
      WRITE (6,472)
  472 FORMAT ( /50X, 'X  IN  CM'/ )
      WRITE (6,700)
  700 FORMAT (//15, 'A:C/CO = 0.9 - 1.0',T30,'B:C/CO = 0.8 - 0.9',T55,'C
     1:C/CO = 0.7 - 0.8',T80,'D:C/CO = 0.6 - 0.7',T105,'E:C/CO = 0.5 - 0
     2.6',/T5,'F:C/CO = 0.3 - 0.5', T30,'G:C/CO = 0.1 - 0.3',T55,'H:C/CO
     3 = 0.01 - 0.1',T80,'J:C/CO = 0.001 - 0.01',T105,'K:C/CO = 0.0 - 0.
     4001',/)
  300 CONTINUE
      IF (IWRITE .EQ. 0) GO TO 54
      WRITE (6,415) TSTEP
      CALL MATROP (NCM1, NRM1, DX)
      WRITE (6,416) TSTEP
      CALL MATROP (NCM1, NRM1, DZ)
      WRITE (6,417) TSTEP
      CALL MATROP (NCM1, NRM1, DXZ)
   54 CONTINUE
      WRITE (6,411) TSTEP
      CALL MATROP (NC, NR, CAVG)
      WRITE (6,412) TSTEP
      CALL MATROP (NC, NR, COUNT)
  350 RETURN
   49 FORMAT (/1X, 'LOCATION OF WATER TABLE : '/5X,16E8.2)
   71 FORMAT (/45X, 'THE WATER PRESSURE MAP IS'/)
```

```
 72 FORMAT (/45X,'THE WATER SATURATION MAP IS'/)
 73 FORMAT (/45X, 'THE CAPILLARY PRESSURE MAP IS'/)
 74 FORMAT (/45X, 'THE AIR PRESSURE MAP IS'/)
 76 FORMAT (/45X, 'THE SATURATION ERROR MAP IS'/)
411 FORMAT (/45X, 'THE CAVG MAP AT TSTEP =',I4/)
412 FORMAT (/45X, 'THE COUNT MAP AT TSTEP =',I4/)
413 FORMAT (/35X, 'VELOCITY IN X-DIRECTION AT GRID INTERFACES AT TSTEP
   $ =',I4/)
414 FORMAT (/35X, 'VELOCITY IN Z-DIRECTION AT GRID INTERFACES AT TSTEP
   $ =',I4/)
415 FORMAT (/45X, 'CX TENSOR AT TSTEP =',I4/)
416 FORMAT (/45X, 'CZ TENSOR AT TSTEP =',I4/)
417 FORMAT (/45X, 'DXZ TENSOR AT TSTEP =',I4/)
    END
```